PHD

Experimental and Analytical Investigation into the Two Stage Turbocharging Systems for Diesel Engines

Zhang, Nic

Award date:
2016

Awarding institution:
University of Bath

Experimental and Analytical Investigation into the Two Stage Turbocharging Systems for Diesel Engines

Qingning Zhang

A thesis submitted for the degree of Doctor of Philosophy

University of Bath

Department of Mechanical Engineering

October 2015

Abstract

The work described in this thesis aims to conduct a systematic study of the two stage turbocharging system to improve the Diesel engine transient performance as well as NO_X and CO_2 emissions with a focus on the improved turbocharger matching and the control of the charging system, through the use of high fidelity engine models backed by experimental results. To perform the analytical study, commercial 1D simulation software has been used in the process of system characterisation and control strategy design. To validate the analytical results, a two stage turbocharging system was installed on a production diesel engine and tested on a transient engine test bench. The test results were then used to further calibrate the 1D engine/turbocharger model. Several other technologies were also investigated in simulation to explore their potential to further improve the system. Unlike most studies in the literature, this project focused on the system benefit of the engine and turbochargers, instead of conducting optimisation solely at the component level. The engine global parameters, such as the engine fuel consumption, emission levels and the transient response were the main parameters to be considered and were also best suited to the strengths of the 1D simulation method. The interactive use of both the analytical and experimental methods was also a strong point of this study.

A novel control strategy for the system was proposed and demonstrated in the simulation. Experiments confirmed the validity of this control strategy and provided data for further model calibration. The comparison of the test results of the baseline engine to those obtained with the two stage turbocharged engine system verified the benefits of the novel turbocharging arrangement and control scheme. Transient response (T1090) was improved, with a 50% faster

torque rise at 1000 rpm; the fuel consumption over the NEDC was 4% lower and NOx emissions over the NEDC were 28% lower. In the meantime, the study also revealed shortcomings of the system, such as the lack of EGR control at low speed, low load condition and a mid-speed fuel consumption deterioration of 13% on average at 3000 rpm due to excessive back pressure.

With a novel 1D model corroborated using test results, exploratory simulation was done to rectify the aforementioned shortcomings and to further improve the system. Simulation results showed that by implementing VGT and ball bearing technology in the high pressure stage of the two stage system, the EGR controllability at low speed was regained and the excessive back pressure at high speed was improved. Consequently, the fuel consumption was only increased by 1.3% compared to the baseline NEDC operation and the transient response was on par with the original two stage system, with only 0.05s slower in torque rise at 1000 rpm, and still 48% faster than the baseline VGT system. Furthermore, the NOx emission can be expected to be greatly improved in the upcoming more intensive drive cycles compared to the NEDC cycle, with simulation showing NEDC NO_X emissions dropped by 1%, comparing to a substantial reduction of 11% in WLTC.

Acknowledgements

I would like to first express my gratitude to my supervisor, Professor Chris Brace, who has been consistently providing support throughout my study. I have learned more from Chris than from any other education institution that I have attended.

I would also like to thank Professor Gary Hawley. His vision and kindness brought me to Bath and made my study possible.

Meanwhile, I can never forget the countless and generous helps I received from our experienced laboratory and testing experts who helped setting up my test cell, Dr Sam Akehurst, Mr Allan Cox and Mr Vijay Rajput.

Very special and sincere thanks to our technician team, Mr Bob Gusthart, Mr Jim Cansell, Mr Graham Rattley, I cannot imagine to finish my study without you guys. It has been a fun ride.

I especially enjoyed the company of colleagues studying or working with me in Bath, Richard Burke, Colin Copeland, Tomasz Duda, Andrew Lewis, Chris Vagg, Huayin Tang, Deepak Hari, Karl Giles, Bo Hu, Dian Liu and Dom Parson. You have set the standards quite high for my future colleagues and friends.

My parents had always been there supporting me, even though they would not be able to read a single paragraph in this long document. 谢谢你们，爸妈.

Thank you all very much.

Table of contents

List of figures

List of tables

Chapter 1 - Introduction

The work presented in this thesis was a comprehensive investigation of the two stage turbocharging system. 1D gas dynamic engine models have been extensively used during the whole process including building of the baseline engine model, sizing of the turbocharging hardware, design of the control strategy and finally the exploration of potential hardware improvement. Although largely a simulation based research, the experimental work was conducted as a crucial component in this study to provide data for model calibration and simulation results validation. To increase the credibility of the exploratory simulation, potential hardware improvements, such as the variable turbine geometry and the ball bearing turbo rotor, were first individually tested and then built into the two stage turbocharging model as virtual hardware. Among other studies conducted on the novel turbocharging systems, this study took a cautious and critical view of the extrapolative capability of the currently prevalent 1D modelling methodology and endeavoured to always relate the simulation results to experiments. The experience gained in this study was hopefully useful for similar work during engine development in the future.

1. Background and motivation

The use of two stage turbocharging systems on the internal combustion engine is gaining popularity in the context of worldwide fuel efficiency mandates and emission regulations. In comparison to the single stage turbocharger, the two stage system provides inherently better transient response and rated power fuel economy due to the two differently sized turbochargers working in their respectively optimal operating region. NO_X emissions can also be reduced due to the more flexible control of EGR gas allowed by the two stage system. Various examples found in the literature have shown that the correct matching and control of such two stage turbocharging systems is the key to fully exploit the potential of the two turbochargers.

The turbocharger uses a turbine to harness the enthalpy in the exhaust gas of the engine to drive a compressor so that the air fed into the engine is boosted to higher density, therefore producing more power from the same engine (up-rating), or the same power from a smaller engine (downsizing). The consensus now is that when choosing the size of the turbocharger to be matched to a reciprocating engine, usually a compromise has to be made between fast response and good efficiency. Meanwhile, a two stage system allows both the fast response time of the small turbocharger and the high efficiency from the large turbocharger: at low engine speed, the small device works more effectively to spin up to high speed and build up the boost at the request of a torque rise; at mid-engine speed, the two turbocharger works in series and boost the engine in two stage to high pressure level; at high engine speed, engine control system actively bypass the smaller device and the large device works solely at its optimal efficiency region. The higher boost level not only leads to more power, it also allows better combustion efficiency and EGR capability.

However, the sizing of the two turbochargers is crucial: the low pressure turbocharger (large) should be sized to the engine rated power condition; a high pressure turbocharger sized too

small would throttle the engine and create a valley on the engine full load curve, while too big leads to poor low end torque and EGR capability. Moreover, the controller is required to robustly decide when the high pressure turbocharger should be phased out of operation and handover the boost control to the low pressure turbocharger to avoid throttling the engine at high mass flow. A poorly designed control strategy can lead to poor fuel consumption, sluggish transient response and even dangerous operation such as turbocharger over-speeding and engine over boosting. The sizing and control of the turbocharger system together should also be able to provide suitable back pressure for pumping EGR gas when needed.

To explore the aforementioned topics, pure experimental studies would require a large amount of expense and labour in the test cell. Therefore, a simulation study, corroborated by sufficient experimental work was proposed here to systematically investigate the two stage turbocharging system.

A few other doctorate research theses have been dedicated to the topic of the two stage system, including the one of Varnier at Universidad Politecnica de Valencia (Varnier, 2012) and the one of Lee at University of Michigan (Lee, 2009). The two studies have both contributed valid research results and provided a solid foundation for this thesis. Nevertheless, the experimental side of these studies was hardly at the same level of sophistication compared to their simulation side, possibly due to the difficulties in hardware implementation. Therefore the study presented here aimed to make contributions on top of the previous study: a large amount of effort was made to experimentally characterise the turbocharging system, facilitated by the simulation study; while the simulation results were corroborated by the test data. The potential weakness and problematic assumptions of the modelling methodology was always considered. Furthermore, the study benefited from a robust partnership of a university - industry collaboration and has received numerous guidance from highly experienced specialists and was

given ample technician hours on the test bench. Moreover, the engine and turbocharging devices used in the experiments were all production hardware which ensured a relatively smooth experimental phase. The successful test bench work guaranteed the quality of the model and produced reliable test data for future work.

2. Aim and objectives

The aim of this piece of work can be summarised as to implement, characterise, control and improve the two stage turbocharging system used on a Diesel engine using 1D engine model corroborated by experimental investigations.

The specific objectives to achieve the aim can be summarised as the contents of the following chapters as follows:

1. To perform a detailed literature survey on the topic of complex turbocharging systems to achieve a thorough understanding of the benefits and characteristics of the two stage system and the other alternative turbo arrangements.
2. To set up the test cell environment and install hardware for the experimental work. To design the test schedule for this study and test the baseline hardware thoroughly to debug the system and obtain baseline test results for model calibration.
3. To build a 1D engine model based on the engine hardware and calibrate the model against test results to be used as a reliable foundation for the subsequent simulation study.
4. To conduct an experimental and analytical study on ball bearing turbocharger technology. The outcome from this piece of work can be useful to explore the potential of a ball bearing system to further improve the two stage system.

5. To perform an analytical study of the two stage system using the calibrated model before the experimental work on the two stage system so as to understand the system characteristics of the two stage hardware to be tested and also design the control strategy based on the simulation results.
6. To test the two stage system using the control strategy proposed and compare the two stage system and the baseline VGT turbocharger system, identifying the weakness of the two stage system.
7. To perform the second phase of the simulation study on the two stage system using the calibrated two stage turbocharging model, exploring the potential technologies which can further improve the two stage system.
8. To conclude the major findings from this thesis and propose recommendations for future work.

Chapter 2 - Literature review

This literature survey aims to provide a thorough understanding of the existing research and the state of the art technologies relevant to this thesis. Specifically, the various important aspects of sequential turbocharging are identified, with an emphasis on automotive diesel engine applications. First, turbocharged Diesel engine is introduced briefly and the limitations of the conventional turbocharging technologies are explained. Then the candidate technologies for improving the conventional device are discussed, within which, the most promising multi-turbo systems are highlighted: variants of sequential turbocharging systems are described along with their relative advantages and limitations. Performance factors such as achievable boost pressure, transient response, and range of possible flow rates are investigated and contrasted across possible architectures of sequential turbocharging. To select the most suitable modelling method for the simulation study and the control method for the experimental study, the review then details turbocharger modelling and control approaches used thus far can be applicable for sequential turbocharging, and the advantages and disadvantages concerning performance and robustness offered by these methods. It is identified that, as one of the most commercially viable solutions, the series sequential turbocharging technology has not been systematically discussed in academia and the industry alike. Therefore, it is proposed in this study to carry out a thorough research on this technology with joint efforts in experimentation and simulation.

2.1 Introduction

The modern high speed Diesel engine is a fast response machine: it can be operated at a lean air-fuel ratio such that increments in the fuel supply rate can be rapidly burned using the readily available excess air in the cylinder to generate additional torque right from the engine cycle when the pedal was pressed. In a conventional naturally aspirated diesel engine, the intake airflow rate is limited by the engine speed and swept volume (Heywood, 1988). This, in turn, limits the maximum load that a diesel engine can achieve to a rather low level without some form of pressure charging. Therefore, supercharging and, in particular, turbocharging technologies are often used on Diesel engines to increase the density of air in the intake manifold and thereby increasing the mass flow rate of air available to the cylinders for combustion (Watson, N. and Janota, M. 1982).

Downsizing is the replacement of a larger displacement engine with one of higher specific power. There is a benefit to running at higher specific loads in a downsized application since the engine friction losses typically increase more rapidly as a function of engine speed than as a function of load (Chen, S. and Flynn, P., 1965). At higher specific loads, therefore, the frictional losses represent a smaller percentage of the total work and so result in a more efficient operating condition. Furthermore, a downsized engine yields a lighter vehicle and thus even better fuel consumption. For gasoline engines, downsizing also allows the degree of throttling to be reduced, leading to lower pumping losses (Lecointe, B. and Monnier, G., 2003). Note though, that since the specific loading of the engine is very high in a downsized application, the bearings may well need to be larger than in a similar sized engine developing a lower specific torque, and so frictional losses are likely to be reduced by less than initially

hoped (Fraser, N. et al, 2009). Engine boosting is the enabler technology to achieve the engine downsizing.

Supercharging technology utilises power from the crankshaft for boosting and thus draws energy for compression directly from the engine, acting as a parasitic loss. It is therefore less popular for passenger car applications than turbocharging which uses otherwise wasted energy in the exhaust gas (Lecointe, B. and Monnier, G., 2003). Indeed, the turbocharger has, for many years, been a standard component of diesel engines due to its ability to increase engine output (Watson, N. and Janota, M. 1982; Fraser, N. et al, 2009). In addition to the up-rating effect, the level of emission production can also be lowered. Hydrocarbon (HC) and carbon monoxide (CO) emissions are reduced due to the higher charge temperature, while the nitrous oxides (NOx) formation can be a problem under high engine loading, yet can be alleviated through injection retardation and high levels of exhaust gas recirculation (EGR) enabled through engine boosting control (Watson, N. and Janota, M. 1982; Stone, R., 1999; Galindo, J. et al, 2010).

One drawback of conventional single stage turbocharging is that at part loads, the turbine area may be too large to be suitable for the low gas flow rate and temperature, causing inefficient operation. Furthermore, variable engine speed and torque conditions can lead to compressor surge (Winkler and Ångström, 2008), especially during load tip-outs. Downsizing the turbochargers can prevent surge from happening while improving transient response; but will limit the engine rating because smaller turbochargers may over-speed at rated power. Traditionally, several turbochargers have been installed in stages to increase the boost pressure on large commercial Diesel engines. In recent years, however, in order to provide boost over a wide range of flow rates on smaller high speed Diesel engine (and gasoline engine in the state of the art applications (Bowyer, S., 2012), several turbocharger units can be used in combination in place of a single unit in order to achieve the higher level of boost required by

downsizing. The turbochargers can be connected in a series or parallel architecture, or even both (Steinparzer, F., 2007); moreover, the various turbocharger units can either operate continuously, or sequentially, where they are phased in and out depending on the engine operating conditions (Langridge, S. and Fessler, H., 2002).

Between the in series and parallel arrangement of turbochargers, there is a clear trend of preferring the series sequential arrangement due to its high boost capability and smooth transition of operating mode. However, it is not without its weakness: the basic setup of using two fixed geometry turbochargers lacks the flexibility to accurately control EGR gas; while the small turbocharger can produce high back pressure, deteriorating the engine fuel economy. Therefore, the VGT technology has been used in the niche product for EGR control and also to alleviate the other problems (Steinparzer, F., 2007). In the meantime, as the ball bearing technology in turbocharger becomes available at an affordable price, it can also be a key component to overcome the weakness of the two stage system (Davies, P. et al, 2013).

2.2 Turbocharging technologies

2.2.1 Turbocharger

Turbocharging is a technology that uses turbo machineries, such as turbines and compressors, harnessing the waste energy in the exhaust gas of an engine, to achieve the effect of supercharging. The result of this is that the air is introduced into the engine cylinder at a density higher than the ambient condition. Such increase in air density allows a higher amount of fuel to be burned in the engine and thus the engine power output is increased (Watson, N. and Janota, M. 1982). For the modern high speed Diesel engine, this technology allows the engine to be downsized for the benefit of engine efficiency (Mayer, A. et al, 1982).

The turbochargers in automotive applications are usually composed of a turbine, a compressor (both radial flow types) and a turbo-shaft connecting the turbine and compressor wheels inside the turbocharger housing. By changing the momentum of the exhaust gas flow, the turbine gains a reaction torque to drive the compressor, which then pass on the energy to the charged air flow in the form of static pressure.

One of the critical tasks in designing a turbocharged powertrain is that of matching the turbocharger with the engine. First, a basic frame size of the turbocharger is determined by estimating the quantity of air required by the engine. Then the compressor is chosen by placing the engine operating lines of its entire speed and load range inside a suitable sized compressor map with sufficient margin from surge line while ensuring as much of the high efficiency area on the map is used. Based on the frame size already chosen, the turbine is then matched by altering the nozzle ring and volute, so that the suitable effective turbine area is selected (Watson, N. and Janota, MS. 1982). The turbine speed will increase with the decrease of effective turbine area and gives good low end response, yet will face over-speeding at high engine speeds. On the other hand, increasing the effective turbine area avoids this problem but the low end response is poor. For the automotive applications which employ a wide flow range, the final matching is usually a compromise between transient response and rated power efficiency (Mayer, A. et al, 1982).

Traditionally, matching of a turbocharger was mainly conducted using the method of characteristic analysis or the filling and emptying modelling method, as will be discussed in the modelling section. Such low level programs can generate relatively a reliable result by using minimal computational power (Yang and Campbell, 1997). However, with the advancement of computer science and the more stringent requirement on the powertrain system, 1-D or even 3-D simulations are becoming common practice in refining the turbocharger matching and validating the powertrain design (Vitek, O. et al, 2006; Shingne, P. et al, 2010; Bozza, F. and De

Bellis, V., 2011; Gautier et al, 2008). As can been seen from the aforementioned research, due to the expectancy of the model accuracy rises, it becomes universal to calibrate the engine model against experiment data before generating any useful simulation results. Even for exploratory research, where the combined turbocharger-engine system does not physically exist at the time of building the model, a rough combustion calibration was still conducted using an existing baseline engine so that the engine model behaves as closely as possible to reality (Gautier et al, 2008).

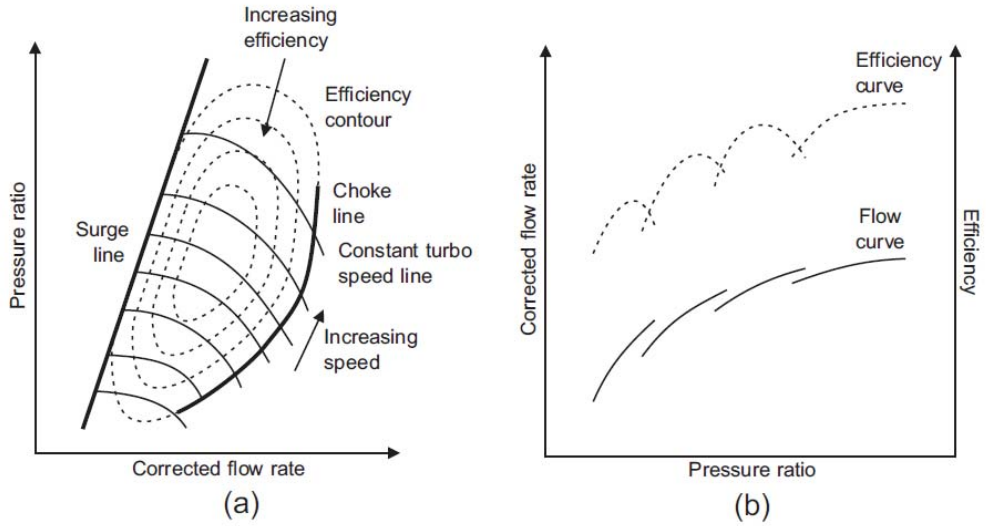

Figure 2.1 typical compressor and turbine maps.

2.2.2 Wastegate

As was previously mentioned, matching of the turbochargers on automotive applications is usually a compromise between low engine speed transient response and rated power efficiency. On many of the low end Diesel engines and most gasoline engines nowadays, this compromise is achieved through the use of a relatively small turbocharger equipped with a wastegate structure. The low inertia and small turbine effective diameter ensures fast response at low engine speeds; at high speeds, however, the excessive exhaust gas is bypassed

through the wastegate to prevent over-speed/boost. The limitations of this technology is that the exhaust gas bled off through the wastegate is a pure loss of energy which means a bigger turbocharger could have been used to work in higher efficiency region and within a wider flow range (Moody, J., 1986).

2.2.3 Variable geometry turbine (VGT)

As the prevalent technology of the Diesel engine turbocharging system, the variable geometry turbine is capable of actively changing the effective turbine diameter. It can operate as a small sized turbocharger (still with inertia of a big one, though) at low engine speeds when transient response is crucial and can also operate as a large and high efficiency device at higher engine speeds (Moody, J., 1986). Therefore, the exhaust energy is better utilised especially at low engine speed while over-speed or over-boost can also be prevented. The technology shows improvements at load speed/load in terms of boost pressure, smoke emission, turbine inlet temperature and specific fuel consumption (Watson, N. and Janota, MS. 1982).

2.2.4 Ball bearing turbocharger

The ball bearing turbocharger technology has only in recent years started to be adopted for mass-production engines due to the potential benefit in transient performance and fuel consumption. Compared to the conventional journal bearing, the ball bearings offer around 40% friction reduction at constant speed (Tanimoto, K. et al, 2000). This allows the turbocharger to accelerate faster so that the engine can be supplied with boost pressure more quickly following a transient torque request and under steady state offers reduced engine back pressure, which can reduce engine fuel consumption (Davies, P. et al, 2013). Apart from the engine performance, the ball bearings on the turbocharger also reduced repair frequency and increased life due to its improved rotordynamics and resistance to contaminated lubricant (Griffith, R. et al, 2007). The challenges to the application include cost and noise consideration.

2.3 Multi-Turbocharger Boosting Arrangements

As mentioned earlier, VGT technology can effectively alleviate the dilemma between transient response and rated power efficiency by changing the effective turbine area. However, stricter emission regulations and rising customer expectancy for performance forces engineers to seek for even better solutions. After all, the VGT turbocharger is still a big device with large inertia; and the efficiency of the VGT deteriorates at low gas flow conditions.

The problem can be better coped with by employing several differently sized turbocharger units. High efficiencies can thus be delivered at a wider range of operating speeds. By using the operating regions of several turbomachinery units, the problems of surge at low flow rates and choked flow at high speeds typically faced by single stage turbochargers can also be alleviated. Higher boost level is also expected to be reached in the meantime (Knecht, W., 2008).

Nevertheless, using multiple turbocharger units can introduce an additional layer of complexity. For instance, although implementing a multi-turbo boosting system to a diesel engine offers more opportunity for adjustment than a single stage solution, it is not a simple task. In addition to the engine breathing performance requirements, several essential limit values must be considered, including peak cylinder pressure, exhaust gas temperature, smoke number, compressor outlet temperature, speed limits, surge margin, choke limits, efficiency from mid to high engine speed at high load, and the engine back pressure limit. Compromises between the various performance factors must therefore be made (Watson, N. and Janota, MS., 1982). An approximated configuration is often used as a first approach to matching, and mass flow multipliers can be then used to select the sizes of both stages (Navrátil, J., 2006). Alternatively, an iterative procedure based on physical modelling can be used to size the turbocharger units (Lee, B. et al, 2008).

The two main forms of multi-turbocharger boosting systems are parallel and series arrangements of the turbocharger units. Since one of these two arrangements is selected to be systematically studied, the merits of the two systems in comparison are discussed in the following sections in greater details.

2.3.1 Parallel Arrangement

In this form of turbocharging, both turbochargers are connected in parallel to a common manifold connecting all cylinders. The basic arrangement of this form of turbocharging is shown in Figure 2.2. During low flow rates, the main unit can be operated solely so that the exhaust energy can be extracted with high efficiency. The peak unit is then phased in as the flow starts to become choked on the main turbocharger. The two turbochargers are usually smaller than a single stage turbocharger on a similar sized engine.

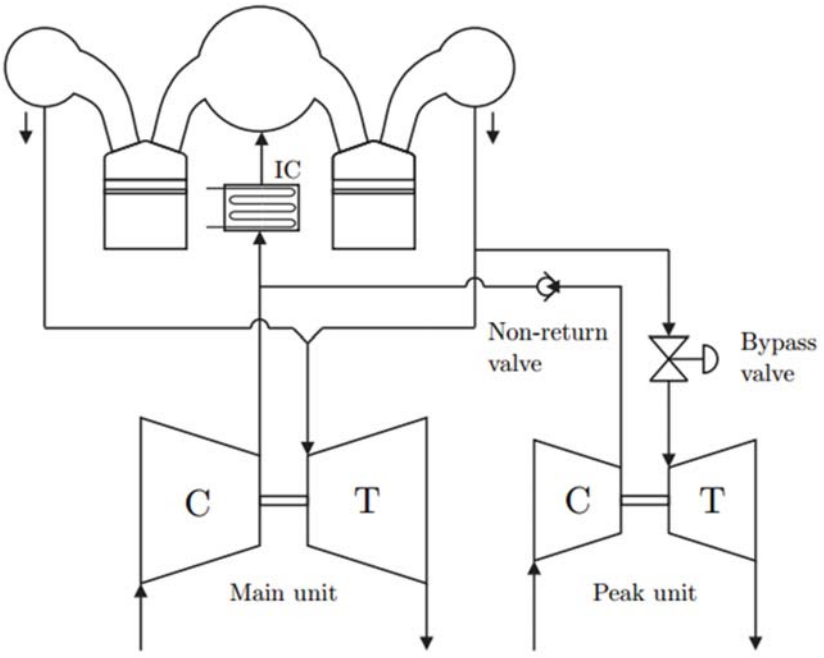

Figure 2.2 parallel sequential turbocharging setup, incorporating compressors (C), turbines (T), Intercooler (IC)

The use of a smaller main turbocharger improves the transient response due to its lower inertia and its full usage of engine exhaust flow when working solely. On the other hand, a wider engine flow range is possible because at higher engine speeds, the second turbocharger phases in when the flow through the first turbocharger begins to become choked (Galindo, J. et al, 2009; Galindo, J., 2007). Depending on the relative sizes of the matched turbochargers and the design objective, which can be different for research and commercial applications, the sequencing used for the two turbochargers has varied, as discussed in the following paragraphs.

In general, during parallel turbocharging operation, the different turbocharger units are phased in and out of operation depending on the engine operating state. This transition between the different phases of operation represents one of the most crucial challenges of parallel turbocharging. Much effort has to be made in creating a controller governing in which operating conditions the transition should be performed in order to avoid unpleasant or even dangerous torque oscillations (Galindo, J. et al, 2009; Zhang, Z. et al, 2008). Fluctuations in torque occur due to pressure variations in the intake and exhaust manifolds, acceleration of the turbocharger units and transients in the thermal conditions (Galindo, J. et al, 2009). The transients in air flow can also interfere with smoke control mechanisms, leading to fuel supply reductions.

Various regimes for switching on and off the individual turbochargers have been devised. Galindo (Galindo, J. et al, 2007; Galindo, J. et al, 2009) used two modes of operation where only one turbocharger is operated at low speed conditions, while both turbocharger units are used at higher speed conditions. Zhang (Zhang, Z. et al, 2008) used a three phase approach, where the first two phases corresponded to operation of the smaller and larger turbochargers only, respectively, and the third phase consisted of both turbocharger units being utilised for boosting. The phase applied depended on the position in the torque-speed space: the engine

used only one of the turbochargers to boost the engine at low engine speed conditions, where the exhaust energy was lower in both cases.

A number of studies have compared the transient and steady state performance of parallel arrangements with single stage turbocharging. Zhang (Zhang, Z. et al, 2008) compared the brake specific fuel consumption and smoke emissions of the parallel turbocharger system with a conventional, single stage turbocharged engine. The parallel turbocharger system displayed lower smoke emissions during transient operation, and achieved better fuel efficiency than its conventional, single-stage turbocharger counterpart.

Ren (Ren, Z., et al, 1998) investigated the operation of a parallel sequential turbocharging system on a medium speed 24 L diesel engine. Two differently sized turbochargers were connected in parallel to a six cylinder marine engine, with the larger (main) unit being used initially, and the smaller (peak) unit being phased in as engine speed and load increased. Despite some degree of air leakage due to the long, flexible steel pipe used to connect the peak unit compressor to the intercooler, performance in terms of brake specific fuel consumption (BSFC) showed improvement. However, the parallel arrangement used in the research was not an optimal design. Firstly, the inlet of the peak unit turbine was on the far side of the exhaust manifold, separate from the main unit. Since the exhaust manifold was not likely designed for providing exhaust gas to two turbochargers at either end, some kinetic exhaust energy is lost from one of the units (probably the peak unit). The second unfavourable aspect of the design was found in the air path of the peak unit compressor. While the non-return valve was very effective and necessary for blocking reverse flow from the main unit and reducing the control complexity, it completely blocked the air path of the peak unit during the transition between sequences when the peak unit began to accelerate. Over-heat, noise and possibly mechanical damage from compressor surge are consequently very likely during the transition.

Controls of air flow, and in particular, protection against compressor surge, are important aspects of parallel turbocharging. Galindo (Galindo, J. et al, 2007) addressed the control of air flow through the compressor by introducing a recirculation circuit, in which the peak unit valve is kept with a slight opening area, even during the single turbocharger operating mode. On the compressor side, the continuously spinning compressor drives air through a recirculation valve back to its inlet. A minimal spinning speed of the peak unit is thus maintained, which has benefits for lubrication and could perhaps also help to avoid the surge issue observed during transition reported by Ren (Ren, Z., et al, 1998).

Building on the above work, Galindo (Galindo, J., Climent, H. et al, 2009) carried out further research in order to develop an optimised controller and tested the control regime over drive cycles. With smoothness during transition being achieved through extra fuelling, the controller focused heavily on over-speed and surge control with a slightly lower emphasis on fuel efficiency than their earlier approach. The controller provided a good illustration of how much effort is needed in order to control a parallel turbocharging system: four valves were controlled interactively and an additional fuel injection control was achieve through the engine control unit (ECU). Moreover, the work highlighted the vulnerability of parallel arrangements to compressor surge during the phasing in and out of the additional turbocharger. Although it was stated in the paper that surge only causes real damage when maintained for several seconds, the compressor map showed a disturbingly wide range of behaviour in the transition region, possibly requiring a re-match to alleviate this problem.

In a further investigation, Galindo (Galindo, J. et al, 2009) explored a number of control strategies aimed at reducing oscillations in torque output following a transition in operating mode. A corrective fuel control strategy achieved significant reductions in torque oscillations but resulted in a low air-fuel ratio at full load. A further, ‘pre-lift’ strategy involved slightly opening the valve responsible for controlling the second turbine during a transition in order to

accelerate the corresponding compressor and pressurise the air downstream of the latter. This strategy effectively reduced the fluctuations by more than a factor of two. A third strategy applied a slow actuation to the valves controlling the turbochargers but proved less effective than the other approaches with respect to reducing oscillations under transient conditions.

Qian (Qian, Y. et al, 2012) applied various switching and valve strategies to a three phase, two-stage parallel turbocharging system. The use of asynchronous valve operation when switching from the larger to the smaller turbocharging units and vice versa were compared with simply opening and closing the compressor and turbine valves simultaneously. For instance, during switching from the smaller to the larger turbocharger, the valve of the larger turbine was firstly closed, and subsequently, only when the boost pressures of the two compressors are equal were the valves of the larger compressor and the smaller turbine respectively opened and closed, followed by the closure of the valve regulating the smaller compressor (see Figure 2.1 for an illustration of the surge limits at different pressure ratios and flow rates). Through this strategy, the surge observed during synchronous valve operation was avoided. Furthermore, in addition to demonstrating reductions in fuel consumption and smoke emissions in steady state for the parallel turbocharging as compared to single stage turbocharging, the authors explored the use of different switching boundaries for transient operation. For example, in the transition between the smaller turbocharger and both units operating, the smaller unit was operated for as long as possible before engaging the second unit; such strategies reduced the acceleration time by around 20%.

A major disadvantage of the parallel arrangement is that since the differently sized compressors share the same pressure ratio, the boost level is limited by the maximum pressure ratio of the smaller turbocharger (Galindo, J. et al, 2010). Nevertheless, some research has suggested that, in some cases, the parallel architecture can cover a higher flow rate range than the series setup (Tashima, S. et al, 1994). This is essentially because in the

series arrangement, the whole air flow has to pass through all the compressors in turn, whereas in the parallel setup, several flow paths are available, leading to a greater range of feasible flow conditions (Rakopoulos, C. and Giakoumis, E., 2009) . This has led to some authors suggesting a stronger role of parallel turbocharging for the gasoline engine which uses lower boost pressures, since the ability to cope with large variations in air flow rate is more crucial in this case (Lee, B., 2009).

However, this potential advantage in the range of flow rates depends on the properties of the turbo-machinery. In the parallel setup, both compressors must provide the full pressure ratio. When the flow rate narrows towards the upper regions of the compressor map, a parallel turbocharging architecture is unlikely to offer benefit in terms of flow rate capacity.

2.3.2 Series Arrangement

In series turbocharging, the intake and exhaust air flows through several turbocharger units in turn. Typically, a larger, low pressure (LP) turbine utilises the exhaust energy of the gas leaving the smaller, high pressure (HP) turbine while the smaller HP compressor further compress the air passed on from the LP stage compressor. The air is thus compressed in two stages; achieving high boost pressures and thus high brake mean effective pressure (BMEP) (Watson, N. and Janota, M., 1982). The basic setup of series turbocharging is depicted in Figure 2.3.

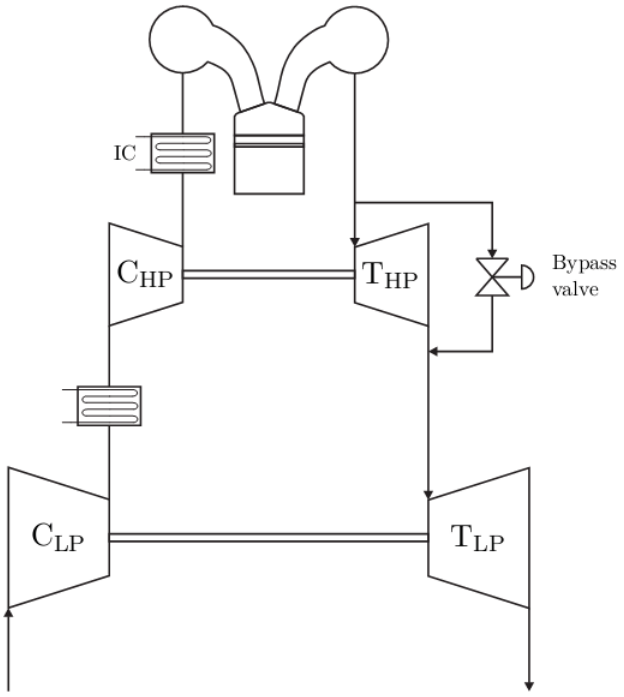

Figure 2.3 two stage turbocharging with high pressure bypass. A low pressure compressor and turbine (C_{LP} and T_{LP}) are combined with high pressure units (C_{HP} and T_{HP}) and intercoolers (IC).

The most distinctive feature of series turbocharging is arguably its ability to achieve very high boost pressures whilst also enabling manageable pressure ratios across the individual turbomachinery units, thereby maintaining high efficiencies (Lee, B. et al, 2009). Due to these advantages, unregulated (that is, without the high pressure turbine bypass valve depicted in Figure 2.3) two stage series turbocharging have already been used on a variety of marine and commercial diesel engines since the late 1970s (Watson, N. and Janota, M., 1982).

However, this unregulated form of two stage turbocharging is not well suited to modern, high speed diesel engines. Firstly, the main benefit for the marine applications is the high boost pressure achievable, whereas on modern automotive diesel engines, the transient response, fuel consumption and emissions production are also crucial factors. Secondly, major changes need to be made on the two-stage turbocharging structure so that it can be adapted to

automotive engines. For instance, the optimal turbine area (and thus machine size) relationship between the HP and LP turbochargers was originally found to be 1:2 so that the compression work was shared equally between stages, achieving high efficiency (Watson, N. and Janota, M., 1982). While this is often true for marine and commercial diesel engines running under a limited range of speeds and loads, on a high speed diesel engine, the much wider speed and load range renders this ratio less desirable. Frequently, a smaller HP compressor is preferred so that boost pressure can be built up quickly at low speeds while the bigger LP compressor allows a high overall boost rating. The 1:2 size ratio would thus not provide optimal sizing of the stages.

Same as in the parallel turbocharging, the phasing in and out of the sequential operation of the different turbocharger units is an important aspect of series turbocharging. As the air flow rate increases, the capacity of the smaller turbocharger unit will be approached and the flow will consequently become choked. Therefore, in order to avoid excessive back pressures and overspeed of the turbocharger shaft, the high pressure unit is normally bypassed at high flow rates (Lee, B. et al, 2009; Pflüger, F., 1998). Nevertheless, switching between the turbochargers can be problematic: phasing in of the second unit may result in high engine back pressure resulting from the two-stage expansion (Moulin, P. et al, 2008).

One of the main benefits of series turbocharging is its ability to improve fuel economy by running in more efficient regions of the turbocharger units' operating spaces. This has been confirmed experimentally; for instance, Researchers in Valencia (Galindo, J. et al, 2010) compared the brake thermal efficiencies of a series turbocharged engine with a conventional, single stage turbocharger set-up. The multi-stage turbocharged engine demonstrated better thermal efficiency, particularly at high boost pressures which were difficult to attain with only a single turbocharger. Engineers in Hyundai (Choi, C. et al, 2006) compared two stage series turbocharging with a VGT-controlled turbocharging set-up. Using the two stage series

arrangement allowed a faster transient response at 1000 and 2000 rpm, and also greater low speed torques than the VGT. Following engine optimisation, the brake specific fuel consumption was reduced for the same level of NOx for the two stage arrangement as for the VGT.

The use of several turbochargers in series also has benefits in terms of power and transient performance. Borg Warner engineers (Schmitt, F. et al, 2004) conducted a study on the Borg Warner Regulated Two Stage (R2S) system, with the test results showing significant improvements in starting torque and rated power over a variable geometry turbine (VGT) system, as well as enhancements in the transient response.

It has been demonstrated that series turbocharging can also help to reduce NOx emissions. In a simulation study, Nitta (Nitta, J. et al, 2011) used a one dimensional modelling approach to compare the boost pressures and EGR rates feasible at various levels of excess air ratios using single, two-stage and three-stage series turbocharging. It was demonstrated that the multi-stage approach allowed higher boost pressures and greater proportions of EGR at a given quantity of excess air, thus reducing NOx and maintaining soot emissions within acceptable limits. The high EGR at full load is therefore an important route to meeting EURO5 emission standards (Pflüger, F., 1998; Schmitt, F. et al, 2004).

Watel (Watel, E. et al, 2010) focused on using series turbocharging technology in order to reduce NOx emissions. Simulation points were chosen according to the New European Drive Cycle, and the turbo-matching was performed solely with emissions reduction in mind. Consequently, the system behaviour was markedly different from other work: a larger than normal HP turbine was chosen to reduce back pressure, and a low specific power was selected, rendering a relatively slow transient response. Nevertheless, a faster torque response was achieved by the series turbocharging than by the single stage VGT scheme. Furthermore, a

higher torque was maintained at low speed by the series turbocharging scheme compared to the single stage turbocharger with a VGT.

Millo (Millo, F. et al, 2005) combined early intake valve closing (EIVC) technology with series turbocharging. A model was developed and validated with experimental data: the results demonstrated significant engine up-rating and NOx emissions reduction. The BSFC was found to be 2% lower with the peak cylinder pressure also being well controlled right below 160 bar, especially considering the high BMEP of 25 bar.

2.4 Modelling Approaches

Various modelling techniques have been employed as part of control design and validation approaches for series and parallel turbocharging. In common with many other control engineering applications, there is a trade-off between the accuracy and fidelity of any given model, its computational demands and ease of calibration (Canova, M. et al, 2009).

Quasi-linear models use steady-state operating points to represent the engine and turbocharger behaviour, neglecting, for example, capacitance effects due to accumulation volumes (Rakopoulos, C. and Giakoumis, E., 2006; Rakopoulos, C. et al, 2007). The main advantage of this type of model is its simplicity, and it can thus be solved rapidly. This notwithstanding, these models often require a large quantity of data for parameter tuning, and the interpolation and extrapolation techniques used to find the response of the engine between or outside the available data points can be unreliable.

Mean value models can represent both steady state and transient engine behaviour using averaged values and maps for the compressors and turbines over many revolutions; engine characteristics such as the volumetric efficiency can be included (Karmiggelt, R., 1998). The

time scale is typically of the order of between three to five revolutions (Jensen, J. et al, 1991). Due to their relatively low complexity, short solution time and ability to simulate important transient phenomena, mean value models have been extensively applied to modelling and control of turbocharging. However, the quality of the model often depends on the quality of the maps, which can be poorly discretized and may not cover a wide enough flow area (Martin, G. et al, 2009).

Canova et al (Canova, M. et al, 2010) used a mean value approach to model a two-stage turbocharged diesel engine and validated the model with experimental data. Using the model, the influence of the variable geometry turbine and bypass valves on the response could be investigated, with the results highlighting problems relating to the use of the VGT to regulate the boost pressure while the bypass valve of the high pressure turbine is open.

Zero order models utilise a chain of control volumes linked by valves and orifices, applying the 'filling and emptying' approach to represent the capacitance of the induction and exhaust systems by means of control volumes (Rakopoulos, C. et al, 2007; Chevalier, A. et al, 2000). It is a common modelling approach which can represent some elements of the transient response. Details such as loss mechanisms and heat transfer effects have to be taken into account, while the parameters needed to describe the geometric and material properties are usually minimal. Therefore, the model can be applied to different turbochargers without a great deal of individual adaptation if the lower predictive accuracy can be tolerated (Nakhjiri, M. et al, 2011).

Yang and Zhu (Yang, X. and Zhu, G., 2010) employed a zero order, filling and emptying approach to modelling a dual-stage spark ignition turbocharger set-up, and validated the model using more complex one dimensional (1D) code (described in subsequent paragraphs). The model was to be used in a hardware-in-the-loop structure for control development. Good

agreement between the two modelling approaches was demonstrated for steady state conditions, though the transient behaviour of the model was not validated. Plianos and Stobart used a zero dimensional approach to modelling a two-stage, series turbocharger for a diesel engine (Plianos, A. and Stobart, R., 2008). This modelling basis was subsequently utilised to derive local, linear transfer functions in order to develop a series of Linear Quadratic Gaussian (LQG) controllers for the various operating points of the engine.

On the other hand, first order models utilise a one-dimensional (1D) approximation of the Navier-Stokes equations, and are derived by transforming the partial differential equations into ordinary differential equations using a mesh; finite difference methods are then used for solution (Chevalier, A. et al, 2000; Vitek, O. et al, 2006). One of the main advantages of 1D models over their zero order counterparts is that the 1D structures can incorporate wave effects, which consist of disturbances in pressure (e.g. due to a rapid opening of the throttle plate) that travel along the induction pipes at the speed of sound and interact with other such waves (Chevalier, A. et al, 2000). Though they are more computationally intensive, 1D models have been used in various control-centred applications including simulation (Nitta, J. et al, 2011) validation of control strategies (Galindo, J. et al, 2010; Millo, F. et al, 2005), turbocharger design (Galindo, J. et al, 2007), optimisation (Kech, J. and Klotz, H., 2002) and engine calibration (Almeida, F. et al, 2010). Saulnier and Guilain (Saulnier, S. and Guilain, S., 2004) used 1D code to investigate the transient and steady state performances of combinations of various compressor and turbine units in a two stage series turbocharging set-up.

One dimensional models have the accuracy capability to investigate transient details such as the surge in turbocharger compressors. In a study by the Valencia group (Galindo, J. et al, 2009), a 1D wave action model was constructed to predict the surge development under pulsating flow. The model corroborated experimental results highlighting that surge margins can be improved through pressure pulsations (which are normally induced by the sequential

operations of the engine cylinders) close in frequency to the surge frequency; this would then increase the range of possible operating conditions for turbocharging. A 1D model developed by Winkler and Ångström (Winkler, N. and Ångström, H., 2008) was used to simulate the transient performance of a two-stage turbocharging system. It was necessary to adjust the turbine maps in order to achieve a match between the simulated and measured results, partially due to uncertainty regarding the behaviour at low speeds. Though good agreement was achieved between the measured and simulated results for pressure, the simulated gas temperatures showed different behaviour to the measured cases due to mass-averaged temperatures being used in the model. Almeida (Almeida, F. et al, 2010) used 1D modelling for a dual-stage turbocharger, achieving close agreement between modelled and measured results for brake mean effective pressure, fuel consumption and turbocharger speed.

Three-dimensional (3D) models include computational fluid dynamics-based simulation and can incorporate more complex flow effects such as turbulence. They have been used to study in-cylinder processes including fuel injection, spray and mixing (Chen, M. et al, 2011), unsteady flow in turbocharger compressors (Dickmann, H. et al, 2006), and frictional losses in turbocharger bearings (Deligant, M. et al, 2011). Moreover, 3D computational fluid dynamics code representing in-cylinder processes and flow through the turbomachinery has also been integrated into an engine model, mostly based on 1D modelling (Chen, T. et al, 2008). Though this type of model can provide insights into the underlying physical processes and also provide a wider range of physical effects, its application in control design and implementation can be limited due to the far greater complexity and much longer solution time.

As an alternative to the approaches discussed above, analytical models can offer detailed insights into the underlying physical processes. Galindo (Galindo, J. et al, 2010) developed an analytical model of a two-stage turbocharging system in order to investigate coupling effects

between the engine and the turbochargers, and thereby evaluate the influence of various parameters on the performance of the overall system. The model also demonstrated the ability of the two-stage turbocharging architecture in increasing efficiency over single-stage turbocharging.

The individual components of the turbocharged engine have been modelled in standard ways throughout much of turbocharging research and development. The behaviour of the compressors and turbines is normally approached using assigned efficiencies via maps, usually obtained experimentally. The dynamics of the turbocharger unit itself are modelled using Newton's second law based on the torque balance of the turbocharger, with individual torques arising from the turbine, compressor and friction. This is combined with the moment of inertia to determine the acceleration of the turbocharger shaft. The mass flow rate of air into the engine is often based on the volumetric efficiency, which is, in turn, determined from an empirical function with arguments of engine speed and intake manifold pressure. Intercoolers are normally modelled as basic heat exchangers, assuming negligible pressure drops (Guzzella, L. and Amstutz, A., 1998), or using an empirical model for the latter. Furthermore, the effectiveness is determined from empirical relationships depending on the type of heat exchanger (e.g. cross-flow, single pass) (Gambarotta, A. et al, 2009). To model flow through orifices and valves - e.g. the EGR valve or inlet throttle - a common approach is to approximate the approach as an isenthalpic or isentropic process (Guzzella, L. and Amstutz, A., 1998).

2.5 Control Strategies

The control design and implementation are a challenging, yet crucial aspect of using two or more turbochargers for boosting: control underpins the efficient, stable operation of the turbocharged engines. In general, turbocharger controllers seek to operate in regions of high

efficiency whilst also avoiding over-speed and choked flow regions of the turbomachinery (Chasse, A. et al, 2008). The majority of turbocharger control research has, thus far, been conducted on single stage turbochargers; consequently, the majority of the literature discussed in this section is focused on that application. However, the results and outcomes of this research are highly relevant to the series and parallel turbocharging cases as they represent effective approaches to dealing with the inherent challenges of turbocharging, discussed in the sections below.

The variables to be controlled in turbocharging are typically the boost pressure (Schwazmann, D. et al, 2006; Kotman, P. et al, 2010; Colin, G. et al, 2007), back pressure, inter-turbine pressure (Schwazmann, D. et al, 2006), and EGR rate (Kotman, P. et al, 2010). Alternatively, some controllers have regulated the air-fuel ratio, power ratio between the turbines and the burnt gas fraction (Plianos, A. and Stobart, R., 2008; Rajamani, R., 2005). The available control inputs (the variables manipulated by the controller to drive the output variables to the desired values) are normally the effective areas of waste-gates, bypass valves, the EGR valve and VGT openings. Some of the variables to be regulated are not directly measurable, and therefore, alternatives such as the pressure in the intake manifold and mass flow through the compressor have often been used instead to reflect variables such as the air fuel ratio and exhaust gas fraction (Stefanopoulou, A. et al, 2000). Observers such as Kalman filters based on the model structures outlined in the previous section are thus common features of turbocharger controllers.

The control difficulty of multi-turbocharging boosting arises from several sources: the underlying dynamics are complex and nonlinear, and furthermore, there are interactions between the different subsystems (Plianos, A. and Stobart, R., 2008; Chasse, A. et al, 2008). Conventionally, ECUs use individual single input single output (SISO) loops in order to control different variables such as intake manifold pressure and the flow rate of fresh air (Ferreau, H.

et al, 2007). Conversely, multiple-input-multiple-output (MIMO) control allows internal dynamic coupling between the controlled variables to be included (Ferreau, H. et al, 2007; Ortner, P. and Del Re, L., 2007). Using two or more turbochargers in a parallel or series arrangement introduces an additional layer of complexity for regulation in that transitions between the different compressors and turbines must also be controlled. In addition to coping with the highly nonlinear nature of the underlying dynamics, the controller must be sufficiently robust in order to deal with uncertainties arising from errors in the turbomachinery maps, fluctuations in ambient conditions and cyclic variations of the engine (Chevalier, A. et al, 2000; Jankovic, M. and Kolmanovsky, I., 2000).

The inherent nonlinearity has been approached using a variety of techniques. These have included the conventional use of linear models representing the system's local behaviour at different operating points, feedback linearization, and other nonlinear control methods such as sliding mode control.

Stefanopoulou (Stefanopoulou, A. et al, 2000) used a nonlinear engine model to calculate appropriate setpoints for the measured outputs of compressor flow rate and intake manifold pressure, based on desired values of the air-fuel ratio and burned mass fraction. A set of linear controllers was used to control the EGR valve and VGT positions. Though good tracking of the reference outputs was achieved, the actuators showed redundancy: they could not manipulate the output variables independently. Malkhede (Malkhede, D. et al, 2005) used a Taylor series approach to develop linear models from a more complex, nonlinear engine model in order to cover the operating range of the engine. A reduced order version of the set of differential equations was then used to synthesise a proportional-integral (PI) controller for engine speed control using pole placement. The transient performance was enhanced through anti-windup implementation which handles situations of actuator saturation. Plianos and Stobart (Plianos, A. and Stobart, R., 2008) aimed to drive the air-fuel ratio, power ratio between the two

turbines in a two stage boosting system, and also to drive the EGR rate to setpoints determined via maps for maximum fuel economy under emissions constraints. A system identification approach was used to generate linear models in different regions of the torque-speed space, enabling a linear quadratic regulator to be synthesised. The system showed a satisfactory transient response, though the control regime had a tendency to give rise to saturated control inputs.

Jung and Glover (Jung, M. and Glover, K., 2006) used a linear parameter varying (LPV) modelling approach to apply a gain-scheduled H_∞ loopshaping methodology for control design. This approach is frequently used to ensure robustness against a wide range of modelling uncertainties. In order to make the optimisation problem feasible, the parameter space was discretised as a grid, allowing optimal control parameters to be calculated offline. The manifold pressure and air mass flow rate were effectively tracked by the controller across the range of operating conditions covered by the NEDC. The effect on emissions of the novel controller was not investigated, however. Däubler (Däubler, L. et al, 2007) also used an LPV approach, deriving linear models representing the system's behaviour at different operating points via a gradient method. The model structure allowed the PI parameters to be adapted online.

Feedback linearization is a further method used to address the inherent nonlinearity of the plant. In this approach, a linearised version of the highly non-linear dynamics is produced via feedback and variable transformation (Charlet, B. et al, 1989). In the turbocharging application, feedback linearisation has often been applied to a simplified model of the dynamics, formulated, for example, using the singular perturbation method (Moulin, P. et al, 2008; Moulin, P. and Chauvin, J., 2011). Rajamani (Rajamani, R., 2005) used a feedback linearisation approach to control the level of burned gas and the air-fuel ratio of a turbocharged, waste-

gated engine. Due to the large number of terms yielded through differentiation of the outputs, a hierarchal structure consisting of an upper and a lower controller was used. An estimator was used to determine the states of the model based on pressure and flow rate estimates. Moulin and Chauvin (Moulin, P. and Chauvin, J., 2011) applied feedback linearisation to a simplified engine model developed previously (Moulin, P. et al, 2008). Anti-windup was incorporated to address potential saturation of the actuators. The system was tested at various speed and load conditions and performed satisfactorily over the operating range of the system using only one set of control parameters. Jancovic and Kolmanovsky (Jankovic, M. and Kolmanovsky, I., 2000) used a constructive Lyapanov function derived via feedback linearisation to control the air-fuel ratio and exhaust gas fraction. By using a domination redesign (Sepulchre, R. et al, 1997), the control design did not rely on exact cancellations in the system's dynamics which may not be feasible or desirable in practice. Furthermore, the control approach ensures robustness against unmodelled dynamics and parametric uncertainties. The system behaved satisfactorily in simulation and engine testing, though large under- and overshoots where observed in the latter.

In addition to feedback linearisation and linearised local models, various other approaches have been utilised in order to cope with the underlying nonlinearity in the dynamics. For instance, Kotman (Kotman, P. et al, 2010) derived a simplified plant model to design a feed-forward controller based on the flatness property (Murray, R. et al, 1995) (analogous to the controllability property of linear systems) of the dynamics.

Furthermore, various established methods are available for ensuring robustness against uncertainties in the model of the dynamics. For example, sliding mode control has been applied to control of turbocharged engines in various forms. Sliding mode control involves the definition of a sliding surface along which the system is forced to move along (Slotine, J. and Li, W., 1999), and can provide robustness against unmodelled dynamics and parametric

uncertainties (Utkin, V. et al, 1991). Sliding mode control was used by Ouenou-Gamo et al (Ouenou-Gamo, S. et al, 1997) in order to drive compressor power to reference values closely with acceptable chatter, a common disadvantage of some realisations of sliding mode control (Slotin, J. and Li, W., 1999). Moreover, Utkin (Utkin, V. et al, 1991) used sliding model control to drive the air-fuel ratio and EGR fraction to reference levels. A reduced order model with an isothermal assumption concerning the intake and exhaust manifolds was used to synthesise the controller. Wang (Wang, J., 2008) applied a sliding mode scheme in order to control a turbocharged engine in two different combustion models, employing a finite-state machine-based supervisory controller to control switching between modes. To avoid chattering, a continuous approximation of the control law was applied around the surface, while using integral action helped to reduce oscillations about the sliding surface. The nonlinear approach demonstrated much better performance in transient response than the conventional control approach based on steady state engine calibration.

The various model structures described in the preceding section can also be used for control schemes based on optimisation. Model predictive control (MPC) calculates control inputs such that a cost function in those inputs and a forecast of the system's behaviour is minimised. Colin et al (Colin, G. et al, 2007) applied linearisation to a non-linear artificial neural network model of a single stage turbocharged engine in order to utilise a model predictive control regime. The latter minimised a cost function based on a desired output and the control inputs. The linearised variant performed almost identically with an exact neural predictive control in simulation, but was far less computationally demanding, and furthermore, performed well during engine tests. Ortner and Del Rey (Ortner, P. and Del Rey, L., 2007) used MPC to regulate pressures and flow rates in a turbocharged engine. The dynamics were represented using a set of linear models across the operating space of fuel injection rate and engine speed. Better

performance in tracking was achieved using the MPC, though this was achieved at the cost of greater NOx output.

2.6 Further improvements

Until now, it has been established in this review that a commercially viable multi-turbo charging system on a high speed Diesel engine should comprise of two differently sized turbochargers; connected in series, while regulated by at least one turbine bypass valve at the high pressure stage. In most cases, a high pressure stage compressor bypass valve is a must to isolate the smaller high pressure turbocharger at high air flow operations. Such a system has been used in several applications in the market (Carscoop, 2007). However, such a system has the weakness of not always being able to generate enough EGR gas at low engine speeds. Therefore, several systems with VGT technologies on the high pressure stage turbine have been seen in the market (Steinparzer, F., 2007; Bauder, R., 2011). Such systems showed great improvement in terms of engine power rating, transient response and emission control. The Audi engine was able to produce 650 Nm from a 3L engine displacement (27 bar BMEP), which was the highest available in the market at the time (Bauder, R., 2011). The upgrade of the BMW engine with a VTG equipped high pressure turbine has bring a large area of the low speed and torque region on the engine map into the regulated area. The high pressure turbocharger can also cover a wider engine map with a high level of efficiency, boost pressure is thusly increased, which leads to higher torque at low engine speed (Steinparzer, F., 2007).

Due to the synergy between technology advancement and emission regulations, other technologies such as ball bearing turbocharger technology will become commercially affordable on a multi-turbosystem. One such application has been experimented on a large commercial vehicle engine. The test results showed the expected improvement in transient

response, fuel consumption, emission control and warranty cost (Griffith, R. et al, 2007). The solution on a smaller passenger car engine will have the similar potential to further improve the transient response and cold start performance of the two stage charging system without changing the aerodynamic design; in the meantime, the high engine back pressure weakness of the high pressure turbocharger is expected to be alleviated.

2.7 Summary

The use of two or more turbochargers in series and parallel arrangements has a number of advantages over the single stage turbocharging, including an increased range of feasible flow rates, enhanced boost pressure and augmented efficiency of operation. The increased boost can also allow operation of exhaust gas recirculation at high loads. These properties make series and parallel turbocharging important routes to meeting future emissions and fuel economy limits via engine downsizing.

Higher boost pressures can be reached by using a series turbocharging setup than its parallel counterpart. A series architecture would thus be most appropriate for systems requiring more extreme levels of boost. Nevertheless, the potentially wider range of flow rates offered by the parallel turbocharging setup could make this form more appropriate for turbocharging the gasoline engine which is usually mildly boosted.

Control of turbocharging in commercial vehicles has thus far relied on the application of individual single input, single output control loops derived via linearisation and system identification, addressing the regulation of different engine variables separately and neglecting important coupling between the different variables. Though more complex, multivariable, nonlinear and robust control approaches take the important underlying nonlinearity and

coupling into account and have consequently demonstrated significant improvements in performance and robustness for single stage turbocharging, and, with some modification, represent effective approaches for series and parallel turbocharging applications.

Finally, the variable geometry turbine and the ball bearing turbo-shaft can be useful addition to the two stage charging system and are areas worth research into.

The content of this chapter was published in:

Zhang, Q., Pennycott, A., Brace, C., 2012. A Review of Parallel and Series Turbocharging for the Diesel Engine. In: Proceedings of the Institution of Mechanical Engineers, Part D: Journal of Automobile Engineering, 227(12), pp1723-1733.

Chapter 3 - Test facilities and baseline engine test results

The experimental work of this study benefited from a highly instrumented engine test cell (internally coded 'Cell3') with full transient capability at the Powertrain and Vehicle Research Centre (PVRC) at the University of Bath. The building of hardware was supported by three experienced technicians and the engine calibration side was adequately supported by the industrial partners.

This chapter first described the experimental environment in which the research was undertaken, including details about the test cell, instrumentation, data capture and the rapid prototyping control system used for controlling prototype turbochargers. The reason behind the choice of each system was explained.

The test engine specification and the test plans were also explained in this chapter. With the baseline VGT turbocharger, the engine has been thoroughly tested as the first phase of the project. The test results are useful for understanding the working characteristics of the baseline engine equipped with the variable geometry turbine. The data generated in this phase of work was later used for calibration of the baseline 1-D engine model, so that the subsequent experimental research can be validated analytically and that the exploratory simulation is based on a relatively accurate model with sufficient predictive capability.

3.1 Test cell environment

The building of the test cell host system was outsourced to *Sierra Instruments* (formerly *CP Engineering*). The CADET Automation System (V14) software was used for the general test cell management, including ambient control and ventilation, water system, dynamometer control, gravimetric fuel consumption meter, communication with engine calibration software and fast data capture system and most importantly, data logging.

3.1.1 Ambient control and ventilation

The adequate ambient control and ventilation of an engine test cell feeds the engine with properly conditioned fresh air to ensure the quality and repeatability of the test data. The test cell at PVRC was ventilated by a variable speed fan driven by a 7.5kW 4-pole motor (ABB variable speed drive) provided by *Alfa Fans Ltd*. The routing of air flow is illustrated in Figure 3.1. The ventilation full capability was excessive for a 2.2L Diesel engine and therefore was constantly set at 25% level during the tests which ensures that the temperature was stably controlled and that the noise level from the fan was acceptable.

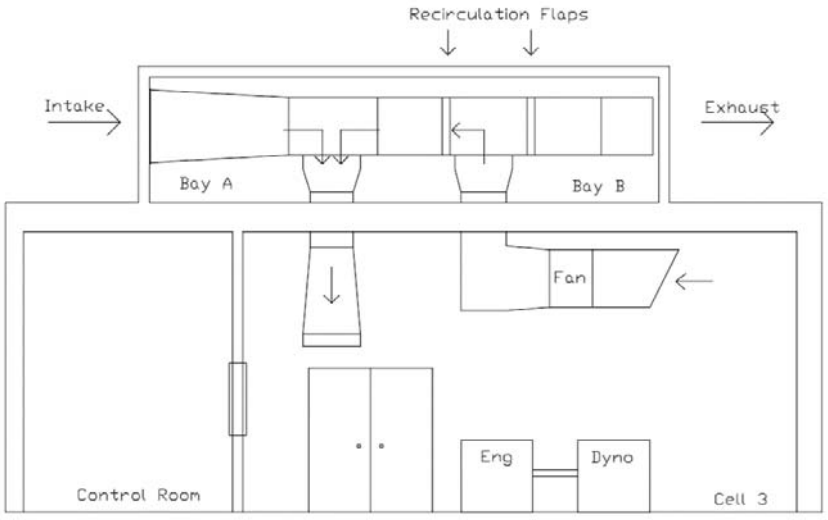

Figure 3.1 routing of the air flow in the test cell

The test cell temperature was controlled by heating and cooling the air into the test cell to match a target temperature. The heating was achieved by CADET system controlling the on and off of the heating cables inside Bay A. Similarly the cooling was achieved by controlling the flow of coolant through the coolant pipes. The coolant is supplied by a water chiller unit (TAEevo 251) provided by *MTA*. During a British summer day, the system is capable of cooling the test cell down to 7 °C. For the cold start tests, the test cell was thermal soaked overnight to 15 °C before the morning test. For the hot engine tests, the test cell is controlled stably at 25 °C. The choice of this temperature was to align with historical test data so that system fault-finding was easy to perform if needed.

3.1.2 Water system

Cooling water was needed to cool down the dynamometer, engine heat exchanger and the intercooler. The cooling water for the test cell was supplied by a water pump (Calpeda Ltd) driven by a 15 kW 2-pole motor (WEG). The water is pumped in from a water reservoir exposed to the outside ambient environment with a large enough capacity and fed into the dynamometer cooling circuit, engine heat exchanger circuit and the intercooler circuit. Strictly speaking, the cooling water from outside environment is of different temperature depending on the weather (usually within 10 °C temperature difference in Southwest England during late January to May 2014). However, since the water flow was always more than enough to cool down the dynamometer and the engine heat exchanger, the influence of the outside ambient temperature has on the test bench operation is kept to a minimum. On the other hand, the in-house made intercooler was using the same source of cooling water and the difference in cooling water temperature can have an impact on the engine gas exchange, especially at a high engine load condition. To solve this problem, the cooling water flow was controlled by a flap valve to match a set post intercooler gas temperature (45 °C). The water supply schematics is shown in Figure 3.2.

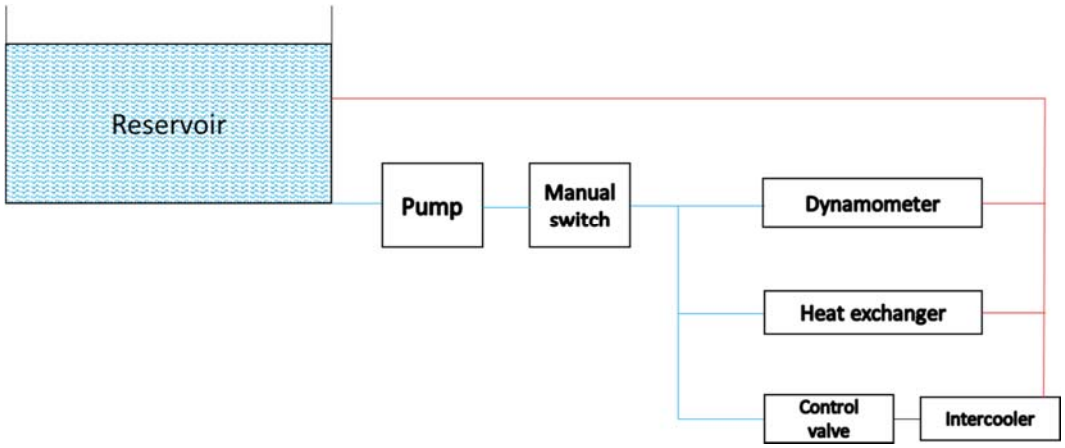

Figure 3.2 cooling water system schematics

3.1.3 Dynamometer

The dynamometer was used as an electric brake applied on the engine crankshaft. The dynamometer used in the project was a David McClure 215kW transient AC dynamometer. It can be operated to control either the speed or the torque of the engine and allow the engine to achieve the other parameter depending on the pedal signal. In the context of this project, the speed control mode was always used and the engine power is absorbed by the dynamometer while maintaining a constant speed. The engine can be controlled by either a pedal position demand in percentage or a requested engine torque governed by a calibrated PID controller.

3.1.4 Gravimetric fuel meter

The gravimetric fuel meter is an essential device for acquiring the accurate fuel consumption of the engine on the test bench. The fuel flow meter was supplied by *Sierra Instruments* (formerly *CP Engineering*). The system automatically refills and measures the consumption of fuel in grams with an accuracy level of 0.5%. The fluid level cycle was controlled between 200 and 1400 grams. It takes around 20 second to refill the beaker from 200 grams to 1400 grams

to allow stable measurement of fuel mass. The reduction of the fuel mass was measured to calculate the average fuel consumption. Due to the capacity of the fuel beaker, the beaker was also programmed to be refilled before recording each test point to avoid the refill from happening during a recording period.

3.2 Instrumentation

3.2.1 Temperature measurement

The K-type thermocouples were used for the temperature measurement. The wide operative range (from -200 to up to 1250 °C) and the robustness of reading were the main reasons for the use in this project. However, the thermocouples with heat resistive cables were not always readily available and the PVC coated cables on the engine exhaust side frequently melted and shorted the wire inside. In this project before each test the temperature readings were checked for credibility. Faulty or disconnected thermocouples would exhibit a constant maximum value, while partly shorted thermocouples (usually due to cable insulation melting) give unstable random readings. It is advisable, therefore, to choose more of the heat resistive thermocouples in future work to improve test efficiency and to avoid having test points with wrong temperature reading. The different types of thermocouples is shown as in the Figure 3.3, with the standard PVC sheath resistive to maximum 105 °C, the PFA sheath to 250 °C, while the Fibreglass sheath to at least 480 °C.

Figure 3.3 K type thermocouples with various sheaths (*TC Direct*)

3.2.2 Pressure measurement

Pressure measurement using general purpose pressure transducers is a cost-effective approach to accurately acquire averaged engine gas exchange system pressure. Since the experimental work was conducted in an engine test cell which is being constantly updated, the pressure transducers used in the projects were from varied producers, including *GE Sensing*, *Druck*, *Gems* and *RS*. The operating ranges of the transducers were carefully selected according to the locations of the measurement and all the sensor were calibrated using a DPI-510 pressure calibrator (*Druck*) before each test setup. It is also advised to regularly clean the transducers used on the exhaust side for water and coke accumulation to ensure the reliable reading.

3.2.3 Fast pressure measurement

To accurately model the engine combustion process, it was necessary to measure the pressure inside the engine cylinder with crank angle resolution - preferably with the intake and exhaust manifold pressure, as well. However, during the experimental phase of the project, it was not always possible to gather all the required data because of issues such as broken sensors or alteration to loaned hardware was not allowed. Fortunately, the test engine was a production

engine which exhibited robust repeatability with various test setups. Therefore, it was considered sufficient to calibrate the combustion model using the test setup with the most complete dataset (the two stage turbocharging setup) and apply the combustion model to all the other test setups.

The cylinder pressure trace was acquired using a Kistler 6058A pressure transducer coupled with a made-to-order Kistler 6544Q glow plug adaptor and installed in the cylinder 1 of the engine. The sensors measure a range of 0 - 250 bar with a work temperature up to 350 °C. It should be noted that as the emergence of downsized engines, smaller glow plug hole will also become more popular. Care should be taken to choose suitable sets of transducers and glow plug adaptors of smaller sizes.

The pre-compressor and pre/post intercooler pressure trace was gathered using Kistler 4008 miniature pressure sensors. The sensors measure a range of 0 - 5 bar and can work in up to temperature of 200 °C.

The exhaust port and pre turbine inlet pressure trace was gathered for the production turbocharger setup using Kistler 4049A water cooled pressure transducers. The sensors measure a range of 0 - 5 bar and can survive temperature up to 1100 °C. During the two stage turbocharging system project, these transducers were not instrumented due to the limited accessibility of the integrated exhaust manifold.

3.2.4 Turbocharger speed measurement

The turbocharger speeds of turbochargers were measured by DZ135 eddy current sensors (*Micro-Epsilon*). The pre-amplifiers were used to condition signal across the heavily instrumented test cell with better quality. The measurement speed range was set at 400,000 rpm, and the analogue output of 0 – 10 V was used.

3.2.5 Emission analysers

The emission sample was analysed by a Horiba MEXA - 7000 analyser (internally coded MEXA1). Due to the long delay resulted from the gas transportation duct, only the steady state readings were analysed in this study. The analyser is capable to measure most of the emissions specified by the European legislation, i.e. CO HC NO_X and also CO_2, with the exception of particulates. The NOx, CO and HC index was measured in part per million (ppm), while the CO_2 was measured in percentage. The gas was sampled from both the pre-catalyst location and the inlet manifold where the EGR gas was mixed. Therefore the EGR rate can be crudely calculated by dividing the respective CO_2 percentage:

$$EGR\ rate = \frac{CO_2\%\ (intake\ manifold)}{CO_2\%\ (exhaust\ gas)}$$

3.2.6 Rapid Control system platform

A dSpace system was used to control different non-standard turbocharging systems. With strategies built into the control board, the system sent out control signals to the actuators in accord while monitoring the sensor signals, actuator feedbacks and ECU CAN signals. There are multiple boards available in the system but in this project the DS1006 processor board and the DS2211 HiL I/O board were used. The processor board was equipped with *AMD Opteron™* processor which provides the real-time calculation power and is the interface between the I/O board and the host PC.

The dSPACE system is located in the test cell on the exhaust side of the engine to shorten the wiring between the I/O board and the sensors and actuators. The host PC is located in the control room with Matlab/Simulink and the dSpace ControlDesk. The control model is conveniently coded in Simulink and complied and flashed onto the dSPACE ROM. The user

interface is designed and controlled using the dSPACE ControlDesk software. The rapid control system schematics is shown as follows.

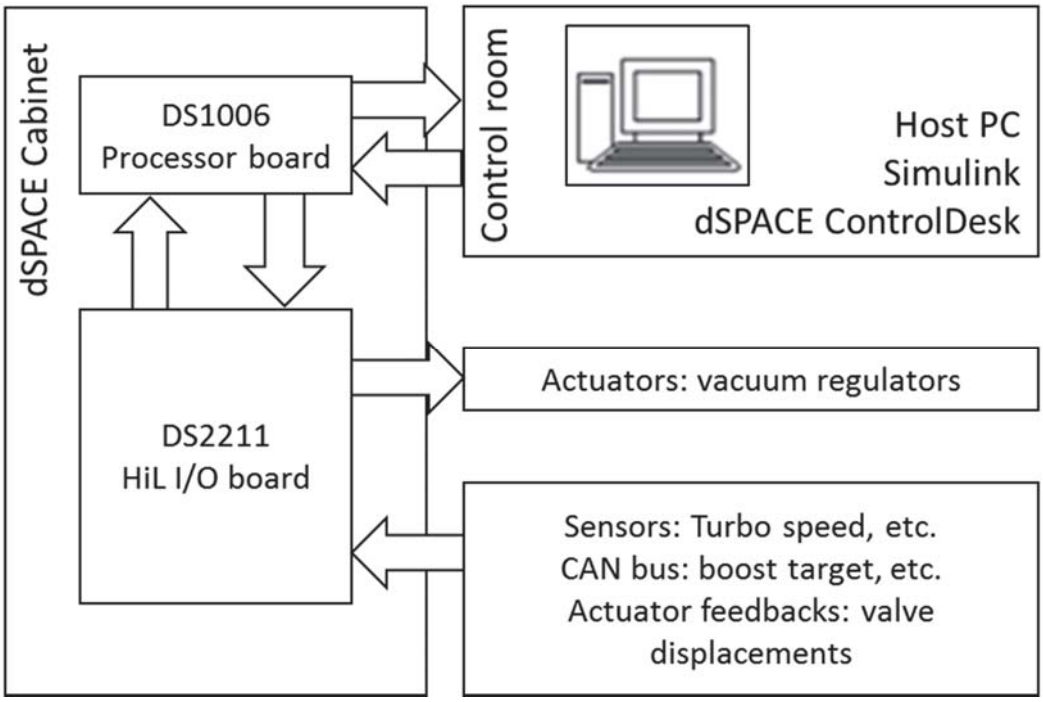

Figure 3.4 rapid prototype control system schematics

3.2.7 Communication with ECU

To monitor the engine operating status and to record the ECU data trace, the host system is reading from a PC with CAN tool via an ASAP3 connection. The CAN tool interrogates the ECU via a USB-to-CAN connection using the ATI Vision calibration software (Accurate Technologies Inc.). The complete signal communication routing is demonstrated in Figure 3.5.

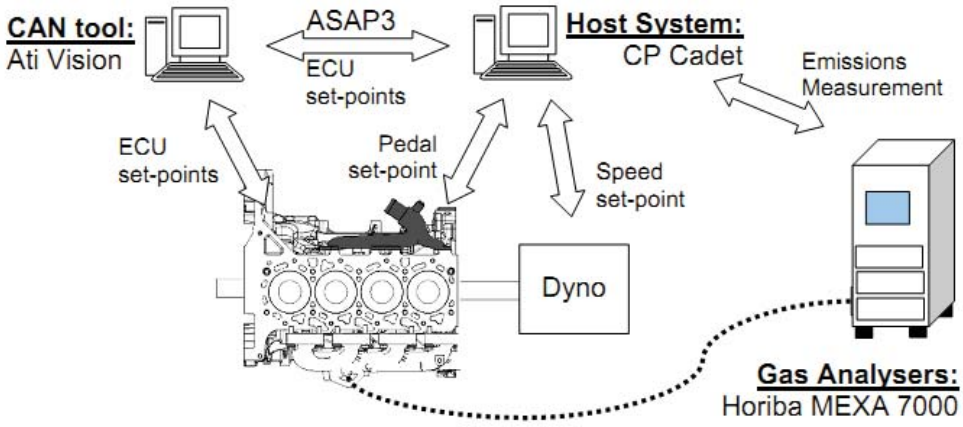

Figure 3.5 test cell signal communication schematics

3.2.8 Data logging

As soon as a test was started, the test data from various subsystems started to be stored automatically as a test trace file with a frequency of up to 10 Hz. For specific steady state test points and transient procedures, the chosen data channel is recorded following a trigger signal as a log files with specified averaging time and logging periods (1Hz) to facilitate data processing for each test.

As an upgrade to the test cell, a Dewetron data acquisition system was built up to record the fast signals coming from pressure transducers and turbospeed sensors. The host system triggers the recording of the Dewetron system by sending a step voltage signal through one of its digital output channels.

3.3 Test engine

The test engine used in the project was a 2.2 litre production Diesel engine (385Nm, 114kW) from Ford. It was intended to be equipped on larger passenger cars (by European standard) such as Mondeo, X-Type and light utility vehicles/trucks such as Transit, Defender, Ford Ranger and Mazda BT-50.

The standard engine was turbocharged by a turbocharger with a variable geometry turbine (VGT) manufactured by *Honeywell Turbo Technologies*. The Continental engine control system manages the engine and it is equipped with high pressure common rail fuel injection system (*Siemens*), with up to six injection events. As a EU5 engine, it used a hot EGR route with an EGR cooler. The after-treatment system, vacuum pump and the original intercooler were dismantled from the engine.

The detailed engine specifications is listed in the table below.

Table 3.1 Test Engine and Turbocharger Specifications

Engine Configuration	L4, Turbocharged, Intercooled
Displacement [L]	2.2
Bore [mm]	86
Stroke [mm]	94.6
Connecting Rod Length [mm]	155
Compression Ratio	15.5:1
Rated Power (kW)	114
Max Speed [rpm]	4900
Max Torque [Nm]	385
Max Cylinder Pressure [bar]	160
Max Turbocharger Speed [k rpm]	213
Max Pre-Turbine Temperature [°C]	830
Max. Compressor Outlet Temperature [°C]	180

3.4 Test plan

3.4.1 Limiting torque curve

In the limiting torque test, the engine accelerator pedal is given a 100% signal at a series of dyno speed conditions and the maximum torque numbers achieved are recorded as a curve dependent on the engine speed. Such a limiting torque curve marks the speed/torque envelope that the engine can achieve. On a Diesel engine, the injector will inject the maximum amount of fuel allowed by the engine control system, limited usually by physical limits such as the smoke, the maximum cylinder pressure and the turbocharger speed, etc.

In this project, the first set of limiting torque test results were compared with an engine manufacturer provided engine torque curve so that the test engine setup was validated. The various physical parameters of the test engine (e.g. temperature, pressure, rotational speed, etc.) were also confirmed to be within the safe limits, allowing the subsequent transient tests. Figure 3.6 below illustrates a typical engine limiting torque curve with the main actuator positions shown below.

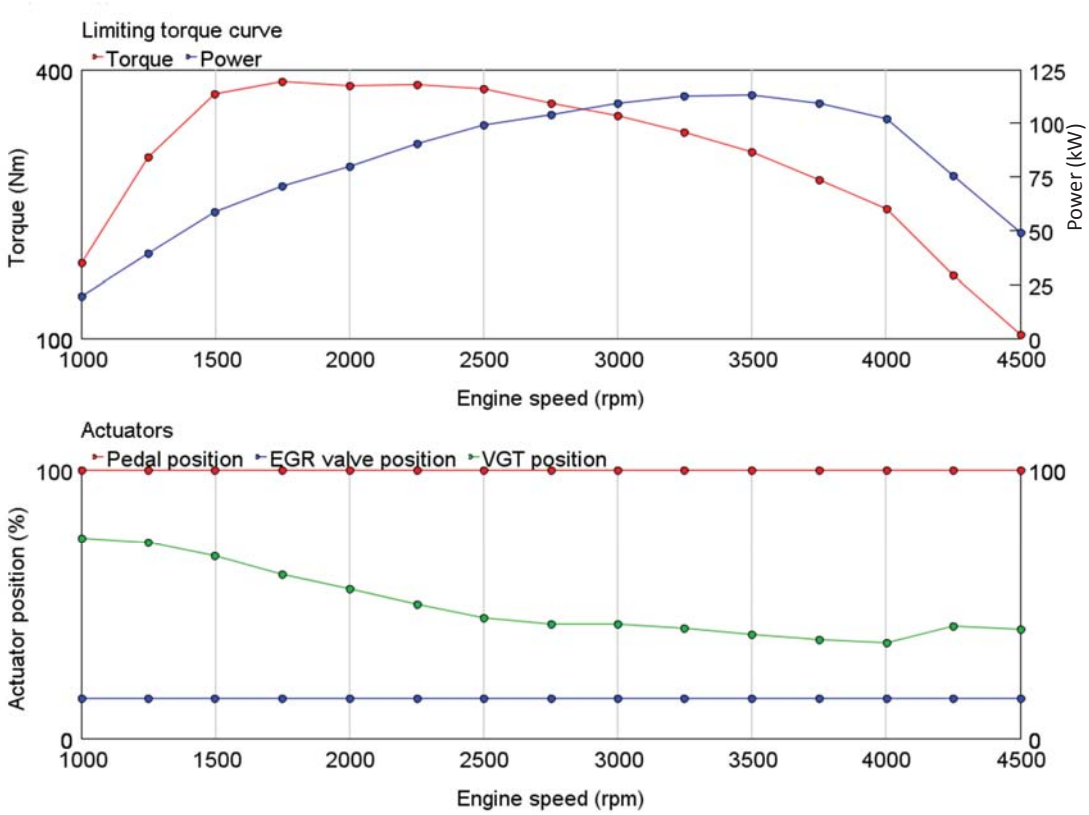

Figure 3.6 a typical limiting torque curve test result

The top graphs showed the behaviour of a typical turbocharged Diesel engine torque curve. At engine speed 1000 rpm and 1250 rpm, the engine torque was limited by the boost pressure due to the fact that the turbine cannot harness sufficient exhaust energy at such low mass flow conditions. Any extra mass of fuel injection would be cut-off by the control strategy to avoid an excessive amount of smoke. At speeds between 1500 and 2500 rpm, the engine exhibited a desirable torque plateau, such data points were usually limited by the structural limit of the engine cylinder, i.e. cylinder pressure limit. At speeds above 2500 rpm, the torque curve starts to decline due to the combined effect of increased engine back pressure, turbocharger protection, increased engine friction and heat transfer losses.

The lower graph in Figure 3.6 revealed the behaviours of the major actuators on the engine during the full load operation. The Pedal signal was held constantly at the maximum location

(thus full load), while the EGR valve was held constantly at a minimal value of 14% (soft limit in the ECU), indicating that no EGR gas was needed as the NOx emission was not a focal point at such conditions.

The behaviour of the VGT position can be better understood with the aid of the compressor map as shown in Figure 3.7 below. The limiting torque curve operating points were plotted on the map as black dotted lines. It was clear that the VGT vane position was being modulated to achieve a calibrated boost target. At speeds up to 1500 rpm, the decision of the boost target was made in according to the requirement to achieve a boost level as high as possible without getting into the surge region on the compressor side while on the turbine side without creating excessive backpressure to reduce the torque. From 1500 rpm to 3250 rpm, the VGT was modulated to provide adequate boost pressure levels while keeping the compressor in the high efficiency region. At high engine speed from 3250 rpm, the calibrated boost target aims to avoid over-speeding the turbocharger and also keeping the efficiency high.

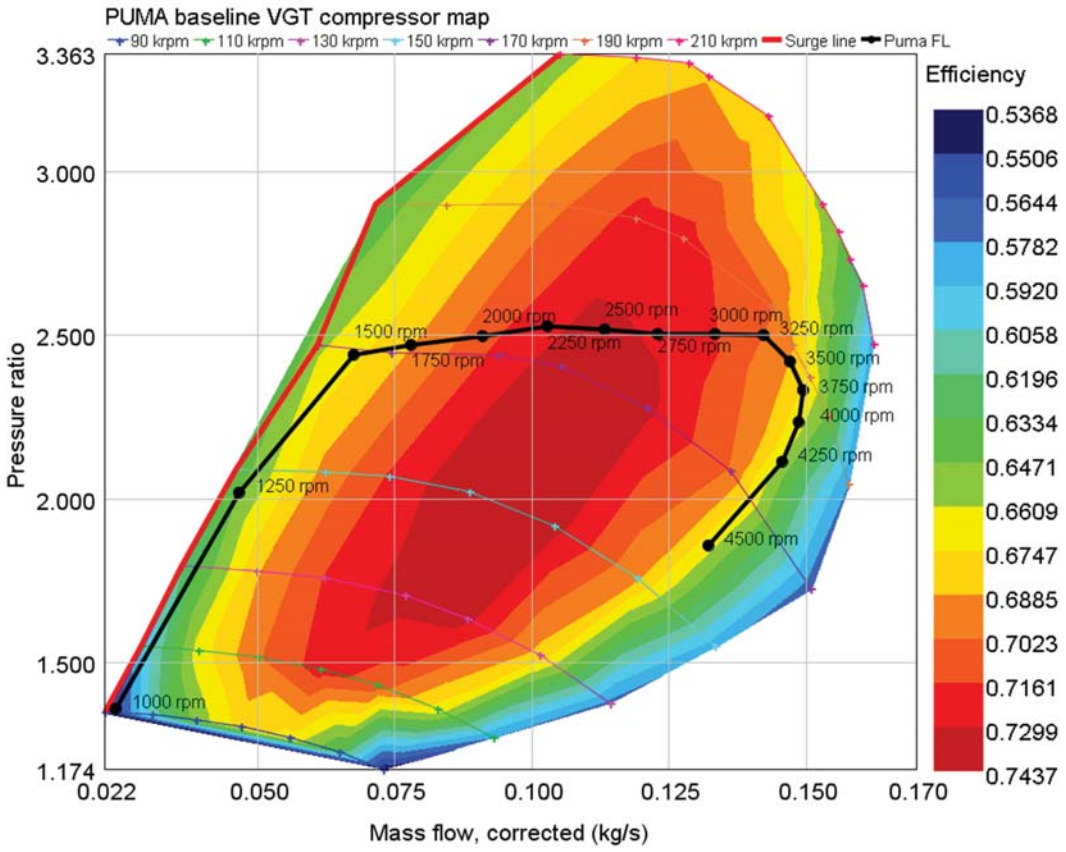

Figure 3.7 limiting torque conditions on the compressor map

Using the test result, the isentropic efficiency of the compressor can be deducted by the following equations:

$$\eta_{tot} = \frac{T_1 \times (PR_{tot}^{\left(\frac{\gamma-1}{\gamma}\right)} - 1)}{T_2 - T_1}$$

Where,

$$PR_{tot} = \frac{P_{2\_tot}}{P_{1\_tot}}$$

$$\gamma = 1.4$$

$$T_1 = pre\ compressor\ temperature$$

$$T_2 = post\ compressor\ temperature$$

Where,

$$P_{tot} = P_{static} \times \left(\frac{T_{tot}}{T_{static}}\right)^{\left(\frac{\gamma}{\gamma-1}\right)}$$

Where,

$$T_{tot} = T_{static} + \frac{v^2}{2 \times C_p}$$

$$T_{static},\ P_{static} = static\ temperature, pressure\ pre\ or\ post\ compressor$$

Where,

$$v = \frac{\dot{m}}{A \times \rho}$$

Where,

$$\dot{m} = mass\ flow$$

$$A = compressor\ inlet\ or\ outlet\ diameter$$

$$\rho = \frac{P_{static}}{R \times T_{static}}$$

Where,

$$R = 287.058$$

The isentropic efficiency of the compressor can also be interpolated from the compressor efficiency maps. However, the efficiency maps were usually acquired in a controlled environment on gas stands by the turbocharger OEM and were likely in very different thermal conditions compared to the turbocharger installed on the test bench. The extra heat transfer effect seen on the engine test bench would deviate the efficiency calculation (using the inlet and outlet condition, i.e. temperature, etc.) of the compressor and turbine from the reality. The comparison of the efficiency measured at the test bench and the efficiency from compressor maps for the same limiting curve test points is shown below in Figure 3.8.

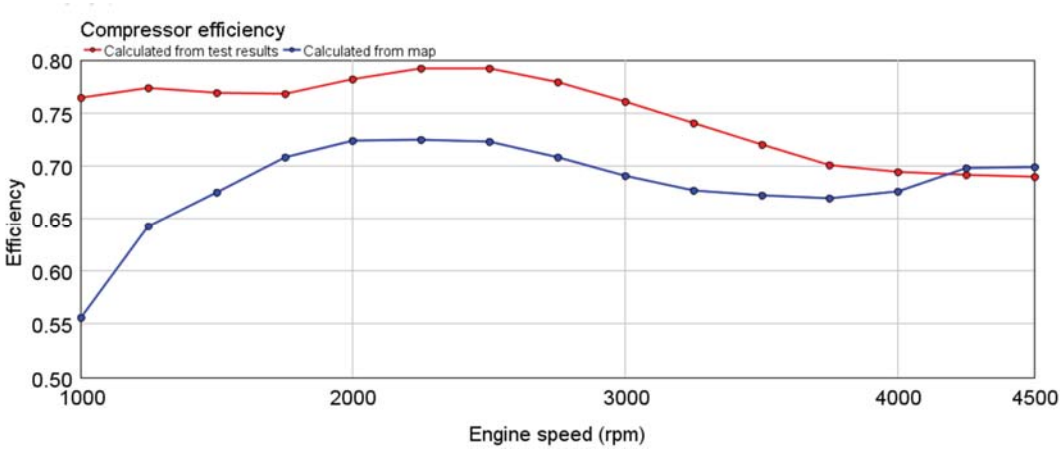

Figure 3.8 compressor isentropic efficiency comparisons

From the graph, it appeared that the efficiency deviation of the map prediction from the test result is especially large at low mass flow conditions and the error reduces to negligible from 4000 rpm and higher. Therefore, directly using the compressor map (and turbine map) in 1D simulation can create large prediction error, especially at low flow operating points. To solve this problem, either the heat transfer and pressure loss effect should be accounted for through extra modelling effort, or the efficiency multipliers should be applied to the compressor map empirically. This will be further discussed in the modelling chapter.

3.4.2 Part-load minimap test points

The part load test points were summarized from the operating trace of the engine used in a standard equipped Ford Transit van running the NEDC cycle and WLTP cycle. The results from such minimap tests can be used to compare the drive cycle performance and is an industry common practice. In the context of the two stage turbocharging project, since the full transient drive cycle test was not performed using the proposed control strategy due to the consideration of hardware protection, this method allowed the comparison of the drive cycle performance among different turbocharging setups.

The speed/torque traces of the NEDC and WLTC drive cycles are shown in the following Figure 3.9 and Figure 3.10, the data points were recorded at 1 Hz.

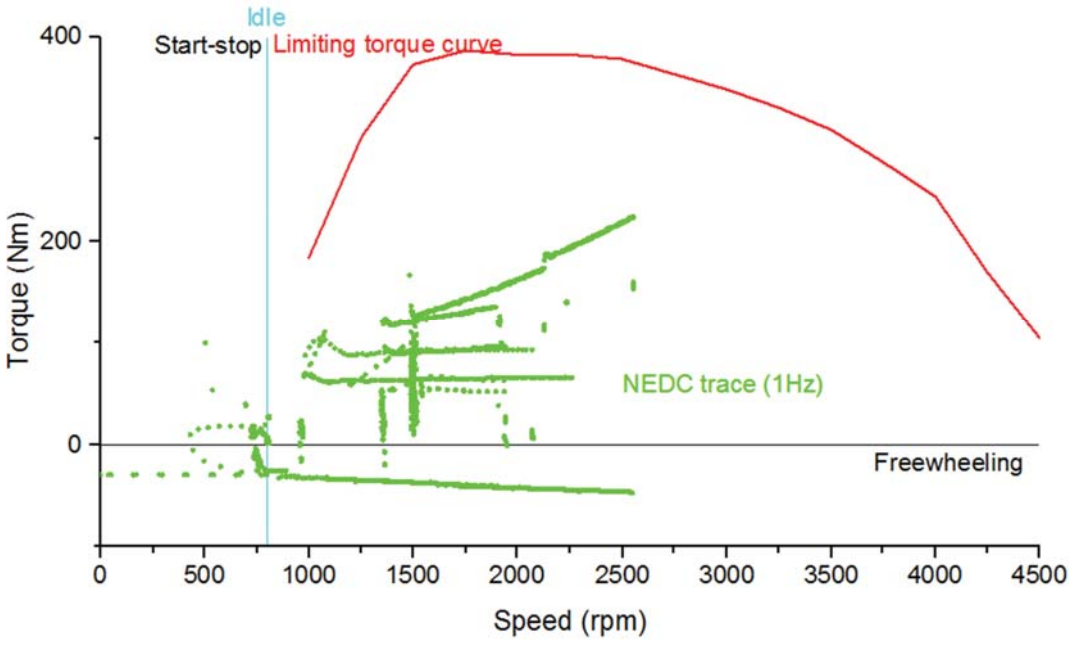

Figure 3.9 baseline engine running an NEDC test cycle with trace points recorded on the speed/torque map

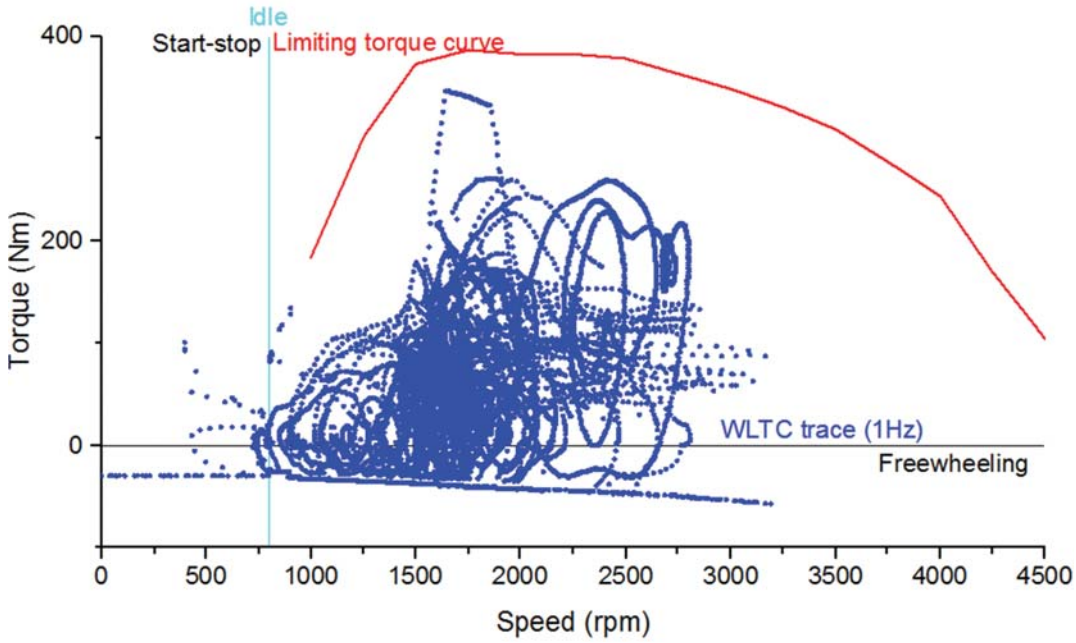

Figure 3.10 baseline engine running a WLTC test cycle with trace points recorded on the speed/torque map

At a glance, the newly proposed WLTC cycle has significantly more transient components and covers a much wider operating region on the engine speed/torque map. When plotting the two drive cycle traces on the same plot as in Figure 3.11, the test points can be chosen to envelop a region that the two cycles resided in, shown as the black square labels.

From the different turbocharging test setups, the raw test results of each of the minimap points will be directly compared to the baseline arrangement. To give a more intuitive comparison of the drive cycle results, these test points were also used to construct the fuel consumption surfaces and NOx emission surfaces, which allowed the results of all the trace points to be interpolated. Although this method lacked the consideration for transients (which could be a significant part) and was also highly dependent on the interpolation accuracy, such comparison would be like compared to like and was more accurate compared to simply applying weightings to each test points.

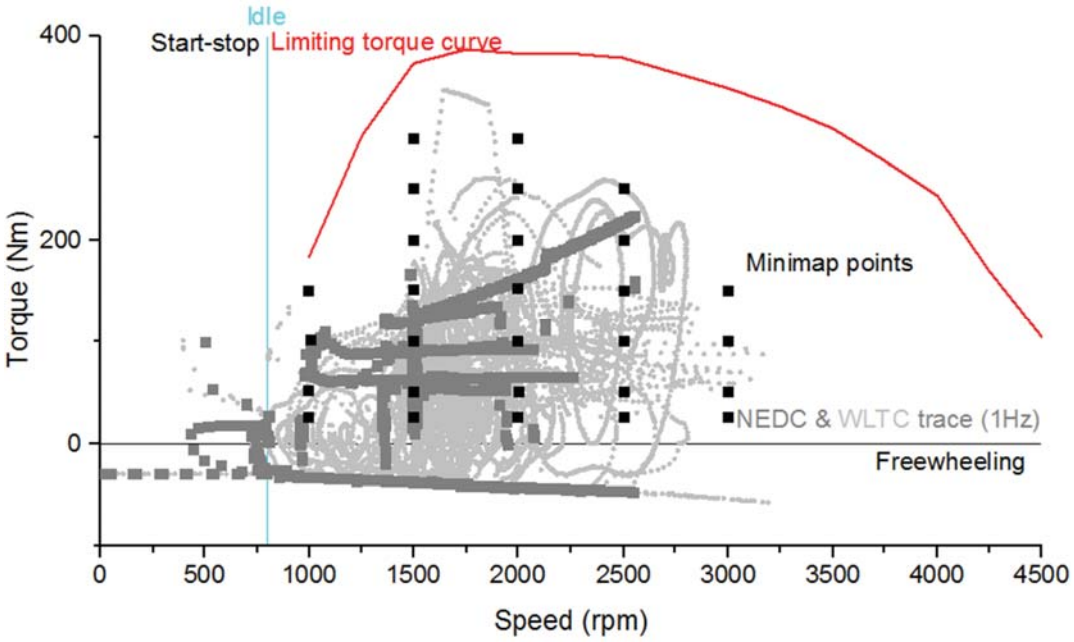

Figure 3.11 chosen minimaps overlaid on the NEDC and WLTC test cycle trace points

3.4.3 Transient test

The transient tests were performed using the 'tip-in/tip-out' of engine torque as shown in Figure 3.12. The engine pedal position was switched between a constant low load pedal position and a 100% full throttle pedal position for 14 times to finish 7 transients in a 7 minutes 20 seconds transient test, as shown in Figure 3.12 below. The transient schedule was arranged in such a way so that both the engine gas exchange dynamics and the ECU controllers operate stably before each tip-in.

To evaluate the turbocharger performance during the engine warm up period, the transient tests were also performed during the engine cold start condition for different engine speeds. In such tests, the engine was kept thermally stable at around 15 degrees overnight before the engine starts and enters the transient test within 30 seconds after cranking the engine, which was to allow time for the fuel beaker to settle and emission analyser to receive the first batch of engine exhaust.

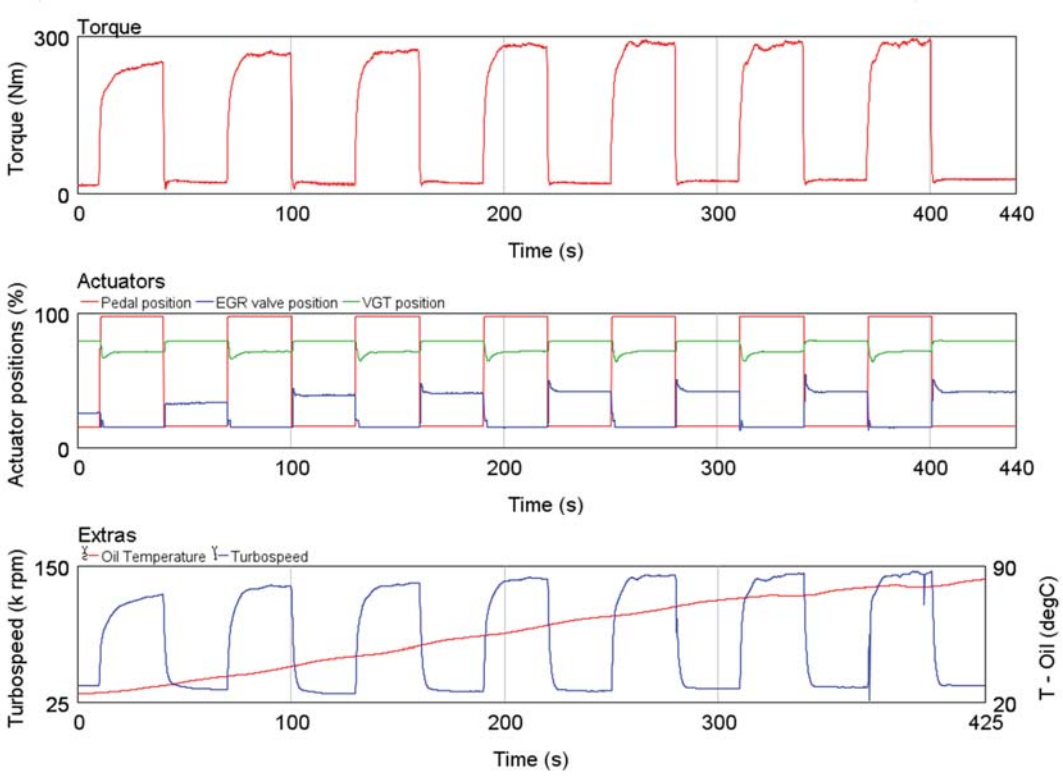

Figure 3.12 example of a cold start torque transient at 1250 rpm

The plots in Figure 3.12 illustrated the key points to look at in the transient test. First of all, whether and how the engine has reached the torque target during the tip-ins are of the utmost importance. Secondly, observing how the actuators behave was the key to understand the behaviour of the whole engine and also provided evidence if the different arrangements were being compared purely on the basis of their turbocharging behaviour or if there was too big an influence from the controllers. Last but not the least, the turbocharger behaviour was the focus in this study. How fast did the turbocharger accelerate seemed to be directly correlated to the torque transient because the transient torque was largely limited by the air mass flow. Also, the oil temperature, used as a global index for the engine thermal condition, provide an important angle to look at the different behaviour of the engine when using different turbocharging arrangements. The evolving behaviour of the controllers in the

warming up phase of the engine was also one of the directions worth looking into to further improve the engine performance.

3.5 Test results

3.5.1 Limiting torque curve

The limiting torque curve test results were first compared with the full load results provided by the engine manufacturer. Such comparison confirmed that the test engine setup in the University of Bath was in working order. The discrepancy can be reasonably explained and all the subsequent work will be compared to these newly acquired test results.

As shown in Figure 3.13 below, the baseline engine test result shown in large red dots in the upper plot achieved the expected torque curve (in small red dots connected by the red line), which was the supplied torque curve by the engine manufacturer. Due to the fact that the test setup was not exactly the same with the production engine (without a catalyst, in house made intercooler, etc.), the VGT controller was not in the same position. As can be observed in the lower plot, except for the 1000 rpm (when the VGT at its most closed position), the test engine at all the other speed points has a more opened VGT vane position. Such result was largely due to the lower back pressure from the test engine (no after treatment system): for the test engine, a more opened turbocharger vane position was capable of boost the engine and provide the mass flow of the same level as the production engine. Also, the back pressure led to lower fuel consumption. It was recommended to have an orifice plate at the downstream of the exhaust system to control the engine back pressure to the same level as the production engine. However, due to the poor performance of the existing valve such arrangement was not used which also allowed the back compatibility with previous test data.

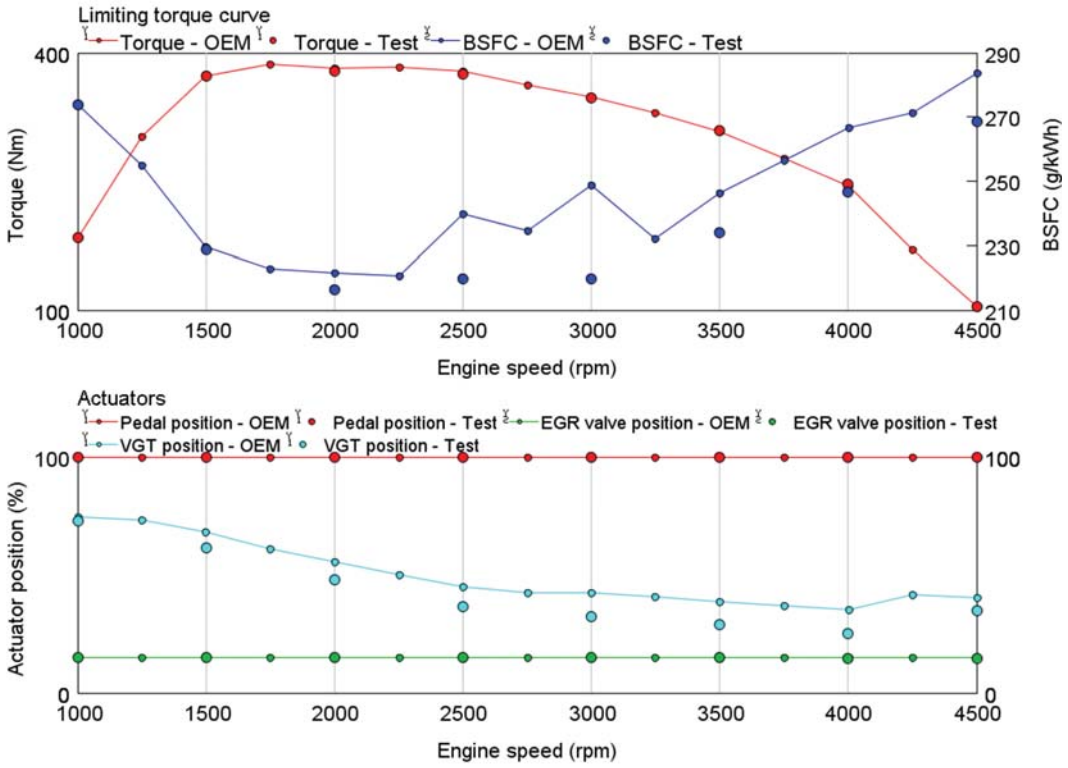

Figure 3.13 baseline VGT engine full load test results compared to OEM supplied data

When looking at the compressor map in Figure 3.14, the turbocharger speed was well within the specified turbocharger limits set by the turbocharger manufacturer. On the map, the limiting torque curve operating points formed a line of the expected shape for such full load conditions.

The 1000 rpm test point was very close to the surge line. Although it was not a big problem in this steady state point, in the transient test later however, the VGT PI controller had to be disabled for this speed to avoid large controller oscillations. The other operating points were keeping a reasonably safe distance from the compressor surge line and choke line. On the other hand, most of the high power points rested in the heart of the compressor efficiency contour, which confirmed the good matching of the turbocharger and the engine.

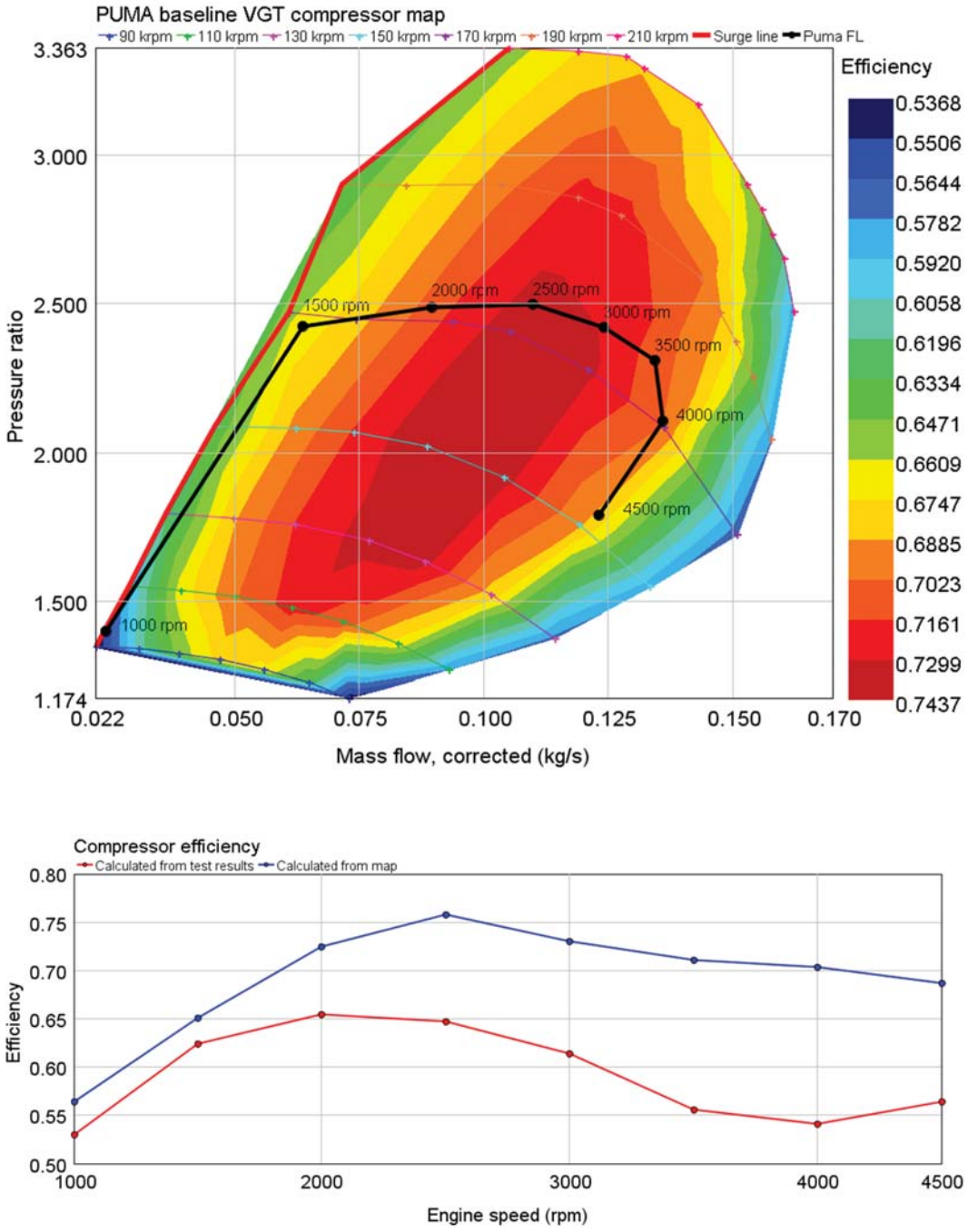

Figure 3.14 baseline VGT engine full load test results compressor performance

As expected, the calculated compressor isentropic efficiency was different from the efficiency acquired by checking the compressor map using the mass flow and pressure ratio. In these tests, the heat transfer from the turbine side was apparently a large influence, with the air in

the compressor heated by the turbine and leading to a lower apparent isentropic efficiency. The discrepancy enlarged as power (speed) increased. This difference will be taken into account in the simulation.

3.5.2 Part-load minimap test points

The brake specific fuel consumption (BSFC) and the nitride oxide emission (NOx) were important parameters to observe in these minimap tests, as they are a static subset of the drive cycle tests, which were designed to test the vehicles of their fuel economy and pollutant emission. These test results were presented in two contour plots which can give an intuitive (yet crude) insight into the contribution that each operating point was making to the total fuel consumption and NOx emission. The graphs also showed the areas of weaknesses that could be improved.

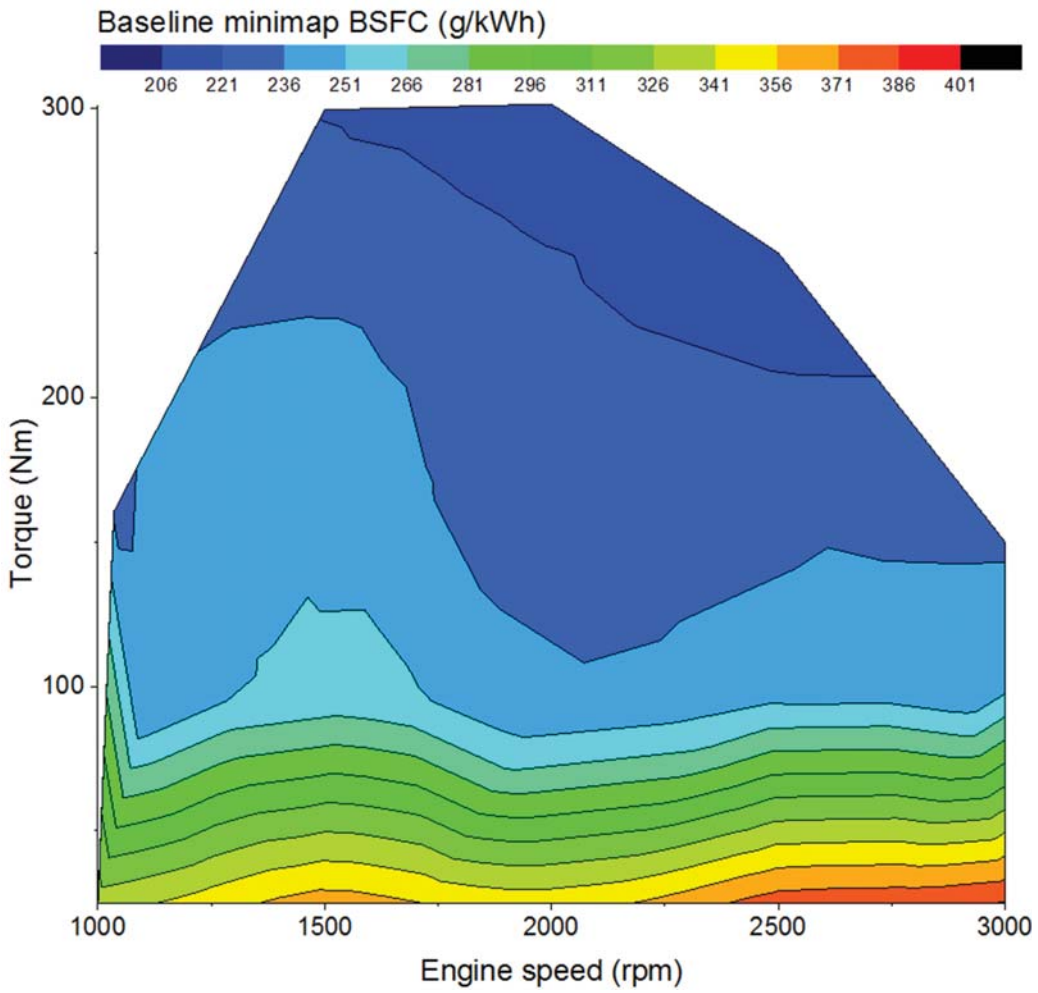

Figure 3.15 colormap of the baseline VGT engine minimap test results: BSFC

The BSFC graph plotted using the minimap data points was a typical **sub-set** of the engine performance map. The mid-speed, mid-load region was the fuel consumption 'valley' on the map due to the good performance from both the combustion and the turbocharging. The contour rose up around this valley to the low speed and low load region due to the increased portion of friction and pumping loss to the total power, the heat transfer loss and blow-by losses, etc. There were several minor regions of non-conformity to this bowl shaped valley due to the stepwise engine calibration method and possibly some test errors. Such nonconformity can be considered common among turbocharged Diesel engines equipped by EGR route.

The NOx map showed that the engine produced very small amount of NOx pollutant in the low load region but much higher NOx emissions at higher load. This was in accordance with the mechanism of NOx generation: at low engine load, the low amount of fuel injection and large portion of EGR gas had been keeping the cylinder temperature low, which inhibited the formation of NOx gas; while at higher load, the larger amount of fuel injected and decreased portion of EGR gas created an ideal hot and oxygen-rich environment for the NOx formation.

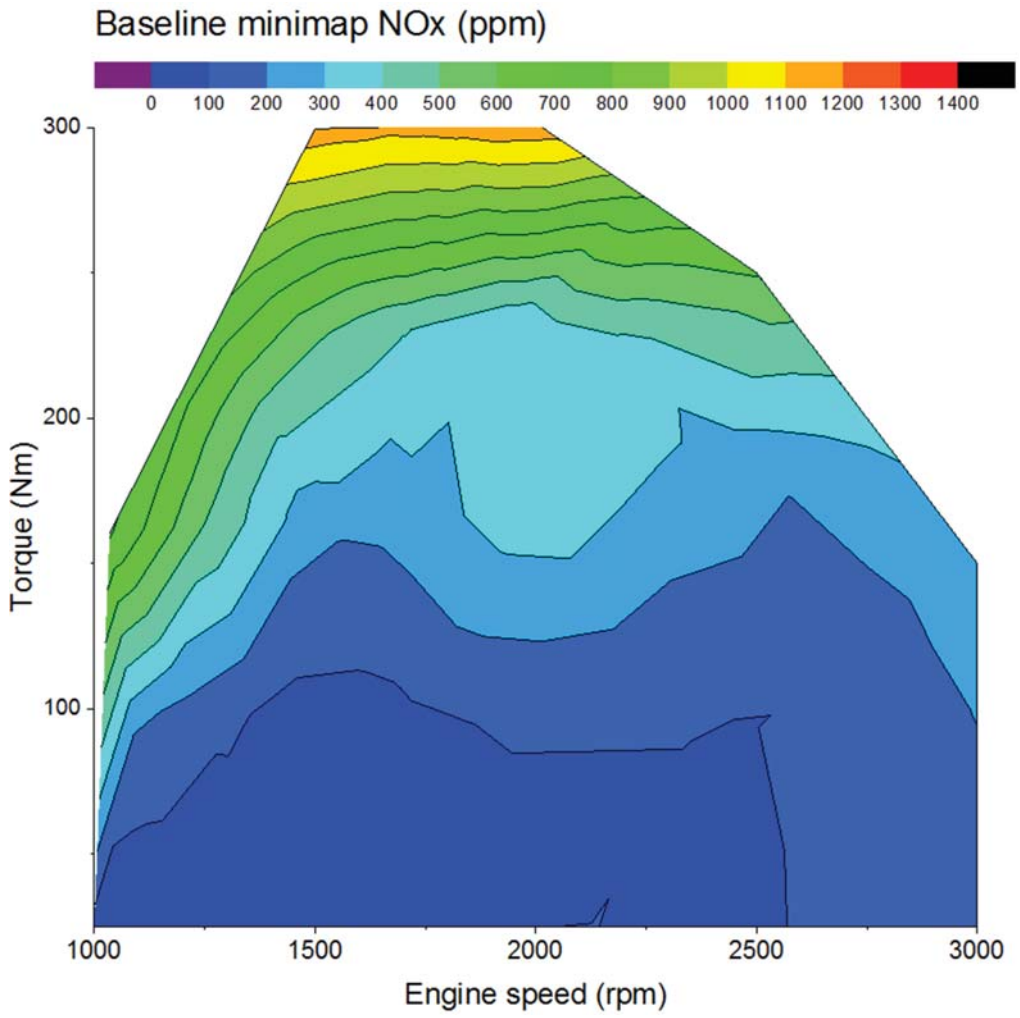

Figure 3.16 colormap of the baseline VGT engine minimap test results: NOx

Although the contour maps can show the whole pictures of the BSFC and NOx across the speed and load map, they were not as convenient as quantitative methods when comparing the different turbocharger arrangements, especially when the difference was small. Therefore, in this study, to conveniently cross compare the emission and fuel consumption benefit from different technologies, a 'quasi drive cycle averaging' method is proposed as follows.

1, the minimap test results (emission or fuel consumption) are used to construct a contour surface, creating a two input – one output model (Figure 3.17).

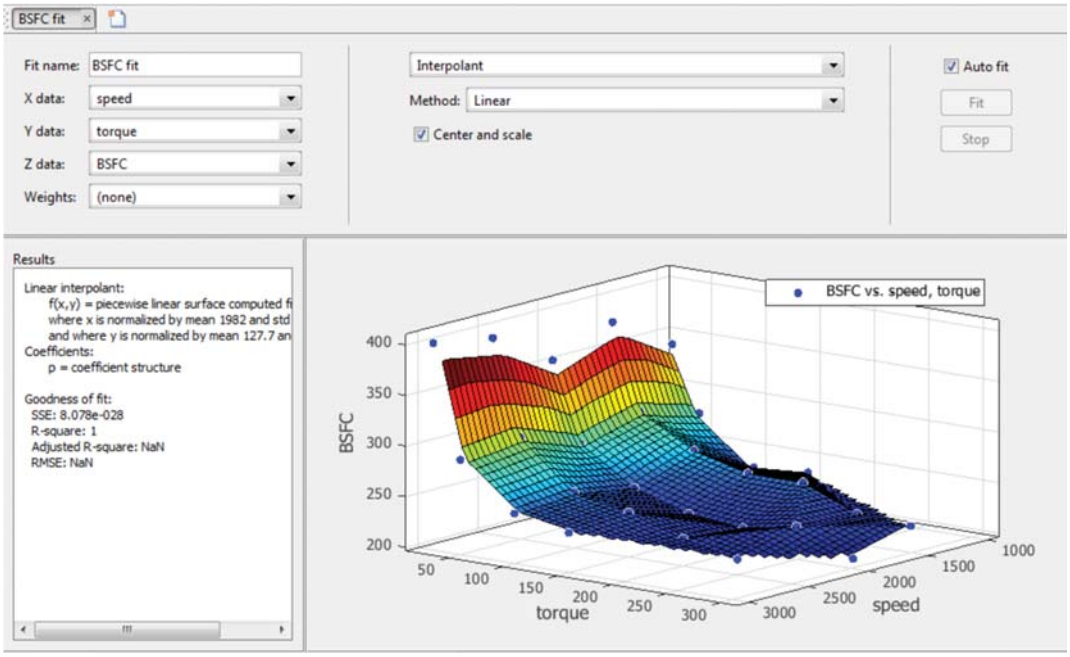

Figure 3.17 contour surface constructed using minimap test results for drive cycle prediction

2, each drive cycle transient operating point (torque/speed sampled at 10 Hz) were fed to the two input – one output model, producing a quasi-steady emission/fuel consumption reading of that operating point. The points closely outside of the contour were extrapolated using the Kriging method and were subject to extrapolation errors. The idling points were singled out and assigned a fixed fuel flow of 0.05 g/s and fixed NOx emissions of 80 ppm from the test

results and the points in the start-stop region and freewheeling were assigned value 0. The complete data list was included in the appendix.

3, all the quasi-static emission and fuel consumption readings were then added up to give an emission or fuel consumption value for the whole drive cycle. The practice was done to NEDC and WLTP drive cycles separately. The comparison of the two drive cycles also provided a new perspective to evaluate the new and old drive cycles using static minimap data. Using this method the test results were calculated to be 6.25 litre per 100 kilometre or CO_2 emission of 165.8 g/km for fuel consumption and 192.7 milligram per kilometre for NOx emission in NEDC and 7.15 litre per 100 kilometre or CO_2 emission of 189.5 g/km for fuel consumption and 292.7 milligram per kilometre for NOx emission in the WLTC.

The result of 7.15 litre per 100 km and 189.5 g/km for fuel consumption were not very far away from the claimed fuel consumption of 7.9 litre per 100 km or 208 gram CO_2 per km and in the same order of magnitude with the 160 mg/km of NOx emission. The lower test CO_2 was mainly due to the reduced parasitic loss on the test engine and the increased NOx emission was due to the fact that the minimap tests were done on a fully warmed up engine. There were certainly also the influence of calculation errors of emulating transient tests using static test results however in this project these errors were ignored and the subsequent work will be compared to the calculated baseline emissions as follows:

Table 3.2 Calculated drive cycle results of CO_2 and NOx emission

	NEDC		WLTC	
Emissions	CO_2	NO_X	CO_2	NO_X
Units	g/km	mg/km	g/km	mg/km
Baseline VGT	165.8	192.7	189.5	292.7

3.5.3 Transient test

The transient performance was charted as shown in Figure 3.18. As mentioned in the previous section, at 1000 rpm full load condition the turbocharger is operating very closely to the compressor surge line and during a full pedal transient, the compressor was pushed into the unstable surge region which led to large VGT controller oscillation in response to the unstable boost. Such oscillation was so large that during this set of transient usable test results could only be recorded by disabling the VGT PID controller. Therefore the VGT position shown in the middle plot were feed forward controlled. This set of results showed that the engine showed excellent repeatability in terms of torque generation, thermal condition, and the turbocharging behaviour.

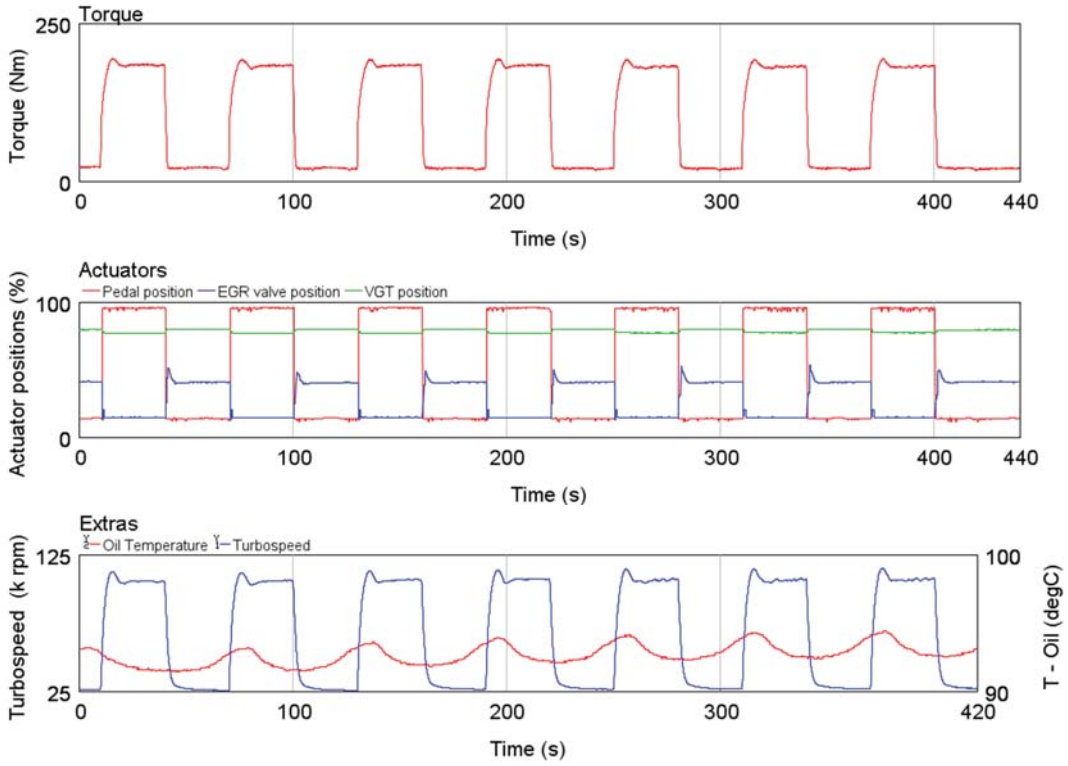

Figure 3.18 baseline VGT engine 1000 rpm transient performance

At higher speeds, i.e. 1500 rpm and 2000 rpm as in Figure 3.19 and Figure 3.20, the PID controller was re-enabled since the operating points had moved away from the surge line. Compared with the 1000 rpm transient operation, there was a period of controller modulating behaviour after the 'tip-out' when the engine was back to low load operation. Such controller behaviour was caused by the EGR and Boost controller interaction and could be improved through further calibration. On the other hand, the transient performance still showed good repeatability and the subsequent simulation was all compared with these test results.

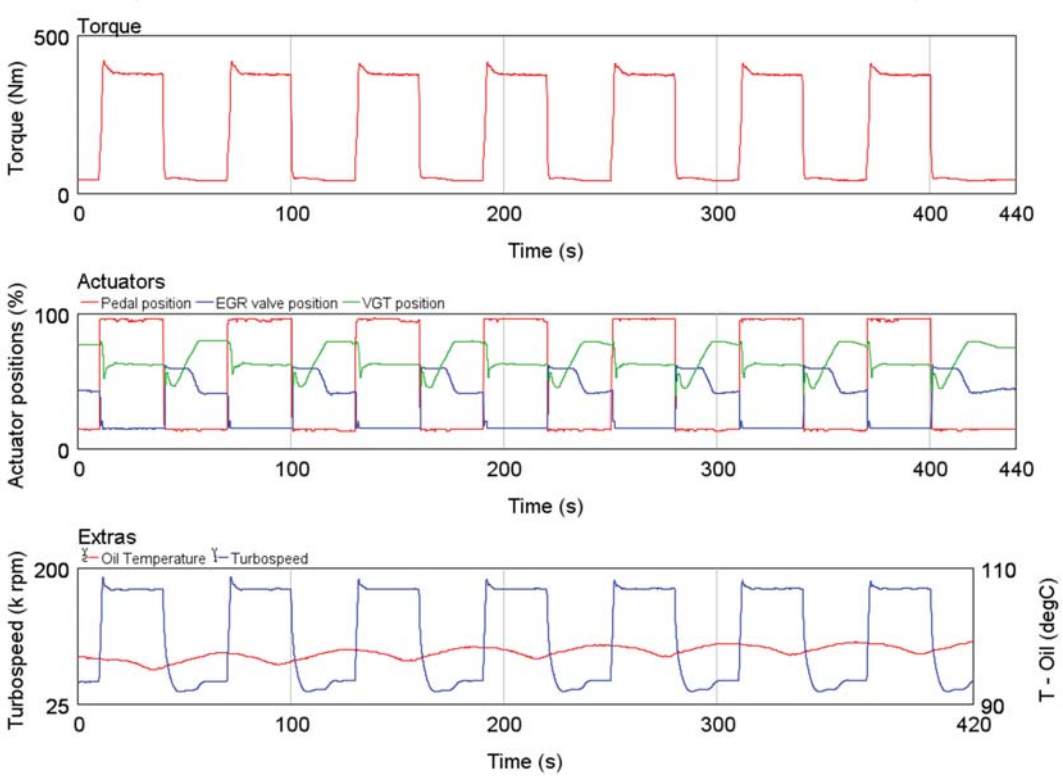

Figure 3.19 baseline VGT engine 1500 rpm transient performance

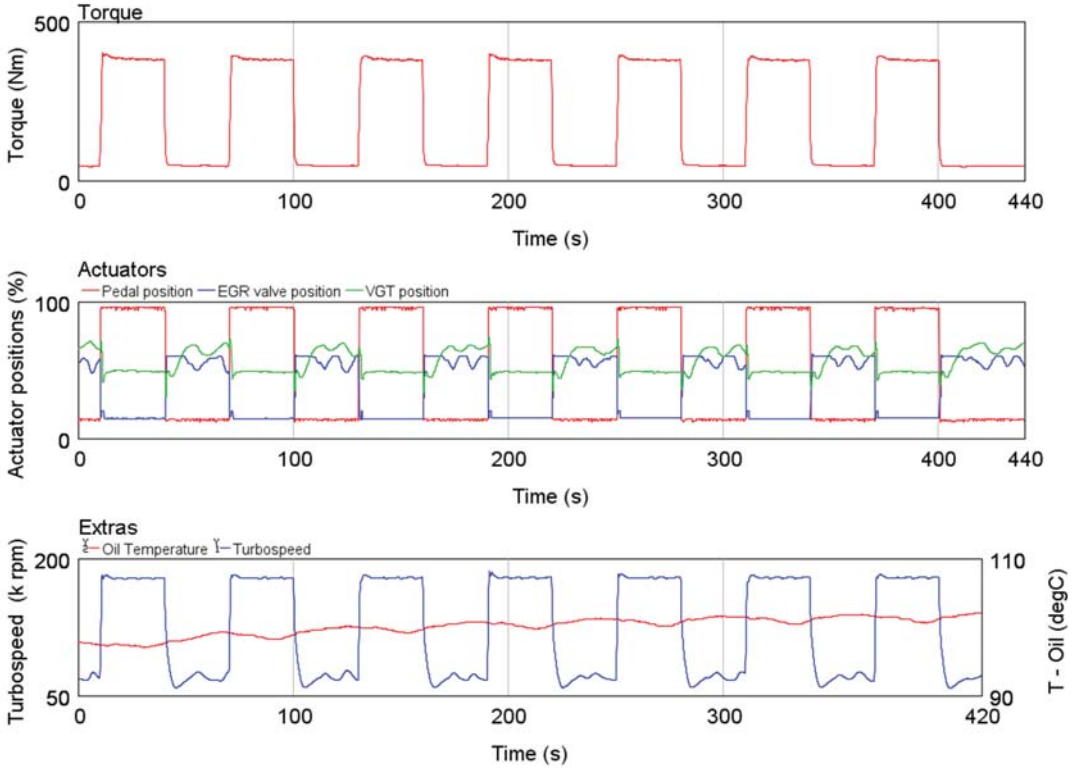

Figure 3.20 baseline VGT engine 2000 rpm transient performance

The cold start transient results were plotted as in Figure 3.21, Figure 3.22 and Figure 3.23.

At 1000 rpm engine speeds, the very cold thermal condition increased the engine friction and the engine was unable to sustain the 1000 rpm set engine speed using the pedal position applied to all other transient test before the tip-in. Therefore, during the first tip-in the pedal position was offset by 5% at the first tip-in and returned to normal at from the second. The torque plot in the upper plot showed the resulting torque curve and it appeared that the engine finally reached its 1000 rpm full load torque level from the 7th tip-in. From the middle plot, it can be observed that the VGT controller almost stayed in a closed location due to the lack of exhaust energy to turbocharge the engine to the boost target. Compared to the hot transient test of 1000 rpm in Figure 3.18, the VGT controller finally started to modulate at high load from the 7th tip-in, indicating the engine and turbocharger was warmed up to meet the

boost target (from half way of the tip-in). The stepwise increase of EGR valve opening during the low load condition indicating also the ECU was requesting more EGR gas as the engine warmed up. The warming up behaviour of the engine and turbocharger was confirmed in the lower graph, with the oil temperature rising and the turbocharger achieving higher turbo-speed during the operation.

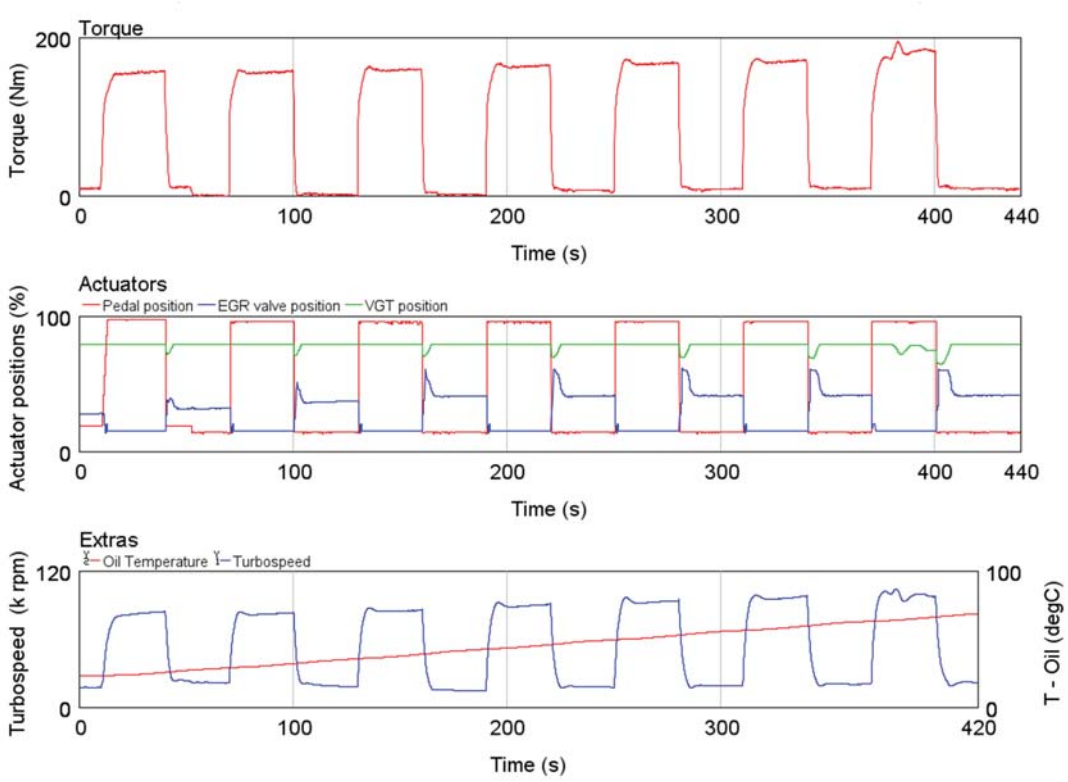

Figure 3.21 baseline VGT engine 1000 rpm cold start transient performance

At 1500 rpm, the engine apparently warmed up much faster, compared with the 1000 rpm, the engine achieved its full load torque from the 3rd tip-in and the VGT and EGR controllers also started working in the same manner as in the 1500 rpm hot test from here.

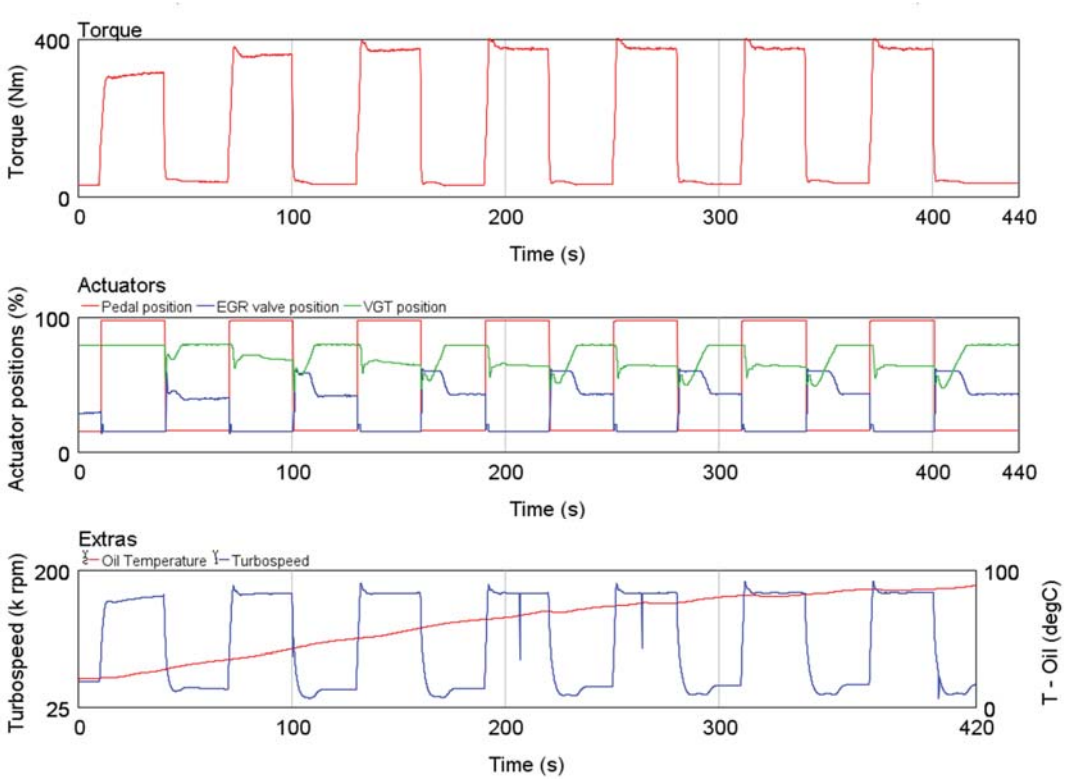

Figure 3.22 baseline VGT engine 1500 rpm cold start transient performance

At high engine speeds from 2000 rpm, however, the engine was able to provide sufficient amount of exhaust energy to the turbocharger and the warm up behaviour in the torque trace was barely noticeable. Only by looking at the controller operation in the middle plot, it seemed that the EGR and VGT controllers were having evolving interactions due to the change in the engine thermal condition.

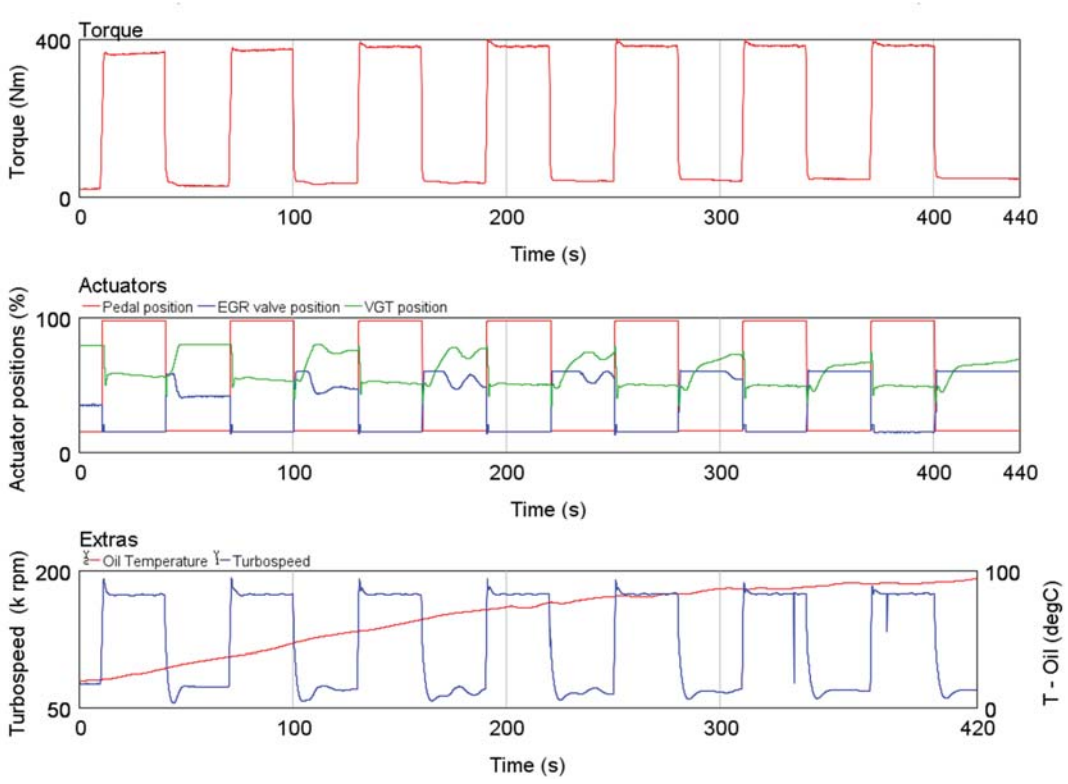

Figure 3.23 baseline VGT engine 2000 rpm cold start transient performance

3.5.4 Understanding of the engine gas exchange controller

To analyse the transient test results it was useful to analyse the ECU control scheme of the gas exchange during the transient.

Before the transients happen, the engine settled at a low load operating condition, the focus of engine calibration was to reduce the NOx emission for the drive cycle paradigm. Only the feedforward term of the boost controller was active and the EGR controller was targeting an air mass flow target. The apparent outcome of such control was that the VGT actuator was set at the smallest vane tunnel cross section to create high engine back pressure to pump EGR and the EGR valve was at an open position to allow as much EGR gas to circulate back to the intake manifold as needed. Such an arrangement also had the effect of maintaining the turbocharger speed at a relatively high level, preparing the engine for an upcoming torque transient. The

negative side effect is that the PMEP of the engine is relatively high, thus the turbocharged engine fuel consumption performance is usually worse than that of a similarly sized naturally aspirated engine at low load.

When the transients happen, the change in pedal position was first translated into the torque target to be achieved and the injection responds accordingly to inject larger amount of fuel, limited only by an air/fuel ratio controller (fuel cutter), resulting in the torque rise. The VGT vanes and EGR valve also worked simultaneously with the torque rise to increase the air intake of the engine, thereby raising the threshold of the fuel cutter until the full load torque was reached. In this transient phase of engine operation, both the boost and EGR control worked in closed loop: the sudden change of the mass flow target would instantly shut the EGR valve, more fresh air could therefore be breathed into the engine cylinder, taking the place of the recirculated exhaust gas; the sudden change of the boost target had a less drastic effect on the VGT controller, as the VGT vane position was already a closed position, and it only opened up when the boost pressure reached the set target, a short while after the transient happens.

After the full load is reached, the gas exchange controllers worked to maintain a stable full load torque. The EGR valve keeps a shut position for the full load condition. The VGT vane position was modulated in closed loop to adapt to small changes from thermal condition of the turbocharger and controller oscillations.

The tip-in ends when the pedal position was returned to the low level setting and the sudden loss of exhaust energy would prompt the engine to modulate the VGT vane position back to its low load setting. In the meantime, the EGR controller would start to allow EGR gas back in to the intake manifold for the low load condition and the two controllers had a short period of interference before the whole system settled to steady state.

3.6 Summary

This chapter aimed to provide a description of the testing environment where the research was conducted. The details of the test cell environment, test bench instrumentation and the test engine was introduced in the first half of the chapter. Thereafter, a test plan made up of limiting torque curve, drive cycle minimap points and the hot and cold transient tests was proposed to be used in the testing of all the different turbocharging arrangement to be studied in this project. Then the baseline engine was tested according to this test plan and the test results confirmed the test bench setup of the engine as the engine performance matched the OEM provided engine data and the drive cycle CO_2 and NOx emission level. Also, the repeatability of the test engine was proved to be acceptable. Therefore, the baseline engine test result will be used as a benchmark for the subsequent test results to be compared to.

Chapter 4 - 1D engine simulation and baseline engine model calibration

This chapter was focused on the analytical side of the study. To begin with, the basic equations of the 1D engine simulation were introduced briefly and the commercial software used to implement the engine model was introduced. Then the details of the baseline engine model were given and the procedures of calibrating a fully predictive engine model were explained. At the end of this chapter, the calibration results with comparison to the baseline engine test results were presented.

4.1 1D Engine Simulation

As mentioned in the literature review, the 1D gas dynamics simulation codes are used to simulate the engine performance. Compared to the mean value models and 3D CFD models, they provide a good balance between prediction accuracy and computation intensity.

The main task of the 1D simulation code is to solve the Navier-Stokes equations in 1D and all the quantities in the equations are averaged on any cross section along the flow direction. By solving the conservation equations of continuity, momentum and energy, the code is able to predict the relevant variables at any cross section on the abstracted flow path. As shown in Figure 4.1 below, the flow paths are abstracted and discretised into small volumes. Volumes

with one inlet and one outlet are connected to represent the pipe components and volumes with more than two openings are modelled as flowsplits.

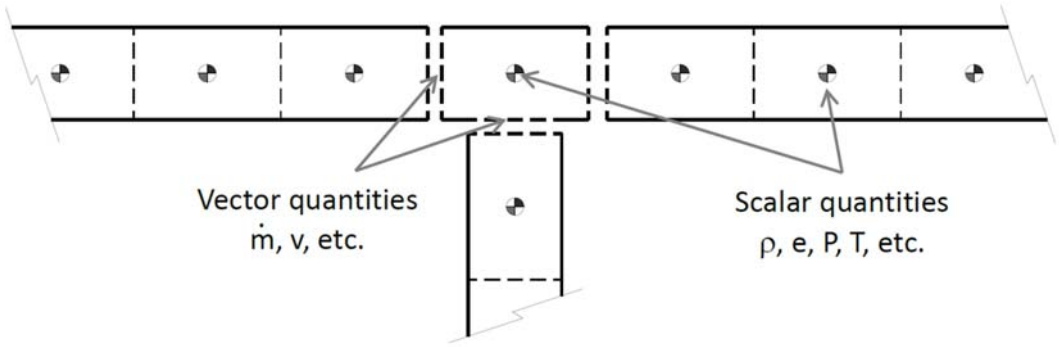

Figure 4.1 Discretised flow path into small volumes were the basic elements to solve the conservation equations

The conservation equations calculated are as follows:

Continuity:

$$\frac{dm}{dt} = \sum_{boundaries} \dot{m} \tag{4.1}$$

Energy:

$$\frac{d(me)}{dt} = -p\frac{dV}{dt} + \sum_{boundaries} (\dot{m}H) - hA_s\left(T_{fluid} - T_{wall}\right) \tag{4.2}$$

Momentum:

$$\frac{d\dot{m}}{dt} = \frac{dpA + \sum_{boundaries}(\dot{m}u) - 4C_f\frac{\rho u|u|}{2}\frac{dxA}{D} - C_p\left(\frac{1}{2}\rho u|u|\right)A}{dx} \tag{4.3}$$

where:

$\dot{m}$	boundary mass flux into volume, $\dot{m} = \rho A u$
m	mass of the volume
V	volume
p	pressure
ρ	density
A	flow area (cross-sectional)
A_s	heat transfer surface area
e	total internal energy (internal energy plus kinetic energy) per unit mass
H	total enthalpy, $H = e + \frac{p}{\rho}$
h	heat transfer coefficient
T_{fluid}	fluid temperature
T_{wall}	wall temperature
u	velocity at the boundary
C_f	skin friction coefficient
C_p	pressure loss coefficient
D	equivalent diameter
dx	length of mass element in the flow direction (discretization length)
dp	pressure differential acting across dx

In each time step, the right hand side of the equation is calculated using quantities from the previous time step. The result can be integrated to yield the quantities of the new time step. The process goes on in iterations until all the variables such as temperatures and pressures achieve equilibrium.

In the application of internal combustion engine simulation, the solving of 1D Navier-Stokes equation method is usually coupled with various mean value sub-models to represent the entire system of the internal combustion engine. When it comes to the components which cannot be abstracted as pipes and flow splits, such as the combustion process and the turbochargers, etc., imposed combustion burn rate, compressor and turbine maps can be filled in the blanks to connect the flow paths. Commercial 1D software also incorporates the possibility of building the controller into the engine model, inserting a whole vehicle powertrain model and connection to other software such as Matlab/Simulink to widen the

application of 1D calculation. The calculations are done in the same iteration manner until all the variables achieve equilibrium.

4.2 Modelling software

In the first phase of the project, Ricardo Wave was used as the modelling software, due to the fact that the original engine model was delivered by the engine manufacturer in Wave format. The software was developed by *Ricardo,* a market leading automotive consulting company and a specialist manufacturer for high performance automotive products. The software has a highly user friendly interface and it is always easy to add in new features to an existing engine model and often the debugging is convenient due to the effective fault finding messages during each simulation. The software also works very well in the Simulink – Wave co-simulation environment.

GT-Suite software is another commercial 1D simulation code developed and licensed by *Gamma Technologies Inc*., an engineering company focused on supplying and supporting this software package. GT-Power, as a component inside the software suite, is another market leading tool in the simulation and optimisation of engine performance. Although the software use the similar physics and algorithms as used in Wave, it has a vastly different user interface and component managing philosophy. As the test results started to accumulate in the project, the study shifted to use GT-Power due to its improved variety of combustion models and also the convenience in template-based method to manage the data and the components. Despite great effort to rebuild the engine model from scratch in GT Power, the software proved to have increased efficiency and was used as the primary 1-D engine simulation software in the latter half of the project. Temperature, pressure, mass flow and turbocharger performance were all carefully calibrated using the test data and the combustion model used was a fully

predictive DIPulse combustion model able to accurately represent the test results with different levels of EGR gas.

The 1-D engine model was first used to explore the possible control strategy of the two stage charging system and then was frequently calibrated using newly acquired test data. When the experimental phase of the project ended, the model was used as a high-fidelity model plant for the further exploration of the system. The co-simulation feature with Simulink was frequently used in this project so that the engine strategy from the ECU was effectively applied and the data was conveniently processed and managed in Matlab.

The Matlab/Simulink software was used comprehensively during this study, as it was a highly effective tool for data storing, processing and plotting. It was also used to automate simulations so that computationally intensive variable sweeping simulation was possible with the Ricardo Wave. Moreover, as a popular tool in the engineering society, it is very well supported on this internet with excessive free resource and many existed codes in the group and various anonymous coders on the internet were adopted in the codes used in this project.

4.3 Baseline engine model

The baseline engine model was built strictly according to the engine geometry provided by the engine manufacturer. As shown in the Figure 4.2, the complete flow path has been represented as pipe and flow split components in Wave environment, shown on the software as the black solid lines and light blue blocks respectively. The green parts represented the orifice components, which marked the change of diameters in pipes which cannot be modelled by a single pipe component. The engine block had the options to define the cylinder geometries and sub models, such as combustion and heat transfer, etc. Turbocharger

assembly was represented by: a compressor component, a VGT turbine component and a turbo-shaft component connecting them. The turbine and compressor maps were defined in the format of a table of four columns: the pressure ratio (P_{out}/P_{in}) is plotted against the corrected mass flow $\left[\dot{m}_{corrected} = \left(\frac{\dot{m}_{physical} \times \sqrt{T_{0,in}}}{P_{0,in}}\right) \times \left(\frac{P_{standard}}{\sqrt{T_{standard}}}\right)\right]$ and, in the case of the compressor map, with constant speed line ($N_{corrected} = N_{physical} \times \sqrt{\frac{T_{standard}}{T_{0,in}}}$) overlaid on the compressor isentropic efficiency ($\eta = \frac{T_{0,out,is} - T_{0,in}}{T_{0,out} - T_{0,in}}$) contour plot. In the case of the turbine map, usually multiple plots are used to represent the same four columns of data due to the fact that the efficiency contours having highly similar slope to the speed line. The exemplary maps have been shown in the previous chapter.

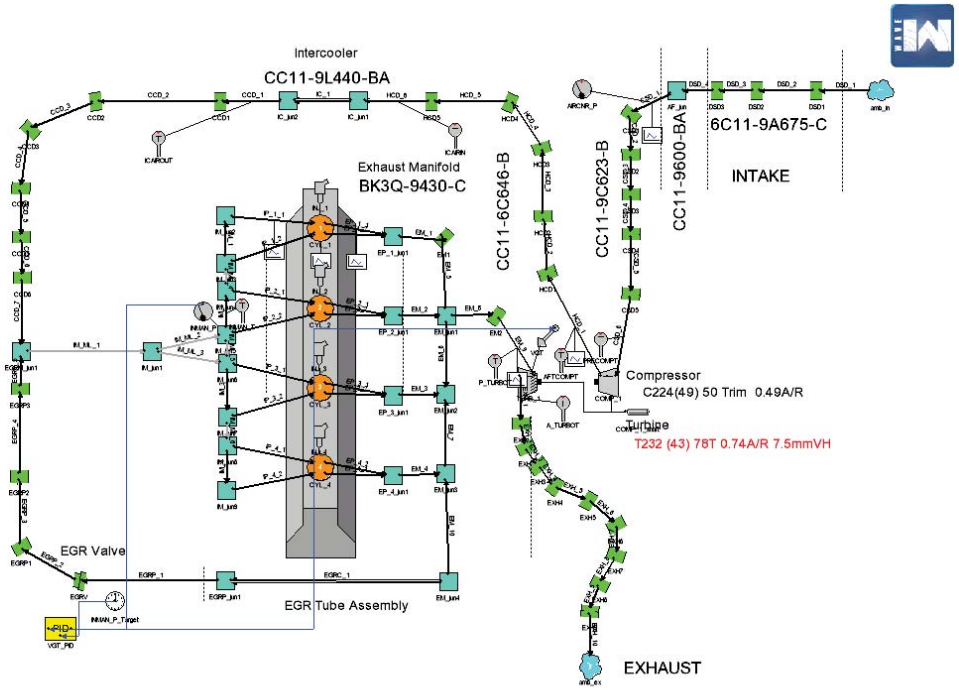

Figure 4.2 Schematics of the baseline engine model in Ricardo Wave environment

There were, however, several sources of error which could not be avoided in this project. One of the source of modelling errors is the intercooler which was made in-house. Due to the

highly non-linear characteristics of the water regulator, tuning of the PID controller was unsuccessful to accurately control the intercooler outlet gas temperature, especially during the transient tests. During the test phase of the project, the intercooler was manually tuned to give an outlet gas temperature around 45±5 °C, and in the model the intercooler outlet gas temperature was controlled to a fixed 45 °C.

In addition, the turbocharger maps were gas stand measured turbine and compressor maps provided by the turbocharger manufacturer. At the first phase of the project, the turbocharger maps were considered to be accurate. However, it should be noted that the heat transfer effect, bearing losses were included in the maps and can only be considered accurate at the gas stand condition. Therefore, modification to the efficiency maps had to be done for the quality of exploratory work.

4.4 Model calibration

4.4.1 Base calibration procedures

The baseline engine model was calibrated using the test data. The focus of the model calibration was to provide reliable exhaust gas condition before the turbine inlet, so that further research on the two stage turbocharging is based on reliable boundary conditions for the turbocharging system. Since there is no need to conduct optimisation/research on the existing engine systems besides the charging system, tuning of many components (e.g. intercooler, EGR cooler, intake system, etc.) was simplified and was done empirically.

To follow the standard calibration procedures specified in the GT-Power manual, the test data was first checked for errors, during which a few faulty thermal couples were identified and ruled out from the data pool. Then the engine model without the turbocharger was used to

tune the engine volumetric efficiency. An EndEnvironment part was used in the place of the compressor to impose the measured compressor outlet pressure and temperature. Pressure loss from the compressor outlet to the intake manifold was modelled by tuning the intercooler empirically. Gas temperature at the intercooler outlet was controlled as 45 °C and the air temperature rise between the intercooler outlet and the intake manifold due to the proximity to the warm engine was modelled by imposed pipe wall temperature that increases with engine loading. The valve lash was tuned to provide the correct air flow under the pre-requisite that the pressures in the exhaust and intake manifolds matched the test results. In the place of the turbine a second EndEnvironment part was used to impose the turbine inlet pressure and temperature (Figures 4.3).

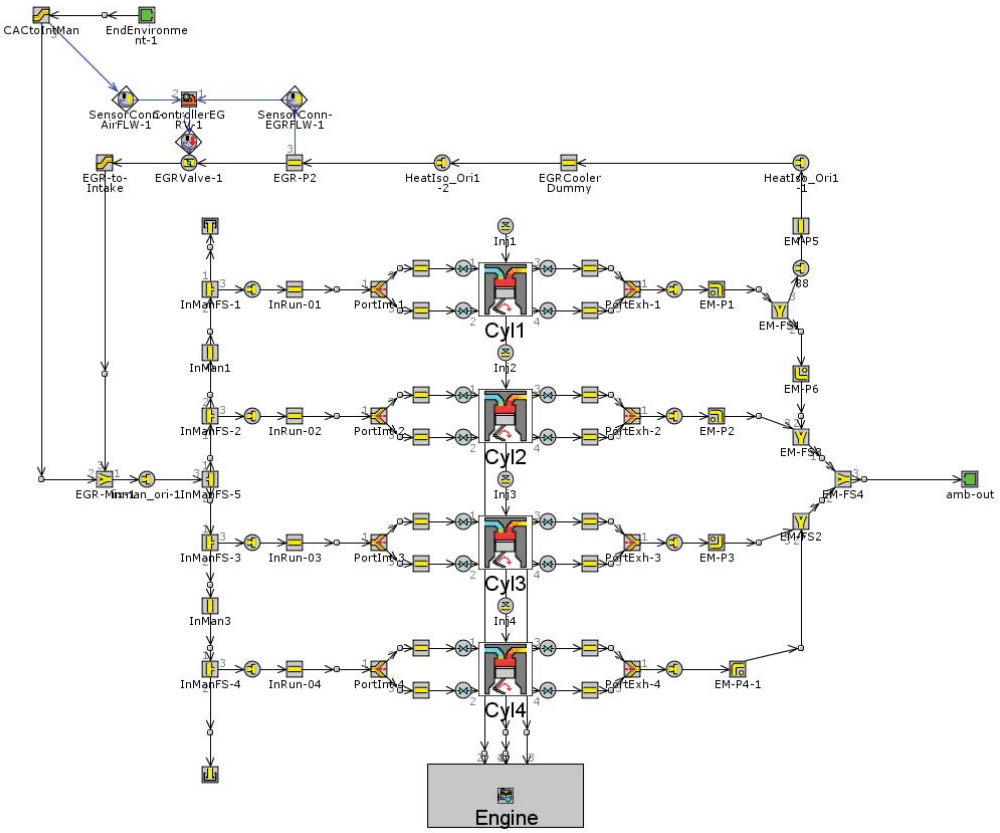

Figure 4.3 Turbocharger was taken out from the complete engine model so that the combustion can be calibrated in isolation of turbocharger influence

A compressor was then inserted into the model, replacing the first EndEnvironment, the compressor was imposed a rotational speed as measured in the test. Together with the compressor, the intake system upstream of the compressor was also included in the model; the pressure loss of the upstream components was matched by tuning the friction multipliers of the pipes. The mass flow and efficiency multipliers of the compressor were also tuned so that the compressor could provide the same air flow as achieved in the previous step.

For the gas exchange system the turbine with imposed rotational speed were inserted into the model (replacing an EndEnvironment component). The VGT rack position was controlled to match the engine back pressure. In addition, the pipes downstream of the turbine were also constructed and tuned to match the pressure drop in the test.

Finally, the efficiency multipliers of both the compressor and turbine were tuned until the two provided similar power. The compressor and the turbine were then connected by a turbo-shaft to form a complete turbocharger.

4.4.2 Combustion model calibration procedures

Before the turbocharger was added to the model, the combustion model should be calibrated so that the subsequent turbocharger calibration would not be hugely influenced by poor combustion prediction. The DIPulse model was chosen to be used as the predictive combustion model. The DIPulse model was a physical combustion model developed by *Gamma Technologies Inc.*, which can predict the combustion burn rate based on the in cylinder conditions, such as pressure, temperature, mixture composition and injection timing and profiles. The model uses several empirical and analytical equations to model the spray penetration, entrainment, droplet size and evaporation and the ignition delay for each pulse is calculated using a correlated equation separately as

$$\tau_{ign} = C_{ign}\rho^{C_{ign2}} exp\left(\frac{C_{ign3}}{T}\right) f(EGR)$$

(4.1)

The premixed combustion is modelled on the calculated evaporated fuel and entrained gas at the time of ignition as propagating flames:

$$\frac{dm}{dt} = C_{pm} m\left(t - t_{ign}\right)^2 f(k, T, \lambda, EGR)$$

(4.2)

The diffusion combustion is then modelled on the continuing mixed and burned evaporating fuel and entrained gas:

$$\frac{dm}{dt} = C_{df} m \frac{\sqrt{k}}{\sqrt[3]{V_{cyl}}} f(EGR, [O_2])$$

(4.3)

Each injection event is treated as a discrete pulse and the predicted burn rate is integrated to predict the combustion.

With adequate calibration using the test data, the physical model was capable of accurately calculating the burn rate of modern Diesel engine with multi-pulse injection with also the emission prediction capability. The model is so far the most advisable Diesel combustion model to provide adequate predictive capability with consideration of EGR. The calibration process is computationally intensive however the calibrated high fidelity model is highly rewarding.

In this project, in total of 44 test points with in cylinder pressure measurement were used to calibrate the combustion model. The test points includes the part load minimap points and the points on the limiting torque curve and covers the full region of the 1000 rpm to 3000 rpm speed region. Higher speeds were not the focus of this project, and were left out to so that the model can achieve a higher calibration quality due to the lesser need to fit the combustion model to a wide speed range.

In the first step, the burn rate profile of the test data was acquired in the GT-Power using the combustion analysis function: the cylinder 1 of the engine was singled out and supplied with both the in cylinder conditions and the cylinder pressure measurement. The in cylinder heat transfer was simulated by a Woschni model adapted by GT and the blowby was set as zero, which is acceptable for the lean burning Diesel combustion. An automatic calculation process was then conducted in iterations so that a suitable burn rate profile was able to match the measured pressure trace.

With the burn rate profile gained accurately from test data as a calculation foundation, the next step was to tune the Entrainment Rate, Ignition Delay factor, Premixed Combustion factor and Diffusion Combustion factor of the DIPulse model, so that the predicted burn rate profile would be able to match the test data burn rate profile. Since the 44 test points were all from different engine speed, torque, engine thermal condition and EGR rate, etc., the fully calibrated combustion model was capable of take these factors into consideration. The tuning of the model factors involved large amount of calculation of DoE cases, which swept through all four parameters in 2000 rounds of calculations for all cases. The calculation results can be subtracted using a GT-supplied Excel spreadsheet tool, which basically acted as an optima-finding code to find the best set of model factors which provides the least prediction error. The optimal set of the factors were then filled in the DIPulse template as a calibrated model to be

used in the full engine model. The 1000 rpm results were plotted as examples in the following Figure 4.4.

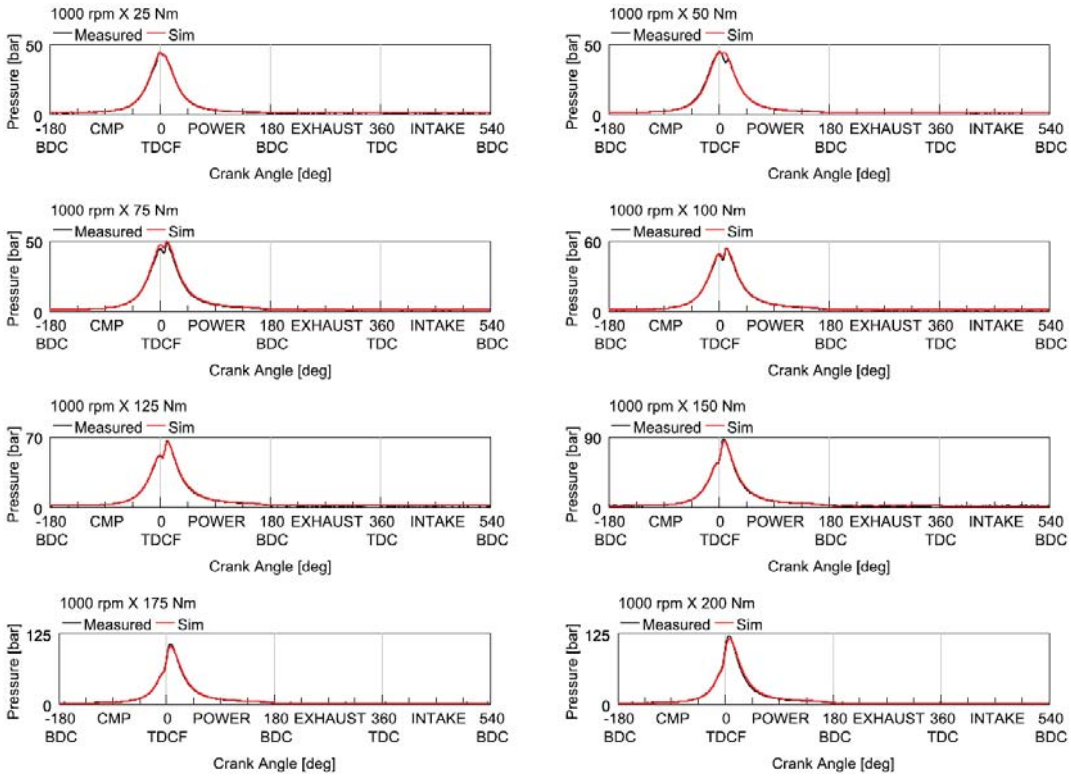

Figure 4.4 results from 1000 rpm in-cylinder pressure simulation plotted with test data showing the quality of combustion model

From Figure 4.4, it appeared that the combustion model accurately predicted the pressure curve in the cylinder at 1000 rpm, with the simulation results almost exactly overlaid on the measured data. Usually an empirical or semi-predictive combustion model would have significant difficulties when predicting the combustion of the pilot-injection, due to the lack of capability to incorporate highly varied cylinder mixture conditions across the speed and load region, leading to the enlarged deviation of the pressure curve at the onset of main injection. The difference will be discussed in the following section.

4.4.3 The impact of the combustion model on turbocharged engine simulation

The combustion model calibration discussed in the previous section was already considered standard practice for engineers working on the engine research and development. However, in many studies on the turbochargers research and development, the quality of the engine combustion model was not always given similar level of attention. More often than not, the engine was considered to be a stable source of hot gas to the turbine so that the performance of the turbocharger can be discussed in isolation. In the modern turbocharged engines which were frequently equipped with closed loop control, such isolation can often lead to inaccurate results.

As an example to explain such situation, an uncalibrated DIWiebe combustion model was applied to the engine model to be compared to quality of the aforementioned calibrated DIPulse model and the performance of both the engine and the turbocharger were shown in the Figure 4.5, and the zoomed version of the two plots in Figure 4.6 and Figure 4.7 which was followed by the error statistics in Figure 4.8.

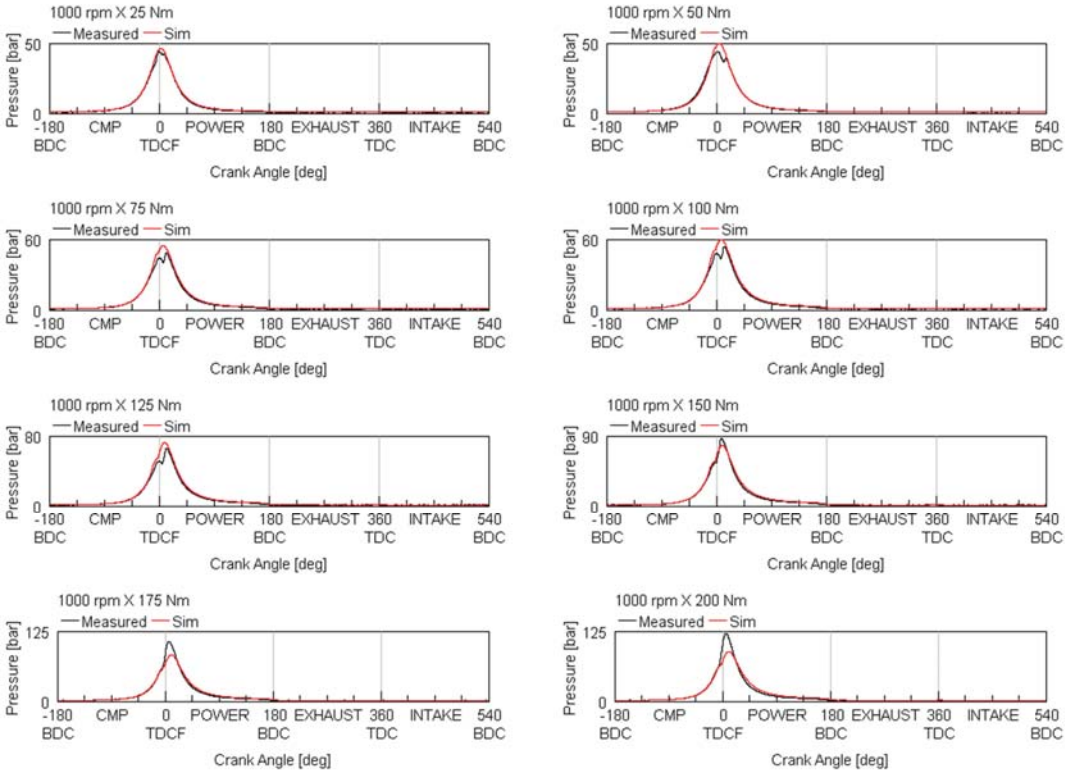

Figure 4.5 results from 1000 rpm in-cylinder pressure simulation plotted with test data showing the quality of uncalibrated combustion model

A closer look at the zoomed plots between crank angle -50° to 50° showed that the empirical model without calibration cannot adequately recreate the heat release rate of the combustion process. The resulting pressure trace was consistently wrong during the combustion. The simulated peak pressure appeared to be overestimated at low loads and underestimated at mid to high load above 150 Nm. Such discrepancy in prediction led to large discrepancy in the turbine inlet temperature and rendered the simulation results of the turbocharged engine unrealistic.

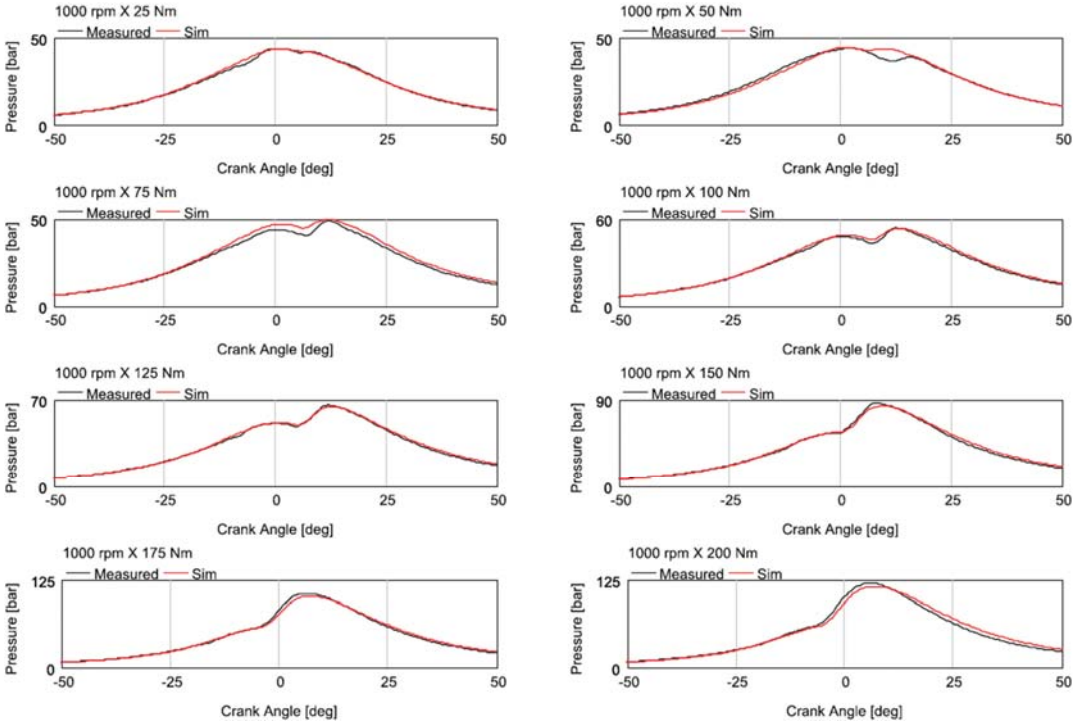

Figure 4.6 zoomed plot of Figure 4.4 showing the quality of calibrated combustion model

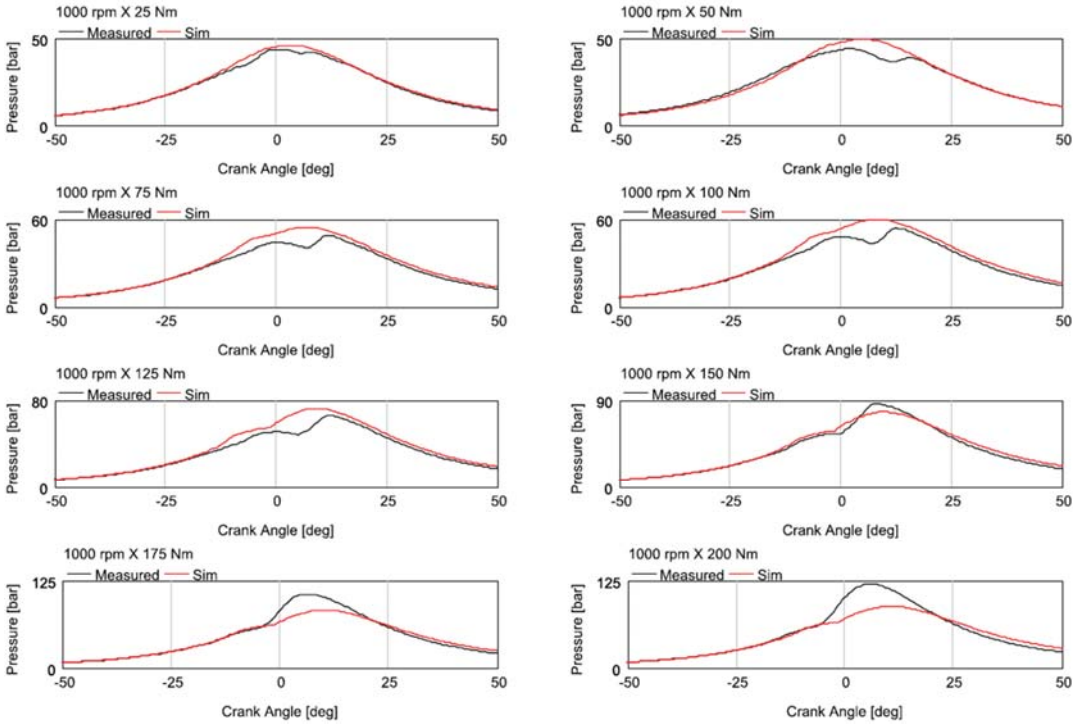

Figure 4.7 zoomed plot of Figure 4.5 showing the quality of uncalibrated combustion model

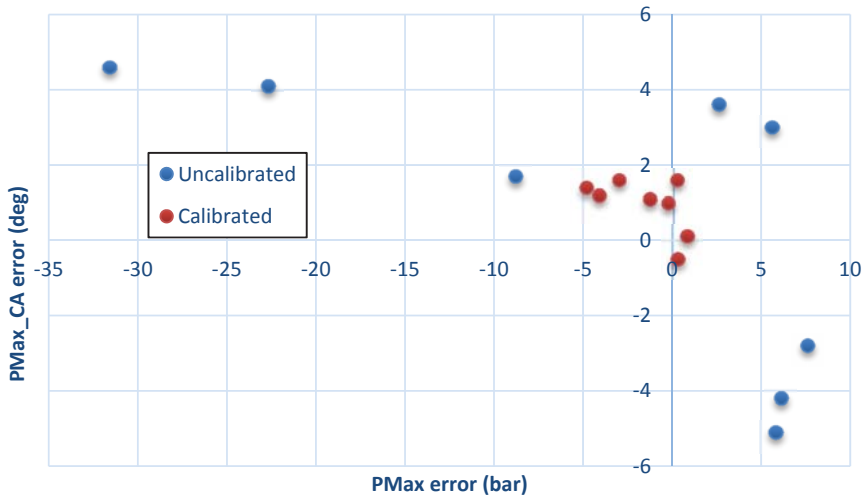

Figure 4.8 Error of PMax and PMax_CA comparison

4.5 Baseline model calibration results

To facilitate the subsequent research of turbocharging systems, the most relevant boundary conditions for turbine and compressor, i.e. engine gas exchange parameters were all in align with the test data after the calibration. As an example to illustrate the model quality, the test points of 2500 rpm are plotted in the following Figure 4.6.

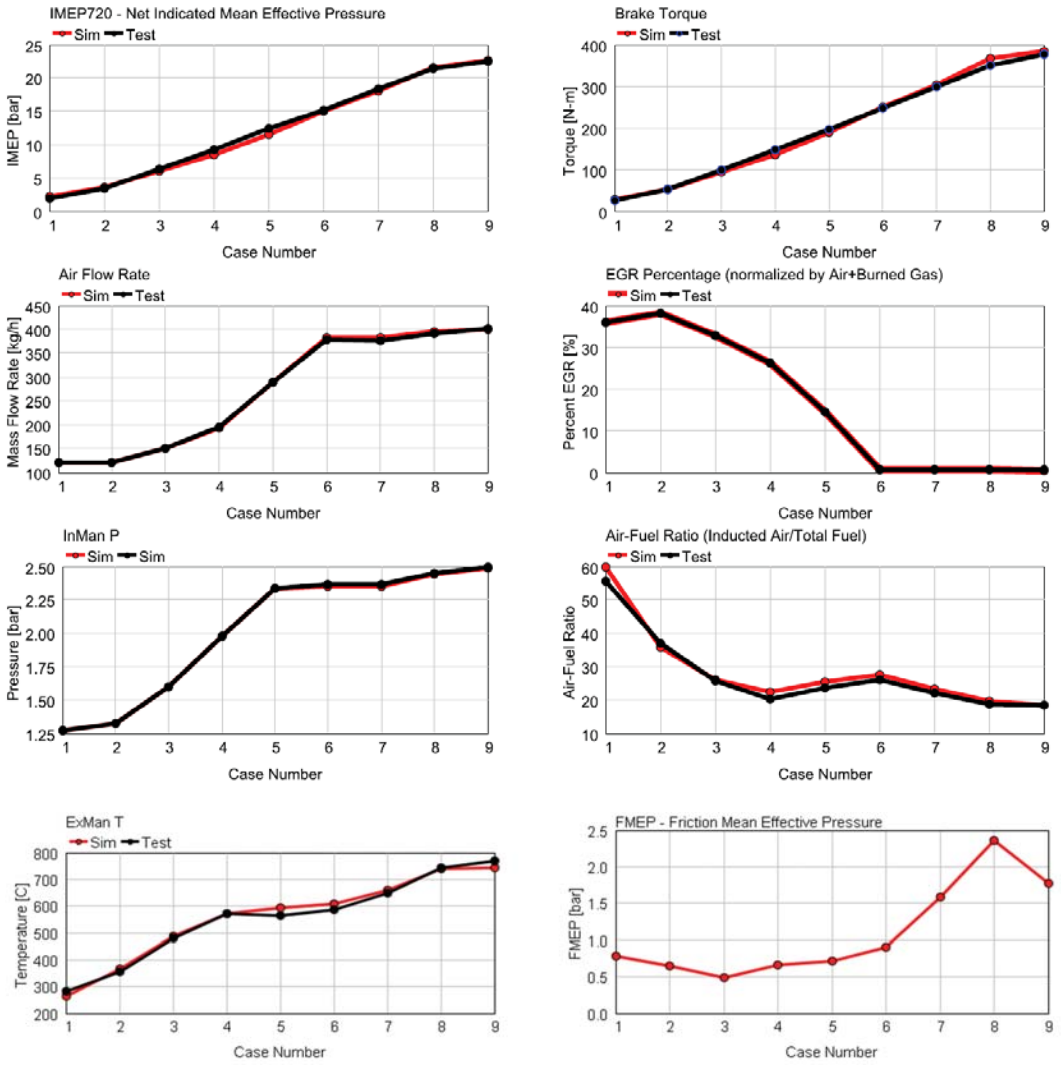

Figure 4.9 baseline engine model calibration results (2500 rpm) showed good matching in most of the relevant parameters

There were a few discrepancies to be noted in the seemingly good matching. One source of error came from the inaccuracies in test data. For example, although airflow was tuned to be almost identical to the test results through tuning of intake system pressure loss and valve lash, the ECU provided fuelling data did not match perfectly with the Air-Fuel Ratio measured by the emission analyser.

On the other hand, as discussed in the previous section, the fully predictive combustion model was considered a necessity for conducting turbocharging research with consideration of the system performance of the whole engine, such as EGR, variable boost and variable injection, etc. However, such predictive model does not guarantee a perfect representation of the combustion. For example, the in-cylinder convection factor had been tuned to match the exhaust manifold temperature test results to achieve the level of matching as shown in Figure 4.6 - ExMan T. However, such tuning should not exceed the reasonable range of physics and further tuning would unrealistically influence the predicted IMEP. Therefore the tuning factor range was limited within 0 ~ 1.2 as advised by GT-Power manual and matching of exhaust manifold temperature were not as good as the other parameters shown in Figure 4.6 and discrepancy as large as 30 °C had to be tolerated.

In addition, to match the torque number with a high level of accuracy, the FMEP curve was manually tuned as in the last plot in Figure 4.6. Although the general trend and data magnitude were acceptable, such a curve could not be perfectly correlated to a Chen-Flynn friction model.

To overcome these unsatisfactory matching between the simulation and the experiment results, with each turbocharger setting in this study, the models were matched to the available test results to the best possible matching quality without using unphysical changes to the model. The calibrated models were then used as the benchmark. The exploratory work in simulation would only be compared with the results from the benchmark model, instead of the test data.

4.6 Summary

This chapter focused on the modelling side of the project with the model methodology briefly explained at the beginning of the chapter. Using the engine geometries and the test results obtained as in Chapter 3, the baseline model was constructed and the quality of the calibration was demonstrated through comparing the test results and the simulation results. With a calibrated combustion model, the simulation results achieved a high level of accuracy compared to the test data, both in the in-cylinder pressure trace and the averaged parameters. In addition, the importance of the calibrating the combustion model was also discussed with comparison with an uncalibrated semi-predictive model.

Chapter 5 – Ball bearing turbocharger testing and simulation study

The aim of this chapter was to conduct a back to back comparison of journal and ball bearing technology both in experiment and in simulation so that the potential of ball bearing technology to improve the two stage system can be discussed in Chapter 8 with a solid theoretical background before two-stage-ball-bearing hardware became available. Two aerodynamically identical turbochargers were implemented on the test engine and modelled in Ricardo Wave. A series of experiments were then conducted covering part load, full load and transient conditions. Test results were then used to verify the model and in return the simulation was used to explore the issues observed in the experiments.

5.1 Ball bearing technology

The bearing system of a turbocharger is an important component not only because it is crucial for the dynamic balance of the high speed turbomachinery, but also it represents a pure energy loss in the transmission of power from the turbine to the compressor. In addition, it must be tolerant of the high thrust loading, oil contaminants, oil supply delay and hot shutdown. The conventional journal bearing solution sad been able to fulfil these stringent requirements and is the prevalent solution nowadays. On the other hand, the ball bearing system has significantly lower friction and has the potential to offer both better fuel economy and faster transient response. However, until the recent decade the high precision

requirement and the high cost had limited its application to niche products, large commercial vehicles and racing cars. After years of technical advancement, the technology has become mature enough to be supplied to the mainstream market; meanwhile the CO_2 emission mandate can well justify the higher cost for the technologies providing better fuel efficiency. A typical turbocharger ball bearing cartridge structure is shown in Figure 5.1.

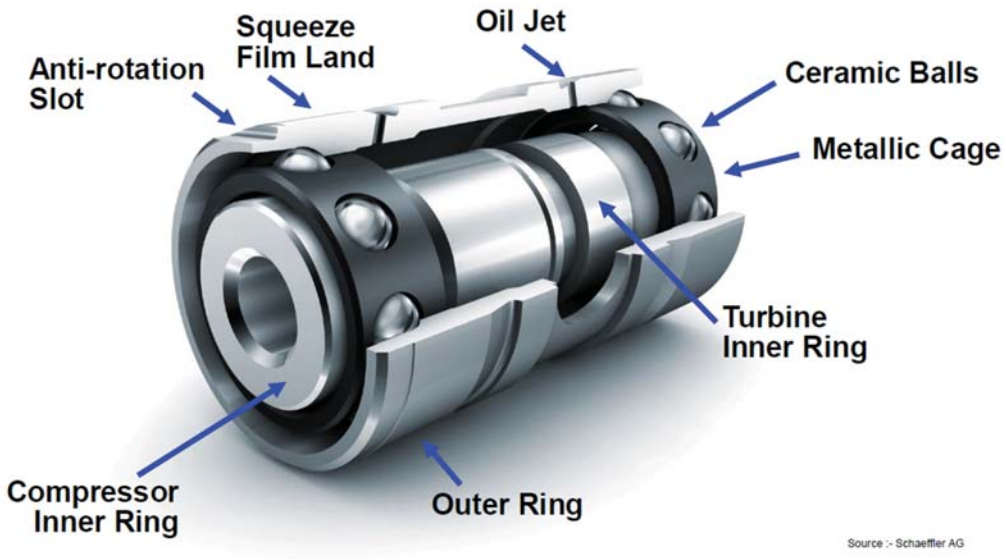

Figure 5.1 turbocharger ball bearing cartridge w/o outer ring (Davies, P. et al, 2013)

Compared to the conventional journal bearing cartridge, the turbocharger shaft was supported by the ball bearing assemblies instead of the floating metal bushes. This ensured much lower friction performance in a wide speed and temperature range. The ball bearing can also take the thrust load, eliminating the need for a separate thrust bearing which can further reduce the friction. The transient response, especially of the cold engine, was expected to be greatly improved. Fuel consumption can also have a moderate reduction due to reduced engine back pressure (Honeywell, 2013).

5.2 Ball bearing model

The characteristic efficiency map of the turbocharger turbine was commonly determined on a gas stand facility based on the measured enthalpy rise in the compressor (equation 5.1). It was determined in this way to avoid the effects of heat transfer in the turbine and was based on the assumption of adiabatic operation of the compressor which was justified at high operating speeds. However, as a consequence the turbine map included the mechanical efficiency of the bearing system.

$$\eta_{map,t} = \frac{\Delta \mathrm{H}_c}{\Delta \mathrm{H}_{s,t}} = \frac{\dot{m}_c c_{p,c}(T_2 - T_1)}{\dot{m}_t c_{p,t} T_{3'} \left(1 - \left(\frac{P_4}{P_3}\right)^{\frac{\gamma-1}{\gamma}}\right)}$$

(5.1)

Where,

$T_1 - Compressor\ inlet\ temp$
$T_2 - Compressor\ outlet\ temp$
$T_{3'} - Turbine\ inlet\ temp$
$P_3 - Turbine\ inlet\ pressure$
$P_4 - Turbine\ outlet\ pressure$

For the purpose of simulating a particular turbocharger on a particular engine, this was sufficient as the requirements were to estimate the overall transfer of power from the turbine to the compressor. However, in the context of this work which was focused on the benefits from a particular bearing system, the turbine map need to be corrected to represent only the aerodynamic performance; this was achieved through Equation 5.2

$$\eta_{s,t} = \frac{\eta_{map}, t}{\eta_{mech}}$$

(5.2)

The mechanical efficiency of the bearing system was determined by the ratio of compressor work to turbine work.

$$\eta_{mech} = \frac{\dot{W}_c}{\dot{W}_t} = \frac{\dot{W}_c}{\dot{W}_c + \dot{W}_{mech}} \tag{5.3}$$

Where $\dot{W}_c$ was defined by the numerator of equation 5.1 and $\dot{W}_{mech}$ was determined through the model developed at Valencia (Serrano, J. et al, 2013) which depended on the internal geometries of the journal and thrust bearings and the oil viscosity. This model was summarised in equation 5.4, but for full details the reader is directed to the original publication. The model has been applied to the manufacturer supplied map using the same conditions of oil temperature and viscosity rating under which the map was originally measured on gas stand. In this way a turbine efficiency map separated from bearing friction has been calculated.

$$\dot{W}_{mech} = K_{jb}\mu_{oil}{N_t}^2 + K_{tb}\sqrt[3]{\left|\frac{F_{ax}(P_{1,2,3,4})}{f(m_{Oil}\mu_{oil})}\right|}\mu_{Oil}{N_t}^2 \tag{5.4}$$

Where,

K_{jb}: $Journal\ bearing\ correction\ factor$
μ_{oil}: $Oil\ viscosity$
K_{tb}: $Thrust\ bearing\ correction\ factor$
F_{ax}: $Axial\ thrust\ force$

Previous studies of ball bearing friction (Griffith, B. et al, 2007; Brouwer, M. et al, 2013) suggest friction reductions of around 50% compared to journal bearings. Therefore, due to the lack of measured bearing friction data for the specific turbochargers used in this study, the

friction model introduced here will be applied to the 1-D gas dynamic model. It was expected that the error introduced by the friction model will only account for a small fraction of the errors by a 1-D model and that the simulation should, to some extent, allow us to look at different control logics that were difficult to check experimentally.

5.3 Experiment setup

The same 2.2L Diesel engine was used as the test engine. The default turbocharger and an updated turbocharger with a ball bearing cartridge were used, in turn, on the engine. In both cases, the only difference between the test setups was the turbocharger bearing while the engine calibration remained unchanged, which was initially intended to allow the back to back comparison of the two turbochargers. The engine controller had two key set-points of inlet manifold pressure and intake air mass flow rate; and the controller will adjust the VGT rack position and the EGR valve in order to meet these two targets.

As described in the previous chapters, the whole intake air - engine - exhaust gas path was monitored by paired temperature and pressure sensors at 40 ~ 80Hz. High frequency pressure measurements using Kistler sensors were taken at crucial locations such as the exhaust ports, post/pre turbocharger so that hot air pressure rise after transients and exhaust gas pulsation details can be recorded and analysed.

The same test plan as in the baseline engine experiments chapter was used to cover the most pertinent engine operating conditions, including:

- Limiting torque curve
    - The engine was tested for steady state full load torque at hot engine conditions.
- Cold start torque transients

- The engine was started from 15 °C and was controlled to enter into the full load transient schedule within 20s (time for the fuel beaker to settle).

- Hot engine torque transients
  - Same test as the cold start torque transients at hot engine conditions.
- Part-load steady state points generalized from combined WLTC/NEDC drive cycles (Figure 5.2).
  - The engine was tested for steady state part-load at hot engine conditions.

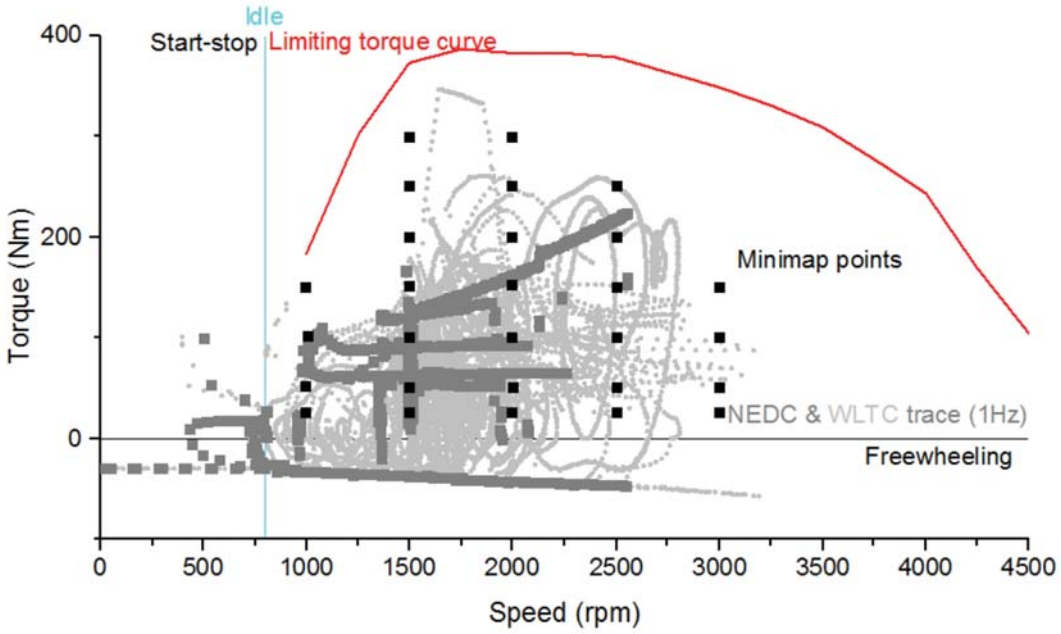

Figure 5.2 combined WLTC/NEDC minimap points

The part-load steady state points were selected to cover the operating range of the WLTC and NEDC drive cycle simulations using a representative vehicle.

Due to the limitation of the chapter length, only representative test results of each of the four tests are presented in the thesis.

5.4 Results and Discussion

5.4.1 Limiting torque curve

At full load, the ball bearing turbocharger did not give an apparent improvement to the engine torque performance. This was largely because the engine full load condition was often limited by factors other than the turbocharger performance (cylinder pressure, exhaust manifold temperature, etc). Therefore, with the same calibrated boost target, the air mass flow rates were similar and the full load torque was only improved up to 6 Nm at 2000 rpm, mostly from reduced pumping work because the engine back pressure was reduced by the ball bearing turbocharger. The averaged BSFC was consequently also only marginally improved. However due to the uncertainty brought in by the BSFC measurement, such improved fuel economy should not be taken as definite (Figure 5.3).

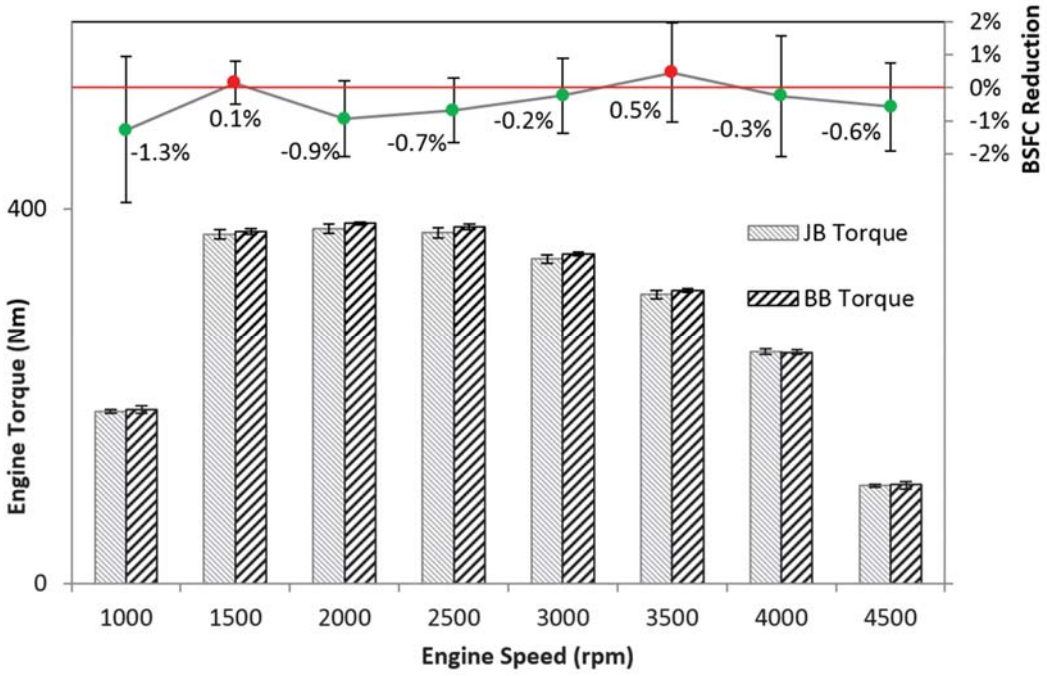

Figure 5.3 limiting torque comparison and BSFC reduction (Negative percentage -> Improvement)

5.4.2 Transient response

5.4.2.1 Cold torque transient

The cold start torque transient tests showed a clear advantage of the ball bearing turbocharger (Figure 5.4). The upper part of the plot showed that the ball bearing turbocharger started off with turbocharger speed 50% higher than the journal bearing turbocharger at low load and maintained a speed at least 10% faster at high load throughout the transient test. The result in torque performance was significant: the ball bearing turbocharger achieved 90% of the full load torque from the very first torque tip-in; whereas the journal bearing achieved only 75% and only reached 90% at the 6th transient. When looking at the first transient response only, the ball bearing T1090 torque rise was 2.7s faster than the journal bearing turbocharger, representing a reduction of 35%. Meanwhile, the torque transient of the ball bearing system also stabilised at a torque level of 40 Nm higher. It should be noted that the full load torque was the same for both turbochargers at this speed and the ball bearing turbocharged engine managed to achieve this torque level from the 5th transient, indicating a necessary warming up behaviour of around 250 seconds. In comparison, the journal bearing did not achieve its full load torque within the transient test period due to the much longer warming up period. It would only happen when the engine oil in the turbocharger is fully warmed up.

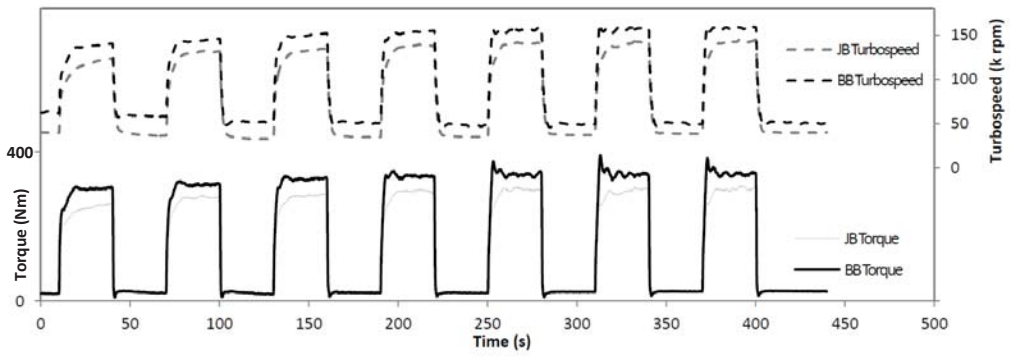

Figure 5.4 cold start torque transient at 1250 rpm and the turbospeed difference

5.4.2.2 Hot torque transient

In the case of a fully warmed up engine, the ball bearing turbocharger out-performed the journal bearing turbocharger in transient behaviour at low engine speed. However, the difference in shaft friction became smaller and the friction loss counts as a smaller proportion of the total work done by the turbine, especially at higher speed.

The transient response comparison at 1000 rpm was shown in Figure 5.5. It was clear that the ball bearing turbocharged engine responds faster than the journal bearing turbocharged engine. The time to 90% JB torque was reduced by 1.2s (41% reduction); and the ball bearing stabilized transiently with a torque level 14 Nm higher than the journal bearing.

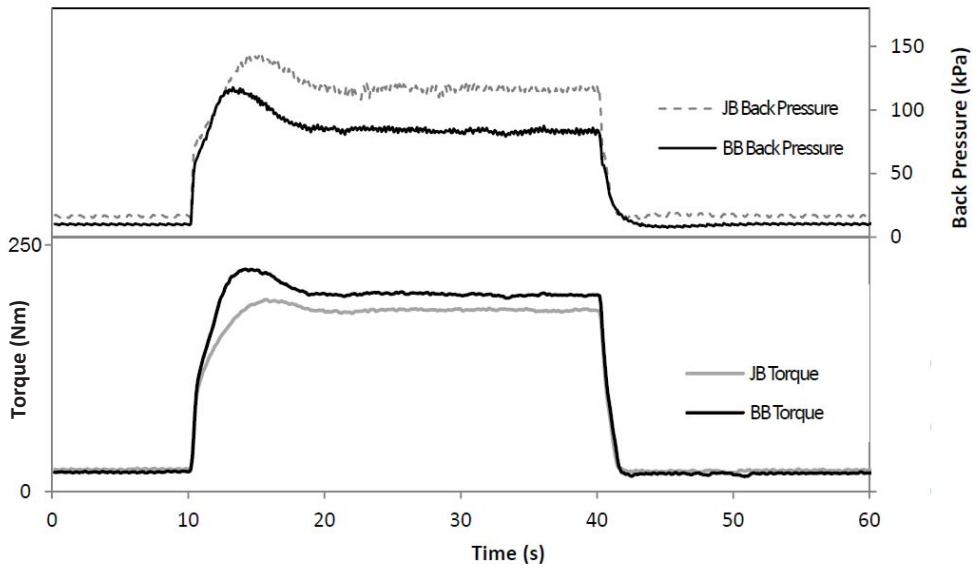

Figure 5.5 hot engine torque transient at 1000 rpm and the exhaust manifold pressure

In both cases, the VGT vanes were at the fully closed position before the transient. This was a calibration setting for the engine to generate high EGR gas at low engine load and to prepare a fast spinning turbocharger for the transients. At such conditions, the ball bearing turbocharger generated a lower engine back pressure. Therefore, the EGR valve in the ball bearing

turbocharged engine was more open to ensure that similar EGR rate can be achieved with the lower back pressure (EGR rate 44% compared to 42% for JB). Although with lower back pressure, the ball bearing turbocharger had a higher speed prior to the transient (35.8 krpm compared to 26 krpm): this led directly to the faster torque rise.

The transient response comparison at 1500 rpm was shown in Figure 5.6. Unlike at 1000rpm, the torque rises were very similar for ball bearing and journal bearing (even slightly faster with the journal bearing); and both reached the same stabilised torque (BMEP 21.5 bar).

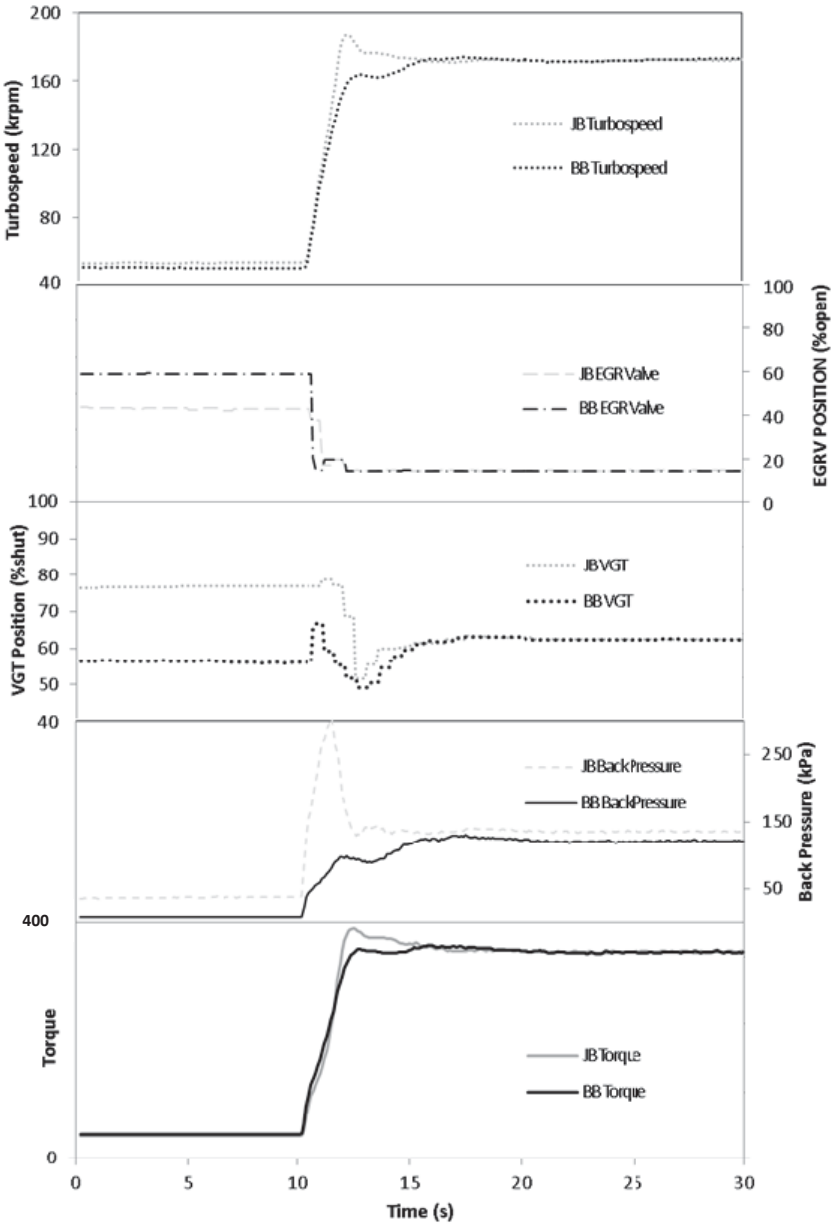

Figure 5.6 hot engine torque transient at 1500 rpm and relevant parameters

Before the transient, the ball bearing turbocharger was able to generate sufficient pressure in the intake manifold to meet the calibration target (VGT 58% shut compared to 78% for JB). The EGR valve was opened wider in the BB case such as to meet the EGR requirements (61% open compared to 42% for JB).

Compared to the 1000 rpm transient test, the exhaust energy was more abundant so that the more closed VGT vane position led to a higher turbocharger speed and back pressure for the JB turbocharger. When the transient happened, the journal bearing turbocharger had faster exhaust pressure build up to accelerate the turbocharger and therefore to provide boost. The overshoot in turbocharger speed and boost also led to an obvious overshoot in torque in the journal bearing transient test. In terms of the torque rise, the benefit of higher back pressure with the journal bearing turbocharger balanced the benefit of lower shaft friction and lower pumping work of the ball bearing turbocharger, therefore the equivalent similar transient performance. However, when considering the exhaust manifold component durability, fuel consumption and controllability, ball bearing turbocharger was the better option.

5.4.3 Part-load points fuel consumption

The part-load quasi steady drive cycle tests can be seen as a crucial indicator of the engine fuel consumption. However, when the test results reveal that the ball bearing turbocharger gave a large fuel consumption benefit, it was clear that without re-calibrating the engine for the ball bearing turbocharger, it was very difficult to generate a convincing engine fuel consumption performance in the drive cycle part-load test.

Figure 5.7 showed the raw fuel consumption benefits for the range of engine loads at 1500 rpm resulting from the back to back comparison of the two turbocharger bearing technologies. These differences are between 3-11% improvement through changing the turbocharger rotor and it was clear that this benefit was not solely a result of reduced turbocharger friction, but in reality due to interactions with other engine systems.

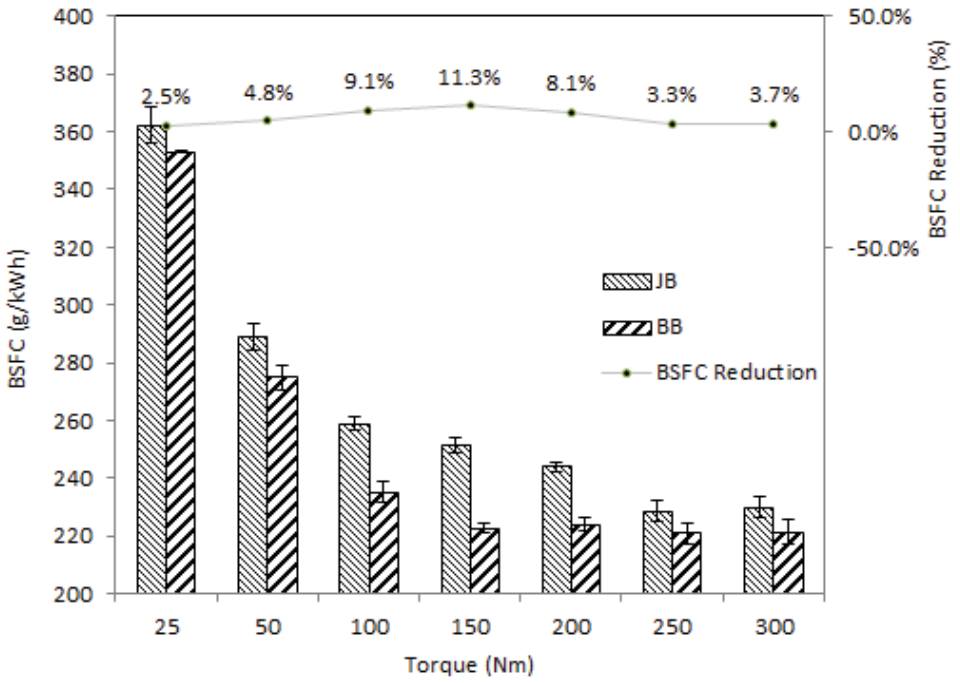

Figure 5.7 BSFC comparison of minimap points at 1500 rpm (Positive percentage -> Improvement)

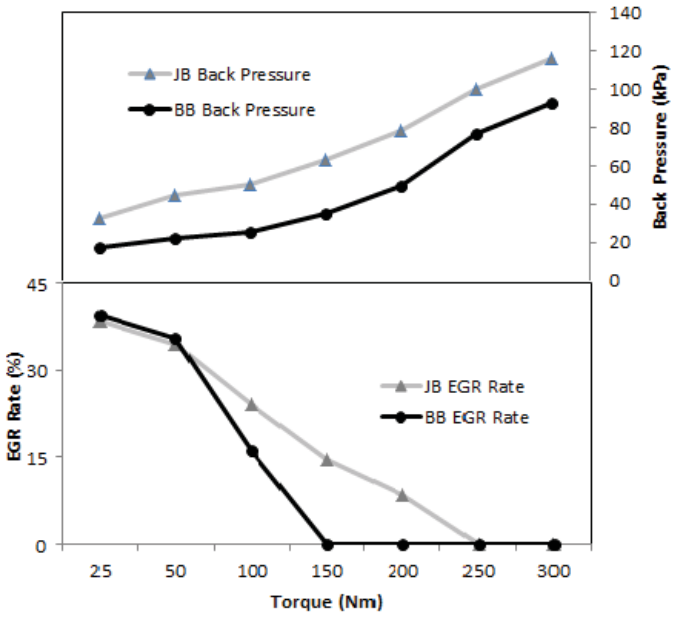

Figure 5.8 back pressure and EGR rate difference between JB and BB equipped engine at 1500 rpm

Figure 5.8 showed the impact of the turbocharger bearing on back pressure and EGR flow. The back pressure was reduced across the load range by 15 - 29 kPa. This reduction in engine back

pressure had a significant effect on EGR rate, notably between 50 Nm and 250 Nm where the largest fuel consumption gains were made. This reduction in EGR rate of up to 15% points would have a large impact not only on fuel economy, but also on NOx emissions

According to the research on the diesel engine back pressure (Hield, P., 2011) and EGR rate (Van Aken, M. et al, 2007), for every 1 Bar of increased back pressure, the BSFC penalty was around 50 g/kWh; while for 1% of EGR rate, there will be a BSFC increase of around 0.3%. In the light of such previous research, a crude calculation of the acquired BSFC benefit through back pressure and insufficient EGR flow was illustrated in Figure 5.9.

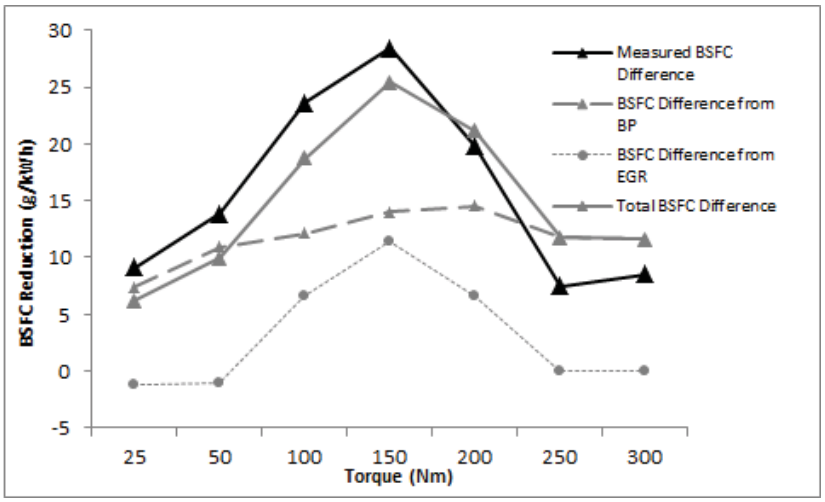

Figure 5.9 BSFC reduction analysis compared to measurement

In Figure 5.9, the expected BSFC reduction correlated reasonably well with the measured BSFC reduction (Total and Measured BSFC Difference). This analysis allowed a crude isolation of the fuel economy benefits due to higher efficiency of the turbocharger and reduction of the EGR flow, with a prediction of 5 - 15 g/kWh benefit in fuel consumption from the reduction in back pressure, and up to 10 g/kWh from reduced EGR rate.

Figure 5.10 was a compiled graph of the rest of the part load points at 1000 rpm, 2000 rpm, 2500 rpm and 3000 rpm. The trend was consistent with the analysis concluded from 1500rpm, with the more EGR reliant points showing large BSFC benefits (mid load, mid speed).

It should be noted that such BSFC reduction was of limited practical use as the engine would still be required to meet NOx emission target which would require the similar EGR level as the JB configuration. Meeting such requirements would involve the complete re-optimisation of the engine controller, notably changing the targets for boost pressure and EGR flow based on the emissions/fuel economy trade off. However such a study is beyond the scope of this project.

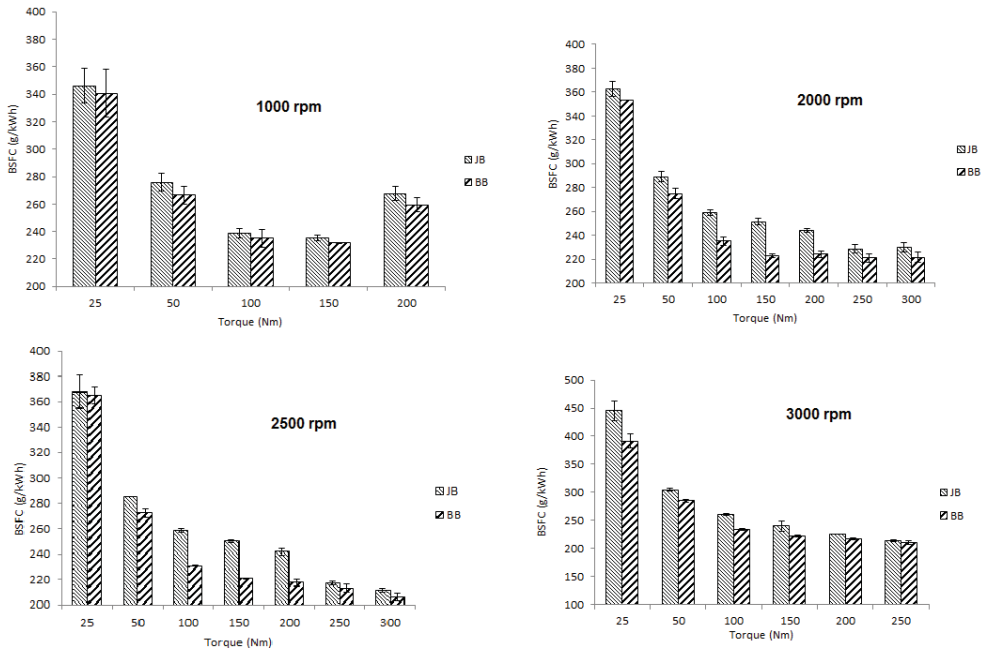

Figure 5.10 BSFC comparison of minimap points at 1000 rpm, 2000 rpm, 2500 rpm and 3000 rpm

Although a fair comparison was intended between the two turbochargers, it was later realized that a perfect back to back comparison was near to impossible in the case of the engine-turbocharger system: any parameter changed would have a chain effect on the parameters in the engine-turbocharger loop. The dilemma suggested yet an optimal solution: by choosing a

slightly smaller turbo-machinery, the higher back pressure was expected to be able to drive the EGR gas back to the inlet manifold which was not so highly boosted. The transient response could be further improved in the meantime.

Ideally the engine should also be recalibrated for the newly fitted ball bearing turbocharger. However, this process was not permitted in the time span of this project. Therefore, it was decided that the engine calibration remained unchanged for both turbochargers. As the result, the experiments gave a comparatively conservative demonstration of the benefit of the ball bearing turbocharger as the calibration was optimized only for the original journal bearing turbocharger. Therefore, the simulation study was designed to cover some of the weakness of the experimental study.

5.5 Simulation study

Since the time and calibration effort required to perform a perfect back to back comparison of the ball bearing and journal bearing device are not allowed in this first phase of the project, a simulation study was conducted in the Ricardo Wave environment using model of the 2.2L Diesel engine. The journal bearing turbocharger was modelled by characteristic maps of the compressor and turbine, supplied by the turbocharger manufacturer; and turbine map was adjusted using the Valencia model to represent the higher efficiency of the ball bearing turbocharger. The model was run in co-simulation with Mathworks MATLAB Simulink to allow a high level implementation of the engine controller software and was calibrated using both high and part load engine operating conditions running up to 3000 rpm.

5.5.1 Hot torque transient simulation

The transient simulation involved improving the 1500 rpm ball bearing turbocharger torque response. It was observed that the ball bearing turbocharger produced slower torque rise at higher speed compared to the journal bearing due to the fact that the more efficient ball

bearing turbocharger rested in lower turbocharger speed compared to the journal bearing turbocharger. Therefore, the boost target of the ball bearing turbocharged engine was adjusted to a higher value at low load, so that the VGT will be at a more closed position to prepare for the torque tip-in. The simulation result is illustrated in the Figure 5.11.

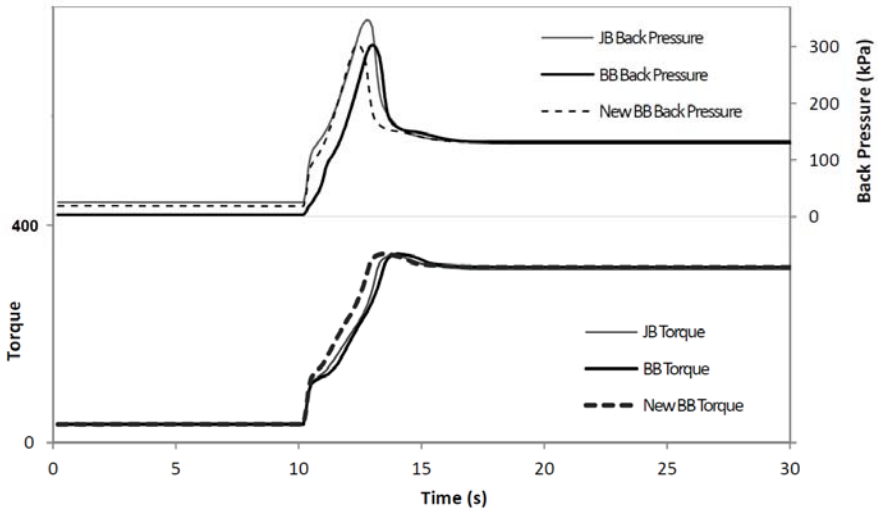

Figure 5.11 simulated hot engine torque transient at 1500 rpm and the exhaust manifold pressure

As shown in the Figure 5.11, with a higher boost target, the ball bearing turbocharger generated a similar level of engine back pressure which implied a similar turbocharger speed. As a result, the torque generated by the ball bearing turbocharged engine has the fastest climb compared to the baseline engine and the ball bearing turbocharger running the original engine calibration. This suggests that an engine re-calibration would benefit the ball bearing turbocharged engine in the transient performance in a wider speed range.

5.5.2 Part-load points simulations

The part-load minimap simulation focuses on the 1500 rpm engine speed that produced overestimated fuel consumption benefits. It was pointed out in the analysis in section 5.3 that when running the ball bearing combined with original engine calibration, the engine will not

achieve the EGR rate required for emission control. Therefore, the simulation was designed to achieve the EGR rate targets instead of the mass flow targets and the results were supposed to reveal the true fuel consumption benefits can be achieved by implementing a ball bearing turbocharger on the assumption that similar EGR rate level would produce similar level of NOx emission. To ensure an as accurate as possible prediction of this steady state fuel consumption simulation study, the original journal bearing turbocharged engine model was especially calibrated manually for the FMEP of each selected brake torque. The results were shown as in the Figure 5.12 below:

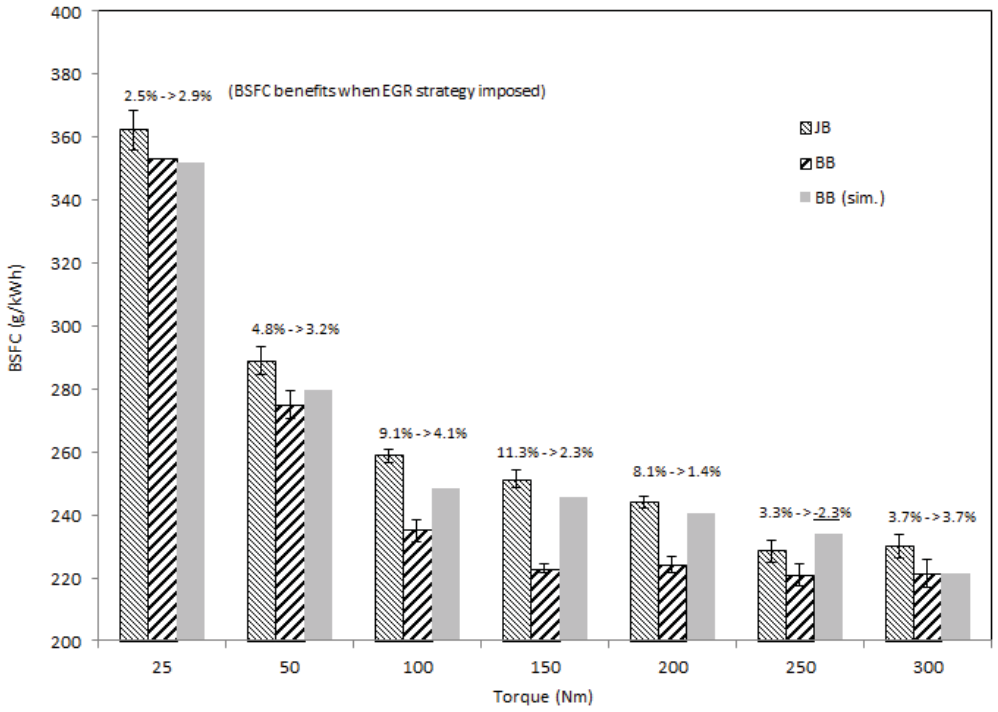

Figure 5.12 simulated BSFC comparison of part-load points at 1500 rpm (Positive percentage -> Improvement)

With a similar level of EGR rate, the engine was expected to produce a similar level of NOx emission. In terms of the fuel consumption as demonstrated in Figure 5.12, the averaged fuel consumption benefit of the ball bearing turbocharger settled to a more reasonable 2.5% BSFC reduction (without the 250Nm negative result taken into account, where the EGR controller

went into instability). The results were also in line with the theoretical fuel consumption benefit from lowered engine back pressure that was discussed in the section 5.4.3.

5.6 Summary

In this chapter, a novel turbocharger equipped with ball bearing rotor was installed on a production engine to evaluate the benefit of using a novel rotor bearing in terms of fuel economy and engine transient response. An aerodynamically identical journal bearing turbocharger was also tested as the benchmark.

The test and simulation results showed that

1. There is a significant benefit of cold start transient response can be gained by implementing the ball bearing turbocharger.
2. Large fuel consumption benefits can be seen when running part-load steady state tests because of the interactions with the EGR system.
3. Simulation results showed that with small modifications to the engine control strategy, fuel consumption benefit of 2.5% could be gained.
4. An engine control system re-optimisation is needed to make a true back-to-back comparison.

The content in this chapter was published in:

Zhang, Q., Capon, G., Davies, P., et al., 2014. Experimental and Analytical Investigation of Implementing a Ball Bearing Turbocharger on a Production Diesel Engine. In: 11th International Conference on Turbochargers and Turbocharging, Paper 0053

Chapter 6 – Two stage turbocharging simulation study

This chapter was intended to understand and characterise the series-sequential two stage turbocharging system through an extensive simulation study before the hardware was available. Using the calibrated baseline 1D engine model, the two stage charging system was implemented by inserting two pairs of differently sized turbocharger maps. A sweep simulation of turbocharger size was conducted to decide on the perfect match of turbochargers to the 2.2L Diesel engine. Then a control valve sweep simulation was conducted to find the best control strategy of the charging system at engine full load operation. Based on these simulation results, the control strategy for the whole engine operating range was proposed with consideration of limiting torque expectancy, fuel efficiency and transient performance. The control strategy will be used in the following chapters to test and further improve the two stage system.

6.1 Two stage system

Matching of a sequential turbocharging system to a diesel engine allowed more flexibility but was not a simple task. The HP stage should be able to provide the necessary air flow and boost pressure at low engine speed to meet vehicle performance attributes such as vehicle launch and overtaking performance. In the engine mid-speed range when the turbochargers boost the air in the two stage mode, the work shared between the HP and LP stage is critical to the

optimal engine performance and therefore the control of the system via bypass valves and wastegates, etc. is a key factor. At high engine speed, the phasing out of the HP stage is also critical to avoid undesirable perturbations to the engine full load torque characteristics. The ever increasing pressure losses due to air duct packaging, charge air and exhaust system updates also exacerbates the difficulty of matching a two stage boosting system. In addition to the engine breathing requirement, a group of limiting factors should also be considered due to the higher boost capability and the more complex turbocharging scheme of two stage system, including engine limitations (peak cylinder pressure, turbine inlet temperature, fuelling limit and smoke number) and turbocharger limitations (compressor outlet temperature, surge margin, choking, engine back pressure and turbocharging efficiency during mid to high flow conditions) (Watson, N. and Janota, M., 1982). When an optimal match of turbochargers is found, an existing engine will need to be recalibrated to be able to utilize the full potential of two stage turbocharging. The process should be done in an iterative manner to finalize the engine-turbocharging system matching.

When a matched engine-turbocharging system is available, characterization of the system is a necessary step towards an optimal control strategy. Research to determine how the valves should be scheduled at full load so that both engine performance and fuel consumption are benefited can be highly informative. However, both the matching and the characterization processes are time and resource consuming if to be done experimentally. Therefore, a 1-D gas dynamic model was used in this phase of work and experimental work will be done in the next phase of the project to validate the simulation study.

The control of the two stage turbocharging system is crucial. The quality of the controller not only decides how well the potential of the two stage arrangement can be exploited, but the turbochargers and the engine could also be seriously damaged if it not designed properly.

Within the safe boost region, control strategies can be implemented to achieve the best steady state fuel consumption and transient performance.

In the first phase of the study, the 1-D gas dynamic model created for the Puma 2.2L engine was used to conduct the study proposed. There were in total three sets of simulation to characterise the system: (1) the turbocharger size simulation confirmed the expected relationships between the turbocharger size and the low speed end transient performance (HP) and mid to high speed end fuel consumption (LP). The small unit size largely determines the launch performance and the bigger unit size is crucial for achieving best fuel economy at rated power. (2) The valve mapping simulation showed the optimal operating scheme of the exhaust bypass valves which ensures both low fuel consumption and engine safe operation at the limiting torque curve and suggested the end position of each valve along the constant engine speed line. (3) The VGT and two stage arrangement comparison simulation showed the advantage of using two stage turbocharging over the single stage VGT turbocharger in terms of fuel consumption, launch performance and EGR potential for NO_X reduction. After understanding of the system through the characterisation simulation, the control strategy was proposed to effectively boost the engine with improved performance in both the fuel consumption and the transient performance.

6.2 Model and System

The same 2.2L direct injection VGT-turbocharged diesel engine was used as the baseline model. The investigated two stage system was governed by three valves: a turbine bypass valve (TBPV) and a passive compressor bypass valve (CBPV) controlled a high pressure stage free floating turbocharger (HP), while the low pressure stage (LP) was controlled by its own wastegate (WG) as shown in Figure 6.1.

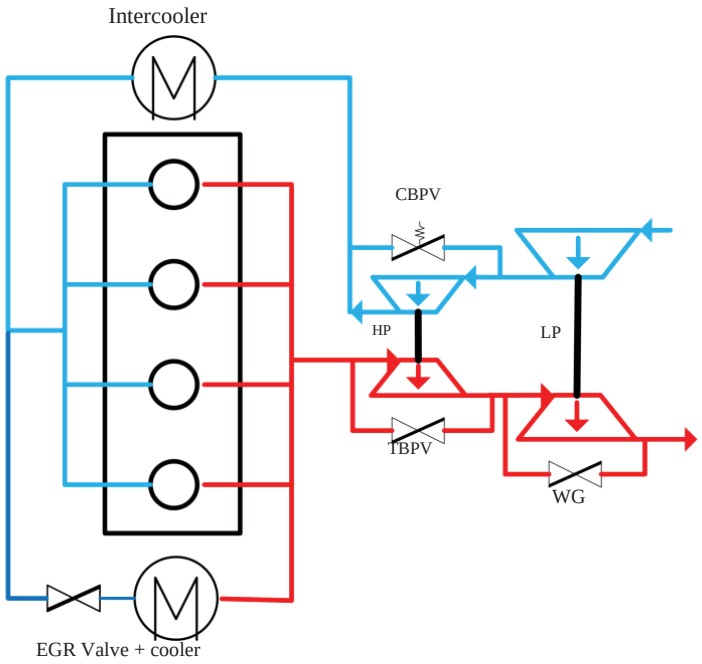

Figure 6.1 system schematics of the two stage turbocharged engine

The engine model was constructed in Ricardo Wave environment and was calibrated for both full load and part load conditions with a particular focus on providing high fidelity exhaust flow in the whole engine operating range. The turbocharging system in the form of the turbine and compressor maps of two differently sized turbochargers was then connected to the calibrated model in the place of the original VGT turbocharger.

A Matlab/Simulink model was constructed as a co-simulation environment to manage the inputs and outputs of the engine model as shown in Figure 6.2. To facilitate future testing work, the modelling and simulation process was designed to represent the realistic situation of installing a two stage system on a production engine: the engine strategy was replicated in the Simulink model to provide the high fidelity ECU control signals; various protective engine limiting parameters were maintained so as to avoid generating simulation results which cannot be verified experimentally; with the exception of those turbocharging-related engine maps being modified, such as an enhanced boost target map, so as to demonstrate the boosting

capability of the two stage system; hot engine condition was assumed throughout the simulation so that the thermal condition related corrections from ECU strategy were minimal.

There are, however, several points to be noted with regards to the simulation works undertaken.

In calibrating the engine model, both the limiting torque across the engine speed range and the low to mid-speed part load test results were used. Pressure and temperature across the air path and exhaust path were matched by calibrating the pressure loss and heat transfer of the ducts and heat exchangers. The combustion model was limited in accuracy due to the use of a semi-predictive Wiebe function combustion model for the EURO 5 multi-injection combustion system. However, by correlating the volumetric efficiency and exhaust port temperature/pressure using heat transfer coefficients and combustion delay parameters, the cylinder in/out gas condition was matched with high fidelity. Therefore the model was considered to be a good starting point for predicting turbocharger-engine interaction. Accuracy of the full load simulations using two stage system was highly dependent on the capability of the Wiebe function model to extrapolate. However, the robustness that the Wiebe function showed in part-load prediction indicated that at least the trend of prediction was trustworthy.

The engine ECU strategy proved to be an obstacle in the way of fully exploiting of the two stage system in simulation. For example, the calibrated injection timing correction would react disruptively to the lack of boost pressure during a transient performance, with which the combustion model was not able to cope well. In spite of these shortcomings, they were considered unavoidable compromises and many were reproducible in the tests so that the simulations and tests were comparable.

The EGR was not enabled for full load operations. Ideally, part-load simulation would benefit from using EGR. However, using uncalibrated EGR rate could allow burned gas more than

needed in the cylinders and thus un-calibrated combustion will occur and produce unreliable results. It was decided that EGR was disabled throughout the sizing and valve mapping simulations so that sizing simulations are comparable to each other. However, the potential of using higher EGR rate in series sequentially charged engine was demonstrated in the two stage-VGT comparison simulation.

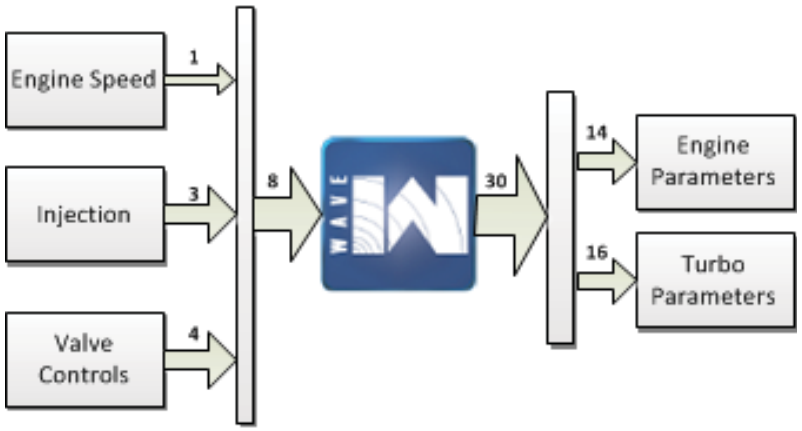

Figure 6.2 schematics of the co-simulation environment (with numbers of channels overlaid on arrows)

6.3 Simulation and Results

6.3.1 Turbocharger size simulation

The turbocharger size simulations aimed to demonstrate the effects of different size combinations of the two stage arrangement on engine performance and fuel consumption. The turbocharger sizes were chosen around a production two-stage system which is to be tested later. As a production unit, the initial size set was assumed to be a good match to each other and to the engine. The effective diameters of each stage were up-scaled or down-scaled

by a factor of 0.8 to 1.2 in turn to show the influences of the differently sized stages. The compressor operating areas were plotted below in Figure 6.3 and Figure 6.4 to give a clear picture of the sizing sweep simulations conducted.

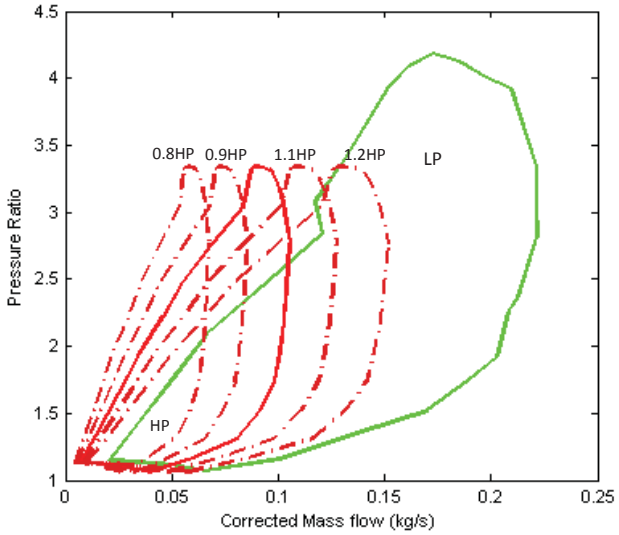

Figure 6.3 HP unit compressor map with several scaled units overlaid on the LP unit compressor map

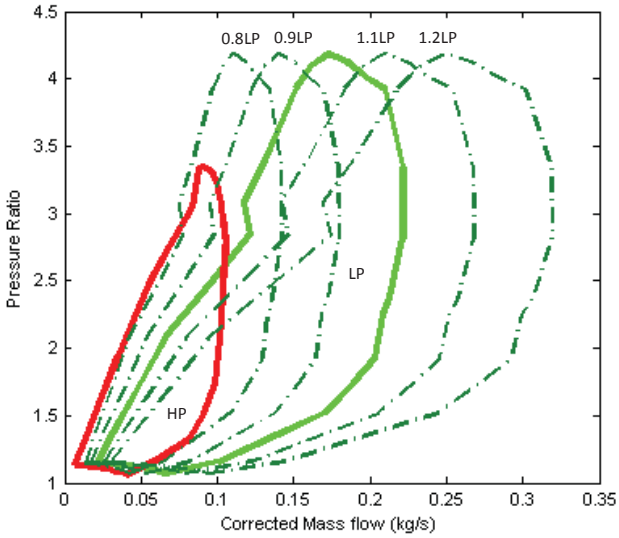

Figure 6.4 LP unit compressor map with several scaled units overlaid on the HP unit compressor map

Simulations as such were based on the assumption that the shaft inertia was proportional to the fourth power of turbocharger effective diameter and that compressor maps can be directly scaled without major deviation of the efficiency prediction.

6.3.1.1 Full load steady state simulations

Full load steady state simulations and transient torque tip-ins have been implemented for a series of constant speeds. For the VGT engine, the limiting torque curve was decided experimentally, which involves pushing the engine to its limits, including mechanical damage limits, smoke emission limits, turbocharging limits with reasonable fuel consumption. The simulation work with regards to the mechanical limits and smoke limits as hard limits which are not to be breached, including in-cylinder pressure, turbine inlet temperature, air fuel ratio. One the other hand, the turbocharger limits, such as boost target and mass air flow, was moderately increased and back pressure limit was slightly relaxed so that the benefit of using a novel charging system can be demonstrated. The results are shown below from Figure 6.5 to Figure 6.14 and will be analysed respectively.

In the full load steady state simulation, an enhanced boost target map allows differently sized turbocharger to boost the engine to their full potential. Under the same smoke limit air fuel ratio (as of the VGT engine), the best sized turbocharger was able to better utilize the exhaust energy to generate higher boost to deliver more air flow which determines the maximum fuel limit. With more fuel being injected, more exhaust energy was available to the turbocharger which further increased the boost. This amplifying loop continued until the engine limits are imposed or the turbocharger was balanced at a point where further increase in exhaust energy would move the operating point away from the high efficiency contour and boost pressure was reduced.

In the HP unit size scaling simulation, the engine torque varied by approximately 30Nm for a scaling +/-20% of nominal size (Figure 6.5), however these differences reduced at engine

speeds above 2750 rpm, where the HP was bypassed. In the low to mid speed range, larger HP size enabled higher limiting torque because lower turbocharger speed was allowed and less energy was required to drive the turbocharger. However, too big an HP unit failed to utilize available exhaust energy (HP1.2 at 1000 rpm) and too small a HP acts as a throttle to the engine (0.8HP at 1250 to 2250 rpm). The sudden improvement of 0.8HP at 2500 rpm was due to its phasing out by a back pressure limiter. The detailed two stage system control strategy is explained in the control strategy study section.

It can also be observed from the simulation that the sequential turbocharging greatly enhanced the low to mid-speed range limiting torque. Compared to the red line which was the engine test bench calibration data, the engine limiting torque in this region was improved by at least 15%, with even more torque possible if the simulation was not limited by an ECU torque limiter for engine protection.

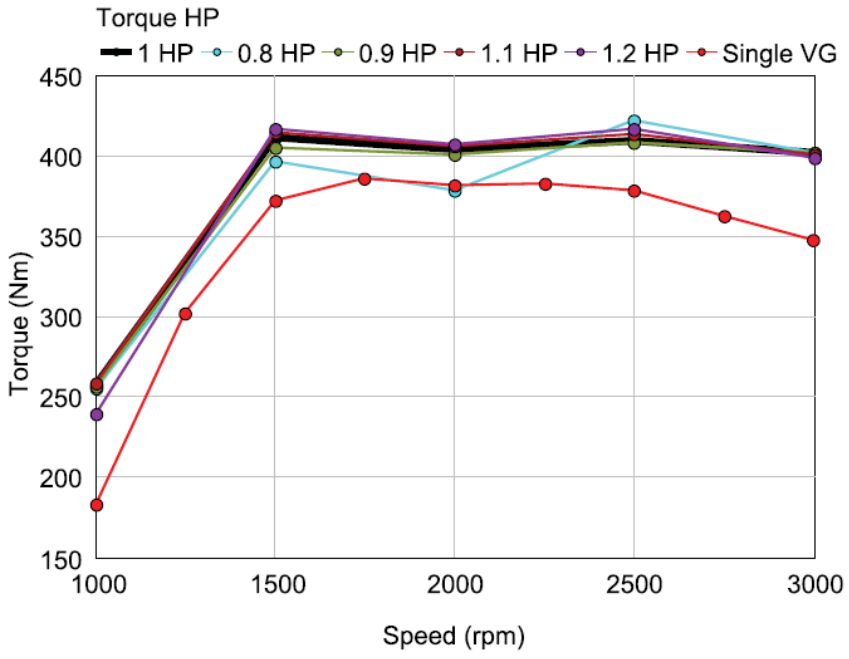

Figure 6.5 HP unit size scaling simulation (with baseline LP unit): full load steady state torque

In the LP unit size scaling simulation (Figure 6.6), the full load curve was, as expected, not much influenced by different LP units at low speeds. After 2500 rpm, however, the engine became more sensitive to the LP unit sizes. It was clear that the original LP unit was almost the optimal size in terms of full load performance as the unit sizes smaller or bigger than the LP could not achieve better performance over the whole speed range.

The gap between the two stage system and the VGT system reduced as the VGT comes to its high effeciency region while two stage is losing exhaust energy through wastegating.

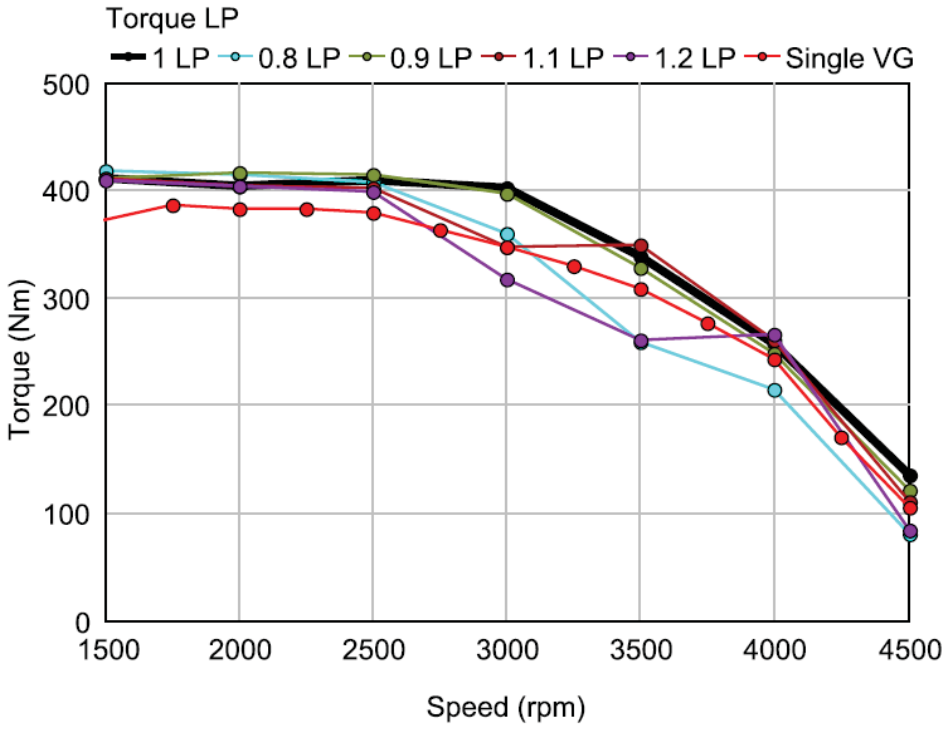

Figure 6.6 LP unit size scaling simulation (with baseline HP unit): full load steady state torque

As can be easily reasoned, the HP unit would influence the brake specific fuel consumption (BSFC) mostly at low to mid-speed region while the LP unit at mid to high-speed range.

It can be observed in Figure 6.7 that the bigger HP units offered BSFC benefits at low to mid-speed range with the exception at 1000 rpm where the HP1.2 could not provide enough boost. Again, sudden improvement of HP0.8 at 2500 rpm was due to its phasing out of the gas paths.

The saw toothed BSFC profile of the Single VG has been due to the combined effect of ECU calibration and experiment data uncertainties.

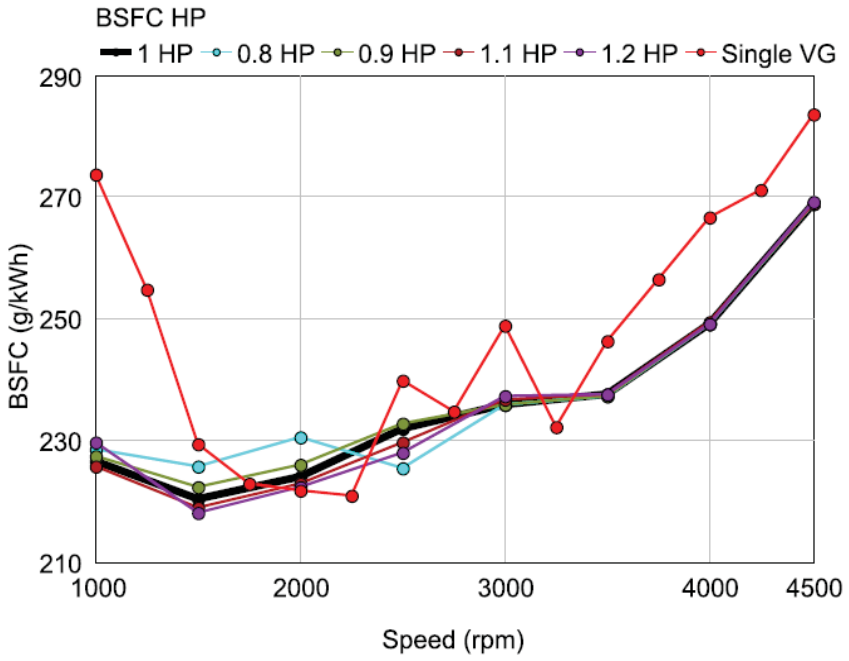

Figure 6.7 HP unit size scaling simulation (with baseline LP unit): full load steady state BSFC

The LP unit size was a strong factor to the high speed full load fuel consumption. As shown in the Figure 6.8, the original LP was proved to be the best selection, offering good fuel consumption over a wide range while bigger and smaller turbochargers struggled to maintain low fuel consumption at higher engine speeds. The smallest 0.8 LP went into choke region due to the extremely narrow flow range the compressor offered (see Figure 6.9 right end dots of the red line).

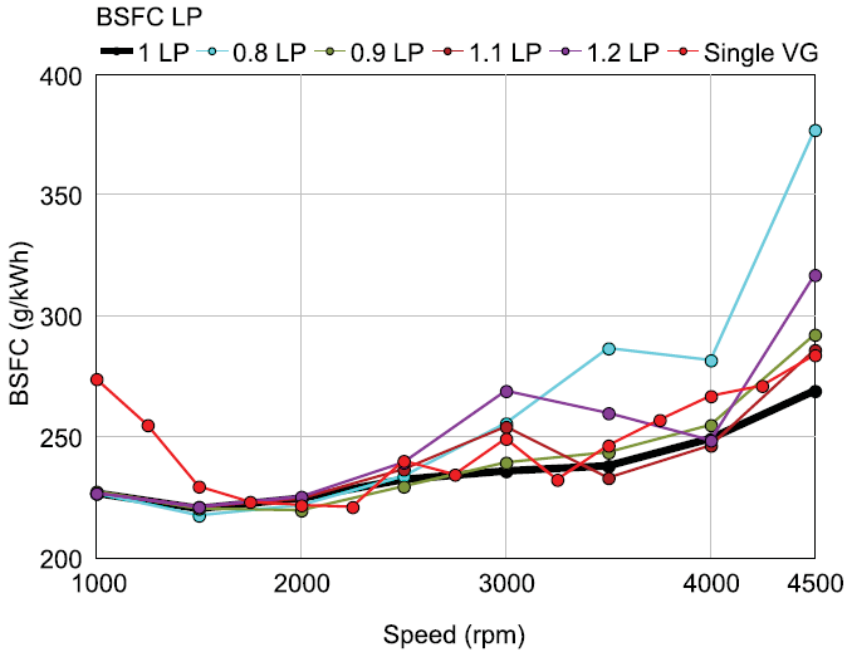

Figure 6.8 LP unit size scaling simulation (with baseline HP unit): full load steady state BSFC)

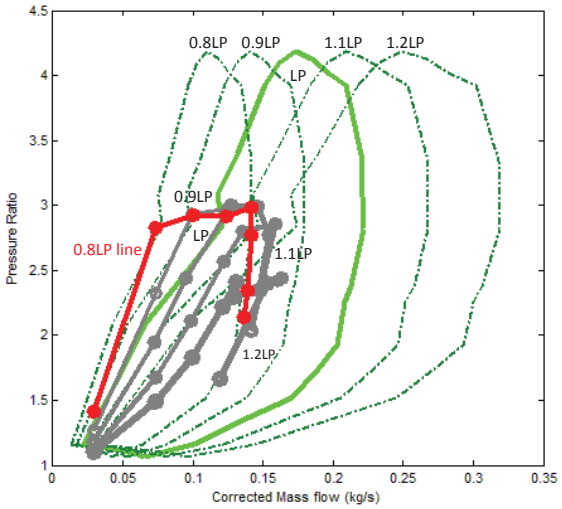

Figure 6.9 Scaled LP unit compressor maps with limiting torque operating points overlaid, 0.8 LP red line goes to the right of the choke line of 0.8 LP map

It should be noted that the scaling of the LP unit was more considerable because a wider flow range was being scaled proportional to the second power of diameter scaling factor. As the

simulation showed the original LP size to be clearly the optimal one, a finer scaling of the LP unit was expected to demonstrate an closer comparison.

6.3.1.2 Transient simulations

The transient simulation was implemented using the engine strategy; with the injection timing sometime plays a disrupting role when it reacts poorly to the sudden change in boost and indicated torque. The influence of the unit size on the transient performance was nevertheless still perceptible. As shown in the transient simulation in Figure 6.10 at 1000 rpm engine speed, a smaller scaling factor offered faster torque reaction which means faster vehicle launching from stand still. HP was able to achieve peak torque within 2 seconds while a bigger 1.1HP took 2.1 second.

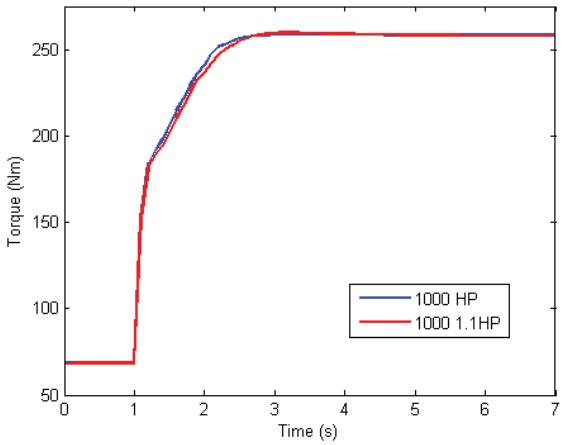

Figure 6.10 HP unit size scaling simulation (with baseline LP unit): torque transient at 1000 rpm

The discrepancy of transient performance increase as more exhaust energy becomes available, as shown in Figure 6.11 at 1500rpm. However, the transient time gap disappeared when exhaust energy was enough to bring LP compressor into its high pressure ratio speed (Figure 6.12). It is worth noticing that before the transient happens, the engine with the smaller HP unit stabilised at a lower torque due to the throttling effect of the small HP.

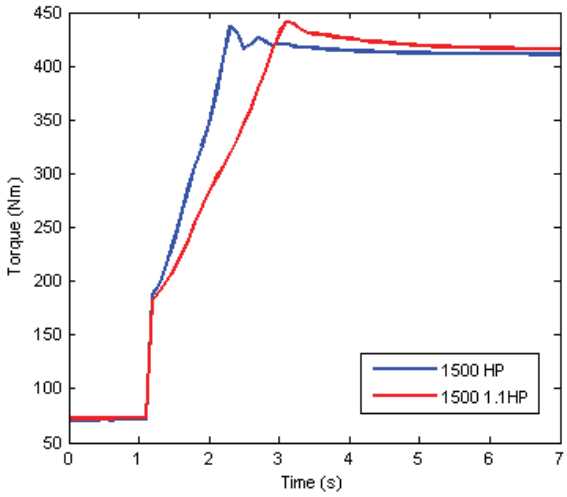

Figure 6.11 HP unit size scaling simulation (with baseline LP unit): torque transient at 1500 rpm

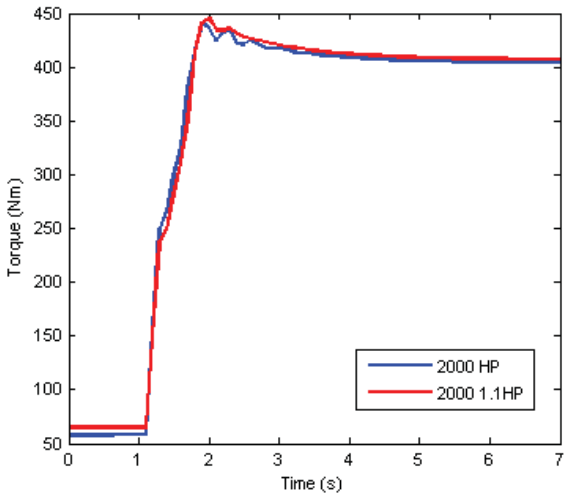

Figure 6.12 HP unit size scaling simulation (with baseline LP unit): torque transient at 2000 rpm

The smaller HP unit eventually becomes an obstacle to the faster transient performance at higher speed. As shown in Figure 6.13, the bigger HP1.1 unit benefits the transient by being less of a throttle to the engine. However, the back pressure controller has bypassed the bigger HP1.1 less completely than the HP, which resulted in the lower stable full load torque of HP1.1 compared to the HP. The HP transient simulation here showed the potential of using a VG

device at the HP stage, which would cater to different flow conditions with different turbine effective area.

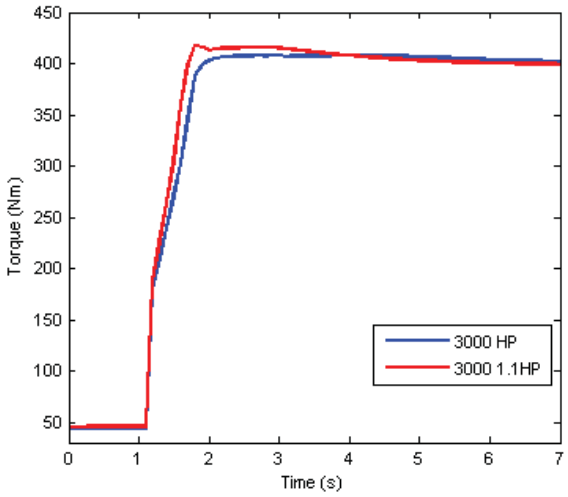

Figure 6.13 HP unit size scaling simulation (with baseline LP unit): torque transient at 3000 rpm

The effect of LP unit size only becomes visible at the mid to high-speed region. As shown in Figure 6.14 and Figure 6.15 the bigger, heavier 1.1LP reacts slower than the original LP unit in terms of torque elevation. The reason for the big deficiency in torque of 1.1LP in 3000 rpm engine speed was the accumulated effect of inefficient extraction of exhaust energy which leads to insufficient boost which then leads back to further insufficient exhaust energy.

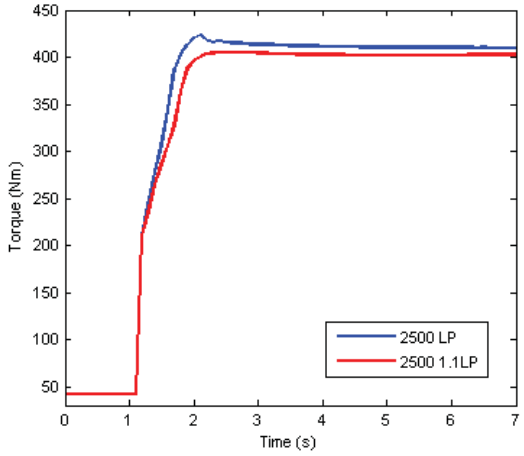

Figure 6.14 LP unit size scaling simulation (with baseline HP unit): torque transient at 2500 rpm

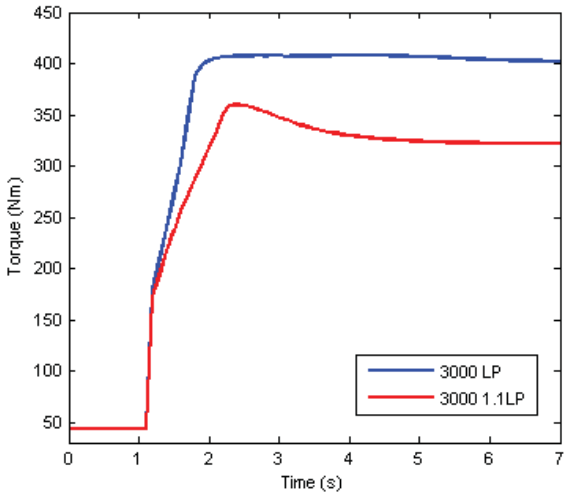

Figure 6.15 LP unit size scaling simulation (with baseline HP unit): torque transient at 3000 rpm

6.3.2 Control valve Mapping Simulation

To isolate the turbocharger from the inaccuracy of the engine strategy so that an unbiased characterization of the turbocharging system can be done, the valve mapping simulation was conducted without the controllers of the engine or the turbochargers. Instead, the inputs were pulled out directly from the full load engine experiment data so that the model was receiving the same inputs (EGR shut position, engine speed, injection amount, timing and duration, etc.) and the generated torque was evaluated to reveal the best control scheme. By varying the two turbocharging control valves: the turbine bypass valve (TBPV) and wastegate (WG), the valve positions that provided the highest torque (thus lowest fuel consumption with identical fuel injection), while conforming to all the engine limiting boundary conditions (Table 6.1) were revealed and are shown in Figure 6.16.

Table 6.1 Limiting conditions to refine the valve operating region

AFR	**16:1**
Turbine inlet Temperature	**830 °C**
Compressor outlet	**200 °C**
Peak Pressure	**160 bar**
Small unit speed	**270000 rpm**
Large unit speed	**190000 rpm**

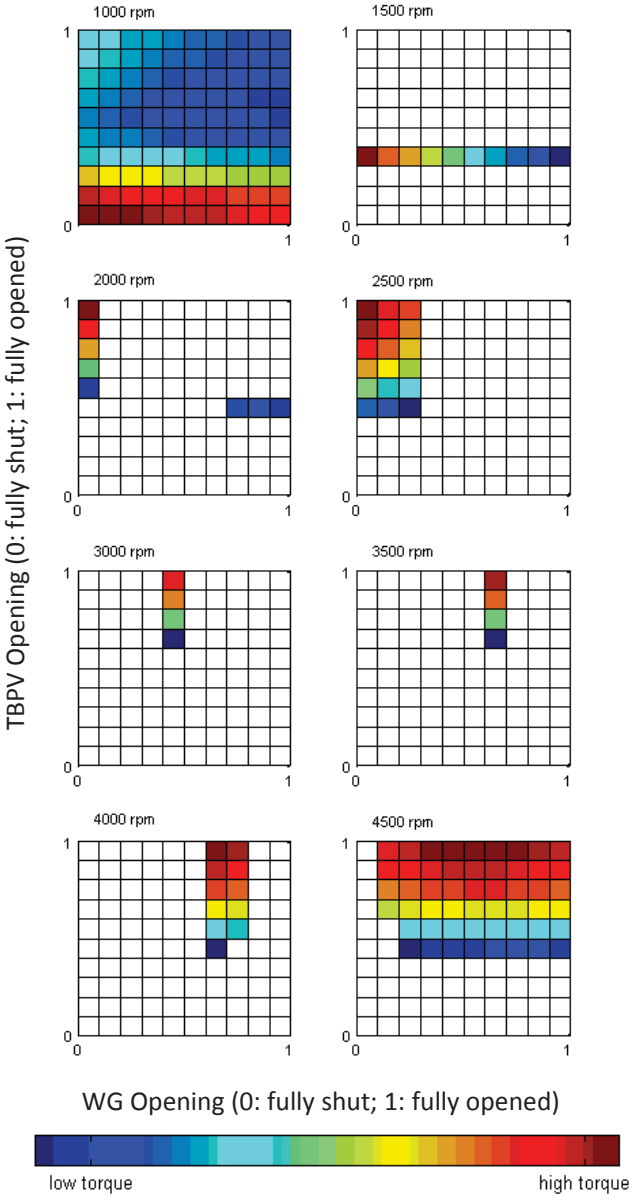

Figure 6.16 valve position mapping for each speed: break torque output using identical fuelling plotted on the operating region of TBPV and WG

Figure 6.16 clearly implies the full load operating points of the two control valves. In the two dimensional maps shown for each speed, the lower left corner represents shutting both control valves and the exhaust gas and inducted air expand and compress through both turbocharger respectively; while the right upper corner represents bypassing both turbochargers which utilize minimal exhaust pressure. The dark red blocks in the torque map represent the optimal operating points, providing high full load torque which also represents the low fuel consumption points. The white blocks are the valve positions which violate at least one of the engine boundary conditions. By finding the optimal points in the limiting torque maps, the optimal valve schedule should be as follows in Table 6.2 and corresponding Figure 6.17:

Table 6.2 optimal valve positions at full load in different speeds

Engine Speed	TBPV	WG
1000 rpm	0	0
1500 rpm	0.3	0
2000 rpm	1	0
2500 rpm	1	0
3000 rpm	1	0.5
3500 rpm	1	0.8
4000 rpm	1	0.7
4500 rpm	1	0.6

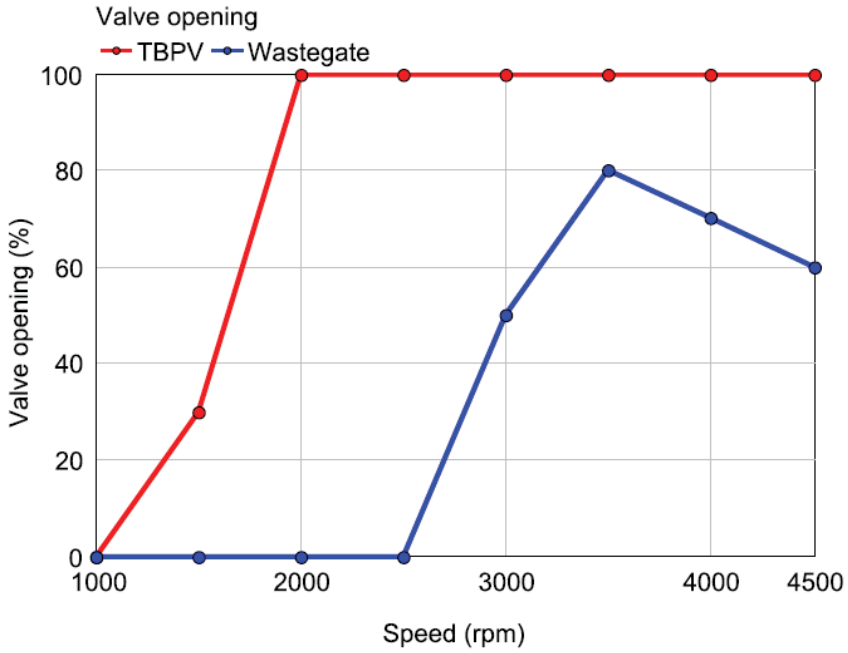

Figure 6.17 optimal valve positions at full load in different speeds

From Figure 6.17, it appeared that the TBPV should be shut at 1000 rpm to reach the full load torque required boost. At 1500 rpm to 2500 rpm, the TBPV opened to modulate the boost level. From 3000 rpm, the wastegate should be opened to maintain the boost.

The simulation results of the valve mapping not only showed the separate good points, but also confined the valves to those safe regions to protect the engine. The full load positions at each speed also act as final points of the controller which provide important perspectives for the proposition of the control strategy.

6.3.3 Two stage turbocharging system and VG Turbocharger Comparison

The advantage of the two stage system over the VGT system in terms of full load torque curve was briefly mentioned in the turbocharger size scaling simulation. To further justify the extra cost and packaging effort, the two stage turbocharging and VGT turbocharger were compared back to back in terms of fuel consumption, transient performance and EGR potential in this set of simulations. Again, the engine controller reconstructed from the ECU strategy was used to

control the models, between the two arrangements only the boost target map was modified for the two stage arrangement. The simulation results are shown below in Figure 6.18, 6.19 and Table 6.3.

As shown in the Figure 6.18, the two stage turbocharged engine can generally have a better BSFC over the full engine speed range compared to the VGT engine when producing the same limiting torque. Fuel consumption of the two stage system is especially good at low engine speed. This was due to the fact that the HP unit can comfortably utilize the limited exhaust energy while the VGT has to shut the nozzle vanes to generate enough boost which entails high engine back pressure, and thus higher pumping losses. At mid to high speed, the two stage system still maintains its advantage by working in the high efficiency region of the LP unit. VGT only rivals two stage system when the dual-turbocharger system switches between stages at 2000 rpm and when VGT has higher efficiency than the wastegated LP unit at 4500 rpm.

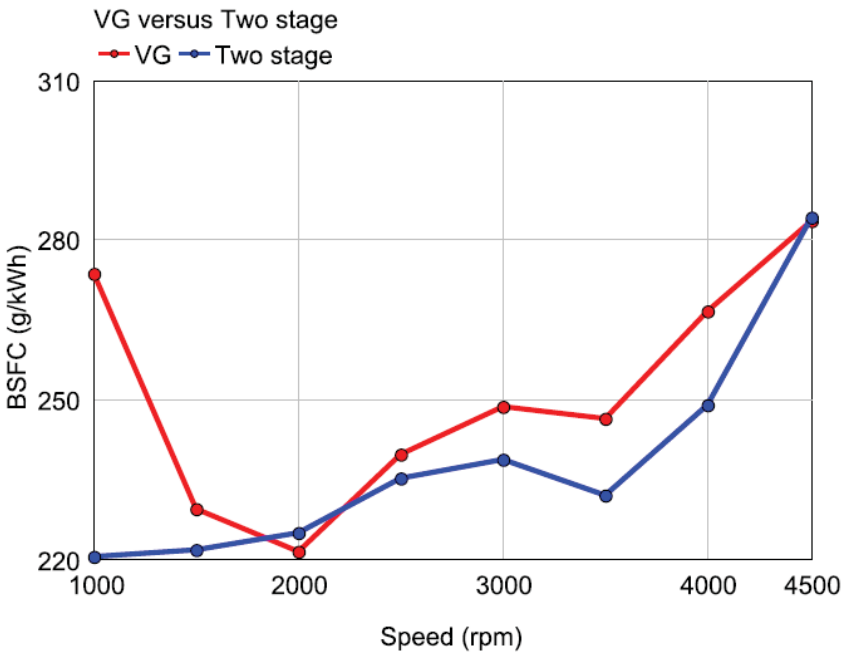

Figure 6.18 fuel consumption comparison of the two stage system and the VGT system

The two stage turbocharged engine has better transient performance than the VGT turbocharged engine over the low to mid-speed range, as shown in Figure 6.19 as an example. However, after 2500 rpm, the two turbocharging systems tend to give similar transient response because the comparison becomes that between the two similar sized VGT turbocharger and LP wastegated turbocharger.

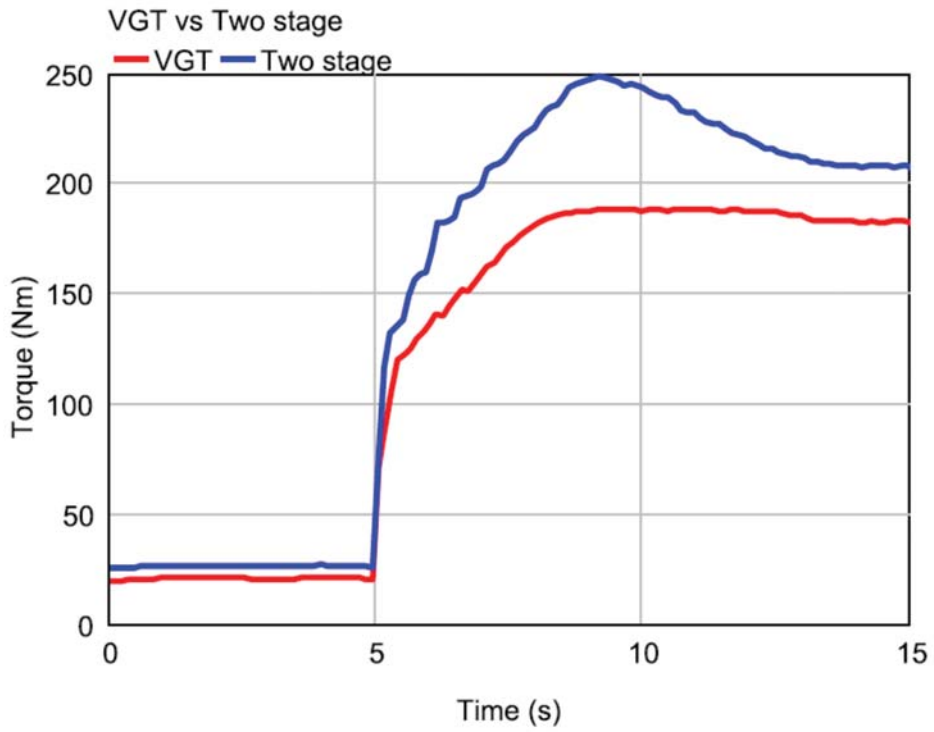

Figure 6.19 transient performance comparison of the two stage system and the VGT system at 1000 rpm

To demonstrate the potential of the two stage system, EGR gas was introduced into the intake manifold to percentage that any more EGR would make the engine failed to achieve the baseline full load torque.

Table 6.3 EGR rate available for the two stage turbocharged engine when achieving the limiting torque of the VGT turbocharged engine

Engine Speed	EGR rate
1000 rpm	0
1500 rpm	4.2 %
2000 rpm	5.2 %
2500 rpm	4.2 %
3000 rpm	5.1 %
3500 rpm	2 %
4000 rpm	0
4500 rpm	1 %

At the full load conditions of the VGT engine, EGR cannot be delivered across the speed range if peak torque is to be maintained. However, for the two stage turbocharged engine, the torque targets of the VGT engine were not yet the limiting torque curve. Assuming a production engine is been upgraded to the two stage turbocharging for the sole aim of reducing harmful emissions without the need for uprating, by demanding the same torque and mass air flow target but using higher boost pressure provided by the two stage system. The EGR rate as shown in Table 6.3 was possible in the simulation. The EGR rate enabled at these relatively high load conditions would be highly appealing when the more intensive drive cycles come into implement.

6.4 Control Strategy Study

The simulations in the previous section showed the optimal control valve operation at the full load operation. To generate a control strategy that was compatible for both steady state and transient operations while providing optimal overall performance, a more systematic study was conducted in this section.

6.4.1 Torque expectancy

First, the full load simulations were implemented to study the torque potential of the two stage turbocharging system. Since the limiting torque curve is the basic index for evaluating an internal combustion engine, the result of this simulation provides the largest candidate pool of valve operating strategies which at least would allow a robust torque curve.

The HP and LP stage match was proved in the previous study as a near optimal pair of turbochargers and in this simulation work the systems were evaluated progressively: in naturally aspirated mode (TBPV open, WG open), HP-only mode (WG open), LP-only mode (TBPV open) and the two-stage mode (TBPV closed, WG closed). TBPV and WG were controlled by a *proportional-integral* (PI) controller so that the boost level was limited to maintain safe peak cylinder pressure. Furthermore, to avoid excessive backpressure at high flow conditions due to the smaller turbine area of the HP stage, another PI controller was used to relieve the HP stage when back pressure was above the engine calibration target. The engine physical torque limit was set as the target limiting torque curve considering the two stage turbocharging should be able to provide enough boost for up-rating. The baseline engine smoke limit was implemented as a fuelling cut-off.

The simulation results were plotted in Figure 6.20. By overlaying the torque range of each configuration, the available operating regions were obvious: the naturally aspirated setup was only able to provide up to around 30% of the limiting torque (thus the motivation of turbocharging); HP stage was able to provide a peaky torque curve in low to mid-speed region, with low speed not achieving target and severe torque deficiency at mid-to-high speed; the LP stage was able to maintain the torque above the baseline engine at mid-to-high speed range, however was unable to provide enough boost at lower speed when the VGT baseline turbocharger was more effective than the wastegate regulation of a larger turbocharger.

On the other hand, the two stage operation scheme was seen to be the most effective strategy in torque generation. The engine torque target was achieved in full speed range. The 1000 rpm engine torque limit was temporarily voided to study the real boosting potential of the system and the result was impressive: without breaching either the smoke limit (Equivalent AFR) or the cylinder peak pressure limit, the engine was able to generate torque above 400 Nm at very low speed, offering generous launch performance and a flat torque curve in a wide region of 1000 rpm to 3500 rpm.

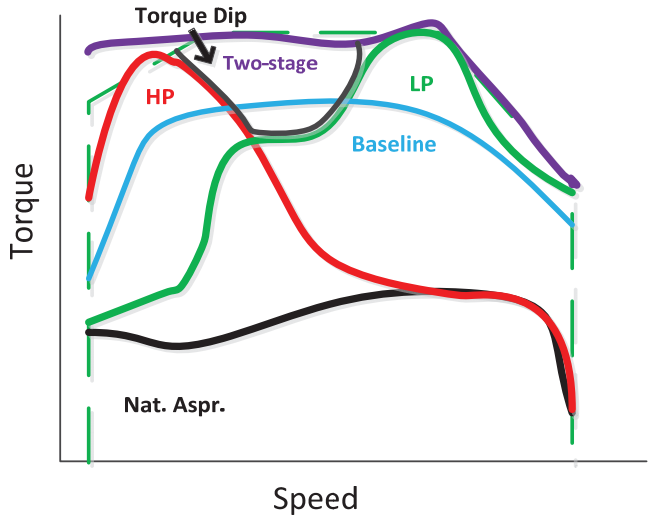

Figure 6.20 achievable torque range using the two stage turbocharging system

From the limiting torque simulation, it would seem that each configuration was useful in at least some regions of the engine-speed torque plane. However, considering the highly varied operating range of the road vehicle, it would be highly undesirable that the HP and LP should be used in isolation from each other, (e.g. due to the torque dip shown in Figure 6.21, an engine under high load accelerating would have to go through HP-Two stage-LP three phases and PI controllers of HP and LP may fight against each other and the slow LP acceleration will eventually render the drivability poor.

Running the two stage setup with only one PI controller was a highly promising option (Figure 6.21): the PI controller gave a common control signal to both devices to modulate boost pressure and the HP stage always opened first to allow the increasing exhaust energy to be passed on to LP stage for more efficient operation. WG modulation would be activated on the fully opening of the TBPV. The control scheme exposed the advantage of a VG device in high pressure stage as prior to the point where the TBPV started to open (and the WG is closed), the response was defined solely by the passive match between the two turbochargers. On the other hand, the effectiveness of such a control strategy need to be further assessed by both fuel consumption level and transient response performance as discussed in the following sections.

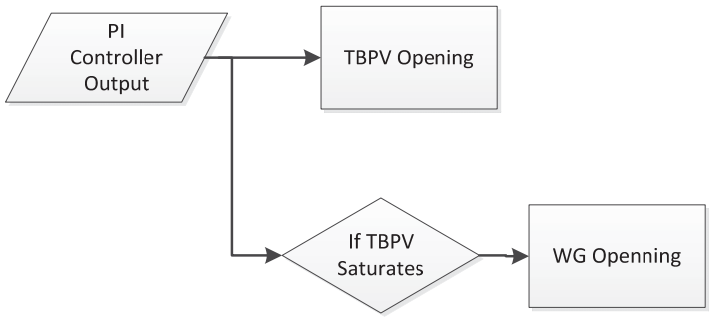

Figure 6.21 two stage system controller single output signal routed to both regulating valves

6.4.2 BSFC consideration

In the simulations implemented in this study, several factors collectively resulted in higher fuel consumption of the two stage system compared to the baseline VGT engine observed in part-load conditions, which include:

1. The back pressures were generally higher (especially at low engine speed) in the two stage arrangement than with the VGT to provide the same level of boost. This was because of the throttling effect of the relatively smaller HP stage turbocharger. Therefore the pumping losses increased.

2. The injection timing map was directly pulled out from the original ECU map. This was because the recalibration of the SOI would demand unaffordable effort, and the initial test plan after the simulation work was to insert the two stage system onto a production engine and to focus on the charging performance. Therefore, the engine optimization was given way to speedily generation of useful results. It can be expected, however, that the engine fuel consumption can be further optimized if new calibrations were implemented.

With the above mentioned reasons in mind, it was beneficial to find the optimal BSFC operating range of the two stage system so that future steady state optimization work can start in the right direction. By plotting the regions where the *brake specific fuel consumption* (BSFC) values are lower than 240g/kWh, the optimal operating range of each setup was revealed (Figure 6.22).

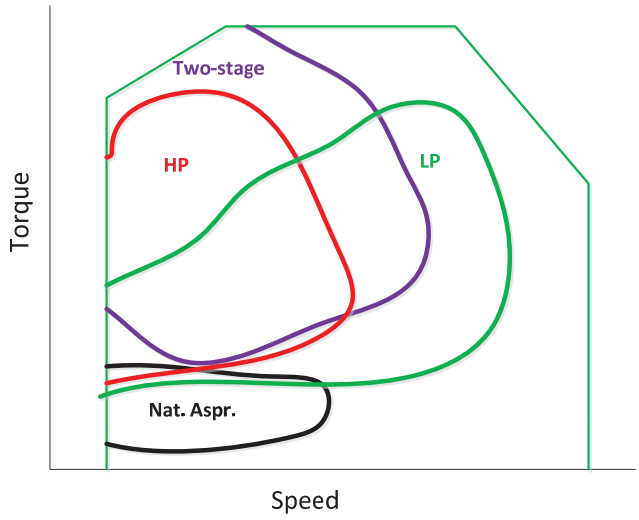

Figure 6.22 BSFC optimal operating range (less than 240g/kWh) using different device

From the Figure 6.22, the naturally aspirated mode was able to provide efficient operation at its limited low speed torque generating region where throttling from the bypassed gas path was minimal and air was sufficient for lean combustion.

The HP-only mode was efficient at low speed mid-to-high load region when the turbocharger is working with high efficiency and exhaust choking was not apparent.

The LP-only mode was efficient in most of the region because of its large turbine area and high efficiency. However, the region was limited in low speed where it cannot sustain the high boost required for more torque.

The two-stage mode on the other hand was not apparently good in fuel consumption, with its low speed region similar to that of the HP mode (influence from the large LP stage was minimal) and the high speed region worse than that of the LP mode due to the throttling of HP turbine.

By comparing the actual BSFC numbers within these optimal regions, the recommended operating regions which give the best fuel consumption are illustrated in Figure 6.23. The operating region was not at all in conflict with Figure 6.20, where the initial operating region was defined. The strategy has become at least half-built with the centre and centre-left of the torque-speed plane, where the two-stage, HP, LP borders, remained flexible since the three setups offered similar BSFC performance which allowed leeway for transient performance improvements to be made.

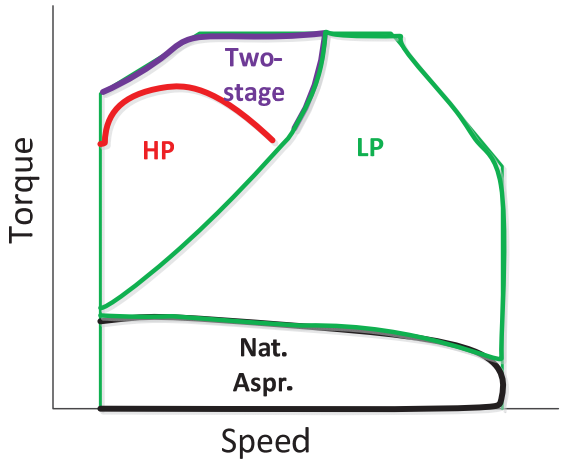

Figure 6.23 optimal operating range for best BSFC

6.4.3 Transient performance consideration

The two stage PI controller proposed in the end of the torque expectancy section was conveniently compatible with the transient operation: when a transient of torque tip-in happened, the PI controller would shut the valve (or remain closed if already shut) so that the boost level would climb to the new boost target. Excessive back pressure, which could cause undesirable performance, was prevented by the back pressure controller which would bypass the HP stage if the transient of the valve was too violent for the engine. By modifying the boost target map and back pressure limit, the controller can be optimized with some flexibility.

For passenger car and light commercial vehicle applications, the main transient performance happens in the low to mid speed range, during the vehicle launch and overtake manoeuver. Therefore, transient simulations were implemented under a load tip-in from around 20 Nm to 250 Nm. Representative torque traces were plotted in Figure 6.24 to Figure 6.27.

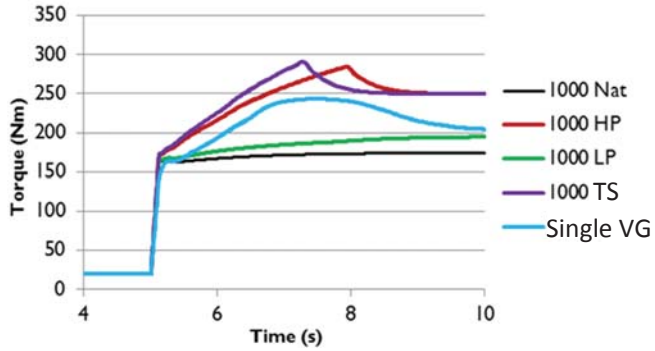

Figure 6.24 transient performance comparison at 1000 rpm

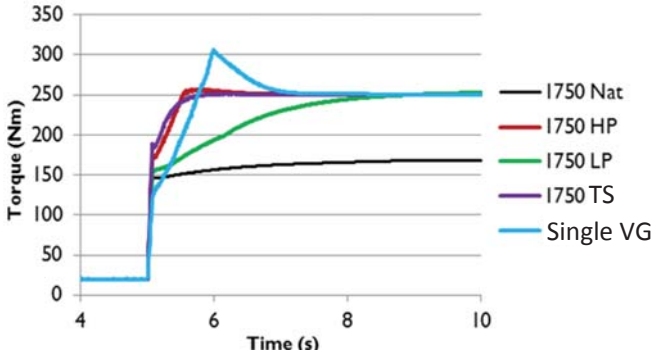

Figure 6.25 transient performance comparison at 1750 rpm

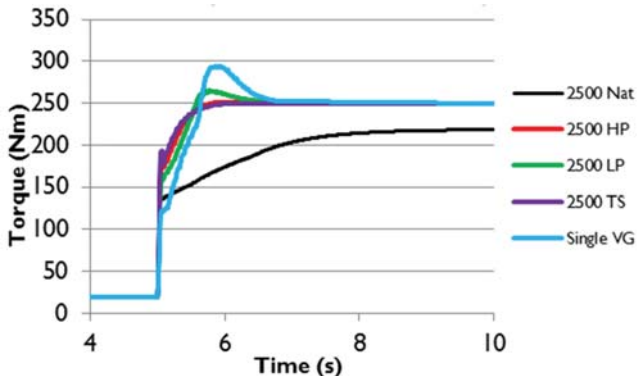

Figure 6.26 transient performance comparison at 2500 rpm

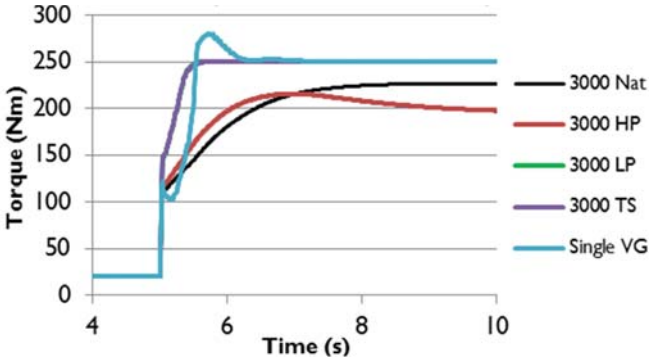

Figure 6.27 transient performance comparison at 3000 rpm

As shown in the graphs, the two-stage (TS) system was able to provide the fastest transient response using its two stage charging from low speed 1000 rpm until 1750 rpm where the HP-only mode managed to catch up with it. HP-only mode then quickly phase out as a fast

performance charger from 3000 rpm when it effectively becomes an exhaust throttle. LP-only became faster than the baseline engine from 2500 rpm onwards and was the fastest from 3000 rpm where two-stage effectively was a LP-only because HP was bypassed through back pressure control.

The summarized optimal operating regions for transient performance were plotted in Figure 6.28, where two-stage mode was in charge of boosting during low speed and high load mid-speed while HP works at mid-speed from 1750 to 2500 rpm. LP mode works from 2500 onwards. The newly revised strategy was still not in violation of the strategies proposed in the previous sections. Further optimization was done in the transient simulations.

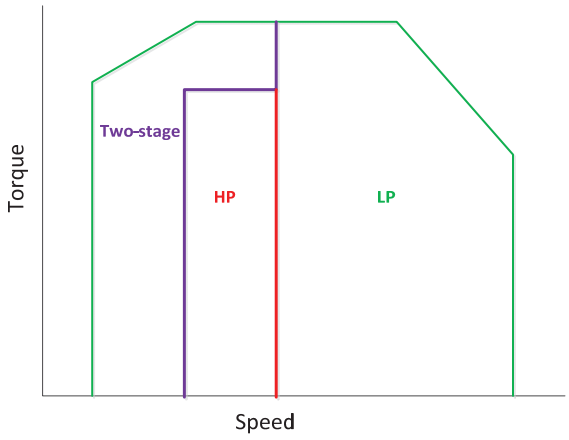

Figure 6.28 transient optimal range for different devices

6.4.4 Further refinement

It should be noted, however, that a large area of BSFC optimal regions, the naturally aspirated low load condition, in the Figure 6.29, was completely negated in the transient simulation. This was due to the fact that naturally aspirated mode where both turbochargers were bypassed will not be able to maintain a relatively high turbocharger speed at low load to cope with any sudden demand in boost and torque (Figure 6.24 to Figure 6.27). However, the low BSFC of the

naturally aspirated mode due to its low throttling could be an inspiration to further refining the control strategy.

When comparing the BSFC value of the two-stage mode and baseline engine or LP-mode, an obvious phenomenon was that the two-stage mode required much higher fuel consumption at low load condition. This was due to the fact that for the same boost level, the two-stage system need to distribute the expansion/compression ratios in two stages, where neither one worked in their high efficiency region. Therefore, two-stage system has to use smaller effective turbine area to achieve the boost target which increases the pumping losses.

An attempt to alleviate such a scenario was implemented in the simulations: boost targets at low load, low to mid speed were reduced so that the TBPV was forced open to reduce throttling. The transient response could be maintained as better than the baseline by carefully scheduling of the boost target reductions. As an example, the 2000 rpm transient simulation result is shown in Figure 6.29. It can be seen that by implementing the new strategy, the BSFC at low load of 50 Nm was reduced by up to 12% (-0.3bar) without a much deteriorated transient performance. This was mainly due the fact that the smaller turbocharger, although bypassed for fuel consumption, can pick up speed rapidly thanks to its low shaft inertia and small turbine area. A further 0.1 bar boost target reduction was unacceptable because the LP stage was also forced open following the full opening of HP stage. Therefore, a meticulous calibration of the boost map will need to be done to fully exploit the exhaust back pressure reduction strategy.

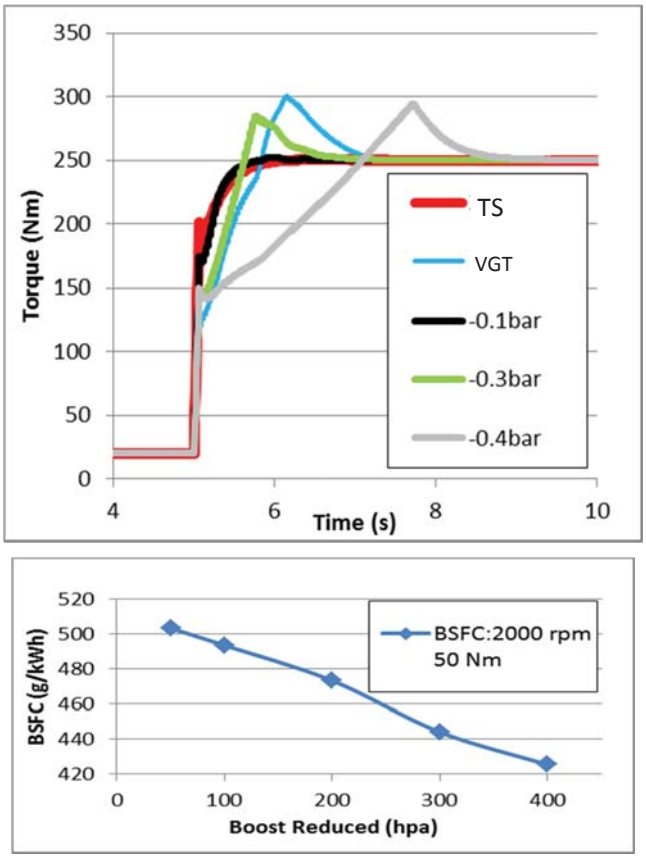

Figure 6.29 transient performance and BSFC benefit of 2000 rpm with boost target reduction

The revised strategy scheme is shown in Figure 6.30. To ensure the transient response at low to mid-speed region where HP-mode used to be, the two-stage was used instead so that LP stage will provide additional pre-boost for fast transient performance.

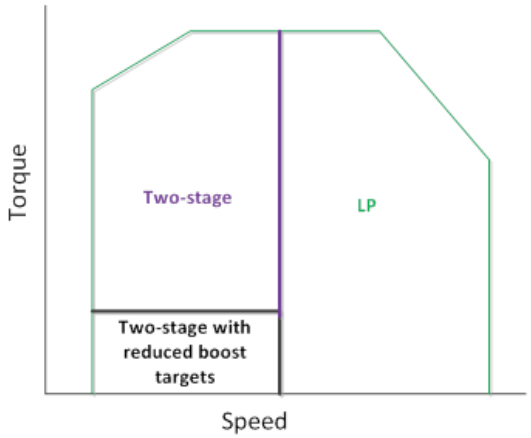

Figure 6.30 optimal operating range for both transient response and fuel consumption with throttling reduction.

6.5 Summary

A simulation based study was conducted on the soon-to-be-popular technology of two stage turbocharging. With the aid of a calibrated VGT model, several simulations was designed and implemented with the feasibility of test validation in mind.

The turbocharger size scaling simulation showed the effect of using differently sized turbocharger in each stage on the engine performance. No definitive conclusion with regards to how to directly size the two interactive turbochargers was attempted. However, by conducting a similar scaling procedure iteratively as in this study, a relatively optimal turbocharger pair can be found.

The two stage valve mapping simulation provides useful insight into the optimal control strategy based on the optimal valve positions at full load. Valve positions which may endanger the engine were also specified for each speed.

The VGT-Two stage comparison confirmed the two stage technology as an effective way to reduce fuel consumption, improve launch performance and alleviate NO_X emission.

Instead of working based on improvement of existing control strategies, the control strategy study started off from the characteristics of the turbocharging system and followed the sequence of satisfying torque expectancy, optimal fuel consumption, improved transient performance and further refinement. A gradually optimized strategy was narrowed down and simulation results were shown.

Even with an imperfect control strategy, the two stage turbochargers were able to push the engine to its physical limit and had the potential to triple the low speed end torque; meanwhile, the transient performance of the system was significantly improved, which then allows some leeway for fuel consumption optimization. The fuel consumption of the two stage system was shown to be higher than its VGT counterpart. The cause of this shortcoming was

summarized and an exhaust backpressure reduction strategy was implemented and achieved typical 12% of fuel consumption reduction without serious transient performance deterioration.

The work in the following chapters will aim to validate the findings in this chapter.

The content of this chapter was published in:

Zhang, Q., Brace, C., Akehurst, S., et al., 2013. Control Strategy Study of the Series Sequential Turbocharging Using 1-D Simulation. In: ASME Turbo Expo 2013, GT2013-94573

Zhang, Q., Brace, C., Akehurst, S., et al., 2013. Simulation Study of the Series Sequential Turbocharging for Engine Downsizing and Fuel Efficiency. In: SAE 2013 world congress, 2013-01-0935

Chapter 7 - Experiment study of the two stage turbocharging system

As discussed in the experiment facility section, the control of the two stage system was implemented using a dSPACE rapid prototype system. The control model was first constructed in the Simulink environment and then compiled on the host computer and flashed into the dSPACE DS2211 board.

Some ECU signals were intercepted via the CAN communication port into dSPACE and were used as several controller inputs (boost pressure) or as 2-D table inputs (engine speeds and indicated torque).

Several important valve opening positions specific to the two stage system were also monitored using suitable displacement sensors.

At the end of the chapter, the test results of the two stage system were used to compare to the baseline engine test results. The potentials and weaknesses of the system were identified.

7.1 Control system configuration

7.1.1 Control model

Based on the simulation study in the previous chapter, the two stage system should use the two turbochargers in series in the low engine speed region and switch to the single

turbocharger (low pressure stage) at higher engine region; the wastegate of the low pressure turbocharger can be opened for fuel consumption benefit in the low load operation.

To implement such control strategy, at low speed region, the two stage system used the high pressure stage turbine bypass valve (TBPV) to modulate the boost pressure, before the boost target was met, the TBPV was kept in a shut position and both stages worked in series. The boost map was applied in the ECU calibration and was reconfigured in such a way that the TBPV was allowed to open when: 1, the boost was achieved and the valve opened to maintain the boost level; or 2, the turbocharger was expect to overspeed soon; or 3, the engine back pressure was too high. The boost level was controlled in closed loop with a PI and feedforward controller. The over speeding prevention was achieved by a D (Derivative) and a P (Proportional) controller. The D gain predicted the turbocharger speed in the next 3 time steps (0.3 second) and opened the valve if it predicted overspeed, the P controller with a large gain could open the valve instantly if overspeed was detected by the speed sensor. The engine back pressure control was implemented similarly with a P control but the danger prevention was also included in the calibrated boost map.

At the higher engine speed region, there were no changes made to the way the TBPV was controlled compared to at the low speed region. However, the high pressure stage turbocharger was barely functional at all due to the back pressure control setting a very low boost target for the high pressure stage so that the small turbocharger was bypassed.

The low pressure stage turbocharger was controlled by a manually configured boost map, and was subject to a scheduled valve minimal/maximum position range so that the wastegate was forced to opened and shut at the region requested. The complete control model schematics was shown in Figure 7.1.

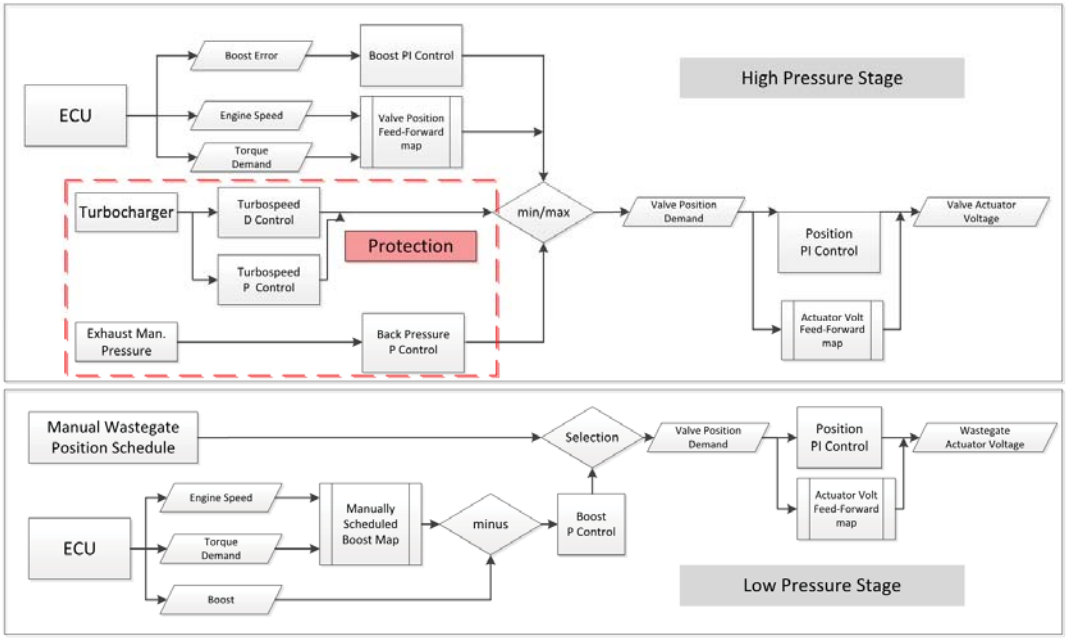

Figure 7.1 Control model schematics (feedback loop omitted)

7.1.2 CAN interception

The controller area network (CAN bus) is a standard for the communication between the microcontrollers and devices on the vehicle. In the test cells in the University of Bath, it was the protocol used by the ATI Vision calibration tool to interrogate the engine ECU to monitor and change the engine parameters. By intercepting this CAN communication, useful ECU parameters can be obtained to be used in the rapid prototype control systems as inputs.

Despite that the CAN was published as a standard, the CAN signals intercepted can be difficult to intercept and process. The CAN standard only described the data structure and data transfer link protocol while the content of the message was open to the ECU designer. Also it was not always possible to acquire a detailed instruction for interpreting the CAN signal. Therefore, great effort had to be taken to work out the CAN grammar used in this engine.

A short piece of the CAN signal intercepted as the engine started was shown as an example in the Table 7.1. The MsgID, MsgData1 and the MsgData2 columns in hexadecimal numbers were the information needed for the control system.

Table 7.1 a typical CAN message intercepted when the engine starts

Msg ID	Direction	Data Length	CAN ID	Data1	Data2	Time	Delta time
1956	0	8	1	7736C455	78355431	0	0
1956	0	8	1	B306BE55	001AC21A	0.000121	0.000121
1956	0	8	1	AC912656	01003B8B	0.000252	0.000131
1956	0	8	1	EA347557	0068CE68	0.000371	0.000119
1956	0	8	1	A9000058	04342C00	0.000496	0.000124
1956	0	8	1	EA68CE59	00000068	0.000618	0.000122
1956	0	8	1	0001675A	50666600	0.000739	0.000121

The MsgID in a piece of CAN message specifies the type of the data, the sending node and the priority. Since the ECU was acting only as the data source during the testing, all the data intercepted in this project was identified as ID 1956 and the message contents in the MsgData* were the ATI Vision requested engine status report.

The next step was to decipher the MsgData channel. It was found that the various parameters can be identified firstly by the first byte of in the MsgData1, ranging from 84 up to 108 in this EUC and this data byte was used in the control model as the channel number. In addition to the channel number, the parameters were identified by the position that they occupied in the 8 byte data. Under such a data structure, the requested ECU data filled in each data channel as three pieces of 2-byte data (used for floating point numbers, such as boost pressure in hpa) and one piece of 1-byte data (used for integers such as coolant temperature).

Table 7.2 break down of a CAN data byte

ID:	MsgData1				MsgData2			
1956	Chn No.	Data 1-1	Data 1-2	Data 2-1	Data 2-2	Data 3-1	Data 3-2	Data 4

The data were then decimalized and cross checked with the calibration software to confirm which parameter is which. The process was extremely tedious and unfortunately the whole process needed to be repeated every time the ATI Vision deletes or added a parameter in its parameter list because the parameters would be in totally random positions again. This parameter locating process could not be avoided without spending large amount of coding effort in order to achieve automatic channel identification and was not attempted in the context of this project. When the locations of the necessary parameters were identified, these information were coded into the simulink model so that the control system can correctly identify and convert the ECU values.

7.1.3 Compressor bypass valve travel measurement

The compressor bypass valve was a spring loaded passive device enclosed in cast aluminum shell. The opening of the valve was crucial for estimating the bypass flow yet is difficult to get access to.

A displacement sensor with neither contact friction nor loaded spring force (MicroEpsilon LDR-25) was used to measure the opening of the valve. The solution is show as in the Figure 7.2 below. The light-weight plunger weighs only 2.2g, introducing minimal influence on the dynamics of the valve. The location of the sensor also ensures there is no significant influence on the engine and the compressor aerodynamically.

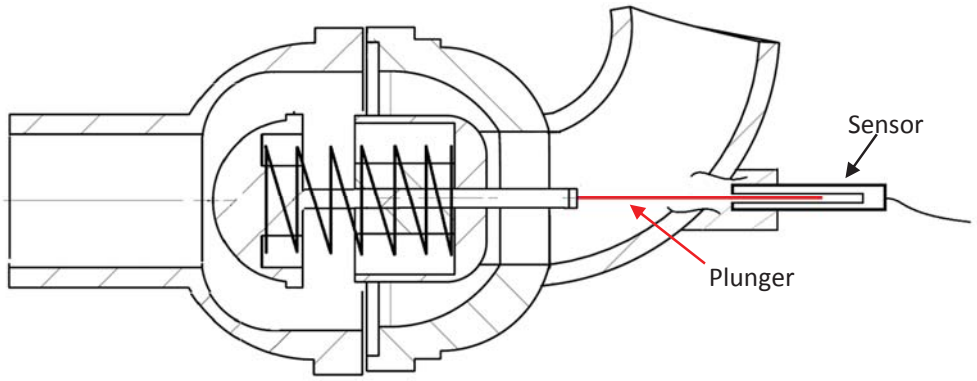

Figure 7.2 the compressor passive bypass valve and the valve position sensor solution

The measured valve position was converted into flow coefficient through a 2D table against the valve lift. The flow coefficient was then used in the 1-D engine model.

7.1.4 Active valves travel measurement

The active valve positions, including those of a high pressure stage turbine bypass valve and a low pressure stage turbine wastegate were each monitored by a *Micro-epsilon* pull wire displacement sensor (WPS-150-MK30). This type of sensors were the optimal solution in that it provides much wider measurement range with sufficient accuracy, robust installation and lower cost. To protect the sensors from the radiation of the exhaust manifold, aluminum heat shield were installed around the sensors (Figure 7.3).

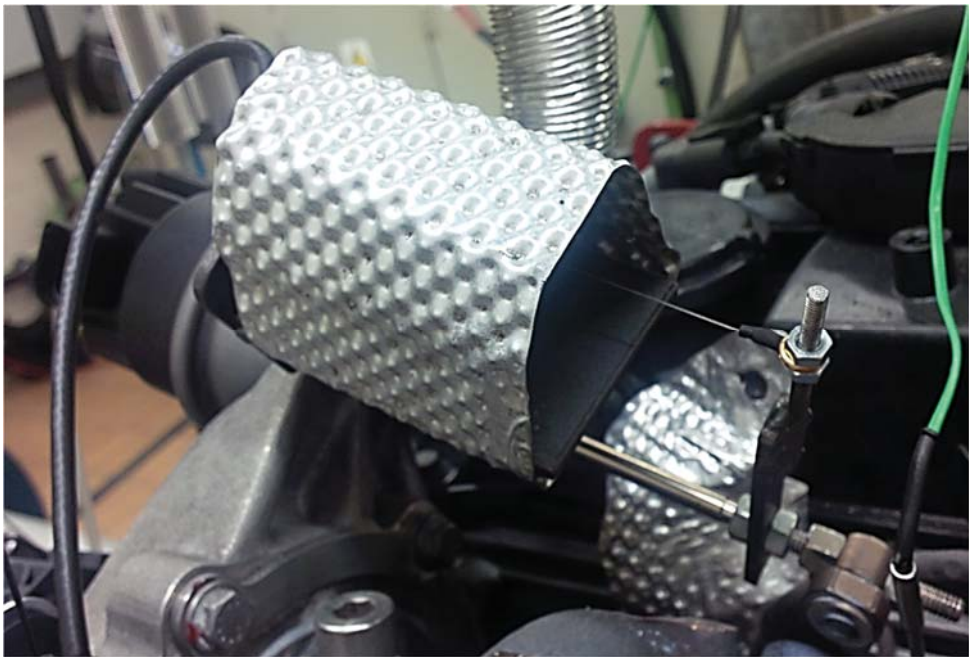

Figure 7.3 pull wire valve travel sensor and the heat shield

The measured valve position was converted into flow coefficients through a 2D table against the valve lifts. The flow coefficients were then used in the 1-D engine model.

7.1.5 Control system connection

The control system includes the dSpace system, host computer, sensors, actuators, pressure regulators and vacuum ejectors. The system is connected as shown in the below diagram.

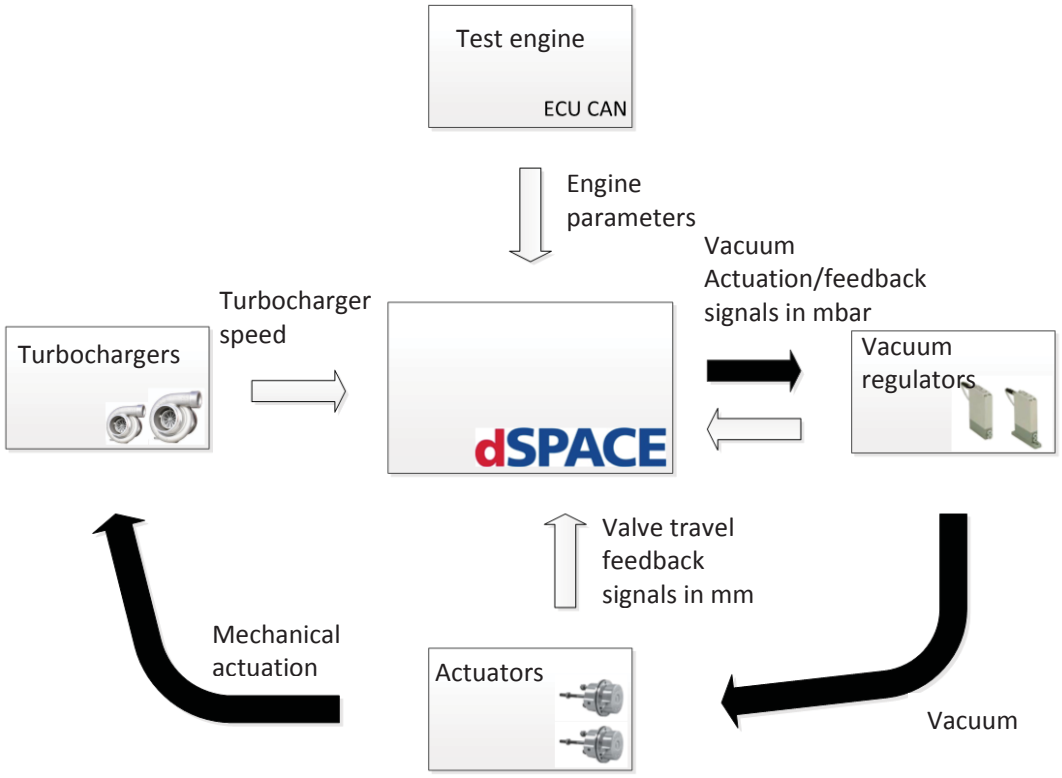

Figure 7.4 two stage turbocharging control system diagram

The dSpace system included the DS1006 processor board which executed the main computation with the AMD Opteron™ processor; a DS2211 HIL I/O board which stored the controller program and conditioned the I/O signals, providing the Hardware-in-the-Loop function and the I/O connection panel

The host controller communicated with the dSpace system through the DS1006 board via a RS232 connection. The host computer worked as the compiler of Simulink model and a user interface for controlling the dSpace system.

The sensors included several pressure transducers in the intake/exhaust manifold and the two turbocharger speed sensors. Since the boost related signals are communicated through CAN bus, the analogue sensors are mainly used for reference record and system protection, such as the exhaust manifold pressure limit and turbocharger over-speeding.

The actuators were the standard pressure vacuum actuators installed on the two stage turbocharger system. Such actuators could have accuracy and reliability issues, yet due to the low cost and perfect immunity to electrical interference, they have been widely used in automotive applications.

To feed accurately controlled vacuum to the two actuators, standard automotive motor driven vacuum pump was initially used but proved to be limited in flow capacity therefore greatly limited the transient response of the bypass valve. A compressed air driven vacuum ejector was later added in the system to provide sufficient flow capacity for the bypass valve; the corresponding regulator was also upgraded to a device with higher flow capacity. The two regulators were shown in the Figure 7.5 below.

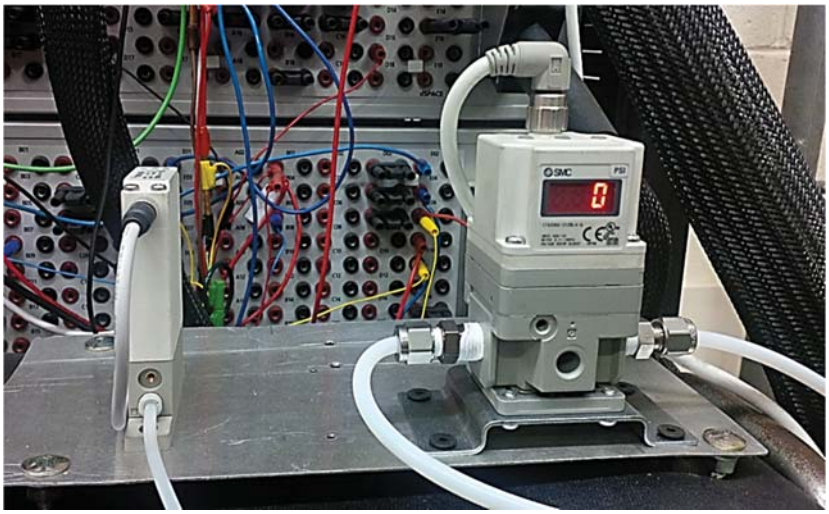

Figure 7.5 vacuum (left) and pressure (right) regulators used in the project to control the vacuum/pressure into the actuator and the vacuum ejector.

7.1.6 Turbocharging system

The two stage turbocharging system used in the experiment were originally matched to a 2 litre Diesel engine with a higher cylinder pressure design limit compared to the test engine, which indicated similar air flow requirements at rated power for both engines. The low

pressure stage turbocharger should be a good match to the 2.2L test engine and the high pressure stage turbocharger was expected to give good transient performance yet high engine back pressure.

The installation of the non-standard turbocharging system onto the engine involved several mechanical changes to the test engine, including removal of obstructive engine structure, building a new oil scavenging system to ensure the oil feeding head, adding adaptor parts for the new exhaust manifold and a newly built engine mount. The influence of the modifications to the engine performance was considered minimal.

The turbocharger had also been adequately instrumented with temperature, pressure and turbocharger speed sensors. The instrumentation diagram was shown in the Figure 7.6 below. The system installation on the engine was shown in Figure 7.7 and the complete test bench setup was shown in the Figure 7.8 at the end of this section.

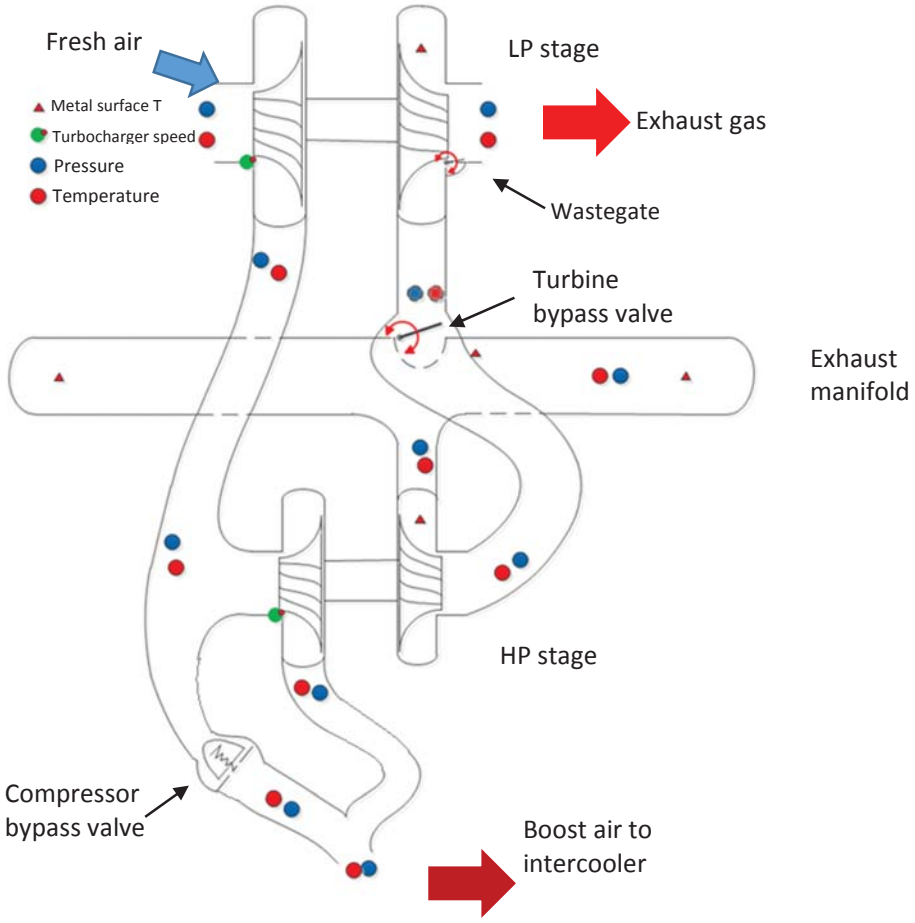

Figure 7.6 diagram of the instrumented sensors on the two stage system

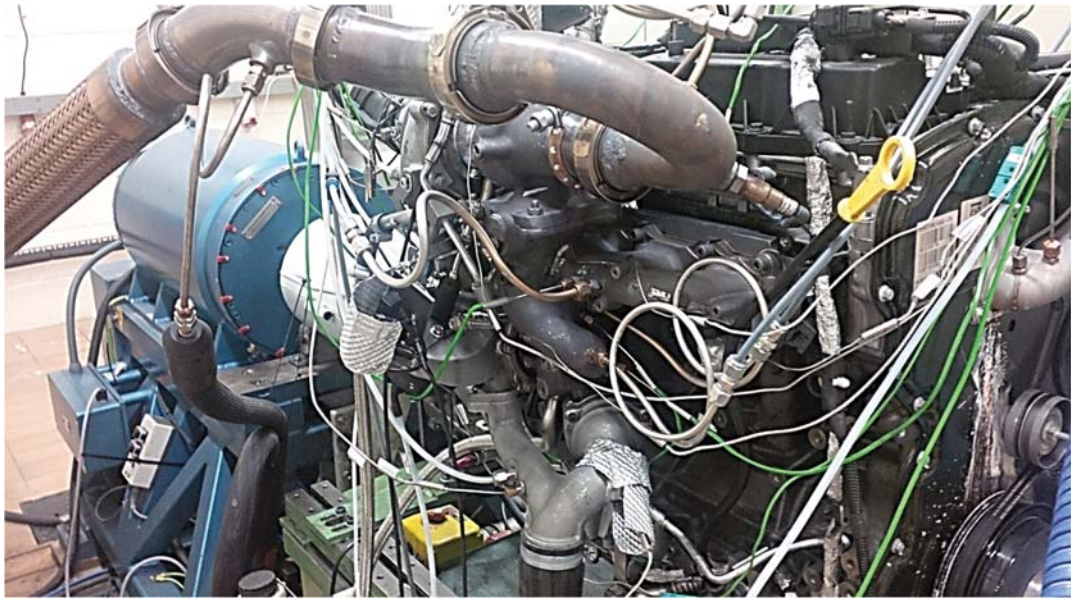

Figure 7.7 the fully instrumented two stage system installed on the baseline engine

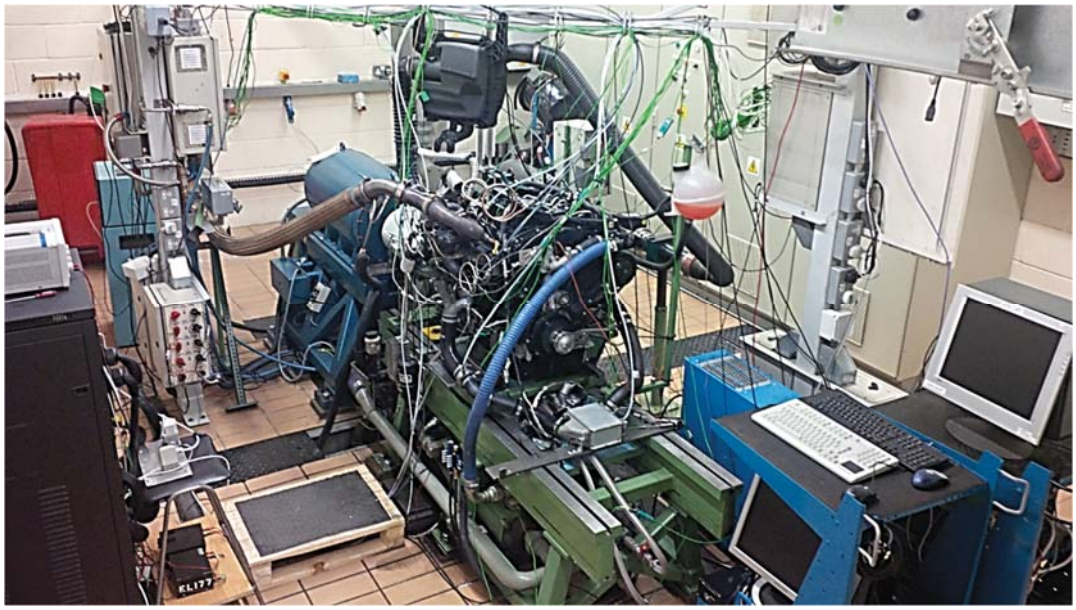

Figure 7.8 the fully instrumented test engine in the test cell

7.2 Test results

Compared to the testing of the ball bearing turbocharger, testing of the two stage turbocharging system was a much more challenging piece of work. Aside from the changes needed to be made to the hardware during the installation, the distributed control of the boosting system need very careful tuning to ensure the safety of the hardware – of both the engine and the turbochargers. The testing work kicked off with a long period of system debugging and durability test in low load operation, during which both the steady state and transient operation were calibrated. Bypass valve leakage, dSPACE system signal interference and sluggish vacuum actuators were among the problems successfully resolved. However, the EGR controllability and the mid-speed high backpressure were examples of the problems could not be solved with the hardware at hand and will be dealt with in the last chapter.

The same test plan introduced in the previous chapters on the topic of VGT turbocharger and ball bearing turbocharger were used in the two stage system testing. The results are presented in the following section.

7.2.1 Full load test results

The full load test was mainly conducted in the speed range 1000 rpm to 3000 rpm. Higher speeds operating points from 3000 rpm were simply the same engine boosted by a wastegate turbocharger and did not provide insightful information therefore the test results presented here will focus on the 1000 rpm to 3000 rpm speed range. The test results were supported by repeated tests to ensure data quality.

As shown in the Figure 7.9, the full load test of the two stage system revealed interesting results of the two stage system. The benchmark torque curve was sufficiently met (part1 upper plot), with significant torque increase at 1000 rpm speed point from 183 Nm to 195 Nm. Since

at the full load operating points the engine was limited by the setting of the ECU, the fuel injection (flow/timing) was almost identical for both the two stage and the baseline (part1 mid plot) - any increase in torque was a gain in fuel consumption. Therefore on the BSFC line lower fuel consumption was seen at 1000, 1500 rpm (part1 upper plot). At higher engine speed, the two stage system generated larger back pressure in the exhaust manifold (part2 mid plot). The higher PMEP value would have led to a torque reduction of almost 17 Nm at 2000 rpm (17.5 Nm is roughly equal to 1 bar of MEP). However, the more efficient two stage boosting system allowed lower compressor outlet temperature, which led to cooler combustion (part1 lower plot). The reduction in heat convection loss balanced some of the pumping loss and therefore the BSFC discrepancy was not as obvious as the PMEP difference.

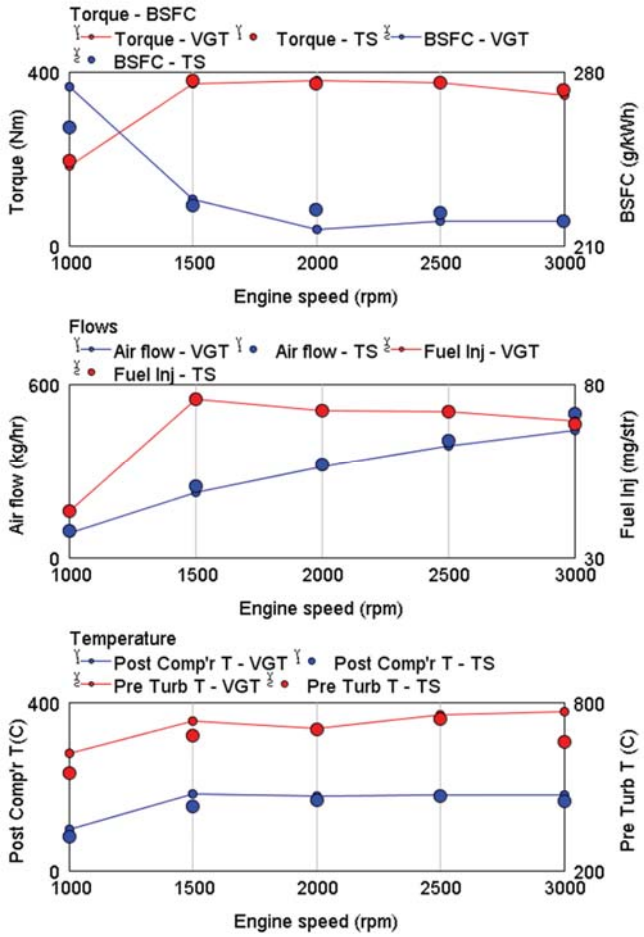

Figure 7.9 two stage system full load test results compared to the baseline VGT test results up to 3000 rpm - part1

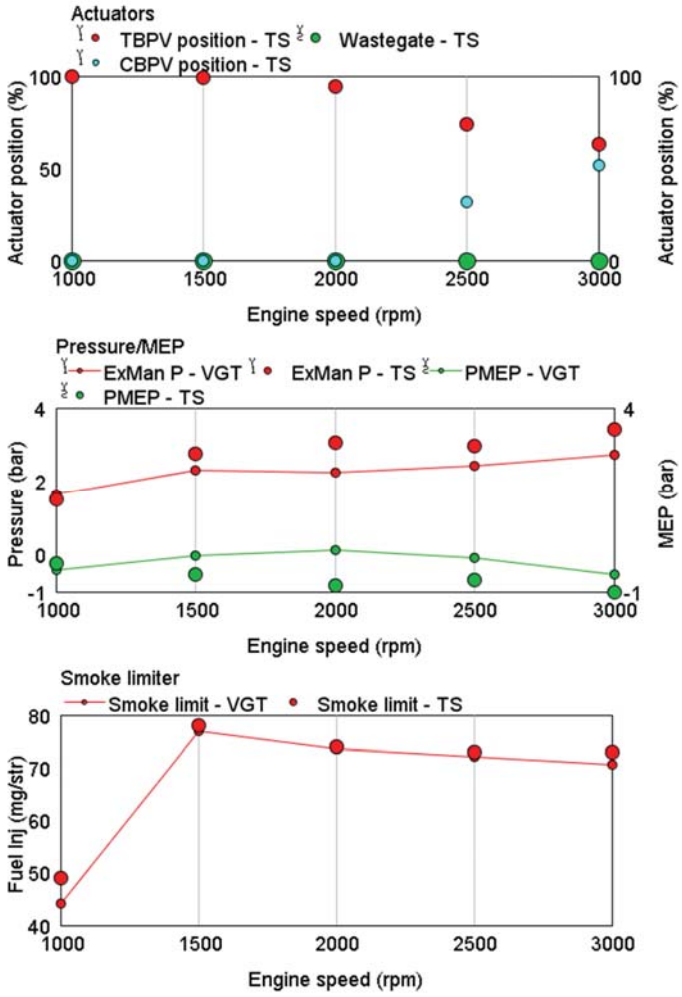

Figure 7.9 two stage system full load test results compared to the baseline VGT test results up to 3000rpm – part2

During the full load tests the back pressure of the engine was a closely monitored parameter to ensure hardware safety. It was obvious that further increasing the boost level would lead to very high engine back pressure. To avoid hardware damage, it was decided that the boost target was kept the same as the baseline test for the full load testing.

It was worth noticing that the air flow was increased in all the speed points when using the two stage boosting system (part1 mid plot). This was mainly due to improved volumetric

efficiency benefited from the compressor efficiency of the two stage system. Although not a significant increase in absolute number at 1000 rpm due to the scale of the plot, the increase from 84.8 kg/hr to 91.8 kg/hr was a substantial increase in percentage. The higher compressor efficiency (part1 lower plot), leaner combustion (part1 lower plot) and the lower pumping (part2 mid plot) loss had contributed to the torque increase from 183 Nm to 195 Nm, a significant improvement in low end torque with exactly the same fuel injection. Should the ECU allowed higher maximum torque at this speed, at least around 30 Nm more torque could have been gained at this speed point, since the smoke limiter could allow an extra 6 milligram of fuel per stroke to be injected (part2 lower plot) and the potentially achievable higher boost level was not considered. The torque at 1500, 2500 and 3000 rpm can also be expected to rise to some extent due to the increased air flow.

The operating points were also marked on the compressor maps of the HP stage and LP stage. On the HP map, the 1000 rpm, 1500 rpm and 2000 rpm full load points were where the HP was contributing to the boost. The apparent drop in pressure ratio at the 2000 rpm point was the effect of opening the turbine bypass valve, thus the drop in compressor power. 2500 rpm and 3000 rpm could not be marked precisely on the HP map due to the opening of the compressor bypass valve, and therefore was marked on the origin of the map.

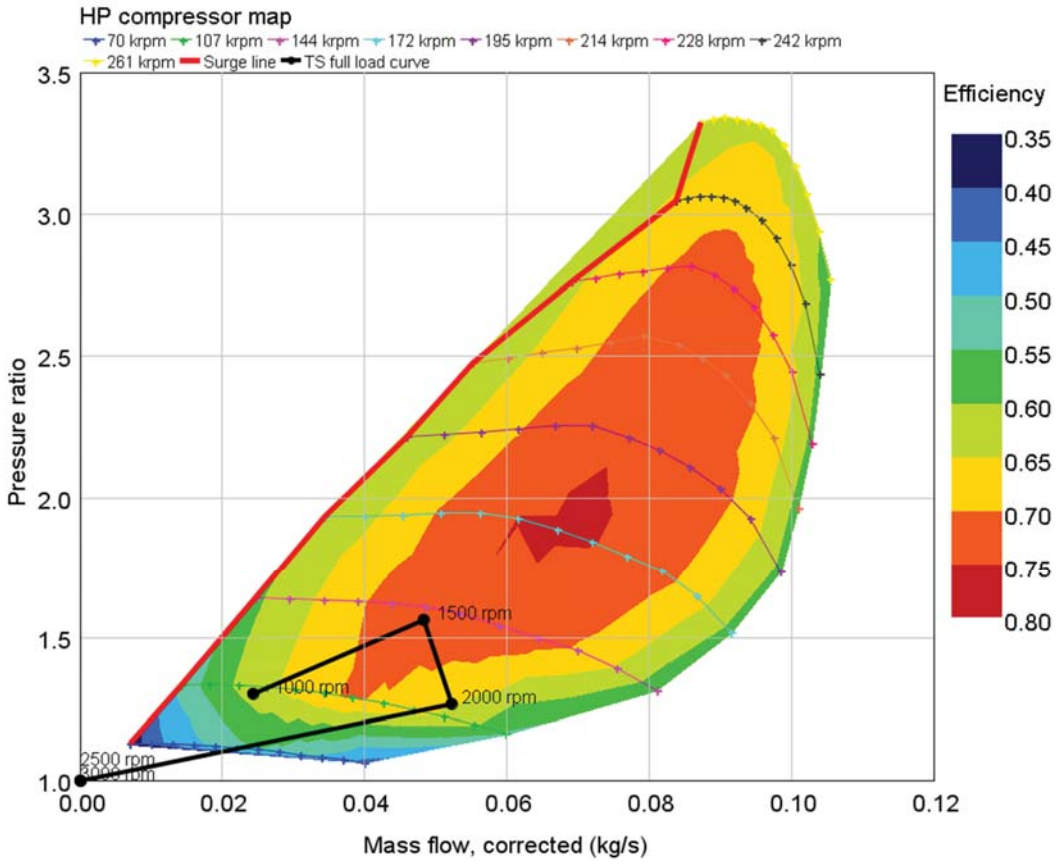

Figure 7.10 the two stage full load test results mapped on the HP compressor map

Apparently only a small portion of the HP compressor map was used and this low flow low pressure ratio region was low in efficiency. A smaller sized compressor would provide better efficiency in single stage boosting but would make the general performance of the complete system unacceptable at the switching point around 3000 rpm. In the context of such necessary compromise, it was advisable that manufacturers should pay attention to compressor efficiency at the low pressure ratio region on the compressor maps when producing the small turbocharger for a two stage system. Higher pressure ratio region would barely be used in the real world operation.

In Figure 7.11, the LP map showed the operating points with very good efficiency performance. On a single stage system, the distance of the low engine speed full load points should be reasonably close to the surge line. The logic behind this was that at rated power (higher engine

speed) point could still sit in the centre of the efficiency contour to provide optimal rated power efficiency although the low speed points would face low efficiency and very likely the compressor surge situation. On the two stage system, such dilemma was avoided since the pressure ratio was shared by the HP stage therefore the low engine speed points were further away from the surge line and closer to the high efficiency region.

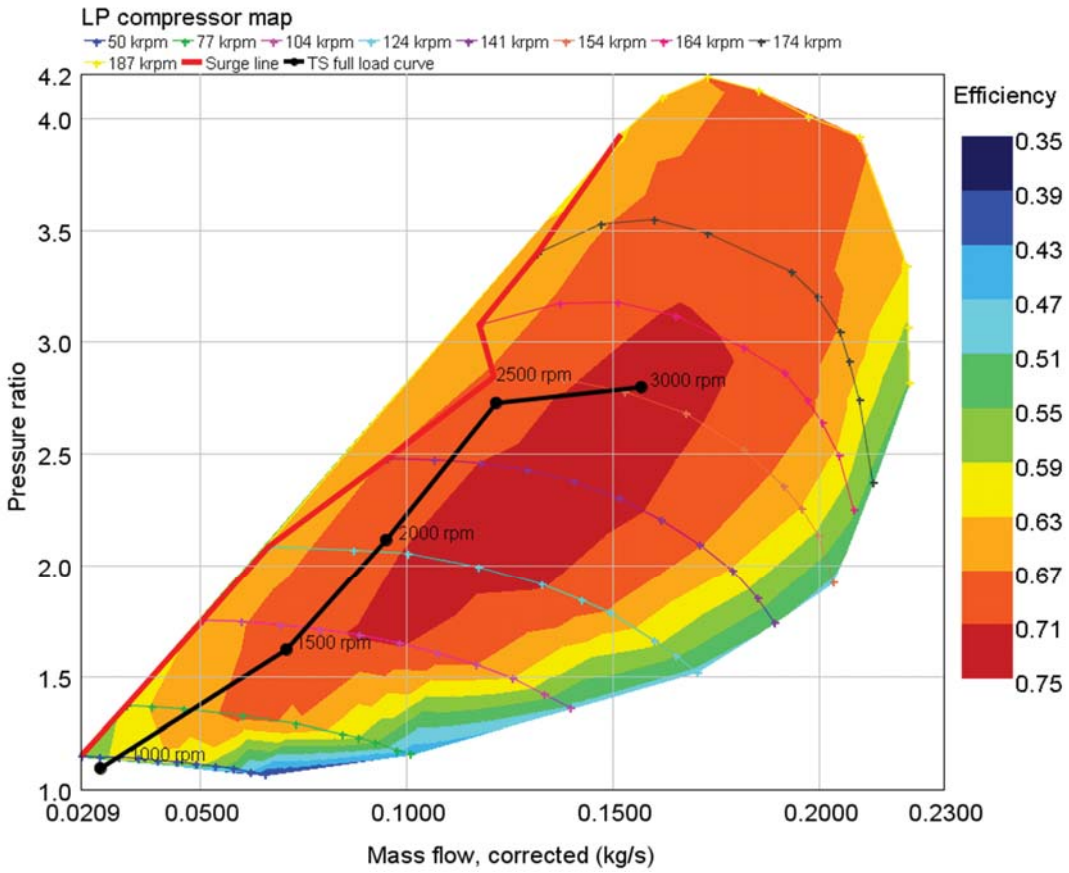

Figure 7.11 the two stage full load test results mapped on the LP compressor map

It was worth noting that although the pressure ratio at 1000 rpm was only a small number, the combined boost level was much higher than can be achieved through singly stage turbocharging without a VGT. Experiments have been conducted with the LP turbocharger wastegate open and the HP stage turbocharger was unable to boost the engine to the same level of brake torque.

7.2.2 Minimap points test results

The minimap test results were presented in the group plot as in Figure 7.12. For the sake of conciseness, only the a few important parameters such as BSFC, NOx, air mass flow and engine delta P (Pressure difference in intake manifold and exhaust manifold) were selected.

In Figure 7.12 part1 the plots showed the engine performance at the 1000 rpm, apparently the two stage system was gaining the best overall performance. At low load (25, 50 Nm) due to the lower back pressure the two stage system gained a large margin on BSFC compared to the VGT turbocharger. Also, the higher mass flow of the two stage system would allow faster response at the request of a torque transient. At 150 Nm, the VGT boost level has plateaued and the ECU algorithm shut off the EGR valve to ensure further torque, while the two stage system met the boost target and allowed 4% EGR gas to significantly reduce the NOx level.

In Figure 7.12 part2 plots, the two stage system was showing a similar trend in BSFC: lower BSFC at low load due to the lower engine back pressure and the advantage diminished as load went higher and back pressure trend reversed. The NOx emissions for both turbocharging system were similar, the only exception being that at 250 Nm the EGR controller was around the switch off location and in the two stage system testing the EGR valve was shut off while in the VGT testing the EGR valve allowed 1.8% EGR gas and reduced the NOx by 250 ppm.

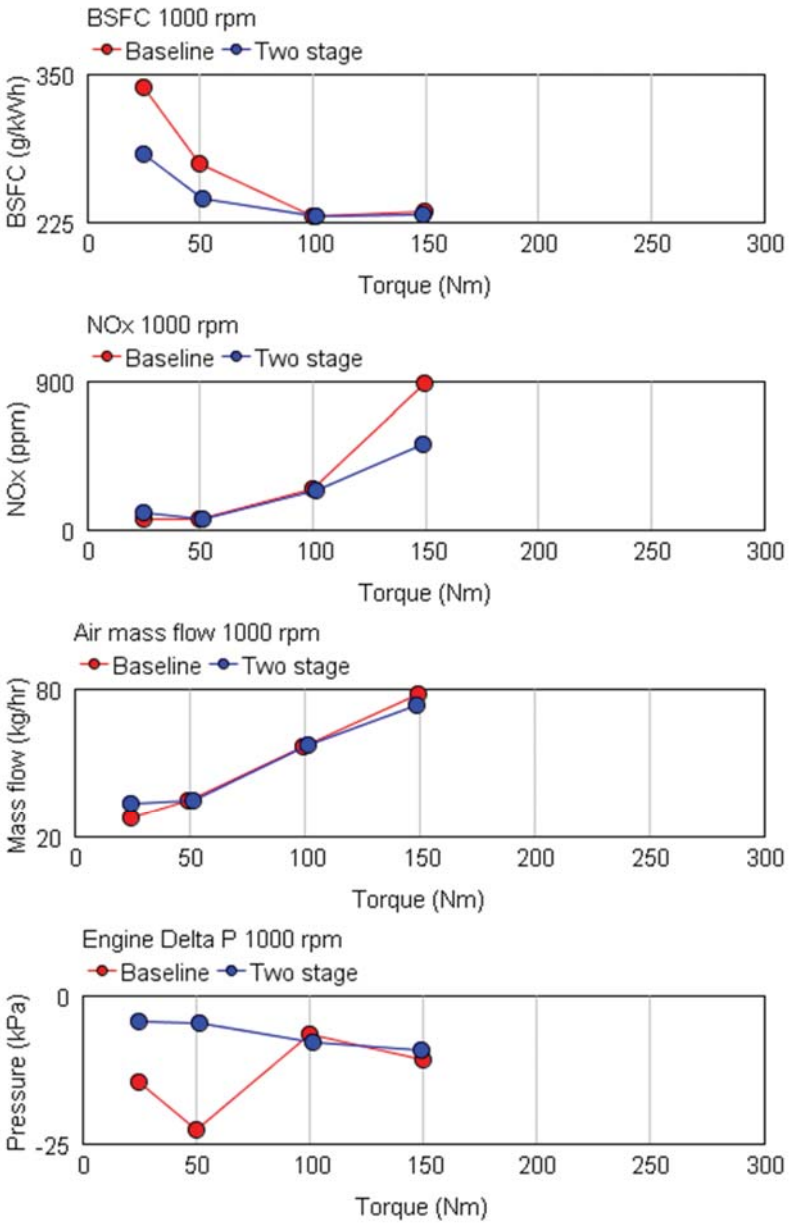

Figure 7.12 the two stage minimap points test results compared to baseline engine (1000 &1500 rpm) – part1

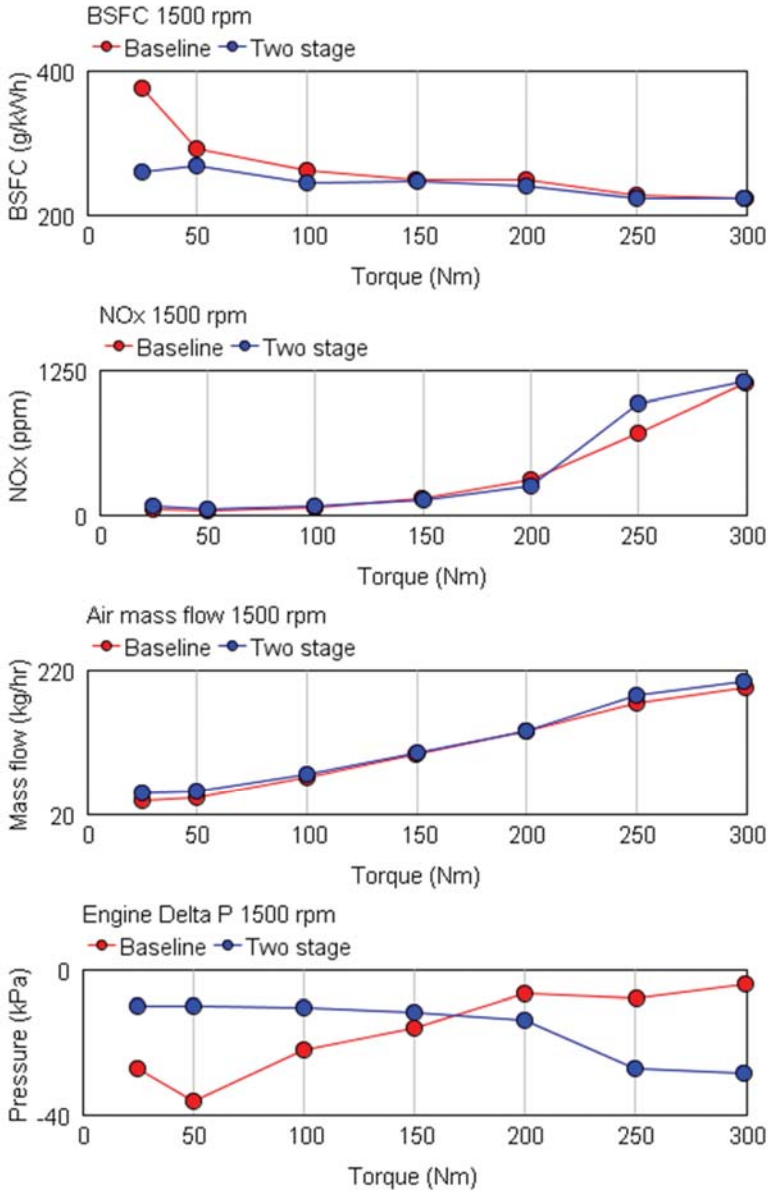

Figure 7.12 the two stage minimap points test results compared to baseline engine (1000 &1500 rpm) – part2

At higher engine speeds the two turbo system were very similar in terms of boosting capability and the high back pressure from the two stage system became a disadvantage. As shown in Figure 7.13 part1 plots, the two stage system at 2000 rpm showed worse BSFC performance compared to the baseline except for the very low load (25 Nm) where the small difference in back pressure had large influence on the EGR rate and thus the combustion. The worse BSFC was alleviated as load increased and EGR was shut off. In Figure 7.14 part2 plots, again no

appreciable advantage was acquired using the two stage system. The lower NOx emission of the two stage system at 150 Nm and 200 Nm was due to the increased EGR mass flow in the two stage system thanks to the higher engine back pressure (indirectly demonstrated through the lower air mass flow).

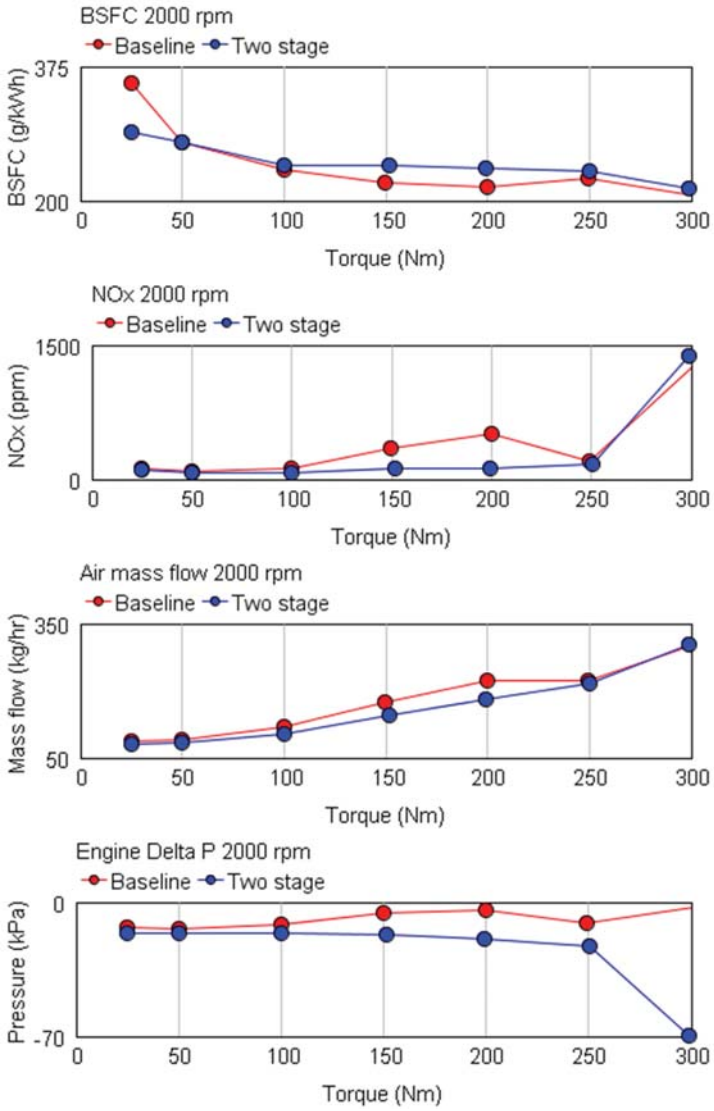

Figure 7.13 the two stage minimap points test results compared to baseline engine (2000 & 2500 rpm) – part1

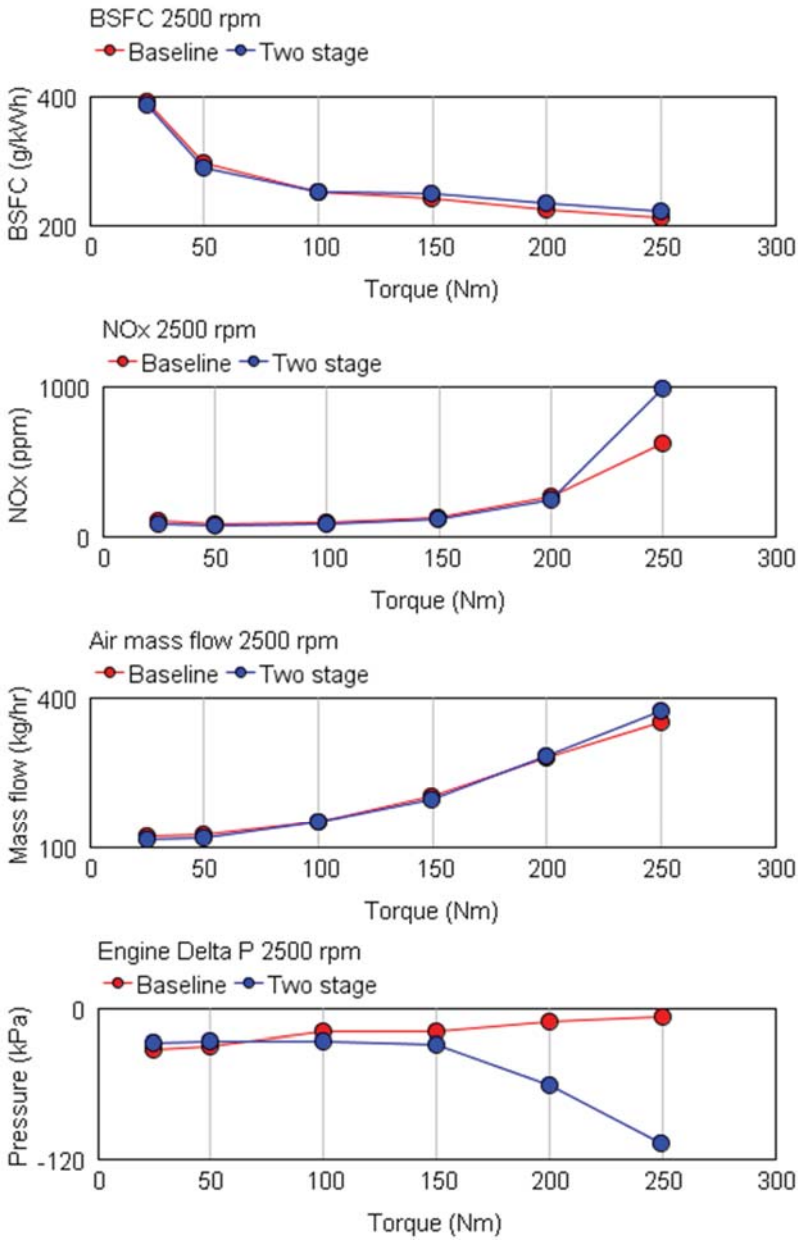

Figure 7.13 the two stage minimap points test results compared to baseline engine (2000 & 2500 rpm) – part2

At 3000 rpm as in Figure 7.14, the back pressure played an even larger influence to the BSFC of the engine. Apparently at this engine speed there was no advantage of using the two stage system. The high pressure stage turbocharger seemed too small for this operation and became a throttle to the system, creating large gradient in engine delta P. EGR controller was not stable for the 150 Nm and was shut off therefore there was a spike in the NOx level.

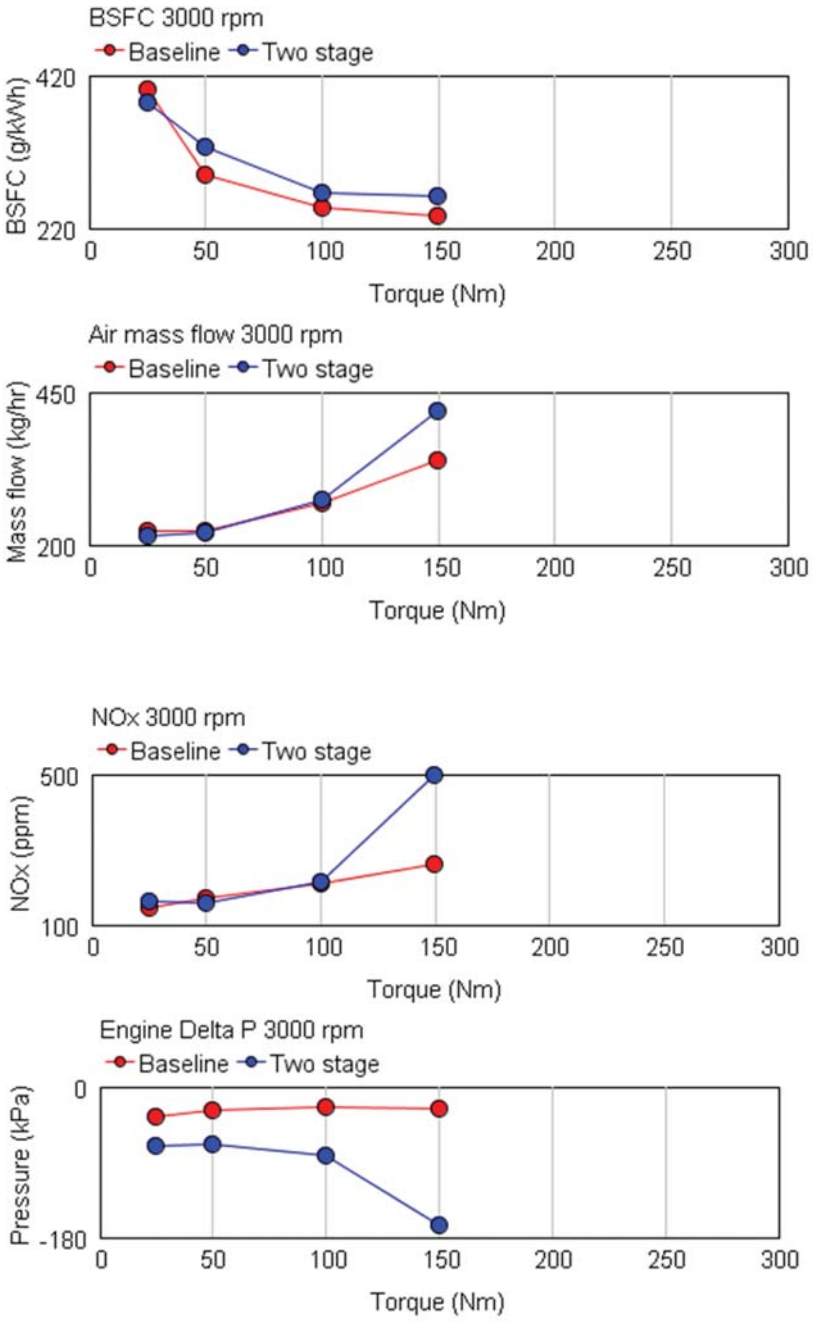

Figure 7.14 the two stage minimap points test results compared to baseline engine (3000 rpm)

As already conducted in the baseline engine experiment chapter, the emulated drive cycle results were derived with the same method and the results were shown in Table 7.3 below.

Table 7.3 emulated drive cycle results from minimap points test results

	NEDC		**WLTC**	
Emissions	CO_2	NO_X	CO_2	NO_X
Units	g/km	mg/km	g/km	mg/km
Baseline VGT	165.8	192.7	189.5	292.7
Two stage	158.9	139	189.1	295.1
Comparison	-4.2%	-27.9%	-0.2%	0.8%

Apparently due to the better performance of the two stage system at low engine speed operating region, the two stage system gained better results in the less intensive NEDC drive cycle. The CO_2 emission was reduced substantially by around 4.2% and the NOx level reduced significantly by 27.9%. In the WLTC drive cycle, which was designed to be a better representation of the real world driving and included more high power operations, neither of the CO_2 emission and NOx was seen to be improved significantly by using the two stage system.

To explain such discrepancy in fuel consumption and NOx emissions, the BSFC reduction in g/kWh was plotted in a contour map as in Figure 7.15 as an example. The graph clearly showed that the two stage system gained benefit in fuel consumption to the left of the '0 reduction' curve, while to the right of the '0 reduction' curve, the baseline VGT system was the more efficient machine. This clearly explained the difference seen in the drive cycle CO_2 emission, since the NEDC cycle mainly resided to the left of the '0 reduction', while the WLTC cycle occupied the right upper region much longer than the NEDC.

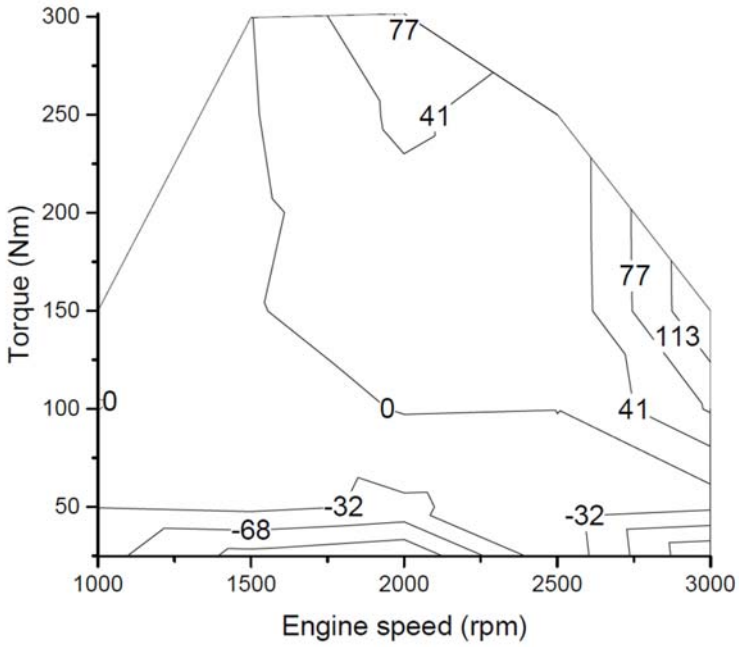

Figure 7.15 Two stage system BSFC reduction in g/kWh from baseline engine (negative -> more efficient)

7.2.3 Transient test results

Since the minimap test only confirmed the comparable performance of the two stage system compared to the baseline setup. The extent to which the transient response can be improved was crucial in justifying the use of the two stage system. It can be expected that the largest benefit in the transient response should be seen at low engine speed region and that the advantage diminished as the engine speed went up and the VGT worked with high efficiency with sufficient mass flow.

At 1000 rpm warm condition, as shown in the Figure 7.16 and the Figure 7.21 upper left for the averaged tip-in analysis, the transient performance of the two stage system was significantly improved. With the transient response time T1090 (torque rise from 10% to 90% of steady state torque) reduced by more than 50% from 3 second to 1.3 second (Figure 7.21 upper left plot). It should also be noted that a wider tip-in torque range was achieved due to the improved boost led to the increased full load torque. The turbine bypass valve controller worked well during the tip-in, with the valve first closed until the boost target reached and

then opened and maintained position with no oscillating behavior. The tip out phase was marked by a large and sudden valve opening behavior which was caused by the sudden reduction of boost target. This maneuver had no apparent disadvantage during the test phase and could be easily avoided by adding in a low path filter to the actuator controller for the sake of hardware protection. On the other hand, the turbocharger was seen decelerating faster than the VGT turbocharger, which might have been beneficial for the system restabilising.

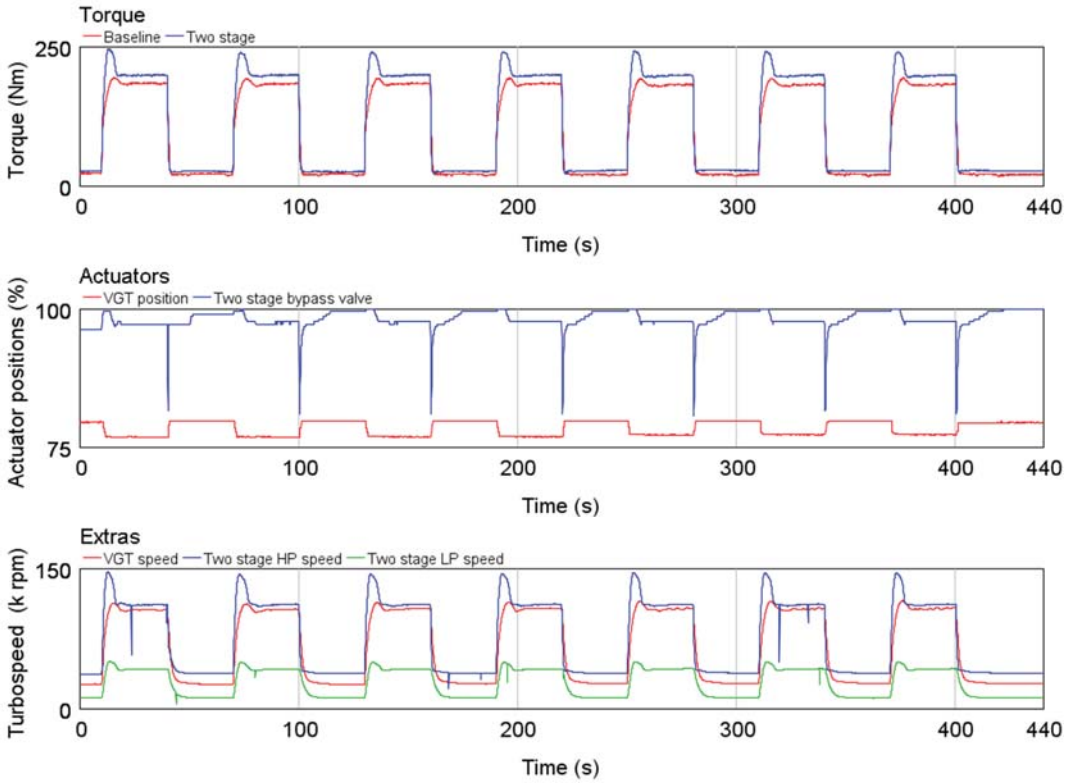

Figure 7.16 two stage transient test results compared to the baseline engine at 1000 rpm hot condition

The advantage of using the two stage system quickly diminished as the engine speed went up to 1500 rpm. As shown in Figure 7.17 below and in Figure 7.21 right upper plot for the detailed tip in/out curve. The two stage system had only a negligible 0.1 second advantage in T1090 compared to the baseline system. Another appreciable improvement of the two stage system was the higher torque at the low load condition which was the result of lower engine back

pressure.

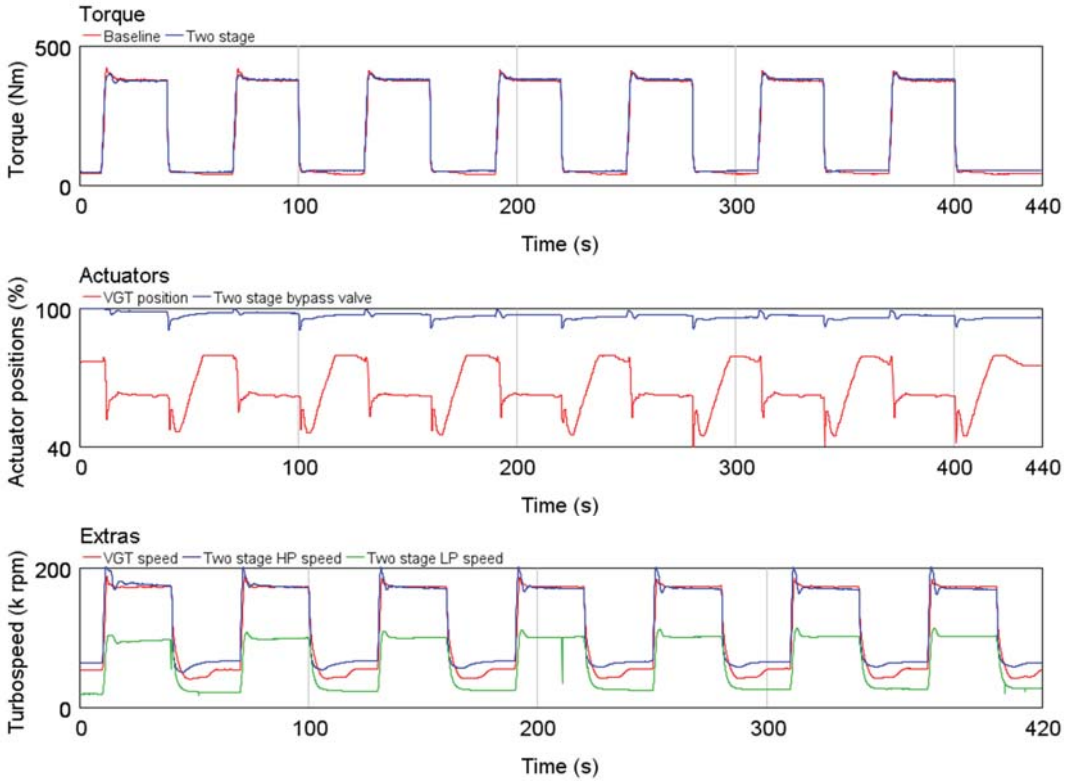

Figure 7.17 two stage transient test results compared to the baseline engine at 1500 rpm hot condition

At 2000 rpm as in Figure 7.18, the transient performance of the baseline VGT system has surpassed that of the two stage system. T1090 was 0.2 second faster for the VGT than the two stage system and the VGT system allowed a higher full load torque. However the difference was still small and the two stage system can be considered to have equivalent transient performance with VGT at 1500 rpm and 2000 rpm. Transient performance above 2000 rpm were no longer a focus in this project and was not tested due to hardware protection.

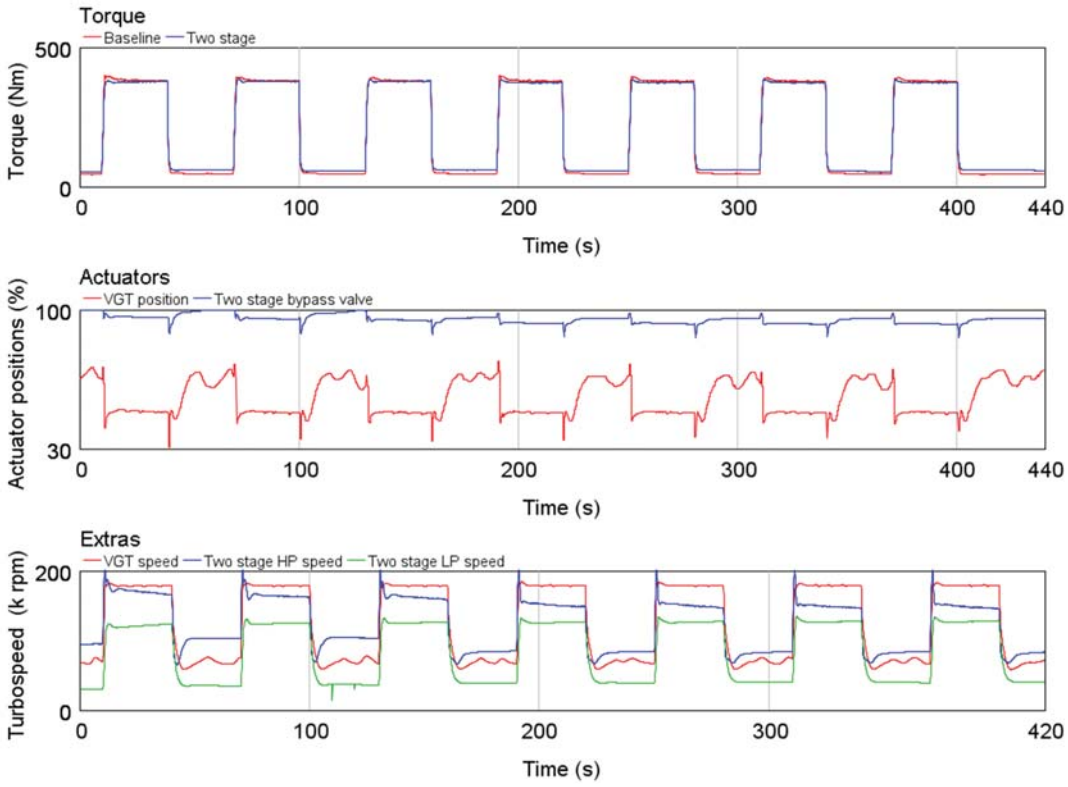

Figure 7.18 two stage transient test results compared to the baseline engine at 2000 rpm hot condition

The cold start transients was another side that the performance was expected to improve by using the two stage system. As shown in the Figure 7.19 below, the two stage system was indeed much faster than the VGT system, with the T1090 reduced dramatically from 4 seconds to 0.6 second. The lower inertia of the HP stage turbocharger was considered the main factor in this drastic comparison. The HP stage turbocharger seemed uninfluenced by the cold oil condition at all and the performance was only limited by the other components in the cold engine system and therefore generating lower full load torque. Another interesting phenomena observed in the experiment was that the engine as a system warm up slower with the two stage system, which could be a disadvantage considering the after treatment system. This had already been expected for the reason of extra mass in the turbocharging system due to the extra turbocharger to warm up, yet the extra mass flow allowed by the two stage system also rendered the combustion to be leaner and colder. The combined effect of lean

combustion and increased thermal inertia should be carefully considered when implementing the two stage system unto production engines.

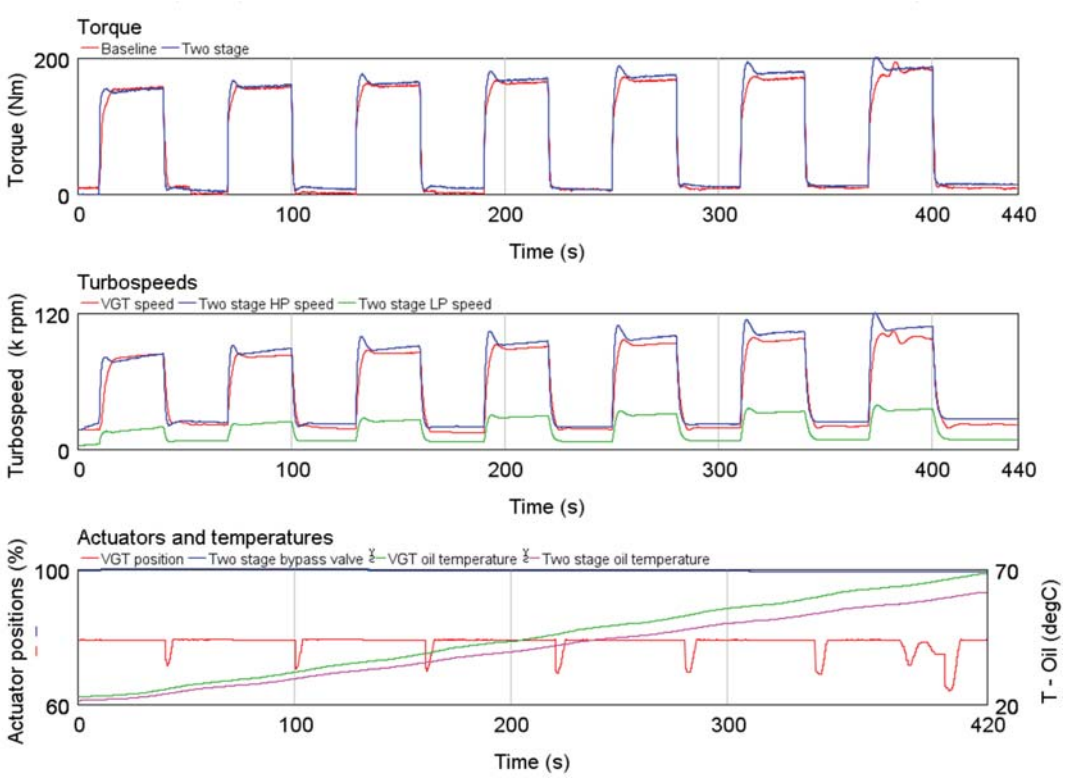

Figure 7.19 two stage transient test results compared to the baseline engine at 1000 rpm cold condition

The cold start at 1500 rpm in Figure 7.20 showed the advantage of the two stage system in boosting the cold engine to the full load level right from the first transient, with a torque difference above 50 Nm. However, the advantage diminished after the first transient since the turbocharger system warmed up faster at higher engine speed and from the first transient the baseline system already reached the boost target, marked by the modulating of VGT control vane position.

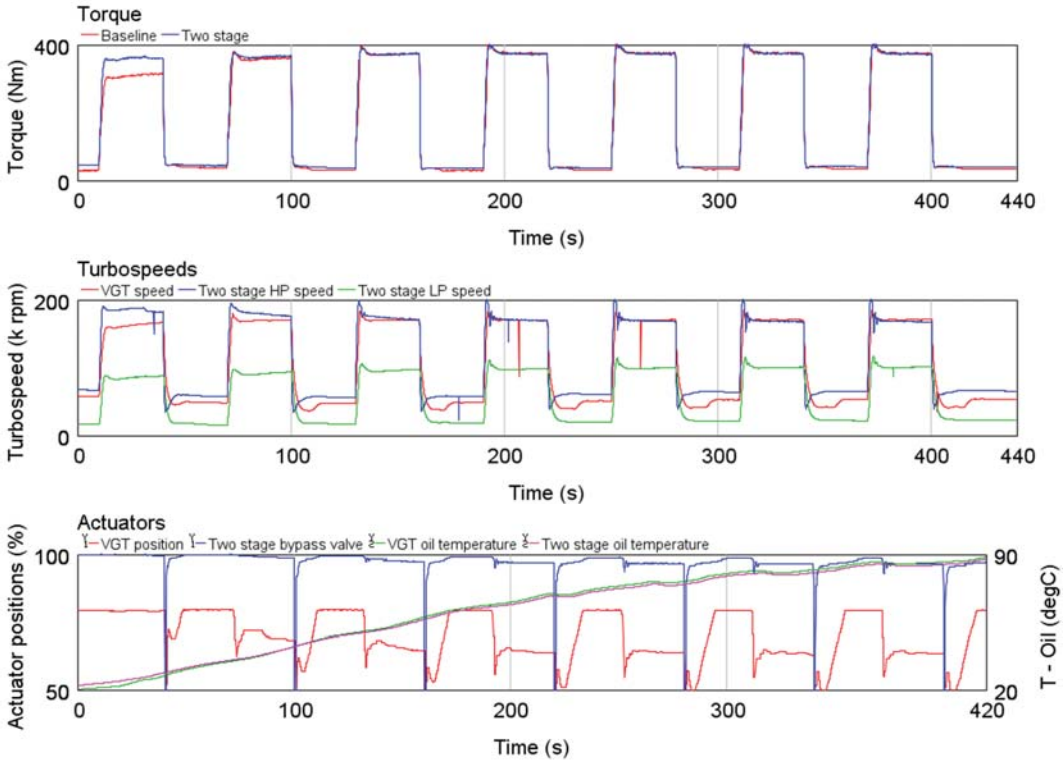

Figure 7.20 two stage transient test results compared to the baseline engine at 1500 rpm cold condition

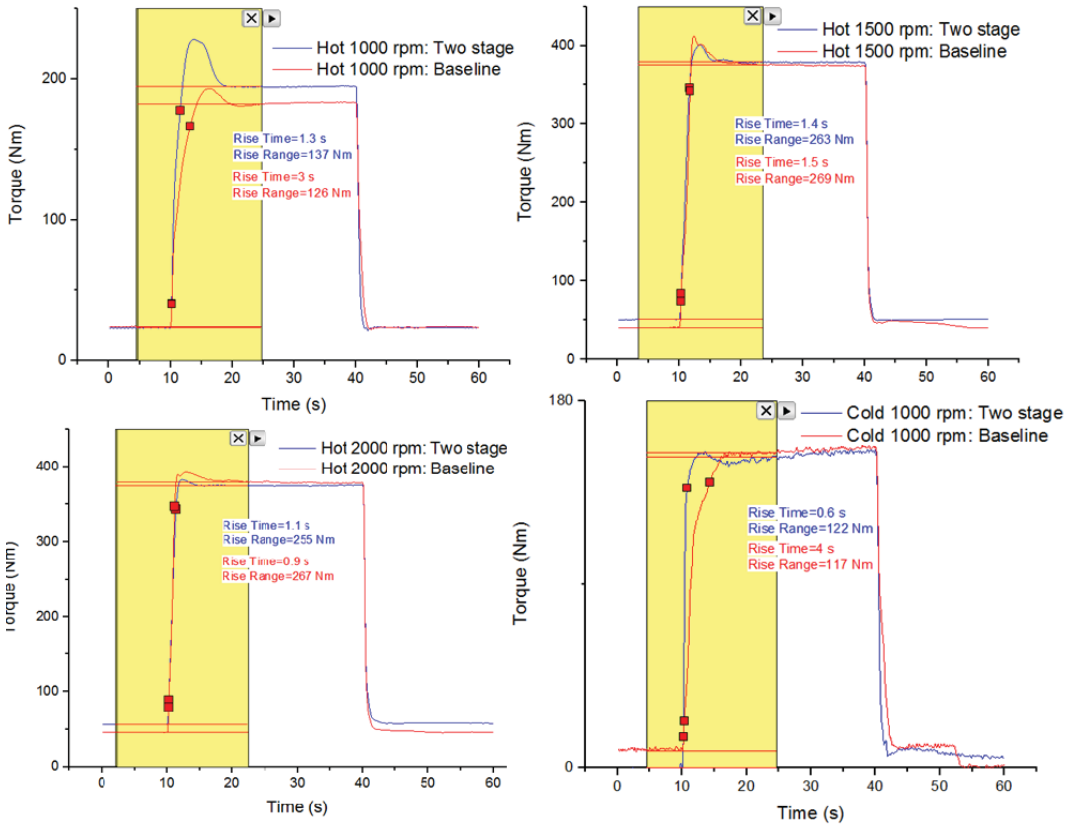

Figure 7.21 two stage system transient performance analysis compared to the baseline engine

7.3 Discussion of the two stage system performance.

The test results presented here did not portray the two stage system as a perfect solution that could improve the performance of an engine in all aspect. For one thing, limited by the available hardware, which was originally matched to a smaller engine, the performance could be improved with a slightly better matched turbocharging system. For another, the control algorithm was constructed without the level of complexity as seen on a production engine, let alone the calibration effort put into tuning the controllers.

However, the test results confirmed qualitatively the findings from the initial simulation studies: the two stage system had the potential to increase the full load torque due to the better boosting capability and the engine saw an increase of 12 Nm at 1000 rpm engine speed.

The transient response would see an improvement due to the low inertia of the high pressure stage turbocharger and dramatic improvements were seen at 1000 rpm in both cold and hot conditions. The improved boost can be used to either produce more torque by burning more fuel, or to reduce NOx emission by allowing more EGR gases.

There were also advantages that were initially not expected. The back pressure of the system was not always as high as indicated in the simulation and in fact was a benefit at the low speed low load condition to reduce the fuel consumption. The better efficiency from the two stage of compression allowed boost air with lower temperature at the same boost level, which cooled down the whole gas exchange path and worked beneficially for the combustion process.

The system inevitably faced compromises as well. As predicted in the simulation study, the hardware used in the experiment would significantly improve the transient performance but in the meantime the engine back pressure will suffer at higher engine speed due to the sizing of the system intended for a smaller engine. The minimap test results confirmed the simulation prediction in that the delta P of the engine was 1 bar higher for the two stage than the baseline at 2500 rpm, and further increased to 1.4 bar at 3000 rpm. Such behavior indicated poor volumetric efficiency and high pumping loss. Certainly this can be alleviated by using a larger HP stage turbocharger but would compromise the transient response.

7.4 Summary

The chapter has discussed the work of implementing the control strategies designed in chapter 6 on the engine test bench to test the two stage turbocharging system. Although most of the experiment results were more or less different from the simulation results quantitatively, the system performance was largely matched with the expectation.

From the test results, the two stage system was confirmed to be a more advanced turbocharging device in terms of the boosting capability. At different engine operating region, the system offered fuel consumption advantage due to its lower engine back pressure, NOx emission reduction due to the EGR capability and also significant improvement in transient response, both cold and hot condition, especially at low engine speed end.

However, the problems of the system was equally obvious. Just as expected, the high back pressure generated by the two stage boosting deteriorated the fuel consumption at mid speed around the switching point. Such problems will be more carefully looked at in the next chapter when the VGT and ball bearing technology will be implemented through simulation to further explore the potential of the two stage system.

Chapter 8 - Further exploration of the two stage turbocharging system

This chapter deals with the potentials and shortcomings of the two stage system identified in the previous chapter. The VGT technology as discussed in chapter 3 can continuously change the turbine area to match the engine mass flow so that a large turbocharger can accelerate faster at the cost of engine back pressure. The ball bearing technology as discussed in chapter 5 can improve the engine transient response and at the same time reduce the engine back pressure. These two technologies were implemented in the 1D engine model to alleviate the back pressure problem of the two stage system while maintaining good transient performance. Other aspects of the two stage system were also studied with the aid of the calibrated engine model.

8.1 Further calibration of model using two stage system testing data.

As discussed in Chapter 4, the baseline model was calibrated using the minimap and full load test data. The calibration was successful in that the model predicts all the turbocharging related engine parameters: mass flow, pressure and temperature with high fidelity. The predictive quality was based on a calibrated predictive combustion model instead of unrealistically scheduling of various multipliers in the model. The steady state baseline model provided a foundation for the exploratory work in this chapter, which relied heavily on the extrapolation quality of the model.

When comparing the two stage system test data with the simulation results in the chapter 6, it was found that simply replacing the baseline model VGT turbocharger with the two stage system was not adequate to replicate the experimental results to the same level of accuracy as the VGT test results: the engine model could not perfectly imitate the real gas exchange process when the turbocharging system was radically different. Therefore, the model was recalibrated using the new test data acquired using the two stage system. Also, this finding confirmed the expectation that the simulation work in chapter 6 was only appropriate for qualitative study to propose a usable control strategy.

Following a standard procedure provided in the GT-Power manual to calibrate the turbocharged engine model, the compressor and turbine models were calibrated separated by tuning of the mass flow multipliers and pressure ratio multipliers so that the turbocharger speeds of both HP stage and LP stage were matched. Then the turbine efficiency multipliers were tuned so that the turbines extracted the same amount of power as was consumed by the compressors; the compressor efficiency multipliers were tuned so that the compressor outlet temperatures matched the test results. The turbine models and compressor models were then connected by turbo shaft components and the calibration of the two stage model was finished. As an example to show the calibration quality, the temperature and pressure before and after

the LP stage compressor were ploted as below in Figure 8.1.

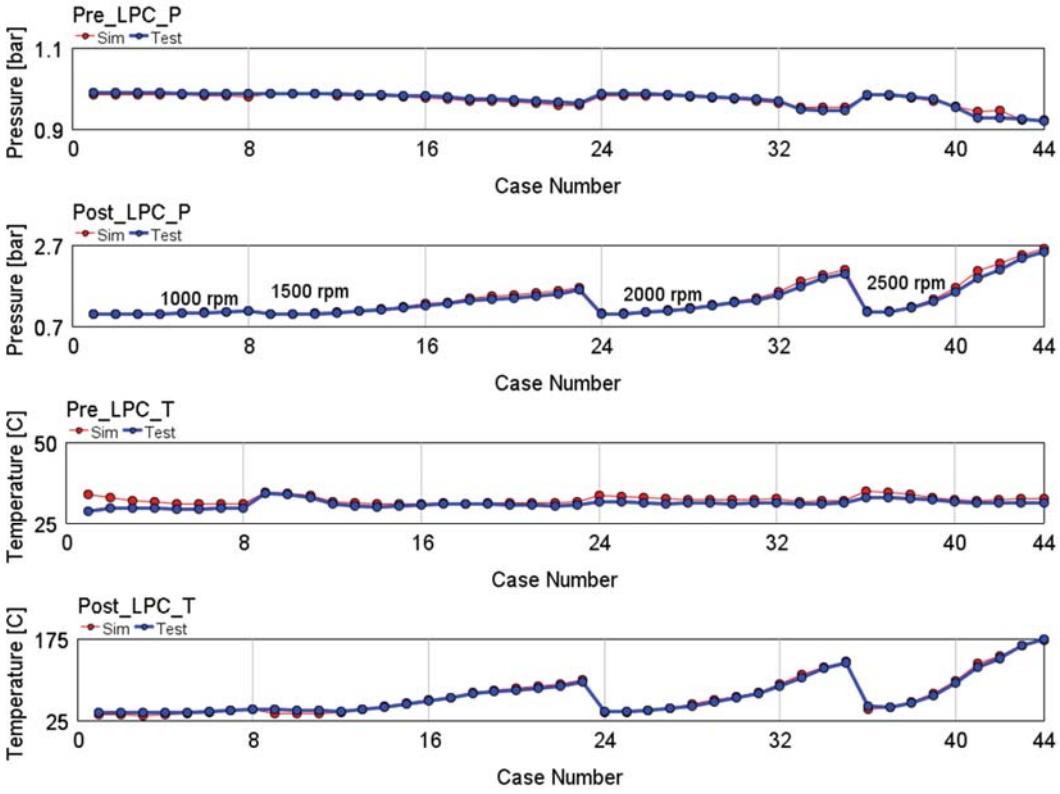

Figure 8.1 the compressor simulation results after calibration of the model using the test data.

It was found that the matching of the simulation results (mainly the compressor outlet temperature) to the test data at the low mass flow region with compressor map extrapolation was not as good as the high mass flow region due to the effect of the heat transfer. However, the difference was within 20 °C and the influence of this error was always absorbed by the larger errors downstream processes i.e. in the intercooler and the EGR gas mixing. Therefore, no scheduling of unrealistic efficiency multiplier was used to match the compressor outlet temperature for these less accurate test points. The procedure was justifiable considering that the exploratory work in this chapter was done by comparison between simulation results only.

Using the simulation results of the steady state operating points, the emulated drive cycle CO_2 and NO_X emission can be compared with those from the test results as in the Table 8.1 below.

Table 8.1 emulated drive cycle performance of the using the test results and the simulation results

	NEDC		WLTC	
Emissions	CO_2	NO_X	CO_2	NO_X
Units	g/km	mg/km	g/km	mg/km
Two stage in test	158.9	139.0	189.1	295.1
Two stage in simulation	149.4	104.3	180.4	268.0

Compared to the results from the experiments, the simulation appeared to have underestimated the emissions by a similar portion in the two drive cycles (10g/km of CO_2 and 30 mg/km of NO_X). The method of emulating the drive cycle proved to be consistent using these two sets of results. On the other hand, considering the collected errors from the test measurement, model prediction, drive cycle emulation, the error seen here was acceptable in this project and the subsequent simulation work will be compared to the simulation result only.

In addition to the steady state operating condition, the model was also re-calibrated to allow transient simulation. As suggested in the GT-Power manual, all the inputs dependent on the engine operating condition were packaged into look-up tables and the pedal position was actuated using a signal generator. Although the model was set up to run in 'speed mode', which indicated a constant speed was imposed and the torque varied with different amount of fuel injected, it was found that the short period of speed variation when a transient occurred had a big influence on the engine mass flow (air pumped in faster) and the calibration set points (set points shifted to the neighbouring matrix). Therefore, despite the instructions in the GT-Power manual, the engine speed was actuated using the test data. Since the improvements expected from the ball bearing and VGT was in the magnitude of less than 2 to 3 %, this practice significantly reduced the prediction error compared to simply presuming the engine dynamometer was an ideal torque absorber which always maintained constant speed.

In addition, the inertias of the turbo shaft were tuned to replicate the acceleration curve as seen in the test results. PID controllers were tuned to match the behavior of the actuators. As an example, the transient simulation at 1000 rpm were plotted in the Figure 8.2 below to demonstrate the quality of calibration.

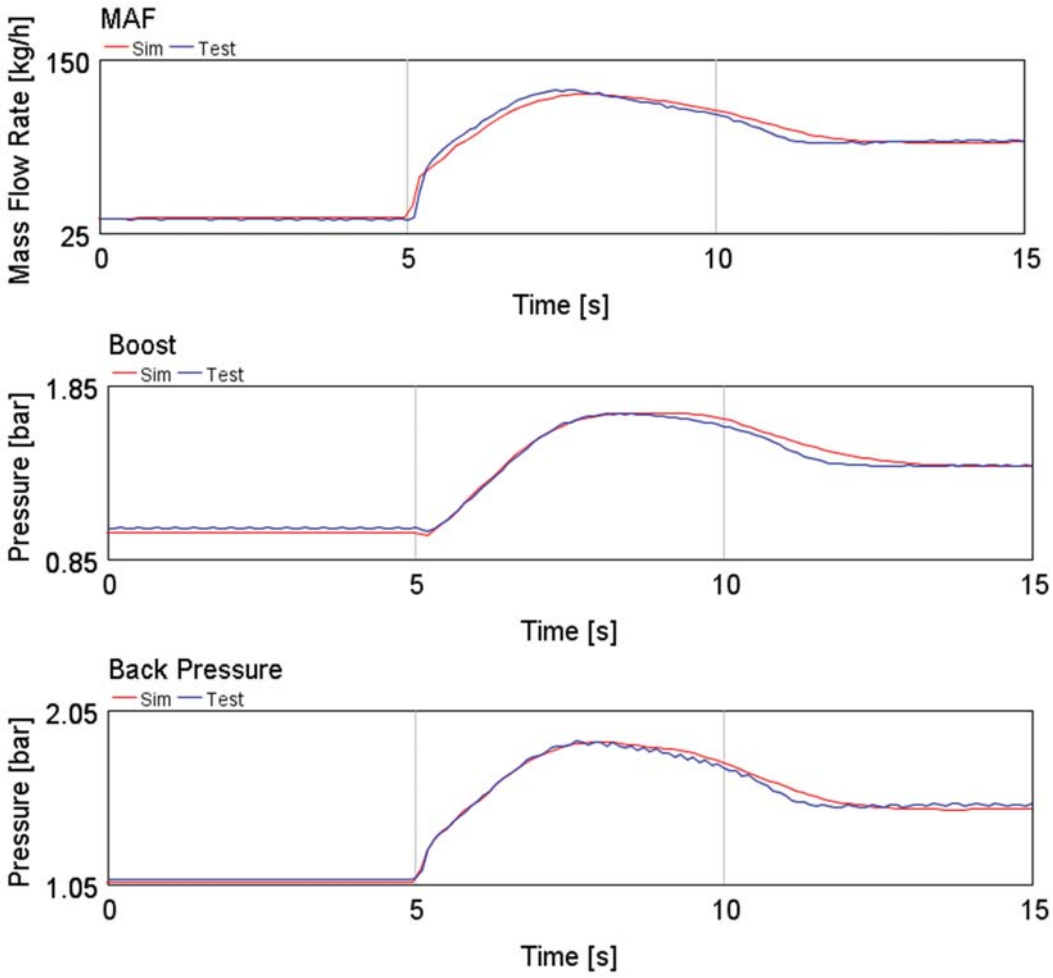

Figure 8.2 calibrated model: engine transient performance simulation results (1000 rpm) compared to test results

As shown in the Figure 8.2, all the three important parameters in the gas exchange process, namely the mass flow, boost pressure and engine back pressure were predicted with high fidelity compared to the engine test data. The slight discrepancy during the system settling was less important than the torque rise period with regards to evaluate the engine transient performance.

8.2 VGT turbocharger in HP stage

To implement the VGT turbocharger into the two stage system, two important decisions had to be made: first, what was the suitable size for the VGT turbocharger and second, whether the bypass valve was still necessary.

There was hardly any specific experience from the literature in sizing a VGT high pressure stage turbocharger in the two stage system. When crudely comparing the three compressors appeared in the two stage system and the VGT system in this project, the mass flow rates of the maximum efficiency points on the three maps were summarized as:

Table 8.2 mass flow rate comparison of max efficiency points of three compressor maps

Two stage: HP	VGT turbocharger	Two stage: LP
0.07 g/s	0.11 g/s	0.14 g/s

When using a VGT turbocharger in the HP stage of the two stage system, the size of the turbocharger should be obviously smaller than a single stage VGT turbocharger while larger than a FGT HP turbocharger in a two stage system. Comparing the numbers listed above, it was reasonable to select a VGT turbocharger for the two stage system HP stage with the maximum efficiency point mass flow between 0.07 g/s and 0.11 g/s. Therefore a turbocharger size sweep of the mass flow multiplier, as was conducted in chapter 6, was repeated here with the multiplier imposed on the VGT turbocharger model between 0.65 and 0.9. The shaft inertia was imposed a multiplier of second order to the mass flow multipliers to reflect the inertia difference.

The resulting trade-off between the peak back pressure and the T1090 indicated that 0.8 was the optimal size as shown in Figure 8.3 right plot below. With the simulation result of the 0.8 VGT plotted at the left.

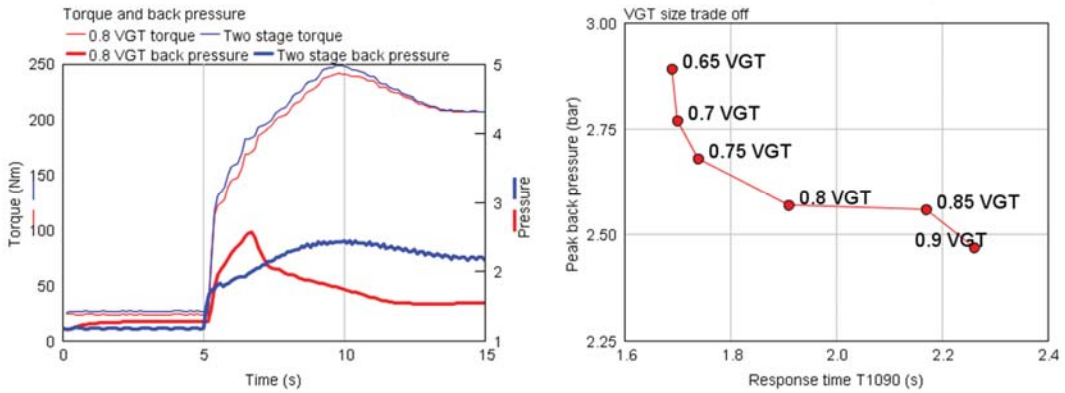

Figure 8.3 trade off of the back pressure and T1090 response time to decide the size of the HP VGT turbocharger

The sweep simulation revealed the expected finding that in all cases the VGT HP turbocharger provided slightly slower torque transient performance (T1090 = 1.7 ~ 2.3 s) compared to the original two stage system (T1090 = 1.5 s), yet due to the lower inertia and higher efficiency of a smaller device at low mass flow, the VGT HP turbo two stage system was still faster than the single stage VGT turbocharger (T1090 = 3s) at the cost of higher back pressure at the onset of the transient.

In all the size sweep cases, the presence of a large turbocharger at LP stage helped with boosting at the compressor side but also contributed to the high engine back pressure at the high mass flow steady state operating points compared to the single stage VGT situation. As shown in the Table 8.3 below, at 3000 rpm 300 Nm, the VGT alone was not able to modulate the boost level by fully opening of the guiding vanes. Without the bypass valve the engine back pressure was 0.5 bar higher than the baseline two stage system, counterbalancing benefit of HP stage VGT turbocharger as a high efficiency device compared to the FGT turbocharger. In addition the compressor outlet temperature was over the limit by 1 °C and it would only get worse when the engine went above 3000 rpm and higher load. Therefore the second question can be answered: the bypass valve was necessary for the two stage system with a HP stage VGT turbocharger.

Table 8.3 boost level, compressor out temperature, back pressure and turbo-speed were used to decide whether the VGT needs to be bypassed

Turbo setup	Boost (bar)	Compressor out T (degC)	Engine back pressure (bar)	HP turbocharger speed (kRPM)
Two stage original	2.34	195	2.91	89
VGT no bypass	2.65	201	3.42	102
VGT bypassed	2.34	174	2.61	43

With the correctly sized VGT turbocharger and the HP stage bypass valve, the drive cycle fuel consumption and NOx emission from the minimap was calculated again as in the Table 8.4 below:

Table 8.4 emulated drive cycle performance of the VGT two stage system compared to original two stage system (negative value -> improvement)

	NEDC		WLTC	
Emissions	CO_2	NO_X	CO_2	NO_X
Units	g/km	mg/km	g/km	mg/km
Two stage original	149.4	104.3	180.4	268
Two stage with VGT	153.1	98.7	183.9	242
Comparison	+2.5%	-5.4%	+1.9%	-9.7%

From the table, unfortunately the use of VGT turbine at the high pressure stage was not seen as an advantage in terms of the BSFC in drive cycles. The fuel consumption actually went up by 2.5% in NEDC and 1.9% in WLTC, mainly due to the increase in back pressure at low engine speed. The fuel consumption was indeed reduced at higher engine speed, which was not as densely populated as in the low speed region in the drive cycles.

The NOx emission, meanwhile, was reduced by 5.4% and 9.7% in NEDC and WLTC respectively. The reduction resulted from the improved EGR gas supply allowed by the VGT turbine at low-to-mid engine load region (where the drive cycle weighting was the highest). Care was taken in the simulation to ensure the EGR rate in percentage was held constant regardless of the total mass flow.

Transient performance was summarised using the T1090 index as in the Table 8.5 below.

Table 8.5 simulated transient performance of the VGT two stage system compared to original two stage system

Turbo setup	T1090 @1000 rpm (s)
Baseline VGT	3 s
Original two stage system	1.5 s
Two stage system with VGT (0.8)	1.9 s

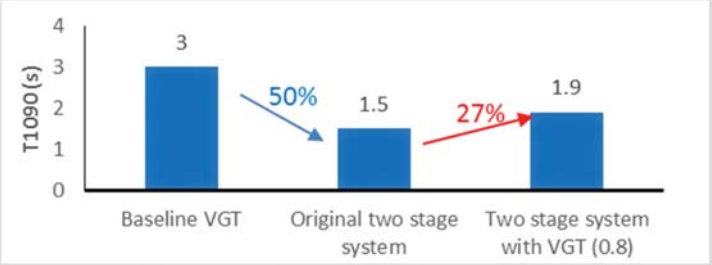

Figure 8.4 simulated transient performance of the VGT two stage system compared to original two stage system

As has already been discussed in the size sweep simulation section, the two stage system did not see an improvement in the transient response by using a VGT turbine at the high pressure stage due to the larger turbocharger inertia compared to the FGT counterpart. However, the penalty in T1090 was not significant (less than 0.4 s) and the margin can be expected to diminish at higher engine speeds.

From the simulation result, it would appear that the use of the VGT turbine in the HP stage can barely justify the extra cost and the extra system complexity. However, when considering the problematic back pressure control of the original two stage system, at low speed low load region the VGT increased the back pressure to allow higher EGR rate while at higher speed the engine back pressure was significantly reduced, allowing smoother EGR controller behaviour. In addition, the NOx emission was seen a significant reduction due to the cooler combustion as a result of better compressor efficiency. One the other hand, accompanied fuel consumption increased and slower transient performance was not significant and can be further alleviated by technologies such as the ball bearing turbocharger rotor.

8.3 Ball bearing turbocharger in HP stage

The ball bearing was implemented with the same method as done in the Chapter 5: the efficiency of the turbine map was modified (increased) to reflect a 50% reduction in the rotor friction losses. The EGR controller was configured to achieve the same EGR rate, instead of targeting a calibrated air mass flow rate. The fuel consumption, the NOx emission and the transient performance, was summarised in the Table 8.6 below.

Table 8.6 emulated drive cycle performance of the two stage system with HP ball bearing (negative value -> improvement)

	NEDC		WLTC	
Emissions	CO_2	NO_X	CO_2	NO_X
Units	g/km	mg/km	g/km	mg/km
TS original	149.4	104.3	180.4	268
TS with HP Ball bearing	147.8	107.8	178.1	260.9
Comparison	-1.1%	+3.4%	-1.3%	-2.6%

By comparing the simulation results, it was clear that the ball bearing at the HP stage achieved the expectation to reduce the fuel consumption. The BSFC was reduced by 1.1% in NEDC and 1.2% in WLTC. The NOx emission was reduced by 2.6% in the WLTC yet was increased by 3.3% in NEDC, indicating that the influence of the ball bearing turbocharger was different for the low load and high load conditions. By replacing the journal bearing with the ball bearing, both the air mass flow and the EGR flow were increased under the same EGR, as shown in the Figure 8.5 below. At low load region, higher air mass flow was trapped in the cylinder due to the lower back pressure and consequently the NOx generation was increased in the oxygen-rich condition (Nakayama, S. et al, 2003; Donahue, R. and Foster, D., 2000). Meanwhile, at higher speed and load region when the combustion was more sensitive to the existence of EGR, more burned mass was allowed in and therefore reduced the NOx generation. As a results, when looking at the cycle emission results, the NEDC which occupied a lower speed

and load region was seen an increase in NOx emission while the WLTC NOx emission was reduced.

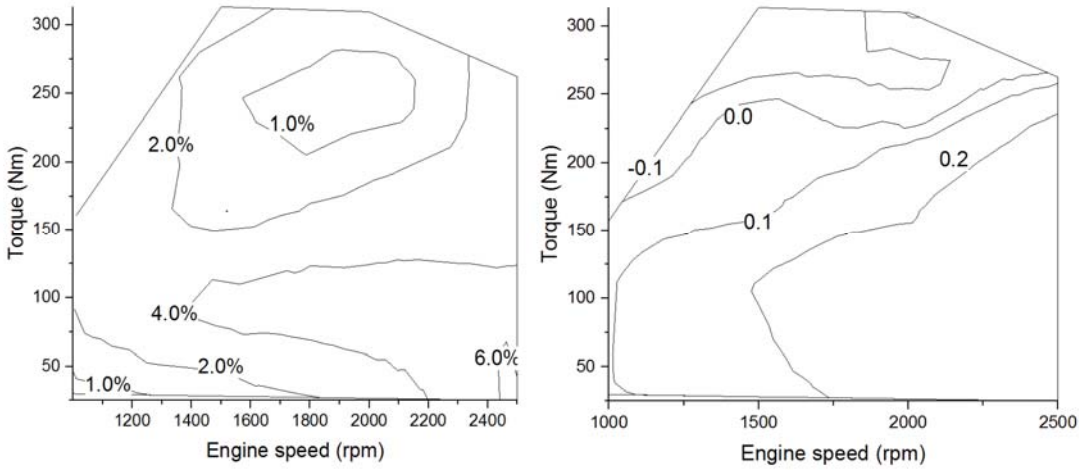

Figure 8.5 increased cylinder trapped air in percentage (left) and the increased EGR flow in g/s (right) through the use of HP ball bearing turbocharger

The transient performance of the HP ball bearing arrangement was summarised as in Table 8.7 and Figure 8.6. It was confirmed that the transient performance can be further improved through using the ball bearing technology in the two stage system. The transient response time (T1090) was reduced a further 0.23s. Such improvement indicated a good prospect to work in synergy with the VGT technology, which on its own would reduce the engine back pressure at the cost of poor transient response.

Table 8.7 simulated transient performance of two stage system with HP ball bearing

Turbo setup	T1090 @1000 rpm (s)
Baseline VGT	3 s
Original two stage system	1.5 s
Two stage with HP BB	1.27 s

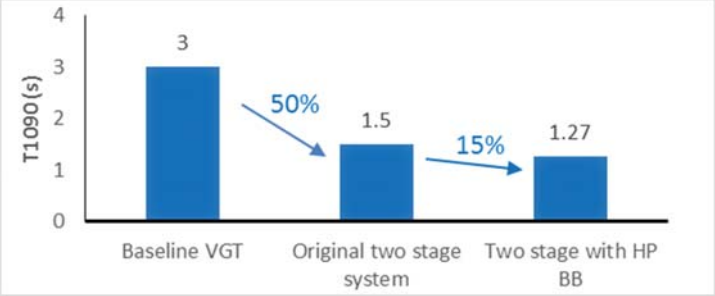

Figure 8.6 simulated transient performance of two stage system with HP ball bearing

8.4 Ball bearing turbocharger in LP stage and in both stages

The same practice in the last section was repeated for the LP stage and in both stages. The results were shown below in Table 8.8.

Table 8.8 emulated drive cycle performance of the two stage system with LP ball bearing and ball bearing at both stages (negative value -> improvement)

	NEDC		WLTC	
Emissions	CO_2	NO_X	CO_2	NO_X
Units	g/km	mg/km	g/km	mg/km
TS original	149.4	104.3	180.4	268.0
TS with LP Ball bearing	148.7	104.1	179.1	252.1
Comparison	-0.5%	-0.2%	-0.7%	-5.9%
TS original	149.4	104.3	180.4	268.0
TS with BB in HP & LP	147.0	109.3	176.8	249.6
Comparison	-1.6%	+4.8%	-2.0%	-6.9%

The simulation results showed that the improvement in terms of fuel consumption was almost linear to the use of HP and LP devices, with the combined benefit of using HP and LP ball bearing in the system equals to the individual benefit of the HP ball bearing system and the LP ball bearing system added together. Meanwhile, the use of LP stage ball bearing did not make as large an impact on the NEDC NOx emission due to the smaller influence on the back

pressure in the NEDC cycle; the impact was larger in the WLTC cycle due to the larger influence on the back pressure in the more intensive WLTC cycle.

Table 8.9 simulated transient performance of two stage system with LP ball bearing and with ball bearing at both stages

Turbo setup	T1090 @1000 rpm (s)
Baseline VGT	3 s
Original two stage system	1.5 s
Two stage with LP BB	1.63 s
Two stage with HP & LP BB	1.27 s

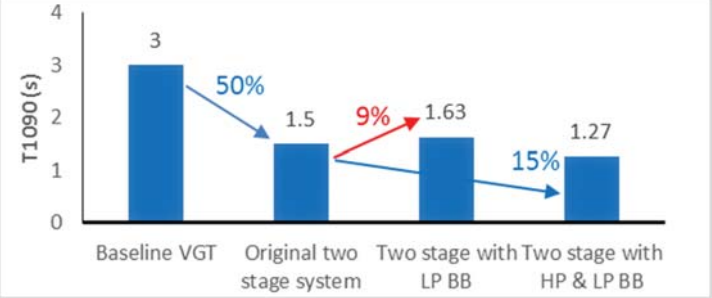

Figure 8.7 simulated transient performance of two stage system with LP ball bearing and with ball bearing at both stages

On the other hand, the transient response as summarised in Table 8.9 demonstrated the interesting effect of the LP stage ball bearing deteriorating the system transient response, which can be explained with the aid of Figure 8.8. With the LP stage ball bearing system, the LP stage now with higher efficiency shared more of the boosting task and consequently the more transient-influential HP stage was not able to provide the boost level quickly enough. As can be seen in HP turbospeed plot, the LP blue curve is much slower than the HP red curve and HLP green curve in both HP speed and boost pressure. The ball bearing at HP stage arrangement, however, had the slowest LP turbospeed acceleration which was not influential in the transient response in the low engine speed. When compared to the ball bearings in both stages (HLP arrangement), the HP stage ball bearing arrangement was slower by a negligible time different in the torque rise.

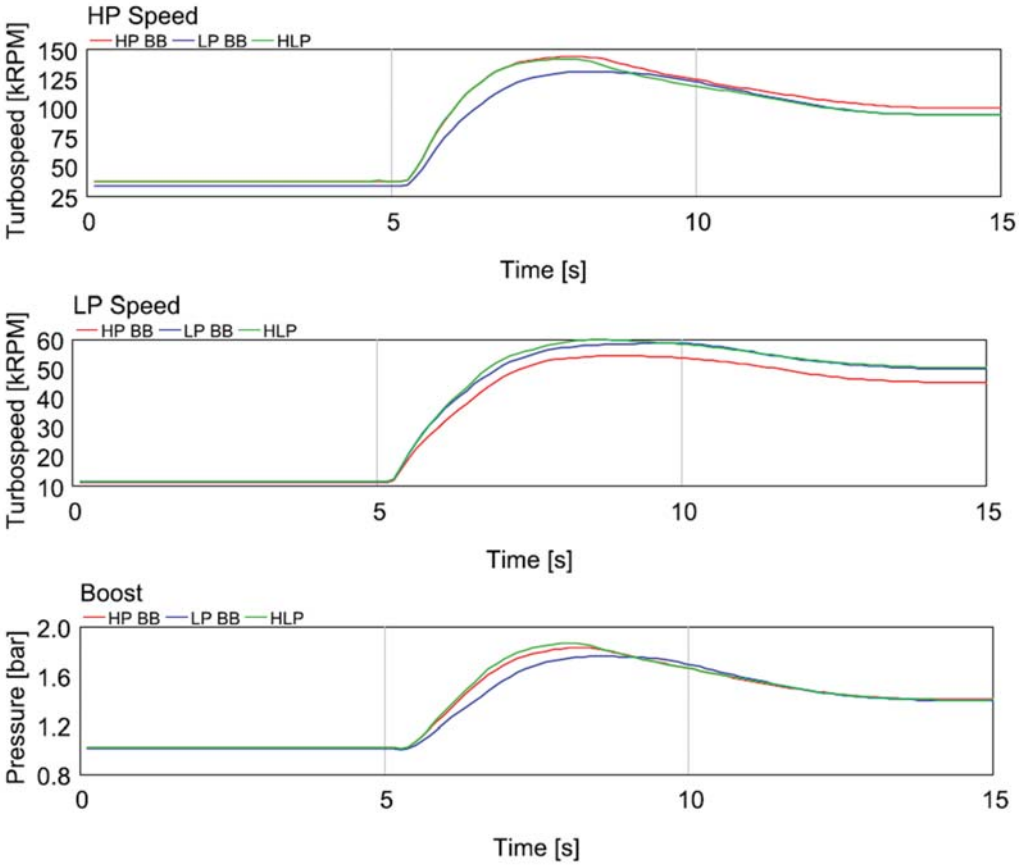

Figure 8.8 simulated transient performance comparison of turbospeed and boost pressure using different ball bearing arrangement.

8.5 VGT and ball bearing in HP stage.

Although the VGT turbocharger chosen for the two stage system was a larger device than the original HP turbocharger which indicated higher flow capacity thus lower engine back pressure, at the very low mass flow region, however, the VGT needed to close the vanes to generate enough boost and therefore raising the engine back pressure. This was not entirely a bad influence because more EGR gas was able to circulate at the low speed low load region, which was a disadvantage of the original two stage system as discussed in chapter 7. Therefore, evaluation of the implementation of a ball bearing rotor on a two stage system with a HP stage VGT turbocharger entailed attention to both the fuel consumption and the EGR capability

influenced by the engine back pressure. The transient response, in the meantime, was sure to be improved further. The simulation results were summarised in the Table 8.10 below:

Table 8.10 emulated drive cycle performance of the two stage system with HP ball bearing VGT (negative value -> improvement)

	NEDC		WLTC	
Emissions	CO_2	NO_X	CO_2	NO_X
Units	g/km	mg/km	g/km	mg/km
TS original	149.4	104.3	180.4	268
TS with BB in VGT	151.3	103.6	181.7	237.7
Comparison	+1.3%	-0.7%	+0.7%	-11.3%

The implement of the ball bearing in the HP stage VGT turbocharger provided the expected fuel consumption reduction of 1.2% compared to the journal bearing VGT situation and was now only around 1% higher than the original two stage system. However, as the previously discussed NOx emission performance in two drive cycles due to low back pressure in section 8.3, the ball bearing technology here showed a similar trend in that the NEDC NOx emission benefit from the VGT was counterbalanced by the HP stage ball bearing system, while the WLTC emission was reduced as expected.

Table 8.11 simulated transient performance of two stage system with VGT and HP stage ball bearing

Turbo setup	T1090 @1000 rpm (s)
Baseline VGT	3 s
Original two stage system	1.5 s
TS with VGT (0.8) and HP BB	1.55 s

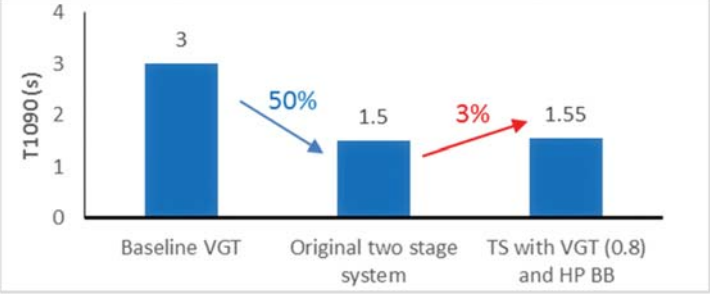

Figure 8.9 simulated transient performance of two stage system with VGT and HP stage ball bearing

As expected, the use of the ball bearing system in the HP stage VGT has reduced the T1090 response time (from 1.9s to 1.55s). With only 3% in response time penalty compared to the original two stage system, the VGT system can be implemented without concerns of deteriorating the transient performance while conquering most of the shortcomings in the two stage system.

8.6 Valve leakage and active control of compressor bypass valve

Much effort has been made to measure the position of the passive compressor bypass valve as it was recognised from the beginning of the project as a weakness in the system. During the test phase which lasted only for a few months, it was found to be free from fault in performance as would have been expected for a production hardware. Nevertheless, it was worth some extra attention into this component for the situations such as valve leakage due to fouling from low pressure EGR. The leakage of the turbine bypass valve was more influential and equally worth investigation but was already conducted by Bauder (2011).

Table 8.12 emulated drive cycle performance of the two stage system with compressor bypass valve leakage (negative value -> improvement)

	NEDC		WLTC	
Emissions	CO_2	NO_X	CO_2	NO_X
Units	g/km	mg/km	g/km	mg/km
TS original	149.4	104.3	180.4	268
TS with CBV leakage	152.7	98.2	185.2	284.2
Comparison	+2.2%	-5.8%	+2.7%	6.0%

Compared to the two stage system with no bypass valve leakage, the BSFC was increased by 2.2% and 2.7% in NEDC and WLTC respectively. Although not significant in the BSFC number, the loss of peak torque was 5 Nm, 8 Nm and 9 Nm in 1000 rpm, 1500 rpm and 2000 rpm respective. Considering the fact that the two stage system could have the potential to further increase torque due to the higher boost available, the potential loss of power due to valve leakage could be much higher.

The NO_X emissions were virtually the reversed (and enhanced) effect compared to the the HP ball bearing case. Due to the reduced air mass flow caused by the valve leakage, low load region NO_X emissions were reduced while the high load region NO_X emissions were increased and therefore the difference between NEDC and WLTC cycles.

On the other hand, the spring loaded bypass valve was not ideal in terms of flow capacity either. As shown in the Figure 8.8, the compressor valve opening was merely 4.6 mm at full load 2500 rpm, which was translated into a pressure drop across the valve of 5.5 kPa. An actively controlled bypass valve can easily increase the flow capacity of the valve at some extra cost. Therefore the benefit of using active control was evaluated here. A flow coefficient sweep simulation at 2500 rpm full load condition indicated a potential pressure drop across the valve of around 4 kPa. Although no significant improvement in BSFC and torque was expected with the identical fuel injection, potential torque rise was definitely possible without breaching the air fuel ratio limit.

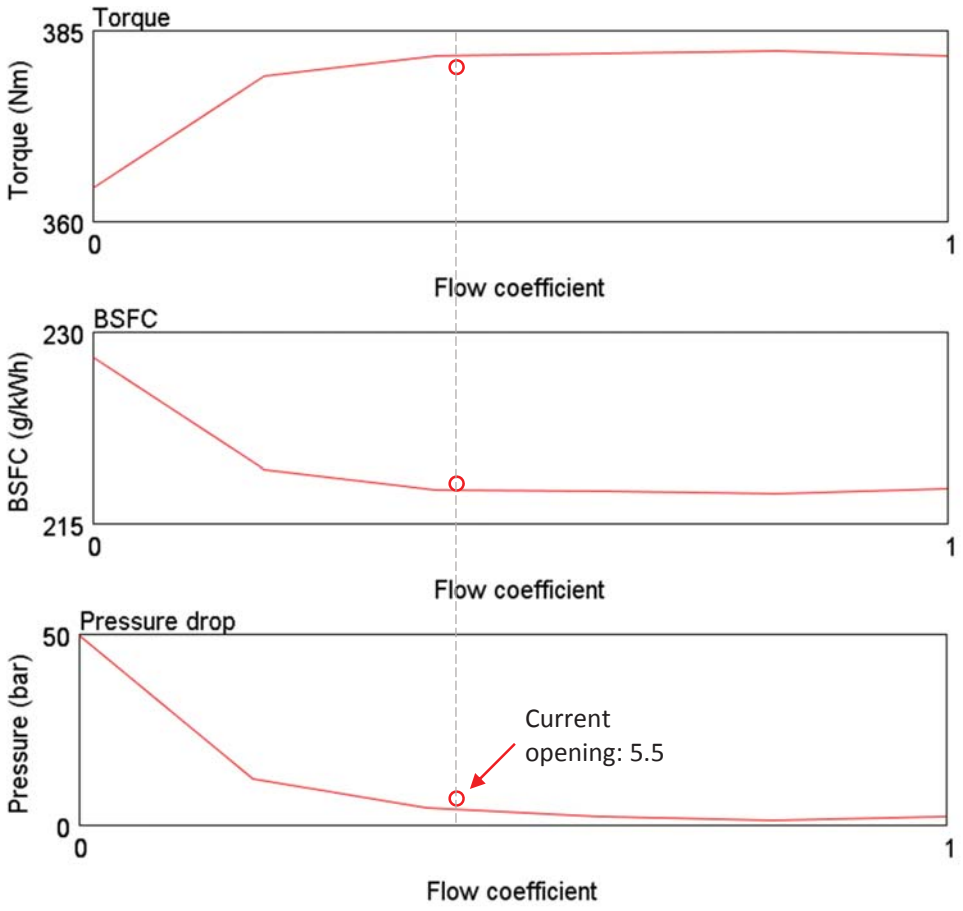

Figure 8.10 potential of improving the engine performance through active compressor bypass valve control

8.7 Summary

The chapter has focused on further exploration of the two stage system with the aid of the engine model. Based on the model calibrated in the Chapter 4 and 5, the model was re-calibrated using the test data acquired during the two stage system testing in Chapter 7 to further reduce the predictive error brought in by the two stage system.

From the simulation results, the VGT technology was found to be a good addition to the two stage system in that it dealt with several significant shortcomings of the two stage system. Although the drive cycle fuel consumption was found to be increased by around 2% due to the higher engine back pressure at low speed region, the NOx emission can be expected to reduce

between 5 to 10 percent due to the better flow capacity of the larger VGT turbocharger and the EGR controllability thanks to the closing of the vane blades. The transient response will not be as good as the FGT system due to the increased inertia, yet the penalty in performance at 1000 rpm was merely 0.4s.

Implementing the ball bearing technology at the HP stage can achieve a fuel consumption benefit of around 1.2%, while at LP stage 0.6% and at both stages 1.8%. The number was on par with the test results in the Chapter 5. The NOx emission however showed a varied results from the two drive cycles with varied load intensity. In addition, it was found that the ball bearing implemented in HP stage can improve the transient response of the system; yet the ball bearing in LP stage showed the opposite effect due to the shift of work load to the LP stage, even with both stages equipped with ball bearing rotors, the transient response was not improved by an measurable amount compared to the single ball bearing at the HP stage.

The implementation of both technologies provided a better compromise of system performance from a two stage system. The fuel consumption and the transient performance was found to be only 1% and 0.05s higher than the original two stage system. The NOx emission can be expected to reduce in the upcoming more transient drive cycle tests. The other shortcomings of the two stage system, such as the low speed EGR control and the high speed engine back pressure were successfully resolved by the use of the VGT technology.

The work presented in this chapter was but only a few examples to demonstrate the scope of work can be achieved using a fully calibrated engine model. Ideally the findings in this chapter should again be validated on the test bench. However, the availability of hardware is usually the limitation during the research and development phase of products and the kind of investigations conducted in this chapter would undoubtedly prove to be useful. Nevertheless, even with the level of calibration achieved in the preceding chapters, care must still be taken when simulation results are to be involved in the design decision making.

Chapter 9 - Conclusions

This chapter summarises the main findings from the project. For each chapter, findings are listed against the work objectives outlined in chapter one. However there were also targets missed due to several unforeseen difficulties and these are included in the weakness section. Future work which could either conquer the weaknesses or further improve the quality of the work are listed at the end.

9.1 Findings from the project

9.1.1 Literature survey

In chapter 2, a comprehensive literature survey was conducted to investigate the background of the two stage system. To understand the logic behind using the two turbochargers in series, comparison with other turbocharging technologies, such as the conventional free floating turbocharger, variable geometry turbine and especially the parallel arranged dual turbocharger system were also given significant attention. Such comparisons aimed to give a thorough study of the pros and cons of each system. By drawing experience from a wide range of studies testing and simulating the multi-turbo system, it was demonstrated that the two stage system, with the two turbochargers connected in series, can provide improved transient response and possibly better fuel consumption at rated power. Depending on the matching of the system, the full load torque can be improved due to the higher boost level when the

turbochargers boost the engine in two stages. It was also recognised from the literature that the matching of the two turbochargers and the control strategy were crucial in safely and effectively operating the charging system, without which the HP stage could easily over-speed and the LP stage can be too sluggish to take over when the HP was bypassed. Although much work had already been done on the two stage turbocharging system, research backed by both experimental and simulation analysis was rare and could be a contribution that this piece of work can aim to achieve.

9.1.2 Experimental facilities and baseline testing

Chapter 3 was focused on the description of the experimental setup and the baseline engine used in the complete research project. Various aspects of the laboratories, including ventilation, water circulation and dynamometer, etc. were briefly introduced. The baseline engine, equipped with a VGT turbocharger, was thoroughly tested following a novel test procedure established in this chapter. The full load experiment were analysed against the engine manufacturer published torque curve and the test results confirmed the engine was installed on the test bench without significant changing the performance parameters, despite the necessary alterations carried out. Other test results, i.e. the minimap points and hot/cold transient tests were presented and the key features of such test results were discussed for the convenience of the subsequent study.

9.1.3 1-D engine modelling methodology and baseline model calibration

Chapter 4 focused on the modelling side of the project with the model methodology briefly explained at the beginning of the chapter. Aided by the test results from the baseline engine experiments, the baseline model was constructed and calibrated. The model quality after calibration was shown to be of high level of fidelity.

9.1.4 Ball bearing turbocharger testing and model calibration

In chapter 5, a geometrically identical VGT turbocharger equipped with a ball bearing rotor was installed on the test engine and the full load tests, minimap tests and the transient tests were conducted as back to back comparisons to investigate the benefit of using the novel turbo rotor. Although the ECU was acting disruptively for the intended back to back experiments, the aid of simulation helped to uncover the true benefit of the ball bearing rotor: steady state fuel consumption can be expected to drop by 2.5% while the transient performance, especially in cold start condition was significantly improved with a drastic 35% reduction in T1090 time.

9.1.5 Two stage system simulation study and control strategy propose

The content of Chapter 6 was devoted to the preparation work for implementing the two stage system on the baseline engine. In several stages, the simulations were designed to characterise, optimise and control the system. The simulation results confirmed the hardware match to the engine size and an initial control strategy was proposed to achieve the optimal torque curve, fuel consumption and transient response.

9.1.6 Two stage system testing

The testing of the two stage system was described in Chapter 7. The test results were largely in agreement with the simulation study and the validity of the proposed control strategy was confirmed. Test results showed that the two stage system was able to significantly improve the engine transient response at low speed end - reducing the T1090 time by 50%. The system also had the potential to improve the engine full load torque, raising the 1000 rpm limiting torque from 183 to 192 without any ECU recalibration. However, the experiment also exposed the excessive engine back pressure of up to 0.8 bar higher than baseline seen at mid to high engine speed which was the results of the use of small high pressure stage turbocharger.

9.1.7 Further exploration of the two stage system using 1D engine model

With the model recalibrated for the two stage system using test data, the model was used for some exploratory study in Chapter 8. A VGT turbocharger at the HP stage with bypass valve was found to be a good addition to the system. Compared to the original two stage system, the NOx emissions were reduced by 5.4 % in NEDC cycle, and by a more substantial proportion of 9.7% in WLTC with only a small penalty in the cycle fuel consumption of 2.5% and 1.9% in NEDC and WLTC respectively. Moreover, the previously discussed ball bearing technology at the HP stage was able to improve the transient response with the T1090 reduced from 1.5 s to 1.27 s. The technology also provided the benefit in fuel consumption of 1.1% and 1.3% in NEDC and WLTC. Meanwhile, the LP stage ball bearing was counter-intuitively not contributing to the engine transient performance due to the interaction of two turbocharger. The combined VGT and ball bearing technologies in HP stage of the two stage system offered the best overall performance. The transient performance was on par with the original two stage system, with the T1090 only slower by negligible 0.05 second. The NOx emissions were reduced by 0.7% in NEDC, yet a much more significant 11.3% reduction in NOx emission was observed in the more intensive WLTC cycle. Fuel consumption was increase by 1.3% in NEDC and 0.7% in WLTC.

In the end, the effect of the leakage and the active control of the compressor bypass valve was briefly discussed and it was found that the around 2.5% in BSFC increase could be seen in a leaky compressor bypass valve; while the active control of the compressor bypass valve had the potential to further improve the limiting torque at high engine speed.

9.2 Weakness in the research

Compared to the other studies on the two stage system, the testing side of this project was given adequate attention. However, due to the inexperience in designing the engine control

system, the two stage control module frequently worked in an unstable manner, fighting with the main engine ECU controller. Therefore, the high speed operating region was not properly tested for the consideration of hardware protection. The data obtained from a wider operating range would greatly improve the quality of the engine model used for simulation.

Also, due to the different exhaust manifold setups used on for different turbocharging system did not give the same accessibility for instrumenting the sensors using the same test plan. In the process of the model calibration, the earlier dataset was not adequate to calibrate the model due to the lack of crucial pressure transducers and it was only in the two stage system testing, the complete dataset was obtained for the combustion calibration.

9.3 Future work

The work presented in this thesis has provided a solid analytical foundation for future studies. The predictive high fidelity 1D engine model is capable of further exploring the potential of the two stage turbocharging system. New technologies and additional charging device can be evaluated through simulation, possible topics include the two stage system with electric supercharger in HP stage, two stage system with electric turbine in LP stage (turbo compounding) and combined parallel and in series charging arrangement.

On the experimental side, although the proposed control strategy and the VGT technology in the HP stage were both intended in the thesis as novelties. During the three year span of the project, BMW and Audi have both promoted Diesel engines with the VGT two stage turbocharging systems installed, running highly similar control logics. However, the highly promising ball bearing technology identified in the thesis has not yet reach the market and therefore could be an ideal next step for the two stage system.

References

Almeida, F., Rodrigues, M., Barbieri, F. and Trevisan, M., 2010. Dual-stage TC modeling and calibration using 1D simulation – correlation with NVH quantities. SAE paper 2010-36-0305.

Bauder, R., Eiglmeier, C., Eiser, A., Marckwardt, H., 2011. The New High-performance Diesel Engine from Audi, the 3.0l V6 TDI with Dual-stage Turbocharging, *Internationales Wiener Motorensymposium*, Vienna, Austria.

Bozza, F. and De Bellis, V., 2011. Map-Based and 1D Simulation of a Turbocharger Compressor in Surging Operation, *SAE Int. J. Engines* 4(2), pp.2418-2433.

Bowyer, S., 2012. The FEV GT^2 Engine – A Downsized & Sequentially Boosted Engine Concept for Fuel Economy. In: *ENGINE EXPO North America*, Novi, Michigan, USA; 23-25, October 2012

Brouwer, M., Sadeghi, F., Lancaster, C., Archer J. and Donaldson, J., 2013. Whirl and Friction Characteristics of High Speed Floating Ring and Ball Bearing Turbochargers, *Transactions of the ASME: Journal of Tribology*, vol 135/041102-1.

Carscoop, 2007. Fiat 1.9 JTD M: New Twin Stage Turbo Diesel Engine Available with 180 & 191 HP, [online] Available at: http://www.carscoops.com/2007/06/fiat-19-jtd-m-new-twin-stage-turbo.html (Last accessed: April 1st, 2015)

Canova, M., Chiara, F., Rizzoni, G. and Wang, Y., 2009. Design and validation of a control-oriented model of a diesel engine with two-stage turbocharger. SAE paper 2009-24-0122.

Canova, M., Chiara, F., Rizzoni, G. and Wang, Y., 2010. Model based characterization and analysis of diesel engines with two-stage turbochargers. SAE paper 2010-01-1220.

Charlet, B., Lévine, J. and Marino, R., 1989. On dynamic feedback linearization. S*ystems Control Lett*; 13(2): 143–151.

Chasse, A., Moulin, P., Gautier, P. et al., 2008. Double stage turbocharger control strategies development. SAE paper 2008-01-0988.

Chen, S. and Flynn, P., 1965. Development of a single cylinder compression ignition research engine. SAE paper 650733.

Chen, M., Zhang, W., Zhang, X. and Ding, N., 2011. In-cylinder CFD simulation of a new 2.0L turbocharged GDI engine. SAE paper 2011-01-0826.

Chen, T., Zhang, Y., Zhuge, W. and Yan, X., 2008. Integrated system simulation for turbocharged IC engines. SAE paper 2008-01-1640.

Choi, C., Kwon, S. and Cho, S., 2006. Development of fuel consumption of passenger diesel engine with 2 stage turbocharger. SAE paper 2006-01-0021.

Chevalier A, Müller M and Hendricks E., 2000. On the validity of mean value engine models during transient operation. SAE paper 2000-01-1261.

Colin, G., Chamaillard, Y., Bloch, G. and Charlet, A., 2007. Exact and linearized neural predictive control: a turbocharged SI engine example. *Trans ASME, J Dynamic Systems, Measmt, Control*; 129(4): 527-533.

Däubler, L., Bessai, C. and Predelli, O., 2007. Tuning strategies for online-adaptive PI controllers. *Oil Gas Sci Technol*; 62(4): 493–500.

Davies, P., Marsal, D., Michel, R., Barthelet, P., 2013. Ball Bearing goes Mainstream, *IQPC*, Wiesbaden, Germany.

Deligant, M., Podevin, P. and Descombes, G., 2011. CFD model for turbocharger journal bearing performances. *Appl Thermal Engng*; 31(5): 811–819.

Dickmann, H., Wimmel, T., Szwedowicz, J. et al., 2006. Unsteady flow in a turbocharger centrifugal compressor: three-dimensional computational fluid dynamics simulation and numerical and experimental analysis of impeller blade vibration. *Trans ASME, J Turbomach*; 128(3): 455–465.

Donahue, R. and Foster, D., 2000, Effects of Oxygen Enhancement on the Emissions from a DI Diesel via Manipulation of Fuels and Combustion Chamber Gas Composition. SAE paper 2000-01-0512.

Ferreau, H., Ortner, P., Langthaler, P. et al., 2007. Predictive control of a real-world diesel engine using an extended online active set strategy. *Annual Reviews in Control*; 31(2): 293–301.

Fraser, N., Blaxill, H., Lumsden, G., and Bassett, M., 2009. Challenges for increased efficiency through gasoline engine downsizing. SAE paper 2009-01-1053.

Galindo, J., Climent, H., Guardiola, C., Doménech, J., 2009. Strategies for improving the mode transition in a sequential parallel turbocharged automotive diesel engine. *International Journal of Automotive Technology*; 10(2): 141–149.

Galindo, J., Climent, H., Guardiola, C., and Tiseira, A., 2009. Assessment of a sequentially turbocharged diesel engine on real-life driving cycles. *Int J Veh Des*; 49(1): 214 – 234.

Galindo, J., Climent, H., Guardiola, C. and Tiseira, A., 2009. On the effect of pulsating flow on surge margin of small centrifugal compressors for automotive engines. *Expl Thermal Fluid Sci* 2009; 33(8): 1163–1171.

Galindo, J., Lujan, J., Climent, H. and Guardiola, C., 2007. Turbocharging system design of a sequentially turbocharged diesel engine by means of a wave action model. SAE paper 2007-01-1564.

Galindo, J., Serrano, J., Climent, H., and Varnier, O., 2010. Impact of two-stage turbocharging architectures on pumping losses of automotive engines based on an analytical model. *Energy Conversion Managmt*, 51(10): 1958 – 1969.

Gambarotta, A., Lucchetti, G., Fiorani, P. et al., 2009. A thermodynamic mean value model of the intake and exhaust system of a turbocharged engine for HiL/SiL applications. SAE paper 2009-24-0121.

Gautier, P., Albrecht, A., Moulin, P., Chasse, A. et al., 2008. A New Simulation Step Towards Virtual Bench Through the Challenging Case of Two-Stage Turbocharger Diesel Engine Control Design, SAE Paper 2008-01-0355.

Griffith, B., Slaughter, S. and Mavrosakis, P., 2007. Applying Ball Bearings to the Series Turbochargers for the Caterpillar® Heavy-Duty On-Highway Truck Engines, SAE Paper Number 2007-01-4235.

Guzzella, L. and Amstutz, A., 1998. Control of diesel engines. *IEEE Control Systems Mag*; 18(5): 53–71.

Heywood, J., 1988. *Internal combustion engine fundamentals*. New York: McGraw-Hill.

Honeywell Turbo Technologies, *Ball Bearing*, 2003. [online], Available at: http://turbo.honeywell.com/our-technologies/ball-bearing/ (Last accessed: Oct 21st 2013)

Jensen, J., Kristensen, A., Sorenson, S. et al., 1991. Mean value modelling of small turbocharged diesel engine. SAE paper 910070.

Hield, P., 2011. The Effect of Back Pressure on the Operation of a Diesel Engine, *Maritime Platforms Division, Defence Science and Technology Organisation*, Australia

Jankovic, M. and Kolmanovsky, I., 2000. Constructive Lyapunov control design for turbocharged diesel engines. *IEEE Trans Control Systems Technol*; 8(2): 288–299.

Jung, M. and Glover, K., 2006. Calibratable linear parametervarying control of a turbocharged diesel engine. *IEEE Trans Control Systems Technol*; 14(1): 45–62.

Karmiggelt, R., 1998. *Mean value modelling of a SI engine*. Report 98.041, Department of Mechanical Engineering, Technische Universiteit Eindhoven, Eindhoven, The Netherlands.

Kech, J. and Klotz, H., 2002. Model-based sequential turbocharging optimization for series 8000 M70/M90 engines. SAE paper 2002-01-0378.

Knecht, W., 2008. Diesel engine development in view of reduced emission standards. *Energy*; 33(2): 264–271.

Kotman, P., Bitzer, M. and Kugi, A., 2010. Flatness-based feedforward control of a two-stage turbocharged diesel air system with EGR. In: *2010 IEEE international conference on control applications*, *2010 IEEE multi-conference on systems and control*, Yokohama, Japan, 8–10 September 2010, pp. 979–984. New York: IEEE.

Langridge, S. and Fessler H., 2002. Strategies for high EGR rates in a diesel engine. SAE paper 2002-01-0961.

Lecointe, B. and Monnier, G., 2003. Downsizing a gasoline engine using turbocharging with direct injection. SAE paper 2003-01-0542.

Lee, B., 2009. *Dual-stage boosting systems: modeling of configurations, matching and boost control options*. Thesis (PhD). University of Michigan, Ann Arbor.

Lee, B., Filipi, Z., Assanis, D. and Jung, D., 2009. Simulation-based assessment of various dual-stage boosting systems in terms of performance and fuel economy improvements. SAE paper 2009-01-1471.

Lee, B., Jung, D., Assanis, D. and Filipi, Z., 2008. Dual-stage turbocharger matching and boost control options. In: *ASME 2008 Internal Combustion Engine Division spring technical conference*. Chicago, Illinois, USA, 27-30 April 2008, pp.267–277. New York: ASME.

Majewski, A. and Khair, K., 2006. *Diesel Emissions and Their Control*, Warrendale, USA: SAE International, pp. 111.

Malkhede, D., Seth, B. and Dhariwal, H., 2005. Mean value model and control of a marine turbocharged diesel engine. SAE paper 2005-01-3889.

Martin, G., Talon, V., Peuchant, T. et al., 2009. Physics based diesel turbocharger model for control purposes. SAE paper 2009-24-0123, 2009.

Mayer, A., Schruf, G., Kirchhofer, H., 1982, Downsizing and Downspeeding of Automotive Diesel Engines – Theory and Practice, SAE Paper 820443.

Millo, F., Mallamo, F. and Mego, G., 2005. The potential of dual stage turbocharging and Miller cycle for HD diesel engines. SAE paper 2005-01-0221.

Moody, J., 1986, Variable Geometry Turbocharging with Electronic Control, SAE Paper 860107.

Moulin, P. and Chauvin, J., 2011. Modelling and control of the air system of a turbocharged gasoline engine. *Control Engineering Practice*; 19(3): 287–297.

Moulin, P., Chauvin, J. and Youssef, B., 2008. Modelling and control of the air system of a turbocharged gasoline engine. In: *17th International Federation of Automatic Control world congress*, Seoul, Republic of Korea; 6–11 July 2008, Vol. 17, Part 1, pp. 8487–8494. Oxford: IFAC.

Moulin, P., Grondin, O. and Fontvieille, L., 2008. Control of a two stage turbocharger on a diesel engine. In: *48th IEEE conference on decision and control*, Shanghai, People’s Republic of China, 16–18 December 2008, pp.5200–5206. New York: IEEE.

Murray, R., Rathinam, M. and Sluis, W., 1995. Differential flatness of mechanical control systems: a catalog of prototype systems. In: *ASME international mechanical engineering congress and exposition*, San Francisco, California, USA, 12–17 November 1995: 1–9. New York: ASME.

Nakayama, S., Fukuma, T., Matsunaga, A., Miyake, T. et al., 2003. A New Dynamic Combustion Control Method Based on Charge Oxygen Concentration for Diesel Engines, SAE Paper 2003-01-3181.

Nakhjiri, M., Pelz, P., Matyschok, B. et al., 2011. Physical modelling of automotive turbocharger compressor: analytical approach and validation. SAE paper 2011-01-2214.

Navrátil, J., 2006. 2-stage turbocharger matching for a light duty diesel engine. Technical Report, *Engine Simulation*, Ricardo Consulting Engineers Ltd, Prague, Czech Republic.

Nitta, J., Minato, A. and Shimazaki, N., 2011. Performance evaluation of three-stage turbocharging system for heavy-duty diesel engine. SAE paper 2011-01-0374.

Ortner, P. and del Re, L., 2007. Predictive control of a diesel engine air path. *IEEE Trans Control Systems Technol*; 15(3): 449–456.

Ouenou-Gamo, S., Rachid, A. and Ouladsine, M., 1999. A nonlinear controller of a turbocharged diesel engine using sliding mode. In: *IEEE international conference on control applications*. Hartford, Connecticut, USA, 5–7 October 1997, pp. 803–805. New York: IEEE.

Pflüger, F., Regulated two-stage turbocharging – KKK's new charging system for commercial diesel engines. In: *IMechE 6th international conference on turbocharging and air management systems*. London, UK, 3 – 5 November 1998, paper C554/035/98. Bury St Edmunds: Professional Engineering Publishing.

Plianos, A. and Stobart, R., 2008. Modelling and control of diesel engines equipped with a two-stage turbo-system. SAE paper 2008-01-1018.

Qian, Y., Zhang, Z. and Deng, K., 2012. Development of a three phase sequential turbocharging system with two unequal-size turbochargers. *Int J RotatingMach*; 951096 (8 pp.).

Rajamani, R., 2005. Control of a variable-geometry turbocharged and wastegated diesel engine. *Proc IMechE Part D: J Automobile Engineering*; 219(11): 1361–1368.

Rakopoulos, C. and Giakoumis, E., 2006. Review of thermodynamic diesel engine simulations under transient operating conditions. SAE paper 2006-01-0884.

Rakopoulos, C. and Giakoumis, E., 2009. Diesel engine transient operation: principles of operation and simulation analysis. Berlin: Springer.

Rakopoulos, C., Giakoumis, E. and Michos, C., 2007. Quasilinear versus filling and emptying modelling applied to the transient operation of a turbocharged diesel engine. *Int J Veh Des*; 45(1): 150–170.

Ren, Z., Campbell, T., and Yang, J., 1998. Investigation on a computer-controlled sequential turbocharging system for medium-speed diesel engines. SAE paper 981480.

Saulnier, S. and Guilain, S., 2004. Computational study of diesel engine downsizing using two-stage turbocharging. SAE paper 2004-01-0929.

Schmitt, F. and Engels, B., 2004. Regulated 2-stage (R2S) charging system for high specific power engines. In: *Congrés le diesel: aujourdhui et demain*, Lyon, France. Suresnes: Société des Ingénieurs de l'Automobile.

Schwarzmann, D., Nitsche, R., Lunze, J. and Schanz, A., 2006. Pressure control of a two-stage turbocharged diesel engine using a novel nonlinear IMC approach. In: *2006 IEEE international conference on control applications*, Munich, Germany, 4–6 October 2006, pp. 2399–2404. New York: IEEE.

Sepulchre, R., Jankovic, M. and Kokotovic, P., 1997. Constructive nonlinear control. Berlin: Springer.

Serrano, J., Olmeda, P., Tiseira, A., Garcia-Cuevas, L., and Lefebvre, A., 2013. Theoretical and experimental study of mechanical losses inautomotive turbochargers, *Energy*, vol. 55, pp. 888-898.

Shingne, P., Assanis, D., Babajimopoulos, A., Keller, P. et al., 2010. Turbocharger Matching for a 4-Cylinder Gasoline HCCI Engine Using a 1D Engine Simulation, SAE Paper 2010-01-2143.

Slotine, J. and Li, W., 1991. *Applied nonlinear control*. Englewood Cliffs, New Jersey: Prentice-Hall.

Stefanopoulou, A., Kolmanovsky, I. and Freudenberg, J., 2000. Control of variable geometry turbocharged diesel engines for reduced emissions. *IEEE Trans Control Systems Technol*; 8(4): 733–745.

Steinparzer, F., 2007. The BMW Six-Cylinder Engine with Two-Stage Turbo Charging, *Auto Technology*, 2007(3), pp. 44-47.

Stone, R., 1999. *Introduction to internal combustion engines*. 3rd edition. London: Macmillan.

Tanimoto, K., Kajihara, K., and Yanai, K., 2000. Hybrid Ceramic Ball Bearings for Turbochargers, SAE Paper 2000-01-1339.

Tashima, S., Okimoto, H., Fujimoto, Y. and Nakao, M., 1994. Sequential twin turbocharged rotary engine of the latest RX-7. SAE paper 941030.

Utkin, V., Chang, H., Kolmanovsky, I. and Cook, J., 2000. Sliding mode control for variable geometry turbocharged diesel engines. In: *American control conference*, Chicago, Illinois, USA, 28–30 June 2000, pp. 584–588. New York: IEEE.

Utkin, V., Guldner, J. and Shi, J., 1999. *Sliding mode control in electromechanical systems*. London: Taylor & Francis.

Van Aken, M. et al., 2007. Appliance of high EGR rates with a short and long route EGR system on a Heavy Duty diesel engine, SAE Paper Number 2007-01-0906.

Varnier, O., 2012. *Trends and limits of two-stage boosting systems for automotive Diesel engines*. Thesis (PhD). Universidad Politecnica de Valencia, Valencia.

Vitek, O., Macek, J. and Polášěk M., 2006. New approach to turbocharger optimization using 1-D simulation tools. SAE paper 2006-01-0438.

Wang. J., 2008. Hybrid robust air-path control for diesel engines operating conventional and low temperature combustion modes. *IEEE Trans Control Systems Technol*; 16(6):1138–1151.

Watel, E., Pagot, A., Pacaud, P. and Schmitt, J., 2010. Matching and evaluating methods for Euro 6 and efficient two-stage turbocharging diesel engine. SAE paper 2010-01-1229.

Watson, N. and Janota, M., 1982. *Turbocharging the internal combustion engine*. London: Macmillan.

Winkler, N. and Ångström, H., 2008. Simulations and measurements of a two-stage turbocharged heavy-duty diesel engine including EGR in transient operation. SAE paper 2008-01-0539.

Yang, J. and Campbell, T., 1997. Development of an IC Engine Simulation Programme for Multiple Turbocharger Configurations, SAE Paper 970056.

Yang, X. and Zhu, G., 2010. A mixed mean-value and crank based model of a dual-stage turbocharged SI engine for hardware-in-the-loop simulation. In: *American control conference*, Baltimore, Maryland, USA, 30 June–2 July 2010, pp. 3791–3796. New York: IEEE.

Zhang, Z., Deng, K., Wang, Z. and Zhu, X., 2008. Experimental study on the three-phase sequential turbocharging system with two unequal size turbochargers. SAE paper 2008-01-1698.